FLOW CYTOMETRIC INVESTIGATION OF THE SIZE SPECTRUM OF NORTH SEA PHYTOPLANKTON COMMUNITIES

Katy R. Owen

A thesis submitted to the School of Environmental Sciences, at the University of East Anglia, for the degree of Doctor of Philosophy, May 2014.

ABSTRACT

Marine biogeochemical processes are closely linked to phytoplankton community assemblages. Cell abundance and biomass are a measure of the successful conversion of inorganic to organic carbon. Carbon estimates are therefore often used to analyse metabolism and energy transfers within marine environments, and carbon is frequently the main parameter used in ecosystem models. Phytoplankton can be divided into functional types based on cell size: microplankton (<200 µm), nanoplankton (2-20 µm) and picoplankton (≤ 3 µm). Differences in cell volume govern variations in carbon content, nutrient uptake and influence cell fate. Reduced diameters equate to lower sedimentation rates and promote participation within the microbial loop and recycling of carbon within surface waters. Larger diameters can increase settling rates, resulting in the loss of carbon from surface waters. Current North Sea monitoring and research programmes typically only consider larger micro- and nanoplankton cells, or the bulk phytoplankton community as a whole: there is little separation by functional type. Inclusion of picoplankton and the delineation of biomass contribution by cell size are required for accurate depictions of phytoplankton productivity within this region, but this is not feasible with current water sampling protocols. Flow cytometry is a new multiparametric analysis technique offering high-speed enumeration and assessment of particles. Phytoplankton cells from 2-200 µm can be easily distinguished from debris and reproducible data on cell size and pigment content is supplied within minutes. This research uses flow cytometry to provide detailed assessments of phytoplankton community structure at a range of spatial and temporal scales. Distribution patterns are related to environmental parameters and observed patterns are used to test existing paradigm and advance current ecological theory.

LIST OF CONTENTS

LIST OF FIGURES

LIST OF TABLES

LIST OF ABBREVIATIONS

ANOVA	Analysis of variance
AT	Adenine thymine
BCP	Biological carbon pump
CCAP	Culture collection of algae and protozoa
CCMP	Culture collection of marine phytoplankton
Cefas	Centre for environment, fisheries and aquaculture science
CEN	Chicken erythrocyte nuclei
Chl	Chlorophyll
CHN	Carbon hydrogen nitrogen
CO_2	Carbon dioxide
CTD	Conductivity temperature depth
DAPI	4',6-diamidino-2-phenylindole
DGGE	Denaturing gel electrophoresis
dH_2O	Distilled water
DIN	Dissolved inorganic nitrogen
distLM	Distance linear model
DMS	Dimethyl sulphide
DMSP	Dimethylsulfoniopropionate
DMSO	Dimethyl sulfoxide
DNA	Deoxyribonucleic acid
dsDNA	Double stranded DNA
DOC	Dissolved organic carbon
FISH	Fluorescence *in situ* hybridisation
FWS	Forward scatter
GAF	Green autofluorescence
GC	Guanine cytosine
GF/F	Glass fibre filter
HAB	Harmful algal bloom

HCl	Hydrochloric acid
HeNe	Helium neon
HPLC	High performance liquid chromatography
I	Iodide
IBTS	International beam trawl survey
l	Litre
MERIS	Medium resolution imaging spectrometer
MDS	Multidimensional scaling
ml	Millilitre
mV	Millivolt
Mya	Million years ago
N	Nitrogen
N_2	Nitrogen gas
NaCl	Sodium chloride
NCMA	National centre for marine algae
nm	Nanometre
OFL	Orange fluorescence
OH	Hydroxide
PAR	Photosynthetically active radiation
PCA	Principal components analysis
PCO	Principal coordinates analysis
PCR	Polymerase chain reaction
PFT	Phytoplankton functional type
PIC	Particulate inorganic carbon
POC	Particulate organic carbon
PO_4	Phosphate
PMT	Photomultiplier tube
PRIMER	Plymouth routines in multivariate ecological research
RCC	Roscoff culture collection
RFL	Red fluorescence

RNA	Ribonucleic acid
rRNA	Ribosomal ribonucleic acid
rpm	Revolutions per minute
RV	Research vessel
TEP	Transparent exopolymer particles
TOxN	Nitrate + nitrite
Si	Silicate
SWS	Side scatter
YFL	Yellow fluorescence

For Mum and Dad

"As soon as you have entered into this pelagic wonderland
you will see that you cannot leave it."

Johannes Muller to Ernst Haeckel in 1853 (Taylor 1980).

"This is an adventure"

Steve Zissou, The Life Aquatic (2005)

ACKNOWLEDGEMENTS

This PhD would not have been possible without a supporting cast of many. I would like to use this space to extend my gratitude towards these people.

I would like to thank my principal supervisor Dr Gill Malin, and co-supervisors Dr Véronique Créach, Dr Rodney Forster and Dr Carol Robinson for their help in developing this research and for their guidance and encouragement throughout. I'd like to thank the Cefas Smartbuoy team, in particular Dave Sivyer, Tom Hull, Neil Needham and Chris Read, for supplying my sea legs, providing endless hours of entertainment (hello sailor) and for teaching me how to cast a CTD at 4 am and not bounce it off the bottom. My time at Cefas supplied me with many amazing colleagues who I now consider to be great friends. These include Thomas McGowan, Rebecca Walker, Elisa Capuzzo, David Stephens and Tina Kerby. Thanks for feeding me, drinking with me and generally being rad. For better or worse Cefas also gave me Michael Godard: alternately my chauffeur, my football mentor, my sushi co-chef, the Goose to my Magnum, and most importantly my best friend. De rien poisson rouge, de rien. I'd also like to thank my long suffering non-science friends who still think I analyse fighter plankton with a flux capacitor. Jen Walke and Sarah Wake thanks for feigning interest convincingly and supporting me through the last four years. Somewhere in between science and the real world is the indispensable Kath Mortimer, supplier of internet memes and giver of good advice. The greatest friend and counsellor I could ever have hoped for. I couldn't find a youtube link that appropriately conveyed what I wanted to express, so I'll just say thanks for the whine and the wine.

Enfin, je voudrais remercier particulièrement ma vrai patronne, une source constante d'enthousiasme, d'inspiration, d'orientation et bien sûr de café. Vous avez été la force motrice de cette thèse et m'avez enseigné à être une vraie scientifique. Je vous remercie de votre patience et de m'avoir appris à jurer correctement en français.

Chapter 1 Introduction

More than 70% of the surface of the Earth is covered by ocean (Suttle 2007). Living amongst the marine mammals, fishes and seabirds are a diverse array of microscopic plants and animals, known collectively as plankton. These tiny organisms are a driving force behind the cycling of energy and nutrients within marine ecosystems. They sustain aquatic food webs, control biogeochemical cycles and regulate global climate, whilst remaining largely invisible to the naked eye. This thesis is concerned specifically with the abundance and distribution of planktonic flora, the phytoplankton, within North Sea ecosystems. In this introductory chapter, I will start by discussing the relevance and diversity of the phytoplankton, and their varying roles within Earth system processes. I will introduce the analysis methods used for phytoplankton observation, including both traditional and cutting-edge techniques and consider the benefits and disadvantages of each. Finally, I will introduce the research objectives of this study.

1.1. What are plankton?

The word plankton is derived from the Greek word "*planktos*", translating roughly as "wanderer", or "drifter" (Graham & Wilcox 2000). It was first used as a descriptive term for marine life in 1887 by Viktor Hensen (Ghosal et al. 2000), during exploration of North Sea biota. He used it to describe "everything that drifts in the water, whether shallow or deep, living or dead" (Taylor 1980). This definition has been refined for modern scientific use, and now refers to microscopic organisms passively advected by currents within the water column (Ghosal et al. 2000; Hoppenrath et al. 2009). Planktonic organisms fall into three main categories: zooplankton (from "*zoon*" meaning animal), phytoplankton (from "*phyton*" translated as plant) and bacterioplankton. These divisions are primarily based on how each individual acquires energy for basic cellular processes, such as growth and reproduction. The zooplankton are composed of a wide variety of organisms, each obtaining carbon, and therefore energy, through ingestion of

either living prey or particles of organic matter. Some, such as crab larvae and juvenile fish are meroplanktonic; settling out of the water column to inhabit the sea floor, or developing into active swimmers and becoming independent of ocean currents. Others, such as copepods and salps, are holoplanktonic and complete their entire life cycle as planktonic organisms. The phytoplankton are composed of unicellular plants, each seldom growing larger than 2 mm, and generally observable only by microscope unless individuals form long chains, colonies, or aggregate in great numbers. In contrast to zooplankton, phytoplankton are photoautotrophic: they require light energy to power photosynthesis and drive carbon acquisition. The bacterioplankton represent the smallest component of the plankton, consisting of heterotrophic prokaryotic organisms (Reynolds 2006). Bacterioplankton cells may be saprotrophic, acquiring energy from dead or decayed organic matter, whilst others are autotrophic, deriving energy from chemosynthesis or even photosynthesis in a similar fashion to the phytoplankton (Thurman 1997).

1.2. Ecological and biogeochemical relevance of phytoplankton

Phytoplankton provide useful indicators of ecosystem state, as cells have minimal buffering capacity against modifications within their environment (Thyssen et al. 2008). Periodic instances of natural or anthropogenic nutrient loading can trigger extremely rapid localised growth of many millions of phytoplankton, known as a bloom (Graham & Wilcox 2000). In such high concentrations, they can impact upon water column conditions by influencing light penetration, heating, and viscosity (Falkowski et al. 2004). They are a vital food source, grazed by zooplankton, fishes, whales and seabirds. These cells are essential for maintenance of marine biodiversity, and are crucial for dependent industries such as coastal and offshore fisheries, and aquaculture. The role of phytoplankton also reaches beyond the ecosystem level. These tiny organisms are major drivers in the global cycling of elements, and produce climatically relevant trace gases (Froneman et al. 2004; Levine et al. 2012; Nishino et al. 2011).

1.2.1. Photosynthesis and the global carbon cycle

Phytoplankton are ubiquitous throughout the uppermost sunlit layer (euphotic zone) of marine environments and are central to ecological systems and biogeochemical processes across the globe (Simon et al. 2009; Morán et al. 2010). Like land plants, phytoplankton are photosynthetic: a process involving the harvesting of solar light by pigment complexes contained within cells (Porra et al. 2005). Energy from photosynthetically active radiation (PAR; wavelength 400-700 nanometres) is absorbed principally by chlorophylls, carotenoids and phycobilins within cells (Porra et al. 2005). The reflected light wavelengths give each of these pigments their characteristic green, golden-brown, and orange colours. Absorbed radiation is converted to chemical energy and used to reduce carbon dioxide (CO_2) to carbohydrate, enabling the production of organic matter. This organic carbon in the form of phytoplankton cells supplies the fuel required for life by non-photosynthetic organisms. Phytoplankton are therefore primary production agents, forming the foundations of marine food webs and underpinning multiple complex trophic layers above them.

CO_2 is often described as a greenhouse gas, due to its influence upon global climate. CO_2 alongside N_2O and methane allows solar energy to pass through the Earth's atmosphere, but prevents the thermal energy radiated back from the Earth's surface from escaping into space (Ducklow et al. 2001). Atmospheric concentrations of CO_2 therefore heavily influence global temperature and climate, making Earth hospitable to life. CO_2 is released into the environment from a variety of sources and processes, including respiration, decay and volcanic eruptions (Ducklow et al. 2001; Suttle 2005). These emissions have historically been balanced with natural CO_2 uptake, principally by photosynthetic organisms, such as aquatic phytoplankton and macroalgae, and terrestrial trees and plants. This is the Earth's natural greenhouse effect, which makes possible the existence of life as we know it. In recent history, this natural equilibrium has been disturbed by increased outputs of greenhouse gases from additional anthropogenic sources. The combustion of carbonaceous fuels such as coal, oil and natural gas has risen with economic growth, the spread of industrialisation and deforestation, resulting

in an excess of atmospheric CO_2 and intensification of the greenhouse effect, as natural sinks reach capacity (de la Rocha 2003). Whilst the importance of the protection and development of conspicuous sinks on land (e.g. woodlands and rainforests) in CO_2 offsetting is well publicised (Adachi et al. 2011), the equal significance of their aquatic counterparts is often overlooked. Despite contributing to just 1% of all photosynthetic biomass, phytoplankton cells are responsible for approximately half of global photosynthesis each year (Field et al. 1998).

The "biological pump" is a term frequently used to refer to a combination of biological, chemical and physical processes that culminate in the removal of carbon from the atmosphere and surface waters and its transfer to the oceans interior (Sigman & Haug 2003). Photosynthetic conversion of CO_2 to organic carbon by phytoplankton cells is central to carbon cycling within marine environments and is tightly linked to atmospheric concentrations of CO_2 (Ducklow et al. 2001, Suttle 2007, Kim et al. 2011). The "soft tissue" pump is driven by biological activity within the euphotic zone. It describes the sinking of photosynthetically-fixed biomass in particulate or dissolved form to the deep ocean where it is respired, thereby "pumping" organic carbon downwards (Volk & Hoffert 1985). The efficiency of this pump is largely determined by the transfer rate of carbon to deeper water, governed principally by the abundance and size structure of phytoplankton communities present and their associated grazers (Froneman et al. 2004, Kim et al. 2011). The resulting net removal of biomass leads to carbon depletion in surface waters relative to the oceans interior, creating a reduction in the partial pressure of CO_2 at the ocean's surface (de la Rocha 2003). This leads to drawdown and diffusion of CO_2 into the ocean which reduces atmospheric concentrations (Froneman et al. 2004, Jin et al. 2007). The existence of transparent exopolymer particles (TEP) and their link to carbon cycling was only discovered relatively recently (Alldredge et al. 1993). TEP are surface active carbohydrates now known to be abundant within oceans (Engel 2002). In marine pelagic systems these particles originate principally from phytoplankton exudates, and promote the aggregation of particulate carbon (Bar-Zeev et al. 2009, Passow 2012). Sinking of

aggregates contributes greatly to the transport of carbon to depth (Alldredge et al. 1993, Passow 2012); in fact the aggregation state of diatoms (measured as total aggregate volume) correlates with TEP concentration (Gaerdes et al. 2010). Sinking TEP supply bacteria with organic carbon substrates and can create 'hot spots' of elevated microbial metabolism and nutrient cycling within the water column (Bar-Zeev et al. 2009). TEP are therefore intrinsic to the efficiency of the biological carbon pump, allowing abiotic transformation of dissolved organic matter into sinking particulate form alongside more conventional microbial uptake. Production of TEP principally by phytoplankton cells further underlines the relevance of phytoplankton community structure to carbon cycling. An overview of the soft tissue pump including the role of TEP is provided in Figure 1.1.

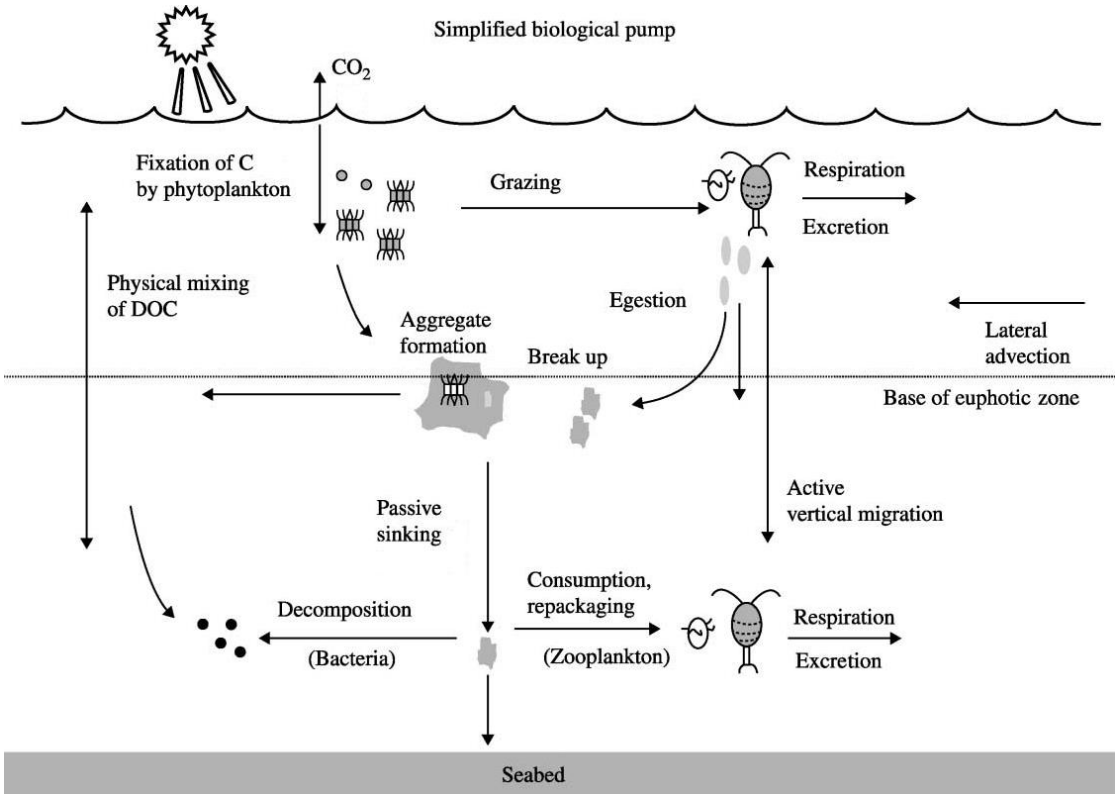

Figure 1.1. The biological carbon pump from de la Rocha (2003), describing uptake of carbon dioxide (CO_2) and fixation of carbon (C).

Many marine organisms also extract carbon from surface waters in order to produce inorganic carbon compounds, principally calcium carbonate ($CaCO_3$; Sigman & Haug 2003). As with organic carbon, some of the $CaCO_3$ from surface waters dissolves whilst sinking or upon reaching the sea floor, contributing to the carbon concentration gradient from the surface to the deep ocean and constituting the carbonate pump (Simpson & Sharples 2012a). A fraction of $CaCO_3$ is preserved and buried in sediments, creating an opposing effect to the soft tissue pump as removal of $CaCO_3$ lowers pH and raises CO_2 (Volk & Hoffert 1985). The pumping of organic carbon and $CaCO_3$ creates vertical chemical gradients which continuously mix surface and interior water. Furthermore, CO_2 solubility is inversely linked to seawater temperature (Sigman & Haug 2003). This temperature dependence results in a surface to deep ocean gradient of carbon concentration. Thermohaline circulation within oceans is driven by cool and dense water masses which originate from deep water at high latitudes and fill the abyssal depths of all the major ocean basins (Simpson & Sharples 2012a). The warmer surface water masses of low and mid latitudes are too buoyant to sink and remain confined to the uppermost water column. Since CO_2 is more soluble at low temperatures, the thermal structure of the ocean imposes a carbon gradient in the same direction as the soft tissue pump and act together to transport carbon from the atmosphere into the ocean's interior (Sigman & Haug 2003). This process may be temporarily reversed during seasonal upwelling events in equatorial regions, where wind currents cause deep water to rise to the surface, replenishing nutrients in the upper ocean but also releasing CO_2 due to reduced solubility of the gas (Simpson & Sharples 2012a).

1.3. Phytoplankton diversity

Phytoplankton are an ancient group of polyphyletic organisms, that evolved over millions of years, interacting with other organisms to produce the huge diversity of physiology and morphology observable both within and across genera today (Tillmann & Rick 2003, Falkowski et al. 2004, Simon et al. 2009, Leliaert et al. 2011) (Figure 1.2).

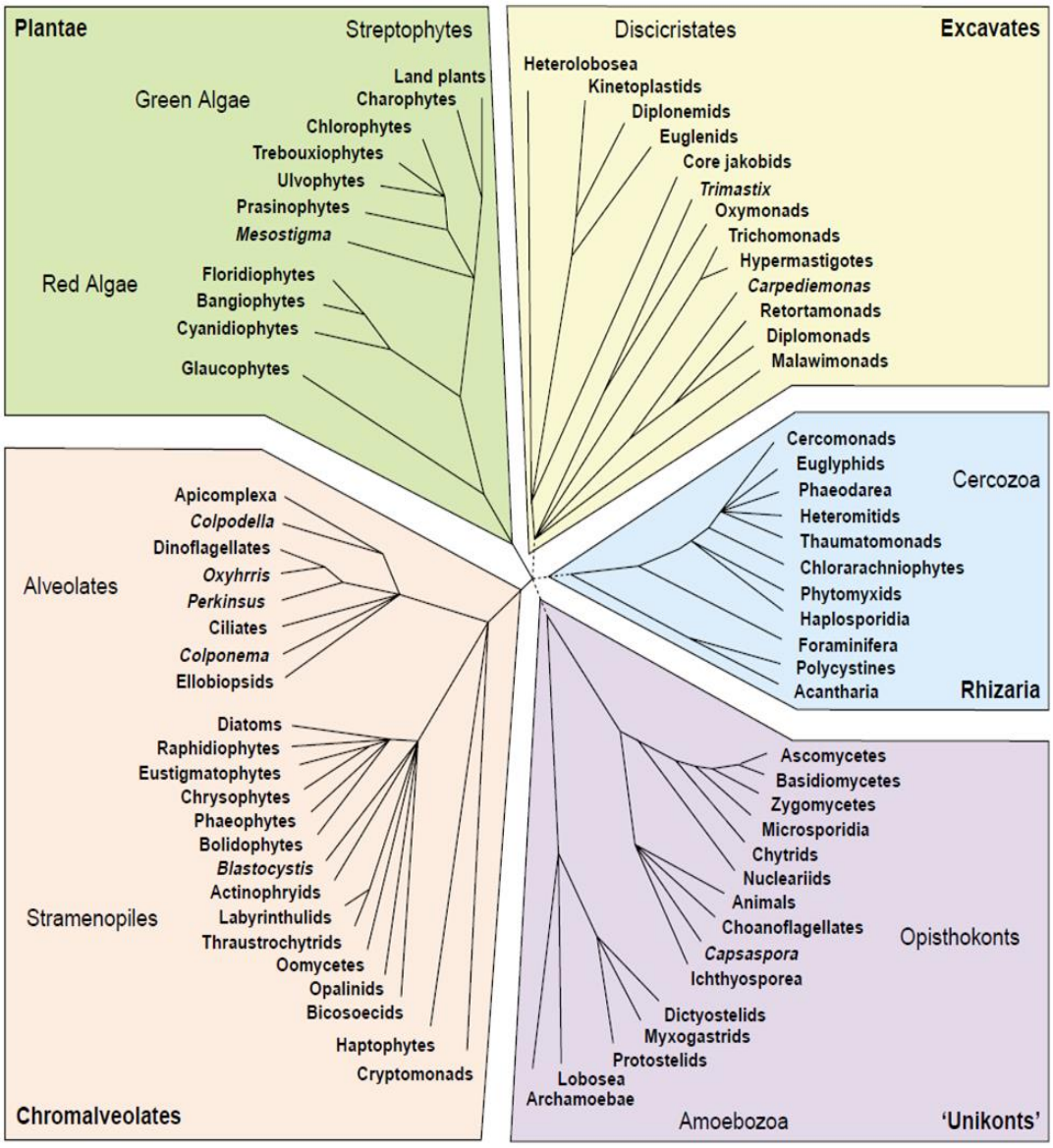

Figure 1.2. A tree of eukaryotes. The tree is a hypothesis composed of molecular phylogenies and morphological and biochemical evidence. Five "supergroups" are shown, each consisting of a diversity of eukaryotes, which are mostly microbial (protists and algae). Branches emerging simultaneously show unresolved relationships where little or no evidence for branching order exists. Dotted branches are used when there are only preliminary indications for relationships. Adapted from Keeling et al. (2005)

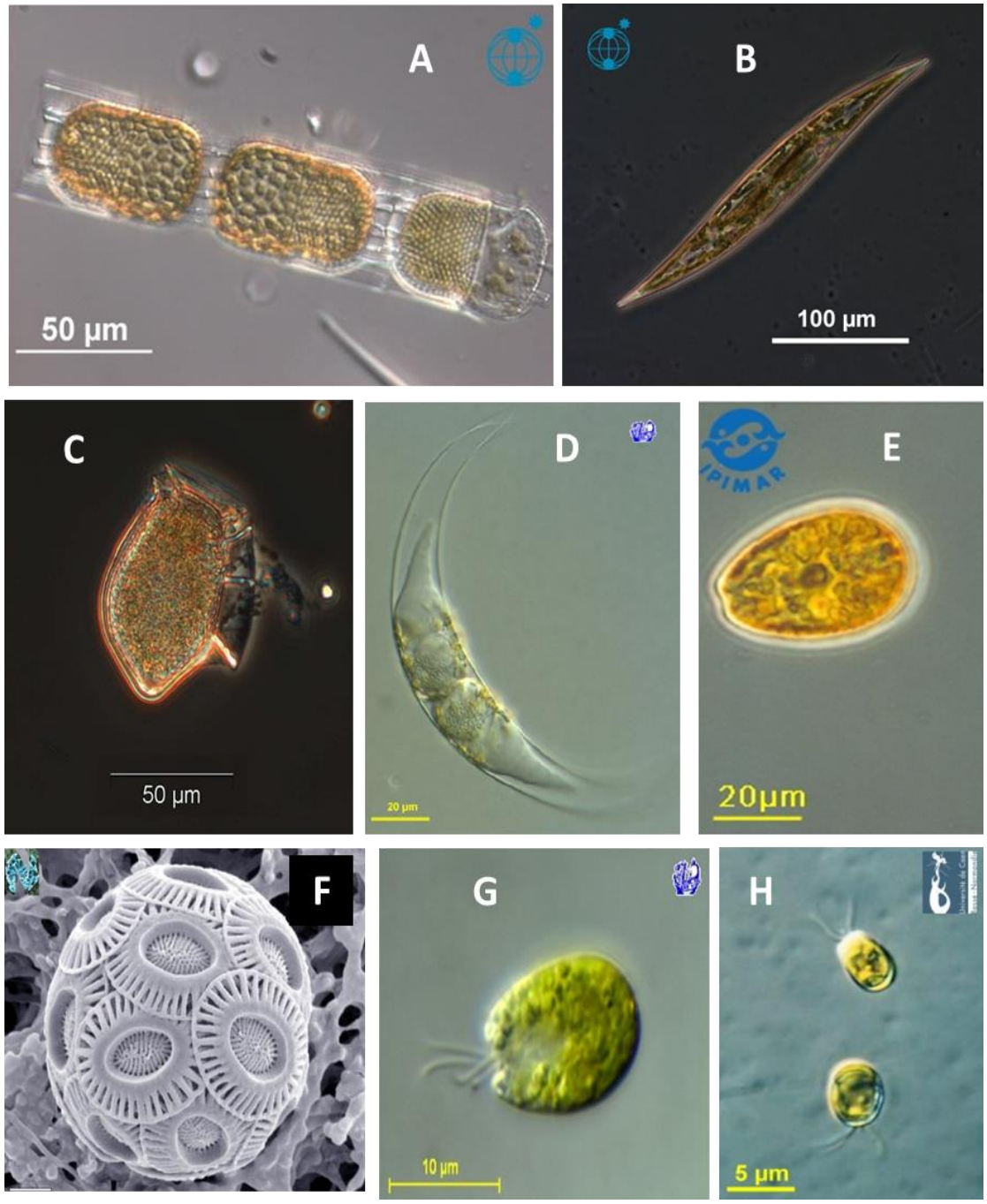

Figure 1.3. The diversity of phytoplankton. Images acquired by light microscopy with the exception of image F acquired by electron scanning microscopy. Images show: (A) chaining cells of *Stephanopyxis turris* (Bacillariophyta), (B) *Pleurosigma* sp. Bacillariophyta), (C) *Dinophysis acuta* (Dinophyta), (D) *Pyrocystis lunula* (Dinophyta), (E) *Prorocentrum lima* (Dinophyta), *Emiliania huxleyi* (Haptophyta), (G) *Isochrysis galbana* (Haptophyta), (H) *Micromonas pusilla* (Prasinophyceae). All images acquired from http://planktonnet.awi.de accessed 06/05/2013.

These cells were the first organisms to release oxygen into the Earth's atmosphere and form the evolutionary origins of the complex array of land plants seen today (Lewis & McCourt 2004). New species from all groups are still being discovered, with little known about the taxonomy and systematics of many divisions and genera (Massana et al. 2004; Medlin et al. 2006; Moon-van der Staay et al. 2001; Simon et al. 2009). A brief description of some of the principal phytoplankton groups follows, with an overview of their diversity of form provided in Figure 1.3.

1.3.1. Diatoms (Bacillariophyta)

The diatoms are a major lineage within the phytoplankton, contributing approximately 40% of all species described to date (Simon et al. 2009). Each cell is contained within a silica frustule which can range in size from 5-200 µm and span volumes over nine orders of magnitude (Jeffrey and Vesk 2005; Leblanc et al. 2012). Each frustule is composed of two halves (valves), containing pores, or straie. The diatoms are subdivided into two groups on the basis of whether cells exhibit radial or pennate symmetry (Hasle et al. 1997; Simon et al. 2009). Pennate diatoms are capable of limited gliding movements through secretion of mucilaginous polysaccharides from longitudinal slits along the valve midline (Round et al. 2007; Hoppenrath et al. 2009; Simon et al. 2009). They exist as solitary cells, but often form long chains or dense colonies of individuals (Simon et al. 2009). Diatoms exhibit very rapid growth rates under favourable conditions and often form dense blooms when nutrient, light and temperature conditions are optimal (Round et al. 2007). Maximum *in-situ* doubling rates for diatoms are generally between 2 and 4 day^{-1} (Furnas 1990), although *Skeletonema costatum* has been known to double at a rate of 5.9 day^{-1} (Furnas 1982). In comparison, growth rates for dinoflagellates, microflagellates and non-motile eukaryotic species are ≤ 2.5 day^{-1} (Furnas 1990). However the absolute requirement of diatoms for dissolved silicon (used in cell wall construction) means populations can crash rapidly when silicate supplies become limited. This pre-requisite controls diatom abundance in the open ocean where silicate levels are often low. The high density of siliceous cell walls also makes

diatoms more prone to sinking: cells are rapidly lost from surface waters without turbulence provided by winds, currents or convection. Some cells possess adaptations which may promote suspension, in the form of long spines or horns (Round et al. 2007). These structures may also serve to discourage grazers and increase the surface to volume ratio of the cell. As with all phytoplankton, the primary photosynthetic pigment of the diatoms is chlorophyll *a*, supplemented by characteristic secondary carotenoid pigments, principally β-carotene, diatoxanthin, diadinoxanthin and fucoxanthin (Round et al. 2007).

1.3.2. Dinoflagellates (Dinophyta)

The dinoflagellates are a genetically distinct division of the phytoplankton, with approximately 1200 described species (Gomez 2012). They are mostly unicellular, and range in size from 5-200 µm (Jeffrey & Vesk 2005). Each cell is divided into two halves by a transverse groove, containing a flagellum which is used to produce rotational movement of the cell. A second flagellum runs longitudinally towards the bottom of the cell and provides forward propulsion (Fenchel 2001, Simon et al. 2009). This physiology allows cells some control over their position within the water column; certain species are known to exhibit diel vertical migration patterns (Hackett et al. 2004). Cells within this group may be armoured (thecate) or unarmoured (athecate), a division based on cell wall covering. Some species have cellulose plates arranged in species specific patterns, with an array of pores, spines, ridges and protuberances, whilst in others these are much reduced or missing entirely (Hackett et al. 2004). Whilst phytoplankton are often described as photoautotrophs, dinoflagellates challenge this definition. Cells within this group are nutritionally diverse, with roughly only half of all species acquiring energy from sunlight alone (Hackett et al. 2004, Gomez 2012). Photosynthetic species contain the major accessory pigments peridinin, dinoxanthin, and diadinoxanthin which give dinoflagellates cells their typical golden brown colour (Jeffrey & Vesk 2005). However many are mixotrophic: species within the genus *Dinophysis* for example, possess chloroplasts but also acquire energy through ingestion of ciliates, bacteria, and other

phytoplankton (Hasle et al. 1997, Palsson & Graneli 2004, Gomez 2012). These individuals blur the boundaries between phyto- and zooplankton, playing dual roles in marine ecosystems as both primary producers and heterotrophic consumers (Qiu et al. 2011). This trophic mode diversity extends to other dinoflagellate genera, where examples of symbiotic, parasitic and kleptoplastidic variations can be found (Hasle et al. 1997, Hackett et al. 2004). Dinoflagellate species, alongside certain diatom species, are also known to form harmful algal blooms (HAB), which pose threats to ecosystem health. This occurs indirectly, through aggregation of cells in the gills of organisms causing physical clogging, or via oxygen depletion when blooms sink and decomposing cells cause anoxia and suffocation of trapped organisms (Ghosal et al. 2000). Direct impacts occur through the production of toxins dangerous to humans as well as marine mammals, fish, seabirds and other components of the marine food chain (Smayda 1997, Van Dolah 2000). Approximately 80% of all toxic phytoplankton species are found within the dinoflagellates (Cembella 2003). Problems arise when toxins accumulate in species of filter feeding shellfish: these can build to levels lethal to humans or other consumers (Shumway 1989) producing paralytic, diarrhetic or neurotoxic shellfish poisoning syndromes (Hackett et al. 2004).

1.3.3. Golden brown flagellates (Haptophyta, Chrysophyta)

These mostly unicellular algae are much less well described than the previous two groups. The golden brown flagellates encompass a wide diversity of polyphyletic organisms, spanning a size range of 2-100 μm and occasionally forming colonies (Jeffrey & Vesk 2005; Simon et al. 2009). They exhibit a wide array of pigment composition, motility, and cell wall structure with many mixotrophic or heterotrophic species. Haptophytes possess dual flagella of slightly unequal length between which extends a unique, defining appendage known as a haptonema (Anderson 2004). Whilst superficially similar in appearance to a flagellum, the haptonema differs considerably in both structure and use. Many haptophyte algae are mixotrophic, generally by phagocytosis of organic molecules (Andersen 2004). This microtubule-supported

organelle is used to capture food particles in mixo- and heterotrophic species, but may also be relevant for other less well-documented purposes (Inouye & Kawachi 1994).

Some of the most prominent members of this group are the coccolithophorids. Many species are calcifying with overlapping calcium carbonate scales (coccoliths) covering cells. The coccolithophore species *Emiliania huxleyi* forms large blooms where detached coccoliths give the surface waters where they occur a distinctive milky-white appearance (Hasle et al. 1997, Houdan et al. 2005). These calcified cells are responsible for nearly half of all $CaCO_3$ production (Brownlee & Taylor 2002) and are of further interest due to their synthesis of dimethylsulfoniopropionate (DMSP) (Franklin et al. 2010). This sulfur compound breaks down to form the volatile trace gas dimethyl sulfide (DMS). Once in the atmosphere, DMS undergoes oxidation to produce aerosols which act as cloud condensation nuclei and influence climate and weather patterns (Shaw 1983; Malin et al. 1992). Whilst the majority of scientific interest is focused on the coccolith-bearing "C-stage" *E. huxleyi*, it is interesting to note that this and the alternate non-calcified "N-stage" life cycle phase are not motile (Andersen 2004). Only cells covered in organic scales during the "S-stage" are flagellated and capable of movement (Houdan et al. 2005). Despite intense interest in *E. huxleyi*, very little is currently known on the physiology, ecology and distribution of this motile phase (Houdan et al. 2005).

1.3.4. Green algae (Chlorophyceae, Prasinophyceae)

This group of flagellates consists of small coccoid to ovoid unicells, spanning a size range from 1- 40 µm. Chlorophycean algae are generally found in freshwater environments, however, some species, such as *Scenedesmus* or *Pediastrum* are occasionally encountered in coastal or estuarine waters. Algae within this class exhibit a great array of morphology, including swimming unicells and large colonies (Lewis & McCourt 2004). Motile cells may have two unequal flagella, or a single flagellum emerging from a pit within the cell structure (Hasle et al. 1997, Lewis & McCourt 2004).

Prasinophytes are important bloom-forming marine algae, and can represent a significant proportion of marine planktonic biomass. They are often described as the cells which gave rise to the first green alga, or the ancestral green flagellate (Lewis & McCourt 2004). They display a diverse assortment of relatively simple cellular structures, with one to eight flagellae (Hasle et al. 1997). Cell surfaces are often covered in organic scales, which are used as taxonomic markers between the major groups of prasinophytes (Hasle et al. 1997; Graham and Wilcox 2000). Prasinophyte algae are amongst the smallest of the eukaryotic planktonic marine flagellates. One well known genus is *Ostreococcus*, thought to be the smallest free-living eukaryote found within marine environments (Courties et al. 1994).

1.3.5. Cyanobacteria

Photosynthetic bacteria were the dominant life form on Earth for more than 1.5 billion years, and were the first organisms to release elemental oxygen into the atmosphere (Graham and Wilcox 2000). The evolutionary formation of photosynthetic eukaryotes is thought to be due to the engulfment and co-development of cyanobacterial cells by phagotrophic hosts (Graham & Wilcox 2000). They are the smallest known photosynthetic cells, and were discovered to exist in large numbers within the marine environment only within the last 35 years. The two key marine genera are *Synechococcus* and *Prochlorococcus*, unicellular species less than 1 µm in diameter (Scanlan & West 2002; Jeffrey & Vesk 2005). *Synechococcus* is widely distributed throughout seas and oceans, whilst the range of *Prochlorococcus* is limited to 40˚S to 40˚N latitude (Partensky et al. 1998) and is therefore not present within the North Sea. Each genera is known to have a variety of ecotypes which dominate in different oceanic regions (Johnson et al. 2006). In contrast to the rest of the phytoplankton, they possess no membrane bound sub-cellular organelles; their photosynthetic pigments are free within the cytoplasm (Partensky et al. 1998). *Prochlorococcus* is exceptional within the phytoplankton, as it is the only species known to possess a unique divinyl derivative of chlorophyll *a* as the principal pigment compound (Chisholm et al. 1988). In

Synechococcus, the green of chlorophyll *a* is often masked by carotenoids (e.g. beta carotene) and water soluble accessory pigments such as phycocyanin, allophycocyanin and phycoerythrin (phycobiliproteins) (Jeffrey & Vesk 2005). *Synechococcus* is thought to have an average *in-situ* daily growth rate of approximately 3 doublings day^{-1} (Furnas 1990), however during daylight hours growth rates of up to 6 doublings day^{-1} have been recorded (Waterbury et al. 1986).

1.4. Phytoplankton Functional Types (PFT)

The complex phylogeny of the phytoplankton makes separation of cells into distinct categories difficult. As a consequence, they are often divided into groups which may be independent of species. These groups, or phytoplankton functional types (PFT), are often based on shared biogeochemical properties. Common segregations include nitrogen fixers, coccolithophorids, DMSP producers, mixotrophs and flagellates (Totterdell et al. 1993). As some phytoplankton possess characteristics of multiple categories during different life cycle phases (such as *E. huxleyi* and diatom species which gain and lose flagella), the most appropriate categories of division are highly dependent upon the research question being addressed. One of the simplest parameters by which to divide the phytoplankton is size. This varies widely between cells (Figure 1.4) and can be determined quickly and easily without requiring identification or complex sample processing. Cell size influences many aspects which control phytoplankton abundance and distribution, further increasing its utility as a basis for PFT division. Sieburth et al. (1978) formally divided and assigned titles to the different size fractions of phytoplankton that are still in use today (Table 1.1).

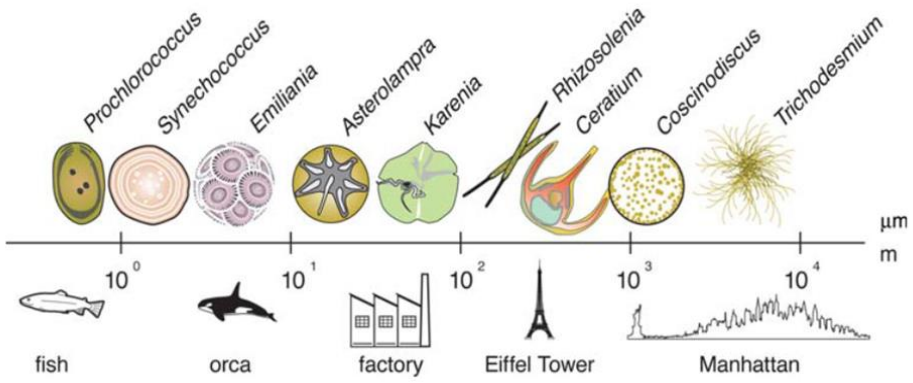

Figure 1.4. A comparison of the size range (maximum linear dimension) of phytoplankton species relative to macroscopic objects (Finkel et al. 2009).

Table 1.1. The classification of phytoplankton according to size (Sieburth et al. 1978).

Maximum linear dimension	*Name*
0.2 – 2 µm	Picophytoplankton
2 – 20 µm	Nanoplankton
20 – 200 µm	Microplankton

The larger cells of the microplankton and nanoplankton include representatives from most phytoplankton groups (Li 2009), whilst the picophytoplankton compose the smallest unicellular eukaryotes and prokaryotic cyanobacteria (Zubkov et al. 2000; Not et al. 2008). These original classifications have undergone some slight revisions for modern scientific use. The word picophytoplankton was originally introduced as an identifying term for bacterioplankton of less than 2 µm. It has since been extended and now includes all photosynthetic organisms within this size range. The upper size limit

definition of this group is subject to some variation within the literature, and varies between either 2 or 3 µm (Li 2002; Calvo-Díaz et al. 2008; Irigoien et al. 2005; Schiaffino et al. 2009). For phytoplankton data collected in the field, 3 µm is generally considered a more practical working threshold, based on the ability of cells to pass through 3 µm pore size filters (Simon et al. 1994; Moon-van der Staay et al. 2001; Not et al. 2008; Vaulot et al. 2008).

1.4.1. PFT distribution

The distribution of phytoplankton is not uniform, but varies over large and small distances and time scales. Phytoplankton density, like weather patterns, exhibits seemingly chaotic dynamics and is influenced by a wide range of conditions and factors. Cell size is a key factor in the ecological and physiological behaviour of phytoplankton, influencing growth and loss of cells and a range of cellular properties. Phytoplankton niches are widely believed to be defined largely by key physiological parameters such as resource acquisition and cell growth, combined with other factors such as resistance to grazing and disease (Margalef 1978). Trade-offs between each of these parameters are used to explain patterns of phytoplankton size distribution across different regions and seasons (Litchman et al. 2007; Jennings et al. 2008; Finkel et al. 2009). Autotrophic phytoplankton cells are dependent on surface area for nutrient uptake and cell cross-section for absorption of sunlight (Cermeño et al. 2006). Increasing cell diameter has two principle effects: the volume of solute exchange decreases due to a thicker diffusion boundary layer (Raven 1998; Agawin et al. 2000) and the quantity of light reaching photosynthetic pigments declines (Cermeño et al. 2006). Small cell size can therefore confer an advantage in resource uptake efficiency and assimilation relative to larger cells (Raven 1998; Beardall et al. 2009). This is clearly beneficial in low nutrient waters, such as in oligotrophic areas of the open ocean where picophytoplankton are observed to dominate both photosynthetic biomass and primary production (Irigoien et al. 2005, Huete-Ortega et al. 2009). These regions also tend to be extremely stratified and reduced diameter is beneficial as smaller cells are less prone to sinking out of the euphotic zone

in calm water (Raven 1998; Ghosal et al. 2000). These environmental conditions do not favour larger and heavier cells, which are reliant on turbulent conditions to remain suspended within reach of sunlight (Smetacek 1999). However larger cells have evolved various strategies compensating for the disadvantages associated with increased size. Diatoms possess vacuoles in which nutrients can be stored, allowing them to proliferate in high nutrient environments and gain a competitive edge over other cells when conditions become less optimal (Cermeño et al. 2006; Maranon et al. 2007; Verdy et al. 2009). Larger cell size, and a propensity to form chains or colonies may infer some protection against grazing (Irigoien et al. 2005), as may increased cell wall thickness (Hamm et al. 2003). Increased volume also alleviates many of the intrinsic difficulties faced by smaller cells. The tiny dimensions of the picophytoplankton make them particularly prone to leakage of accumulated resources and accrue proportionally greater motility costs (Raven 1998). Small cells also risk photo damage to pigments from overexposure to photosynthetic radiation (Raven 1998). These differences in size, and therefore volume and surface area, are thought to control the distribution and high relevance of picophytoplankton in the oligotrophic open ocean (Partensky et al. 1999; Veldhuis et al. 2005), and the greater contribution of nano- and microplankton to productivity in well mixed, nutrient-rich coastal waters (Maranon et al. 2007). This is held accountable for lower photosynthetic rates in the pelagic ocean, in comparison to higher productivity in coastal regions (Agawin et al. 2000, Maranon et al. 2007).

Phytoplankton size distributions also display temporal as well as geographical variability. Within temperate shelf seas the size structure of phytoplankton communities shows seasonal shifts in biomass partitioning, reflecting fluctuations in the abiotic parameters which govern their activities (Not et al. 2007; Schlüter et al. 2012). Throughout the course of a year, two distinct bloom events dominated by larger nano- and microplankton cells are generally observed (Medlin et al. 2006) (Figure 1.5). During spring months, water temperature starts to rise whilst the weather begins to calm. Stabilisation of the water column combined with longer photic periods due to increasing day length cause greater light intensity in the surface waters (Li et al. 2006).

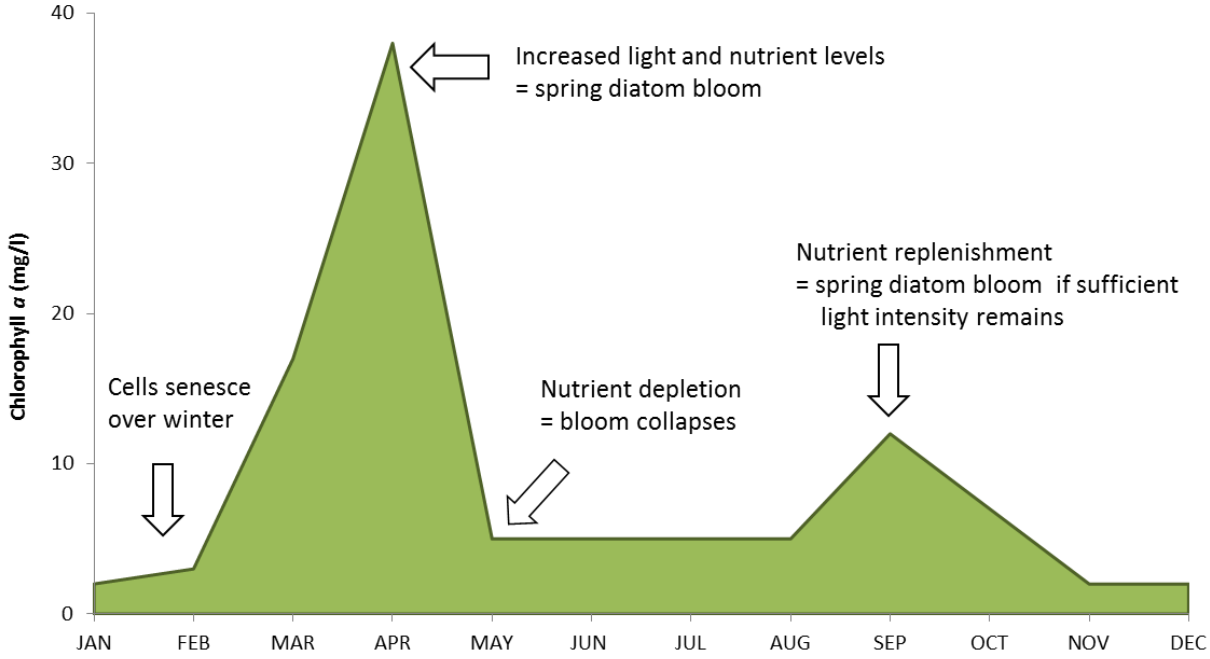

Figure 1.5. Typical annual phytoplankton succession within a temperate marine ecosystem.

Environmental conditions are then optimal for cells to effectively use the nutrients returned to surface waters by winter turbulence (Ghosal et al. 2000, Tillmann & Rick 2003). Rapid phytoplankton growth occurs, dominated by large diatom species and accompanied by small flagellates. Autotrophic biomass can increase by up to three orders of magnitude over a few days, when growth, accumulation and physical advection surpass loss processes such as lysis, sinking and grazing (Irigoien et al. 2005). The exact composition of this spring bloom is determined by the survival of cells through the winter months as the species inoculum in early spring will determine the bloom composition (Colijn and Cadée 2003; Schlüter et al. 2012). The species composition of blooms has great ecological significance. Those dominated by diatoms contribute greatly to global biogeochemical cycles, as these cells have high export: production ratios, caused by increased sedimentation rates through aggregate formation

and inclusion into rapidly-sinking zooplankton faeces (Smetacek 1999, Leblanc et al. 2012). Blooms dominated by haptophytes such as *E. huxleyi* supply significant contributions to DMS production (Liss et al. 1997).

As supplies of essential nutrients (e.g. silica) are exhausted and grazing rates rise, diatom abundance falls rapidly and blooms can collapse as suddenly as they appeared (Hasle et al. 1997; Ducklow et al. 2001; Rousseau et al. 2002). Populations are generally low during summer stratification of the water column, and consist principally of nanoplankton, in particular dinoflagellates (Tillmann & Rick 2003). Cell abundance may increase again during late summer or early autumn, as turbulence causes upwelling events and replenishment of nutrients within the surface layers. Whilst sufficient light intensity remains, a smaller, secondary bloom of diatoms may re-occur (Litchman et al. 2007; Hoppenrath et al. 2009).

This established model of succession accounts principally for the larger species of the nano and microplankton, as a wealth of information on their distribution and productivity is available (e.g. Hasle et al. 1997; Li and Dickie 2001; Falkowski et al. 2004). In comparison much less is known about picophytoplankton within coastal waters, despite increasing evidence indicating their significant contributions to primary productivity (Not et al. 2007). This is due to the low number of studies which have included shifts in picophytoplankton populations within time series monitoring (Li & Dickie 2001). The limited datasets available indicate temporal distribution of picophytoplankton may differ to patterns in nano- and microplankton populations. The abundance of picophytoplankton cells within a Mediterranean coastal system remained relatively stable during high environmental variability (Modigh et al. 1996), whilst *Synechococcus* cell abundance in the coastal northwest Atlantic Ocean peaked during late summer then declined to lowest cell numbers during spring (Li & Dickie 2001). These data suggest that much remains to be discovered about the biogeographic patterns of picophytoplankton and the variety of processes that control their global distribution (Martiny et al. 2006).

1.4.2. Picophytoplankton

The picophytoplankton are the smallest component of phytoplankton populations and are present in all major seas and oceans around the globe. This group is dominated by the cyanobacterial genera *Synechococcus* and *Prochlorococcus* (Scanlan & West 2002), but also contains a diverse eukaryotic component with representatives from many algal phyla (Zhu et al. 2005, Kirkham et al. 2013). This functional group represents less than 10% of all marine photosynthetic biomass, but contributes around 40% to annual phytoplankton productivity (Agawin et al. 2000). Picoeukaryotes are often less abundant than cyanobacterial picoplanktonic genera (Bouman et al. 2012), but are generally slightly larger in size (Hasle et al. 1997). They are therefore often responsible for greater portions of biomass and primary production, despite being numerically outnumbered (Morán 2007). Within the picoprokaryotes, *Synechococcus* is found throughout temperate and warmer oceans, but is rare in polar and sub-polar waters (Li et al. 2009). *Prochlorococcus* is thought to have a latitudinal limit of 60° N in the open ocean (Buck et al. 1996), but distribution within coastal areas is less well documented. It has not yet been recorded in brackish or well-mixed waters, is confirmed as absent from both the Celtic Sea and English Channel (Calvo-Díaz 2004; Zubkov et al. 2000) and is therefore unlikely to be present within the North Sea. These two genera are often found to co-occur, with *Synechococcus* more abundant within the surface layers, whilst *Prochlorococcus* extends deeper into the water column (Partensky et al. 1999; Scanlan and West 2002). This vertical partitioning is due to the lower resistance of *Prochlorococcus* to high light intensity and therefore greater viability in the low irradiance conditions found at depth (Agustí 2004). These differences in water column position and geographic distribution indicate that *Prochlorococcus* and *Synechococcus* occupy different optimal niches due to their varying responses to stressful conditions (Agustí 2004, Zwirglmaier et al. 2008).

Picophytoplankton dominate chlorophyll and biomass in stratified, oligotrophic, warmer waters (Agawin et al. 2000, Calvo-Diaz & Moran 2006, Moran 2007), a relationship linked most closely to nutrient concentration (Agawin et al. 2000). The

relative importance of picophytoplanktonic contribution to photosynthetic standing stock negatively correlates with increasing nutrient load and the consequent increase of micro- and nanoplankton biomass dominance (Agawin et al. 2000). In recent studies, the significance of picophytoplankton in more well-mixed, eutrophic, shallower waters has begun to be re-examined (Carrick and Schelske 1997; Calvo-Díaz 2004; Morán 2007). Despite a deficit of applicable data sets, initial indications show this PFT may also be important outside of the stratified open ocean, in more environmentally variable regions. In the southern Bay of Biscay, a marked seasonality in the picophytoplankton has been discovered. Work by Calvo-Diaz et al. (2008) showed the eukaryotic component dominating picophytoplankton productivity between February and May, with cyanobacteria of greater significance in the remaining months. However, a lack of data from sufficiently varying spatial and temporal locations limits the establishment of any general pattern of succession. This is partly due to the relatively recent realisation of the importance of this PFT, and also because of a lack of sufficiently sensitive analysis techniques capable of recording such small cells.

1.5. The microbial loop

Until the 1970s, it was widely believed that only nano- and microplankton were of any great importance within marine ecosystems (Vaulot et al. 2008). Carbon fixation by these phytoplankton supplies particulate organic carbon (POC) for transport throughout food webs, via consumption of these cells by grazing zooplankton, which in turn serve as food for larger organisms (Azam 1998; Fenchel 2008). This classical description of a typical food chain does not include bacteria, as this system was not thought to produce any significant quantities of dissolved organic carbon (DOC). Since this is the major energy source for bacteria, it was assumed they were unimportant in carbon cycling and largely ignored (Azam et al. 1983; Pomeroy et al. 2007). Marine bacteria were also thought to be very sparsely distributed; an idea perpetuated by the use of inefficient observation methods and the low growth rates observed in culture at that time (Azam et al. 1983, Giovannoni et al. 1990, Suttle 2007). Attempts to challenge these perceptions

(Pomeroy 1974) were met with scepticism or dismissal. It was only in the 1980s with the publication of a hugely influential paper by Azam et al. (1983) describing the 'microbial loop' that the paradigm of food webs underpinned solely by larger phytoplankton cells began to shift. The key roles of picophytoplanktonic bacteria and other previously ignored small organisms, such as protozoa and viruses (Suttle 2007), in the flux of organic matter started to become apparent.

The microbial loop describes separate trophic pathways additional to the established classical linear food chain (Figure 1.6). It was discovered that a substantial amount of organic carbon is in fact dissolved and released into seawater via processes such as: bacterial lysis, leakage from phytoplankton cells, sloppy feeding by zooplankton and the excretion of waste products (van den Meersche et al. 2009). This dissolved organic carbon (DOC) is consequently available for bacterial uptake (Fenchel 2008). Bacteria are consumed by heterotrophic flagellates, which are in turn eaten by microzooplankton (Azam et al. 1983), providing an opportunity for carbon to exit the loop and continue along the classical trophic routes (Veldhuis and Kraay 2000; Pomeroy et al. 2007).

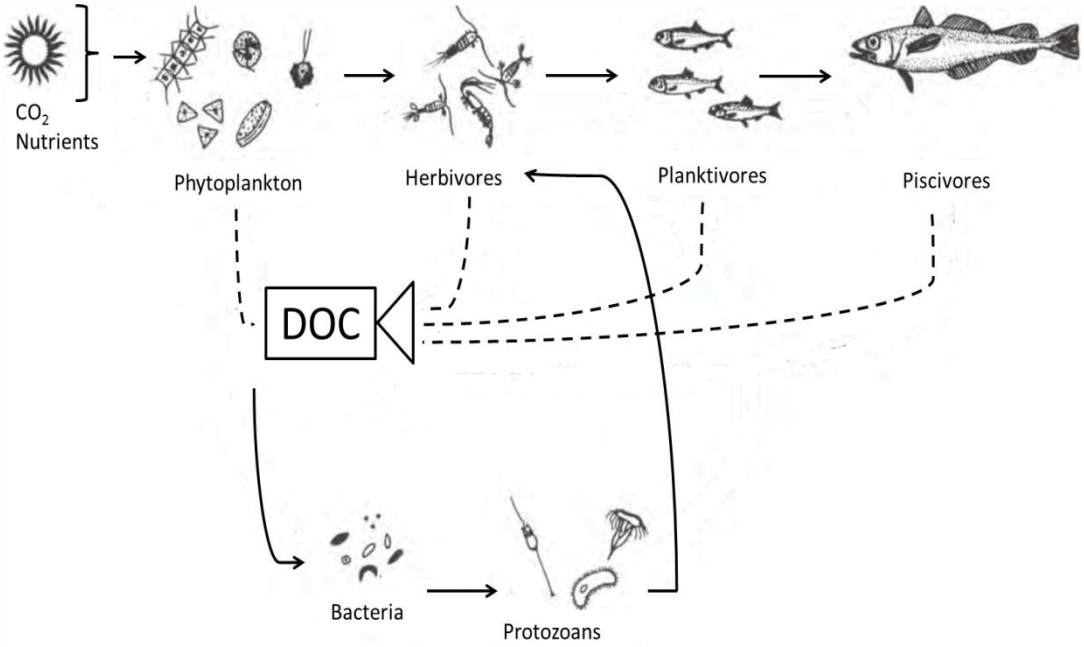

Figure 1.6. Schematic illustration showing the addition of the microbial loop (bacteria and protozoans) to the classical pelagic grazing food chain. Dashed lines indicate the release of dissolved organic material (DOC) as metabolic by-products. Adapted from Lalli and Parsons (2006).

Within the microbial loop, carbon is recycled rapidly, but little is exported to the oceans interior. This is in contrast to the classical food web, characterised by the large-scale transport of particulate organic carbon to the deep ocean via sedimentation of phytoplankton cells, or high-carbon faecal pellets (Froneman et al. 2004). The division of carbon between these two food webs is principally a function of the size structure of the phytoplankton community. Phytoplankton production is generally channelled into the microbial loop in areas populated by small cells, whereas when larger cells are abundant, production drives the more classical food web (Froneman et al. 2004). The picophytoplankton therefore occupy a key position at the base of the food web (Collier 2000) and should be considered of equal importance to the larger cells of the nano- and microplankton.

1.6. Mathematical ecosystem models

The partitioning of phytoplankton biomass across the micro-, nano- and picophytoplankton impacts on many aspects of both primary productivity and carbon cycling (Brewin et al. 2011). Accurate comprehension of phytoplanktonic input to marine ecosystems requires knowledge of the distribution of cells, and therefore carbon, across these groups. Mathematical modelling represents an important tool in gaining understanding on the structure and function of marine communities. Models have been developed for a wide range of applications, from increased comprehension of nutrient fluxes and biogeochemical cycles (Proctor et al. 2003), to those designed to test the potential impacts of eutrophication, aquaculture or harmful algal blooms (Nobre et al. 2005; McGillicuddy 2010; Wild-Allen et al. 2010). However, the representation of phytoplankton within traditional ecosystem models is often very simplistic. Articulation of the distinct roles of varying PFT is normally absent, with all species and sizes aggregated into a catch-all "phytoplankton" category (Anderson 2005; Aumont 2002), despite the diversity of form and function previously described. This is a generalisation referred to as a "black box" within models which do not utilise information on the physiology of phytoplankton to create more dynamic representations of their roles in marine systems (Le Quere et al. 2005; Jardillier et al. 2010).

More modern dynamic green ocean models, such as ERSEM, PlankTOM and PISCES now recognise the importance of separation of the phytoplankton into a range of PFT. ERSEM is one of the more complex lower trophic-level marine ecosystem models currently available. This generic model tracks physiological processes and population dynamics through biomass flux in pelagic and benthic ecosystems (Baretta et al. 1995). The ecosystem is split into functional groups by role (production, consumption and decomposition), and further sub divisions are made based on size and trophic mode. However despite this detail, there remains room for improvement and development of more detailed representations of phytoplankton communities, particularly the picophytoplankton (Jardillier et al. 2010).

1.7. Phytoplankton analysis techniques

1.7.1. Microscopy

The paucity of information on the picophytoplankton in comparison to other PFT is predominantly a factor of their small size. Larger cells can be observed, identified and enumerated by traditional monitoring methods such as the Utermöhl technique (Utermöhl 1931, Paxinos & Mitchell 2000). Water samples are commonly fixed via the addition of Lugol's Iodine or formalin and dispensed into settling chambers, in a volume determined by cell or sediment density (Utermöhl 1931). Phytoplankton are then counted and identified, a laborious and time consuming process largely dependent upon the skill of the analyst (Felip & Catalan 2000, Tillmann & Rick 2003). The large, robust cells of the nano- and microplankton possess recognizable features, facilitating identification to genus, if not species level. In contrast, picophytoplankton cells tend to be morphologically simple and light microscopy generally cannot provide sufficient resolution to resolve species identity (Not et al. 2002). Electron microscopy can provide further details, but is not feasible for high throughput work (Medlin et al. 2006). The preservation of cells necessary for microscopy also creates issues. Chemical fixation can mask chlorophyll fluorescence and dissolve hard structures, leading to cellular distortion (Jeffrey and Vesk 2005). The consequences of preservation on phytoplankton vary widely across species: cells may contort, contract, expand or disappear entirely, depending on their phylogenetic origin and size: effects further complicated by the type of fixatives used and length of storage (Menden-Deuer et al. 2001; Montagnes et al. 1994). However, until relatively recently, there was no other practical means of measuring phytoplankton diversity on a large scale (Azam et al. 1983, Thyssen et al. 2008).

1.7.2. Chlorophyll *a* (chl *a*) and accessory pigments

Data on phytoplankton can also be acquired via measurement of the quantity of chlorophyll *a* within a seawater sample. This photosynthetic compound is universal to

all algal phyla, and consequently it is widely recognized as a valuable indicator of phytoplanktonic biomass (Jeffrey and Mantoura 2005). Measurements of chl *a* are obtained via vacuum filtration of discrete water samples to concentrate cells upon a membrane, followed by mechanical rupture of cell walls and solvent extraction of the chlorophyll within (Aminot and Rey 2000; Jeffrey 2005). The optical properties of the extract are then determined by spectrophotometric or fluorometric analysis to provide a measure of chl *a* content (Bidigare et al. 2005). Conversion factors are applied which permit transformation of chl *a* data into units of carbon allowing phytoplanktonic biomass to be calculated (Riemann et al. 1989; Zubkov et al. 1998; Veldhuis and Kraay 2000). The convenience of acquiring biomass data in this manner has led to chl *a* becoming one of the most commonly measured biochemical parameters in oceanography (Riemann et al. 1989; Jeffrey & Mantoura 2005). Data on *in vivo* chl *a* can also be acquired by the use of *in situ* fluorescence probes, such as those placed on moored buoys (Weston et al. 2008) or within autonomous shipboard monitoring systems, e.g. FerryBox (Brandt & Wirtz 2010) or those deployed manually during research cruises (Röttgers et al. 2007, Garel & Ferreira 2011). Despite the ubiquity of these methods, the biomass estimations they produce only describe bulk phytoplankton contribution; they cannot differentiate by PFT, limiting the use of these data for detailed studies (Toepel et al. 2004).

High Performance Liquid Chromatography (HPLC) analysis of environmental samples is further source of additional information. Water samples are vacuum filtered through glass microfibre filters and the pigments retained by the filter are solvent extracted and analysed by column chromatography (Jeffrey 2005). Liposoluble pigments such as chlorophyll and carotenoids can be detected and quantified in this manner, although watersoluble phycobiliprotein pigments are excluded (Jeffrey 2005). This technique is based on the premise that different phytoplankton groups possess unique marker pigments and therefore phytoplankton communities can be characterised by the presence or absence of certain pigments (Jeffrey et al. 2011). Whilst these can vary amongst cells within a taxon or between taxa, the abundance of diagnostic pigments

generally reflects the major distributions of phytoplankton to the division or class level (Ediger et al. 2006). The data on relative abundances of each pigment produced by HPLC can be quantified by factor analysis and algorithms using specifically designed programs such as CHEMTAX (Mackey et al. 1997), which in turn can be used to generate estimates of the biomass of different groups (Simon et al. 1994, Thyssen et al. 2008, Vaulot et al. 2008).

1.7.3. Coulter counters

A coulter counter is a benchtop machine widely used in phytoplankton research. Developed by Wallace Coulter in the 1950s for medical applications (Shapiro 2004), these instruments operate using the principle that cells surrounded by a lipid membrane are poor conductors of electricity when compared to the saline solutions (seawater or culture media) they are suspended in. In a coulter counter, cells pass in single file through a small opening between two chambers filled with saline. A continuous electrical current is maintained across this aperture and as the cell passes, the electrical impedance increases in an amount proportional to the volume of the cell causing a related increase in the voltage across the opening. Whilst extremely useful in a laboratory setting, coulter counters do not provide a sufficient level of detail for environmental analyses because the necessary distinctions between biological and non-biological particles cannot be made, making accurate quantification of phytoplankton communities impossible.

1.7.4. Flow cytometry

Recent advancements in technology have greatly aided the investigation of phytoplankton, particularly the picophytoplankton (Zhu et al. 2005, Tarran et al. 2006, Marie et al. 2010, Ribalet et al. 2010). Automated flow cytometry was initially designed for use on mammalian cells in biomedical research (Kamentsky 1965), but its

applicability for marine microbial research was soon recognised. A flow cytometer can count and supply reproducible information on the physical and chemical properties of thousands of particles within minutes with no complex sample preparation required (Li 2009; Marie et al. 2005). A peristaltic pump is used to propel a steady stream of seawater into the instrument. The suspended particles within the sample are entrained within a sheath fluid and pumped in single file across the path of a lamp or laser light source (Collier 2000; Marie et al. 2005). The time each takes to pass through the beam and the light scatter produced provide information on cell diameter and structure (Jonker et al. 2000). Flow cytometry is particularly applicable to phytoplankton because of their photosynthetic nature; each cell, without exception, contains a form of the pigment compound chl *a* (Jeffrey 2005). As a phytoplankton cell crosses the laser, this pigment emits a natural strong red fluorescence permitting discrimination of autotrophic cells from debris and sediment (Veldhuis & Kraay 2000). From a combination of these data, it is possible to recognise phytoplankton functional groups present within a sample, and infer conclusions about their composition (Collier 2000; Jonker et al. 2000).

Flow cytometry was first applied to oceanographic data collection in the 1980s (Yentsch & Yentsch 1979, Olson et al. 1983) and was quickly adopted as a valid technique for the analysis of marine microbes (Olson et al. 1985). It is now considered amongst the methods of choice for reproducible measurements of phytoplankton abundance and community structure (Collier 2000). As research activity at this time centred on exploration of the picophytoplankton, this new technology soon yielded advances in this field (Li & Wood 1988, Olson et al. 1990). These tiny cells were shown to exist in the ocean on an unprecedented scale, leading to the discovery of novel genera and species (Pomeroy et al. 2007). *Prochlorococcus* was the first picophytoplankton group to be uncovered by flow cytometry alone (Chisholm et al. 1988). The dim red fluorescence emitted by unique divinyl derivatives of chl *a* and *b*, and its tiny size (0.2 - 0.7 µm), placed it at the edge of cytometric detection limits at that time (Scanlan & West 2002, Jeffrey & Mantoura 2005). Six years later, flow cytometry was responsible for another discovery; this time the smallest eukaryote identified to date, *Ostreococcus tauri*

(Courties et al. 1994). Most recently, flow cytometry was central in the detection of globally distributed unicellular diazotrophs (Zehr et al. 2008).These crucial, yet relatively recent discoveries serve to further illustrate how relatively unexplored the picophytoplankton are as a functional group.

Flow cytometry can also be used to measure phytoplankton biomass. Calibrated light scatter measurements are used to estimate cell size, which can then be used to calculate cell volume. Biomass is determined using empirically derived relationships between cell volume and carbon specific to each functional group (Tillmann and Rick 2003; Menden-Deuer and Lessard 2000; Morán 2007). The first annual picophytoplanktonic carbon to chl *a* ratios calculated using this technique have recently been reported from the Cantabrian Sea (Calvo-Diaz et al. 2008). Flow cytometry is also used in conjunction with fluorochromes, allowing fluorescent labelling of specific cell components. Fluorescent dyes can be used to detect contaminating bacteria or viruses (Marie et al. 1997) or examine enzyme activity (Franklin et al. 2012) or cell viability (Veldhuis et al. 2001). Nucleic acid stains are frequently used to investigate genome size, base pair composition and ploidy within phytoplankton cells (Veldhuis & Kraay 2000). The capability of flow cytometry to collect data on both cell size and DNA content has enabled its use in a more experimental method of phytosynthetic biomass estimation. The positive correlation between genome size and cell size in eukaryotic taxa is well established (Holm-Hansen 1969, Gregory 2001a, Koester et al. 2010). This relationship was first investigated within the phytoplankton using flow cytometry by Veldhuis et al. (1997). Data produced correlated well with cell carbon data derived from other methods, indicating that this technique may supply a useful alternative means of estimating carbon biomass. Furthermore, the ability to rapidly assess genome size within a population which displays apparent morphological constancy may provide useful insights into the mechanisms of speciation (Koester et al. 2010).

The use of flow cytometry to provide large volumes of comparative data on the abundance and distribution of all PFT has enhanced understanding of the seasonal cycles

of nano- and microplankton. It has also provided a tool with which to begin assembling the same depth of knowledge about the picophytoplankton. However, this technique is not without limitations. Problems arise when multiple species possess similar optical characteristics, or when a single species displays a wide range, e.g. cells which are liable to clump or form chains or colonies (Jonker et al. 2000). The vast diversity within and between phytoplankton groups can create issues in inferring taxonomic meaning to flow cytometric output alone (Veldhuis and Kraay 2004). It should also be noted that flow cytometry only provides a snapshot of community diversity. The information gained by analysis of a single sample is enough to give an indication of phytoplankton community composition, but cannot be extrapolated to a population census (Li 1997). The results provided by flow cytometry will also be weighted significantly in favour of the pico- and nanoplankton. This bias is unavoidable, as these small cells are more numerically dominant within the phytoplankton. To attain a more statistically equivalent balance between PFT, greater volumes of water samples need to be analysed in order to counteract lower numbers of large cells in natural assemblages (Li 1997). Problems are also encountered when natural populations occasionally produce parameters which cannot be accurately measured by flow cytometry. Some cells cause light scatter beyond the range measurable by the instrument, e.g. extremely large or highly fluorescent cells cause saturation of the light sensors. Others suffer the converse; electronic detectors may not be sensitive enough to capture very small quantities of light scatter and fluorescence (Li 1997). In efforts to counteract these issues, flow cytometry has undergone many improvements and refinements since its inception for marine use. Instruments have become increasingly sophisticated, with broader detection ranges and greater sensitivity to morphological features (Dubelaar and Gerritzen 2000; Veldhuis and Kraay 2000). With certain types of flow cytometer, it is now possible to acquire an image of each particle analysed (Campbell et al. 2010), or sort them into groups based on size or optical properties (Zubkov et al. 2004). Some models are automated, and capable of continuous analysis whilst submerged under water for weeks at a time (Thyssen et al. 2009); whereas others are equipped with multiple lasers for in depth investigation of multiple pigment fluorescence (Katano & Nakano 2006). Machines are now available

with a range of specifications, dependent on the target population: some focus on a narrow size range (e.g. the Apogee A50-Micro, the Accuri C6 or the BD FACSCalibur), whilst more generalist machines process particles across a large size range (Cytobuoy CytoSense). However, without exception, the resolution and effectiveness of flow cytometric data is greatly increased when combined with additional information sourced from other established techniques.

1.7.5. Molecular analysis techniques

Molecular analyses are powerful taxonomic tools in studies of phytoplankton community structure and an excellent means of gaining genetic information from environmental samples. All eukaryotes contain the 18S ribosomal RNA (rRNA) gene (Guillou et al. 2004). Its transcribed product is used to manufacture ribosomes, meaning there are an abundance of potential hybridisation sites even in the tiny cells of the picophytoplankton (Not et al. 2002; Vaulot et al. 2008). Within this gene are regions of sizeable genetic diversity, alongside others that are evolutionally conserved (Vaulot et al. 2008). This combination of features makes it ideal for investigation of phylogenetic associations, and it forms the basis for an array of genetic analysis techniques (Simon et al. 1988; Fuller et al. 2006; Mary et al. 2006).

Whole cell Fluorescence *In-Situ* Hybridisation (FISH) is an accurate and versatile approach to genetic analysis, widely accepted as a valid technique for investigation of phytoplankton populations (Amann et al. 1995, Gerdts & Luedke 2006, Frada et al. 2006). FISH permits quantitative resolution of the relative abundance of different phylogenetic groups (Mary et al. 2006) through the use of probes selected to detect the presence or absence of features specific to the taxa under investigation (Volpi & Bridger 2008). Probes are labelled with a fluorescent tag then combined with a sample, binding to the area of a chromosome where the complementary sequence is located (Simon et al. 2000). The sample can then be analysed visually for taxa abundance using epifluorescence microscopy (Vaulot et al. 2008). Catalyzed reporter deposition-FISH

(CARD-FISH) offers an alternative to the standardised FISH technique. Assay sensitivity is increased through the use of horseradish peroxidase-labelled oligonucleotide probes, which catalyse the deposition of tyramine molecules and result in fluorescent-signal amplification at the site of the probe hybridisation (Amann & Fuchs 2008). This is advantageous for the detection of microbes such as *Synechococcus* in oligotrophic oceanic environments whose signal may otherwise be below detection levels or lost in high fluorescence background (Pernthaler et al. 2002, Volpi & Bridger 2008).

Denaturing Gel Gradient Electrophoresis (DGGE) is a genetic fingerprinting technique which allows rapid assessment of community diversity within an environmental sample (Mary et al. 2006, Vaulot et al. 2008, Schiayno et al. 2009). The technique is based upon separation of Polymerase Chain Reaction (PCR) generated double stranded DNA in an acrylamide gel (Muyzer & Smalla 1998). As DNA migrates through the gel by electrophoresis, it encounters increasing quantities of denaturing chemicals which alter its structure and slow its progress. This process is sequence dependent, and bands of DNA are deposited at different points across the gel (Muyzer 1999). Each band represents a different DNA sequence and allows the diversity of species within a sample to be calculated. Individual bands can be removed and sequenced for taxonomic affiliation and image analysis software can be used to calculate similarities and relationships between them (Muyzer and Smalla 1998; Mary et al. 2006; Vaulot et al. 2008). However, problems with error and bias in PCR amplifications are well documented: some groups of species amplify much more readily than others and the production of chimeric sequences from complex DNA mixtures is common (Gonzalez et al. 2005; Viprey et al. 2008).

Whilst the data these techniques provide are useful for determining distributions of cultured species, many 18S rRNA sequences recovered do not match those in genetic libraries (Moon-van der Staay et al. 2001, Mary et al. 2006, Vaulot et al. 2008). This is particularly true of picophytoplankton samples, and serves to indicate an extensive range

of species yet to be successfully cultured and formally identified (Shi et al. 2009; Simon et al. 2009).

1.7.6. Remote sensing

An entirely different approach to determining the abundance and distribution of phytoplankton is achieved through use of satellite-based scanners. Measurements of phytoplankton biomass based on chl *a* can be produced via analysis of "ocean colour" (Kroger et al. 2009). Satellite remote sensing is capable of global monitoring of oceanic surface layer ecosystems via measurement of the spectral intensity of radiance reflected from surface waters (Uitz et al. 2006; Kostadinov et al. 2009) which is linked to the concentration of colour producing agents in surface waters (Bratbak et al. 2011).This method of large-scale data acquisition has revolutionised oceanography, offering constant coverage especially valuable for areas that are under sampled or inaccessible by boat. Satellite data have proven extremely useful for surveys of phytoplankton on a synoptic scale, such as monitoring of seasonal cycles, interannual variability and hotspots of phytoplankton productivity (Le Quere et al. 2005, Ribalet et al. 2010). Until relatively recently, remote sensing could not distinguish between the majority of phytoplankton groups (Brewin et al. 2011). However, the development of increasingly advanced bio-optical methods is starting to permit partitioning of marine productivity into contributions by pigment and more recently size-based PFT (Brewin et al. 2010, Uitz et al. 2010, Brotas et al. 2013). Whilst technologically very advanced, this method suffers from reliance on indirect measurements. Satellite data must be retrieved from measurements of irradiance, then undergo further manipulation for conversion into units of carbon or division into PFT (Uitz et al. 2006). This means that final values suffer from the inaccuracies associated with this type of generalised data translation (Brotas et al. 2013). Efforts to address this difficulty are underway, with recent remote sensing work compiling and utilising *in situ* measurements in order to sea-truth data acquired via this method and correct for the inaccuracies in conversion ratios (Li et al. 2013).

1.8. Study area: the North Sea

The North Sea is a small marginal sea of the Atlantic Ocean (Figure 1.7), covering a surface area of approximately 575,000 km^2 between Great Britain and mainland Europe (Otto et al. 1990). It is an epeiric (shelf) sea and is consequently comparatively shallow with an average depth of 74 m (Otto et al. 1990).

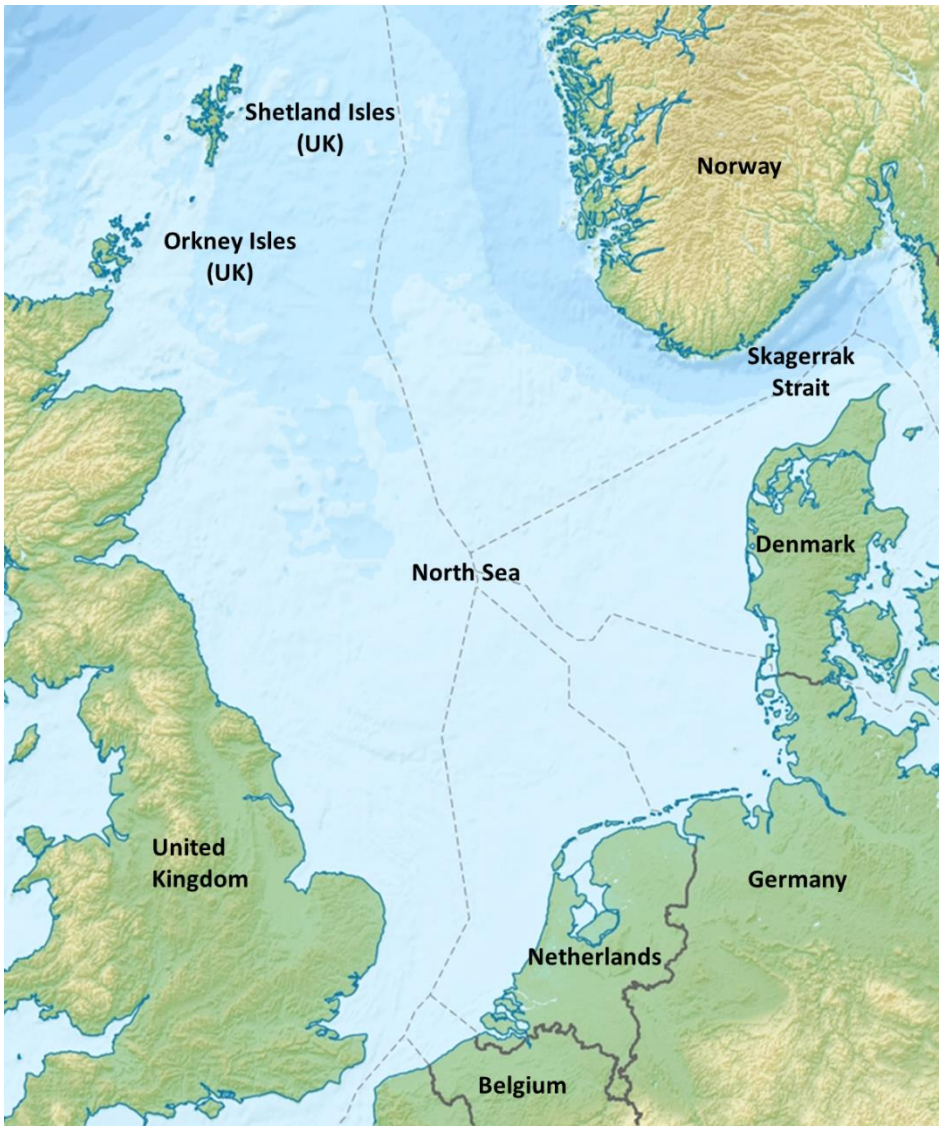

Figure 1.7. The North Sea and surrounding European countries.

The Norwegian Trench is approximately 30 km wide and runs parallel to the Norwegian shoreline from Bergen to Olso; and in this region maximum depth exceeds 700 m (Otto et al. 1990).The Dogger Bank is an area of extremely shallow water in the southern North Sea, caused by a glacial moraine which rises to 15-30 m below the surface (Veenstra 1965). Average water temperatures range between 17 °C in summer months to 6 °C in winter, whilst salinity averages between 34 to 35 grams of salt per litre of water (Janssen et al. 1999). Water flow within the North Sea is generally in an anti-clockwise direction, with water currents entering from the Atlantic Ocean to the northwest and weaker warmer waters currents from the English Channel to the south.

The North Sea is a productive region, supporting a large European trawler fishery industry and commercial harvesting of demersal species including cod, haddock, herring, mackerel, plaice and sole (Reid & Edwards 2001); however continued overfishing has led to substantial declines within this industry, particularly over the last two decades (Kerby et al. 2012). The coastlines of the North Sea form important migratory stopovers and breeding grounds (Bourne 1983), whilst many species of pinnipeds and cetaceans are found throughout the region (Boran et al. 2003). This area is also rich in energy resources, with many oil and gas platforms present throughout the North Sea (Seljom & Rosenberg 2011), and the on-going construction of offshore wind farms along the eastern coast of the UK (Gee 2010). More recently North Sea wave or tidal power has undergone development as a further source of renewable energy (Schillings et al. 2012). As a consequence of the many anthropogenic activities within the North Sea, the region is extremely busy, with high volumes of marine traffic particularly due to the presence of major shipping lanes providing access to the large European container ports located at Rotterdam and Antwerp in the Netherlands, Bremerhaven in Germany and Felixstowe in the UK.

1.9. Project rationale and primary research objectives

It is apparent that to improve understanding of phytoplankton community structure and dynamics, all three constituent size fractions should be studied in detail and on a broad geographic scale. The information provided by investigative techniques both new and old can be combined to produce a more thorough picture of the relationships between primary productivity, carbon cycling and phytoplankton community structure over a massive scale. Mathematical models are increasingly utilised in the study of marine pelagic systems as large quantities of data collected by multiple methods can be collated to create representations of the interactions between functional groups and trophic levels. Data on key traits such as cell size are ideally suited to mathematical modelling, as they possess reliably scalable properties which can be used to predict the effects of future change in environmental or biological conditions (Finkel et al. 2009). The more data that are supplied to these models, the more rigorous they become, increasing their relevance to oceanic ecological systems (Scanlan and West 2002; Le Quere et al. 2005). Flow cytometry is an appropriate technique for modelling purposes as large amounts of high quality data on the PFT present within phytoplankton communities can be collected with relative ease.

This research aimed to assess and document the natural variability of phytoplankton populations within North Sea waters, focusing specifically on the contributions of the micro-, nano- and picophytoplankton functional types. This project presented an opportunity to continue development of knowledge on picophytoplankton ecology outside of typical oligotrophic open ocean studies. Research focused on the determination of picophytoplankton abundance in higher nutrient regimes and regions of environmental variability such as coastal areas is not widespread. In order to broaden our understanding, investigation into both the species composition and population numbers of this functional group is required. However, the picophytoplankton cannot be studied in isolation. Both the nano- and microplankton fractions must be observed simultaneously for any significant conclusions to be drawn. Data must be collected over yearly timescales, in order to identify seasonal cyclical trends present within

picophytoplankton distribution, similar to those observed in larger cells. This work was expanded to uncover the contribution of picophytoplankton to standing stocks of carbon biomass, and extrapolated to determine their contribution to primary productivity, and subsequent ecosystem importance. The findings of this research were linked to prevailing biological and physical parameters within sample collection areas in an effort to better comprehend phytoplankton ecosystem function, and to discover macroecological patterns. This project built upon the foundations laid by research conducted by Calvo-Diaz (2004, 2006, 2008) and Moran (2007, 2009) amongst others. This was an opportunity to examine their overall conclusions that the picophytoplankton may be of greater significance to phytoplankton primary production in more eutrophic coastal regions than previously imagined. The research conducted for this thesis can be divided into three parts focusing on the three major objectives described below:

Objective 1: *Spatial investigation of PFT through participation in the Cefas International Beam Trawl Survey Research Cruise, August 2010 (Chapter 3).*

- On board flow cytometric analysis of phytoplankton community structure across the North Sea during August 2010, supplemented with HPLC and remote sensing data.
- Assess biomass partitioning and chl *a* contribution of PFT, inclusive of picophytoplankton cells.
- Determine whether the data acquired fits with existing ecological theory dictating reduced phytoplankton community biomass at this time of year.
- Uncover and map any contribution of picophytoplankton to phytoplankton community biomass within the North Sea.
- Correlate patterns in PFT distribution and abundance to prevailing environmental conditions.

Objective 2: *Temporal investigation of PFT in the Wash estuary (UK) from 2010-2012 (Chapter 4).*

- Monthly flow cytometric analysis of phytoplankton communities within the Wash estuary over a two year period, supplemented with data acquired by HPLC analysis.
- Assess seasonal fluxes in biomass partitioning and chlorophyll *a* contribution of all three PFT over a three year period.
- Investigate the relevance of picophytoplankton in a well-mixed eutrophic environment.
- Track seasonal fluctuations in diversity and biomass partitioning and relate to prevailing environmental conditions
- Relate to existing ecological conjecture on seasonal succession.

Objective 3: *Advancement of flow cytometric techniques for phytoplankton analysis through development of an environmental DNA staining protocol (Chapter 5).*

- Develop a DNA staining technique effective across PFT encountered within the North Sea environment.
- Application of the staining technique for flow cytometric analysis of phytoplankton DNA content in cultured and environmental phytoplankton populations.
- Conversion of acquired DNA data to units of carbon, in order to supply an alternative to chl *a* in phytoplankton biomass estimation.

The research conclusions of each objective were brought together in final synthesis chapter to provide overall conclusions on the variability of all three sized based PFT within North Sea ecosystems. The key role of flow cytometry in attaining these data was

also discussed, with provision of further details on the potential of this technique for supplying greater insight in phytoplankton community structure.

Chapter 2 General methodology

In this chapter I describe the methodology applied to the investigation of my research objectives, including phytoplankton culturing and environmental sampling techniques, and the instruments used for their analysis. A detailed description of the assessment and optimisation of methods of phytoplankton DNA quantification via flow cytometry is presented in Chapter 5.

2.1. Phytoplankton culturing techniques

Phytoplankton strains were ordered from the National Centre for Marine Algae and Microbiota (NCMA), the Roscoff Culture Collection (RCC) and the Culture Collection of Algae and Protozoa (CCAP). *Stephanopyxis turris* was isolated by Dr. Veronique Creach at the Centre for Environment, Fisheries and Aquaculture Science (Cefas). Strains representative of North Sea phytoplankton populations were chosen, and characterise a diverse array of species each with specific requirements for growth. A list of species used and their culture media is presented in Table 2.1. Cultures were maintained in an incubator (MLR-351 Plant Growth Chamber, Sanyo, Loughborough, UK) at 17 °C with fluorescent light supplied on a 12 h light: 12 h dark cycle, at 40-50 µEin $m^{-2}s^{-1}$ light intensity. Each strain was grown in batch culture, using Erlenmeyer flasks of 100 ml or 250 ml volume. These were filled to approximately one third of the total volume with media, and capped with cotton-filled muslin bungs. Cultures were transferred approximately every 14 days to maintain growth. Cells were harvested in exponential phase to maximise numbers and reduce bacterial contamination. All manipulation of phytoplankton cultures was conducted within a Class II biohazard safety cabinet (ESCO Airstream, UK). Prior to use, the cabinet was cleaned with biocide to ensure sterility. All glassware and culture media were autoclaved at 120 ºC for 20 minutes before use.

Table 2.1. Phytoplankton species maintained in culture. Details include their full names, strain codes, origin, and culture medium

Domain	Class	Species	Strain	Origin	Medium
Prokarya	Cyanophyceae	*Synechococcus*	2370	NCMA	SN
Eukarya	Prymnesiophyceae	*Isochrysis galbana*	927/1	CCAP	f/2
	Prymnesiophyceae	*Emiliania huxylei*	1229	RCC	K
	Eustigmatophycea	*Nannochloropsis salina*	849/6	CCAP	f/2
	Prasinophyceae	*Micromonas pusilla*	1965/4	CCAP	f/2
	Chlorophyceae	*Tetraselmis suecica*	66/22A	CCAP	f/2
	Dinophyceae	*Amphidinium carterae*	1102/5	CCAP	L1
	Dinophyceae	*Prorocentrum minimum*	1136/16	CCAP	L1
	Dinophyceae	*Pyrocystis lunula*	1131/1	CCAP	L1
	Bacillariophyceae	*Amphora coffeaeformis*	1086/19	CCAP	f/2+Si
	Bacillariophyceae	*Thalassiosira punctigera*	1085/18	CCAP	f/2+Si
	Bacillariophyceae	*Thalassiosira weissflogii*	01/12	CCAP	f/2+Si
	Bacillariophyceae	*Stephanopyxis turris*	C001	Cefas	f/2+Si

2.1.1. Media preparation

Media were prepared from enriched seawater obtained from open water during Cefas research cruises. Natural seawater was kept dark at 4 ºC until required, then filtered through a 0.2 µm pore size cellulose acetate filter to remove contaminating organisms and particles before autoclaving. Further nutrients were added aseptically after cooling. The medium used for each species was in accordance with instruction from the supplying institute. For each medium, the required stock solutions were autoclaved or sterile filtered, then combined aseptically with seawater to create the final medium. The pH was adjusted to 8 with 1M NaOH or HCl, although this was rarely necessary. Stock solutions were stored at 4 ºC.

2.1.1.1. f/2 + Si medium

This is a commonly used medium in phytoplankton culture maintenance, containing macro- and micronutrients sufficient for the growth and long-term maintenance of most phytoplankton species (Guillard & Ryther 1962, Guillard 1975). Silicate is required only by diatoms and it is therefore excluded from this formula when f/2 is used for other

phytoplankton groups. The trace metals include elements required by phytoplankton for enzymatic reactions, but which become toxic if present above a threshold, or *trace* concentration (Reynolds 2006). The trace elements and vitamin stock solutions are prepared using distilled water (Table 2.2). Aliquots from each are added to autoclaved natural filtered seawater with the additional compounds shown in Table 2.2 to produce a final medium volume of 1 l.

Table 2.2. Components of f/2 medium. The proportions are listed for the stock solution preparation, the volume of each solution used in the final medium, and the molar concentration of each compound in the final medium (dH_2O refers to distilled water, FSW is filtered seawater).

Stock solutions	Compounds	g/L dH_2O	Molar concentration in final medium (M)
(1) Trace elements	Na_2EDTA	4.36	1.17×10^{-5}
	$FeCl_3.6H_20$	3.15	1.17×10^{-5}
	$CuSO_4.5h_2O$	0.01	3.93×10^{-8}
	$ZnSO_4.7H_2O$	0.022	7.65×10^{-8}
	$CoCl_2.6H_20$	0.01	4.20×10^{-8}
	$MnCl_2.4H_2O$	0.18	9.10×10^{-7}
	$NaMO_4.2H_2O$	0.006	2.60×10^{-8}
(2) Vitamin mix	Cyanocobalamin (Vitamin B_{12})	0.0005	3.69×10^{-10}
	Thiamine HCl (Vitamin B_1)	0.1	2.96×10^{-7}
	Biotin	0.0005	2.05×10^{-9}
		g/L or ml/L FSW	
f/2 + Si medium	$NaNO_3$	0.075	8.82×10^{-4}
	$NaH_2PO_4.2H_2O$	0.00565	3.62×10^{-5}
	$Na_2SiO_3.9H_2O$	30	1.06×1^{-4}
	With:		
	(1) Trace elements stock solution	1.0 ml	-
	(2) Vitamin mix stock solution	1.0 ml	-

2.1.1.2. L1 medium

This medium is commonly used in the growth of dinoflagellate species (Guillard & Hargraves 1993). L1 medium is based on the recipe for f/2, but differs in the addition of supplementary trace elements. Selenium, nickel, vanadium and chromium were added as

these elements are required for enzymatic reactions in certain dinoflagellate species. The vitamin mix and final medium stock were made using a modified version of the f/2 recipe described in section 2.1.1.1. Sodium metasilicate was excluded and the f/2 trace elements stock solution was replaced with the enhanced L1 stock given in Table 2.3. The final medium was made up to 1 l using autoclaved natural filtered seawater.

Table 2.3. Components of L1 medium. The proportions listed are for the trace element stock solution preparation (dH2O means distilled water).

Stock solutions	Compounds	g/L dH_2O	Molar concentration in final medium (M)
(1) Trace elements	Na_2EDTA	4.36	1.17×10^{-5}
	$FeCl_3.6H_20$	3.15	1.17×10^{-5}
	$CuSO_4.5h_2O$	0.01	3.93×10^{-8}
	$ZnSO_4.7H_2O$	0.022	7.65×10^{-8}
	$CoCl_2.6H_20$	0.01	4.20×10^{-8}
	$MnCl_2.4H_2O$	0.18	9.10×10^{-7}
	$NaMO_4.2H_2O$	0.006	2.60×10^{-8}
(2) Vitamin mix	Cyanocobalamin (Vitamin B_{12})	0.0005	3.69×10^{-10}
	Thiamine HCl (Vitamin B_1)	0.1	2.96×10^{-7}
	Biotin	0.0005	2.05×10^{-9}
		g/L or ml/L FSW	
f/2 + Si medium	$NaNO_3$	0.075	8.82×10^{-4}
	$NaH_2PO_4.2H_2O$	0.00565	3.62×10^{-5}
	$Na_2SiO_3.9H_2O$	30	1.06×1^{-4}
	With:		
	(1) Trace elements stock solution	1.0 ml	-
	(2) Vitamin mix stock solution	1.0 ml	-

2.1.1.3. K medium

K medium is designed for the growth of phytoplankton species poisoned by high levels of trace metals (Keller et al. 1978). This medium is similar to f/2 but uses a 10 fold higher EDTA chelation, and excludes sodium metasilicate. Stock solutions were combined as for f/2 (section 2.1.1.1) using the components listed in Table 2.4 and made up to 1 l using autoclaved natural filtered seawater.

2.1.1.4. SN medium

SN medium is specifically for the growth of strains of *Synechococcus* sp. (Waterbury et al. 1986). Stock solutions were made up using distilled water in accordance with the recipe in Table 2.5. These were aseptically combined in 750 ml of autoclaved natural filtered seawater and 235 ml of distilled water, to produce 1l of medium.

Table 2.4. Components of K medium. The proportions are listed for the stock solution preparation, the volume of each solution used in the final medium, and the molar concentration of each compound in the final medium (dH_2O means distilled water, FSW refers to filtered seawater).

Stock solutions	Component	Stock solution g/L dH_2O	Molar concentration in final medium (M)
(1) Trace elements	Na_2EDTA	41.6	1.11×10^{-5}
	$FeCl_3.6H_20$	3.15	1.17×10^{-5}
	$CuSO_4.5H_2O$	0.01	1.0×10^{-8}
	$ZnSO_4.7H_2O$	0.022	8.0×10^{-8}
	$CoCl_2.6H_20$	0.01	5.0×10^{-8}
	$MnCl_2.4H_2O$	0.18	9.0×10^{-7}
	$NaMO_4.2H_2O$	0.006	2.60×10^{-8}
(2) Vitamin mix	Cyanocobalamin (Vitamin B_{12})	0.0005	3.69×10^{-10}
	Thiamine HCl (Vitamin B_1)	0.1	2.96×10^{-7}
	Biotin	0.0005	2.05×10^{-9}
		g/L or ml/L FSW	
(3) K medium	$NaNO_3$	0.075	8.82×10^{-4}
	NH_4Cl	2.67	5×10^{-5}
	Na_2 b-glycerophosphate	0.00565	3.62×10^{-5}
	$Na_2SiO3.9H_20$	15.35	5.04×10^{-4}
	H_2SeO_3	1.29	1.0×10^{-8}
	With:		
	(1) Trace elements stock solution	1.0 ml	-
	(2) Vitamin mix solution	1.0 ml	-

Table 2.5. Stock solution for SN medium. The proportions are listed for the stock solution preparation and the volume of the solution used in the final medium (dH_2O means distilled water).

Stock solutions	Component	Stock solution mg/L or g/L dH_20	Stock solution ml/L FSW/H_20	Molar concentration in final medium (M)
(1) Trace elements	Citric acid. H_2O	6.25	-	3.25×10^{-5}
	Ferric ammonium citrate	6	-	-
	$MnCl_2.4H_2O$	1.4	-	7.08×10^{-6}
	$NaMoO_4.2H_2O$	0.390	-	1.61×10^{-6}
	$ZnSO_4.7H_2O$	0.222	-	7.72×10^{-7}
	$Co(NO_3)_2.6H_20$	0.025	-	8.59×10^{-8}
(2) Vitamin mix	Cyanocobalamin (Vitamin B_{12})	1.0 mg	-	7.38×10^{-10}
	$NaNO_3$	76.5	10 ml	9.0×10^{-3}
	K_2HPO_4 (anhydrous)	15.68	1.0 ml	9.9×10^{-5}
	Na_2EDTA	5.58	1.0 ml	1.5×10^{-5}
	Na_2CO_3	10.7	1.0 ml	1.0×10^{-4}
	With:			
	(1) Trace elements stock solution	-	1.0 ml	-
	(2) Vitamin mix stock solution	-	1.0 ml	-

2.2. Culture sampling

Prior to removal of aliquots, flasks were manually agitated to ensure collection of a homogenous sample representative of the culture. Each flask was gently swirled 2 to 3 times and sampled immediately. Aliquot volume varied depending on the age (and therefore concentration) of the sample, and the removal purpose. For flow cytometry, approximately 3 ml aliquots were taken. This was sufficient to permit multiple analyses, and reduced stress and potential contamination to cultures through repeated disturbance.

2.3. Environmental sampling

Seawater was collected for flow cytometric analysis, and where possible for determination of further biological and chemical parameters to provide environmental

context. These included chl *a* and other pigments, particulate load, nutrients and salinity. The methodology for collection and treatment of these water samples is listed in this section, along with a brief overview of any further laboratory processing required, with the exception of flow cytometry which is described in detail in section 2.4. It should be noted that unless otherwise indicated, all stages beyond sample collection and preparation were conducted by staff at the Cefas nutrients, chemistry or phytoplankton laboratories (Lowestoft, U.K.).

Multiple research vessels were used during data collection for this project, of different sizes and capacities. The R.V. Cefas Endeavour is specifically designed for fisheries and environmental research, and was the largest and best equipped vessel available for use within this project (73 m, capacity for 19 scientific staff). The R.V. Three Counties is a catamaran (18 m, 4 scientific staff) specifically designed for operation in shallow water and was used for data collection within the Wash estuary only. When unavailable, water sampling was performed by the fisheries patrol boat, the ESF Protector III (23.5 m, 4 scientific staff).

Water samples were preferentially collected via 10 l Niskin bottles mounted on a stainless steel framework (rosette), alongside conductivity, temperature and depth (CTD) probes. On smaller vessels, or in rough weather, seawater was collected using a single Niskin bottle mounted on a cable in combination with a mini-CTD data logger. Water was also collected from the continuous seawater supply (unfiltered, from approx. 4 m below surface) of the R.V. Cefas Endeavour when bad weather prevented deck access. In instances where neither of these options was available, a large plastic bucket attached to a length of rope was thrown over the side and allowed to fill with surface water, before being pulled back on board. For each method, water was sampled away from areas disturbed by the vessel's positioning system or engines, to minimise collection of water modified by suspended sediment or oxygenation. Seawater collected for flow cytometry was immediately passed through a 200 µm nylon mesh filter on collection. Water samples for HPLC were also treated in this manner to allow comparison of data.

Filtration removed particles too large to pass through the flow cell of the flow cytometer which may have caused clogging of the machine. Pre-filtration also removed grazing organisms from the sample, limiting cell loss during storage and transport. It is possible that some large phytoplankton cells such as diatom chains or colonies were also removed by this process. Whilst not ideal, this pre-treatment is a common practise in flow cytometry as many machines are restricted by upper size limits.

2.3.1. Chlorophyll determination

The chlorophyll content of seawater was measured by the filtration of a known volume of water through a glass microfibre filter (GF/F). The density of the algal population within the water sample determined the volume filtered. During winter months, cell populations were generally low and as much as 1 l of seawater was filtered in order to produce an accurate reading. However in summer, when cell density increased, the filter became easily clogged. In these conditions, 250 ml was a sufficient filtration volume. Frozen filter papers were returned to the Cefas Nutrients Laboratory, where pigments were extracted in 90% acetone over 18-72 hours at -20°C in the dark. A fluorometer (10AU, Turner Designs U.S.A) was used to excite the extracted sample with a broadband blue light (5-60 blue filter). The resulting fluorescence within the red wavelength (2-64 red filter) was recorded. Fluorescence contributions from phaeopigments were corrected for through acidification of the sample using HCl (1.2 M), converting all chlorophyll to phaeopigments. The sample was re-analysed allowing comparison of the strength of chlorophyll and phaeopigment fluorescence, and permitting calculation of the concentration of each using equations given below:

$$\text{Chl } (\mu g/l) = \left(\frac{F_m}{F_m - 1} \right) \times (F_o - F_a) \times K_\chi \times \left(\frac{vol_{ex}}{vol_{filt}} \right)$$

$$\text{Phaeopigment } (\mu g/l) = \frac{F_m}{F_m - 1} \left(\times [(F_m \quad F_a) - F_o] K_\chi - vol_{ex} \right.$$

Where:

F_m = acidification coefficient (F_o / F_a) for pure chl *a*

F_o = reading before acidification

F_a = reading after acidification

K_χ = calibration factor

vol_{ex} = extraction volume

vol_{filt} = sample volume

A summary of the sampling protocol followed is given below:

The polythene bottle and cap were rinsed thoroughly with the sample seawater twice, and discarded. The bottle was re-filled and labelled with station details.
Samples were filtered immediately or stored in cool dark conditions to avoid chlorophyll breakdown when this was not possible.
The filtration apparatus was rinsed with de-ionised water before use and between samples to avoid contamination. This apparatus was set-up inside, away from direct sunlight and fluorescent lighting.
Forceps were used to place a filter on the glass sinter and the funnel was carefully clamped in place. Care was taken to avoid wrinkling of the filter.

The polythene bottle was inverted twice to homogenise the contents. The measuring cylinder was thoroughly rinsed with some of the sample to remove any contaminating material.

A 250 ml aliquot of the sample was measured out. The pump was turned on (vacuum did not exceed 100 mm Hg) and the sample was poured into the funnel. Further 250 ml aliquots of sample water were added until a sufficient volume was filtered. This was dependent on the time of year and nature of the water body.

The remaining water was passed through the filter. The final filtration volume was recorded. The funnel was unclamped with care taken not to touch the residue collected on the filter.

The filter was folded in half (residue inwards) using forceps, placed on a small square of foil and wrapped. The sample was transferred to a labelled plastic bag and stored at -20°C in a tightly sealed box containing desiccant.

Frozen samples were removed to the Cefas Nutrients Laboratory upon return to shore for further processing. At no point were the filters allowed to defrost. Chlorophyll is labile and will break down in sunlight and fluorescent light. The following protocol was therefore carried out in subdued light. A minimum of two replicates were collected for each sample.

2.3.2. HPLC

Seawater samples for analysis by HPLC were collected using the same equipment and protocol used for chl *a* determination, with the exception that filters were frozen immediately in liquid nitrogen and stored at -80 °C. Upon returning to shore, samples were carefully packed in dry ice and shipped to a specialist laboratory for analysis (DHI Group Laboratory, Denmark). Where possible, replicates were taken of each sample, although these were only analysed when primary samples returned anomalous results, due to the cost of sample transport and processing. Upon arrival at DHI, filters were transferred to vials with 6 ml of 95% acetone with an internal standard (vitamin E).

Samples were extracted at 4 °C for 20 hours, then filtered through 0.2 µm Teflon syringe filter into HPLC vials and placed in the cooling rack of the HPLC (Shimadzu LC-10A HPLC system with LC Solution software). Analyses were performed using the method described by van Heukelem & Thomas (2001).

2.3.3. Nutrient analysis

Measurements of multiple dissolved nutrients (phosphate, silicate, nitrate, nitrite, ammonia and total nitrogen) were acquired from a single seawater sample. Water samples were filtered to remove suspended particles which may influence analytical results and also to reduce the possibility of adsorption of trace constituents onto reactive particles (Kirkwood 1996). However it is possible for filtration to introduce a source of contamination therefore all glassware was thoroughly rinsed with the sample before use to eliminate this source of error. Sample stability was also an important consideration as nutrient concentrations can fluctuate due to the presence of micro-organisms in seawater. As samples collected at sea could not be analysed immediately, they were chemically preserved with mercuric chloride and stored to minimise degradation. A minimum of two replicate samples were collected at each station. Upon return to the laboratory, samples were analysed by the Cefas nutrients laboratory using a continuous flow automated analyser (SKALAR, the Netherlands). A summary of the sampling protocol followed is given below:

The polythene bottle and cap were rinsed thoroughly with the sample seawater twice, and discarded. The bottle was re-filled and labelled with station details.
Samples were filtered immediately or stored in cool dark conditions when this was not possible.
The filtration apparatus was rinsed with de-ionised water before use and between samples to avoid contamination. Using forceps, a filter was placed on the glass sinter and the funnel was carefully clamped in place, avoiding wrinkling of the filter.

The polythene bottle was inverted twice to homogenise the contents. The measuring cylinder was thoroughly rinsed with some of the sample to remove any contaminating material.
A 50 ml aliquot of the sample was measured out. The pump was turned on (vacuum did not exceed 100 mm Hg). The sample was poured into the funnel and an aliquot was allowed to pass through the filtration rig, thoroughly rinsing the filter beaker and collection flask with filtrate. This was then discarded.
100 ml aliquot of sample water was filtered. The resulting filtrate was used to rinse the sample pot and lid before filling the pot to the brim. 0.1 ml of mercuric chloride solution was added to the sample pot to give a final concentration of 20 µg/l mercuric chloride. Samples were stored in cool dark conditions until returned to Cefas for further processing.

2.3.4. Salinity determination

To ensure accuracy, samples collected for salinity analysis were not filtered. Any manipulation exposing the sample to evaporation or dilution invalidates results obtained. Seawater was used to rinse and fill a 200 ml glass bottle, leaving a 10-20 ml headspace. The neck, threads and top of the bottle were dried thoroughly using a tissue and carefully stoppered. Samples were stored in protective travel crates in cool, dark conditions and returned to Cefas upon reaching shore. Salinity was determined via further processing using an 8410 Portasal salinometer (OSIL, U.K.).

2.4. Phytoplankton analysis by flow cytometry

This section describes the inception of flow cytometry and the development of its use within microbial oceanography. I focus on the principles and technology underpinning these instruments, and explain the operational setting and procedures necessary for the

acquisition of robust data. I conclude by providing guidelines for the preparation and analysis of environmental and cultured phytoplankton samples within this study.

2.4.1. Development of flow cytometry

Cytometry can be defined as the process of measuring the physical and chemical characteristics of single biological cells. Flow cytometry is a technique which requires the suspension of cells within a stream of fluid during analysis. The first cytometers began to evolve in the 1930s (Moldovan 1934); early machines were developed in efforts to produce more detailed measurements of tumour cells than those provided by conventional histological staining techniques at that time (Shapiro 2004). Flow cytometers began to appear during the 1950s, when the underlying principles of the hydrodynamic focusing technique that is still in use today were first developed (Crosland-Taylor 1953). Commercial production began in the 1970s, with the release of the ICP 11 machine by Partec, but widespread distribution of flow cytometers within research laboratories did not occur until the 1980s (Shapiro 2003).

A flow cytometer produces measurements similar to those achievable by conventional light or fluorescence microscopy. They provide information on the heterogeneity of cell populations, from mammalian erythrocytes to bacterial communities. Differences in the attributes of these particles are determined by measurements of their optical properties, used to infer detail on cellular structure and content. The popularity and success of flow cytometry over more traditional methods is attributable principally to its speed and automation. All forms of microscopic analysis are time consuming and extremely labour intensive and, as a consequence, only a small percentage of the cells in a sample are typically analysed. Analysis effort is further increased if information beyond simple cell counts is required, such as identification, sizing, or evaluation of stain uptake. Further issues arise in the qualitative nature of microscopy because variability in the skills of analysts combined with an innate risk of human error due to the repetitiveness of the work greatly affect the reproducibility of the

results obtained. Analysis of discrete data (e.g. presence or absence of cells) is relatively straight forward; however problems start to arise when measurements of continuous data are required. For example, accurate and consistent assessment of the fluorescence intensity of stained cells between different samples can be extremely difficult by microscopy. The combination of each of these factors affects the robustness of the data produced, and also confidence in statistical significance.

The analysis of single cells by flow cytometry generates accurate, reproducible, multi-parametric data on individual particles, allowing the heterogeneity of a sample to be quantitatively determined and producing a multidimensional representation of a population. Samples require little or no prior processing, and data are produced rapidly; analysis rates can exceed 1000s of cells per second (Lindström et al. 2002). The reduced labour and increased sampling rate permits greater quantities of a sample to be analysed, further promoting statistical confidence in the data generated, and increasing the likelihood of detecting rare events. Flow cytometers can detect minute variations in fluorescence intensity, removing the subjectivity issues normally associated with the acquisition of this type of data. Flow cytometry therefore provides a powerful tool for high throughput analysis of microbial communities.

2.4.2. Operational principles

Flow cytometers are now widely available, with instruments available for specific objectives such as cell sorting or imaging. However, each operates using the same basic principles and components which can be divided into three main categories: fluidics, optics, and electronics.

2.4.2.1. Fluidics

A blood or water sample contains thousands of different microscopic particles. If these were simply pumped straight through a delivery tube to the measuring point within

a flow cytometer, it is unlikely they would arrive in a reproducible manner. Multiple cells may arrive simultaneously or in a variety of directional planes, making acquisition of coherent data virtually impossible. Narrowing the delivery tube will not resolve the problem, and is likely to create further issues through increased risk of blockages. These problems are overcome by hydrodynamic focusing of the sample stream and the particles within it. The sample is entrained within a larger volume of pressurised, particle-free sheath fluid before being passed through the narrow opening of the flow cell. This constrains cells into a narrow region within the centre of the sample stream (core); forcing them to flow in single file along their longitudinal axis (an effect described as laminar flow). This efficiently delivers each particle one-by-one at fixed speed to the measuring point (Figure 2.1). The flow rate of the sheath fluid is kept constant, whilst the speed of the sample stream can be altered. The difference in pressure between the two liquids is used to control the sample volume flow rate: the greater the differential, the wider the sample core. If the difference in pressure becomes too great, core stability, and therefore laminar flow of particles, will be lost. The diameter of the sample stream is proportional to sample flow rate, but this does not impact velocity of flow within the injector and flow cell.

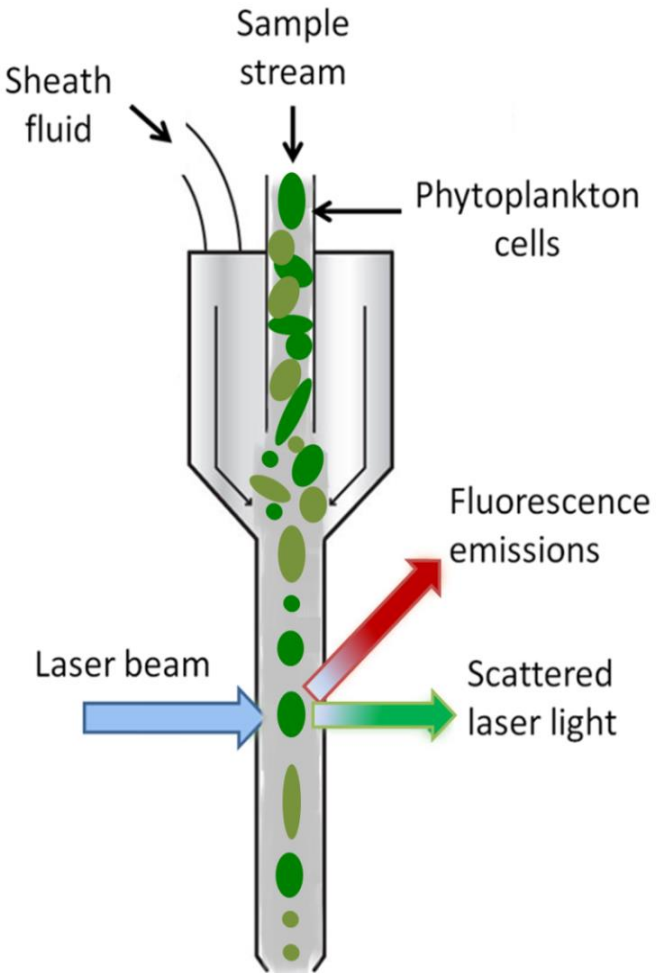

Figure 2.1. Diagram showing the basic principles of particle delivery and analysis within a standard flow cytometer. Adapted from Introduction to Flow Cytometry (http://www.abcam.com/index.html?pageconfig=resource&rid=11446, accessed May 2013).

2.4.2.2. Optics

The measuring point within a flow cytometer consists of a high powered light source, most commonly a laser. Lasers are monochromatic; providing a single coherent wavelength of light with a strong, reliable signal. A 488 nanometre (blue) argon laser is used for many types of analysis, but is particularly suited to investigation of

phytoplankton communities, due to good excitation of chl *a*. Other instruments may be fitted with a 544 nm (green) or 633 nm (red) helium-neon (HeNe) laser, or less frequently mercury or xenon arc lamps which supply a white light source. Modern flow cytometers are commonly fitted with multiple light sources, greatly increasing the scope and flexibility of their analysis capabilities. As a particle passes in front of the light source, it interrupts the beam causing light to be scattered in all directions (Figure 2.2). Light dispersed at a low angle in a forwards direction (along the same axis as the main beam) is called forward scatter (FWS). This light is captured by a FWS detector and its intensity can be used to provide a rough indication of cell size (Figure 2.3). FWS is linearly proportional to cellular cross section only for optically large cells (tens of microns in diameter and/or highly absorbing) and shows fluctuating behaviour at intermediate size. For these reasons, it should not be used as an absolute indicator of cell size. Light scattered at a wide angle to the path of the main beam is termed side scatter (SWS) (Figure 2.2). The strength of this signal is proportional to the amount of cytosolic features of a cell, such as granules or inclusions. SWS may yield the most proportional relationship to particle cross section for particles of low refractive index (sized from 1 µm upwards), but is extremely sensitive to the presence of any small external cellular structures which cause large variations in data. When the information provided by both FWS and SWS is combined, it permits differentiation between cells which might otherwise appear to be a homogenous population. It should be noted that scatter is affected by preservation of cells. Dilution, chemical fixation, staining and cell damage will all cause alterations in light scatter signals.

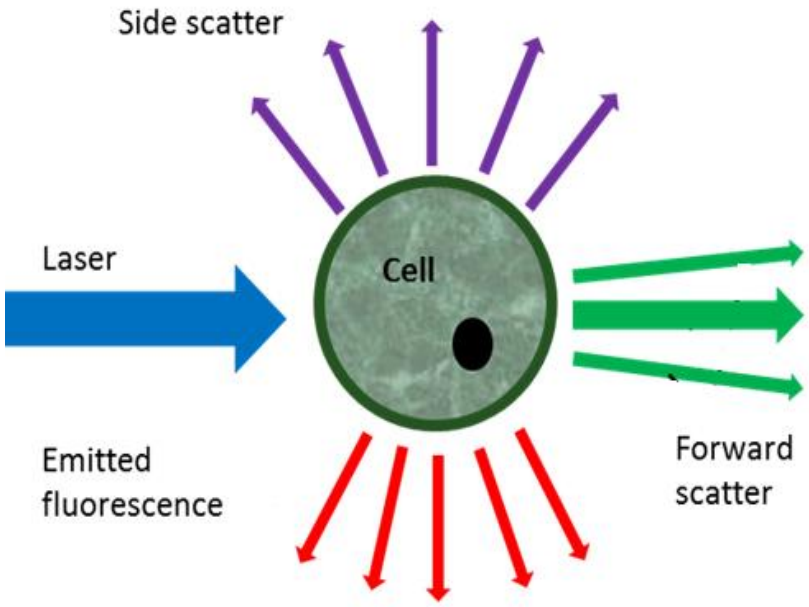

Figure 2.2. Diagram showing light scatter, absorption, and re-emission by a cell crossing the path of a laser beam. Adapted from Shapiro (2010).

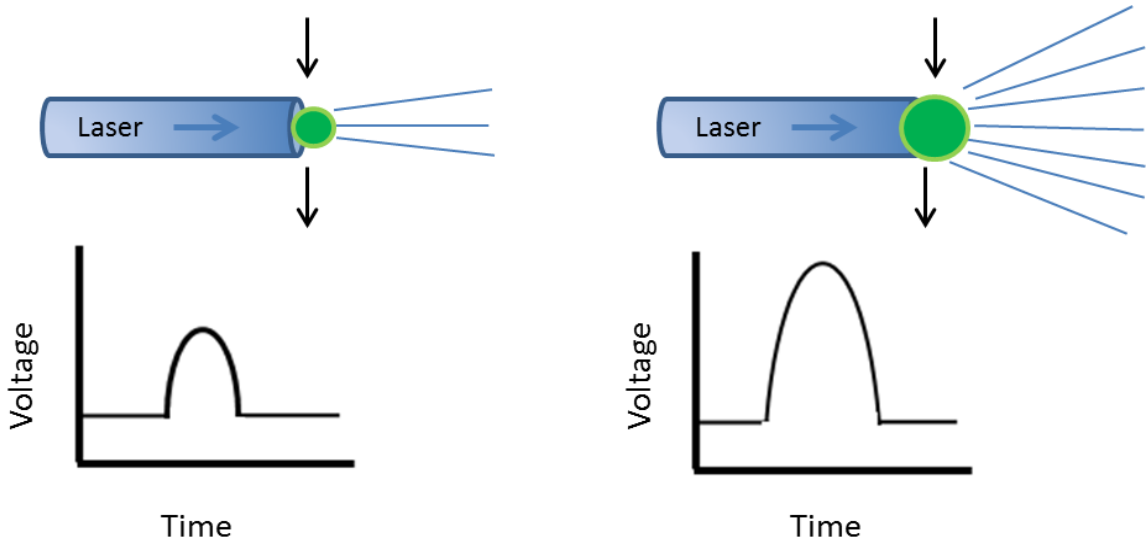

Figure 2.3. Diagram indicating how light scatter intensity from forward scatter provides an indication of cell size.

Interrogation by a light source also provides further information on certain particles. The energy supplied by the beam is absorbed by naturally occurring or artificially added fluorochromes, leading to their excitation. This energy is then released at longer, lower energy wavelengths to the initial beam. The emitted light is channelled through a series of optical filters and lenses and is ultimately collected by photomultiplier tubes (PMT). These are more sensitive than the photodiode detectors used to collect scatter, as the amount of light re-emitted is often very small. Optical filters are required to separate this emitted light and ascertain the intensity of each emitted wavelength independently. Each filter is specially designed to reflect or absorb certain wavelengths of light, whilst permitting others to pass through. A long band pass (BP) filter transmits all wavelengths greater than the specified minimum, whilst a short BP filter allows wavelengths below a pre-determined value to pass. These filters are placed directly in front of each PMT, limiting the specific range of light it can detect, thereby increasing accuracy.

2.4.2.3. Electronics

As each particle passes through the beam of the light source, it creates what is termed a "voltage pulse". More and more light is scattered until the cell is in the centre of the laser (maxima). As the cell leaves the path of the laser, light scatter decreases. After a set amount of time, the window closes until another object scatters enough light, exceeding the threshold for data to be collected. The photons of light which reach each detector or PMT within a flow cytometer are converted to a current and transformed into a digitised value which can then be further processed. A voltage is applied to each detector or PMT, supplying it with electrons. These electrons are then "picked up" by a proportional number of photons of light. As light intensity increases, so does the quantity of photons, resulting in greater uptake of electrons and a larger current output from the detector. The sensitivity of each detector and PMT is controlled by the amount of current supplied to it; as voltage increases the same quantity of photons will have a greater current output. Adjustments to this sensitivity, often referred to as the instrument threshold, define the minimum amount of scatter or fluorescence intensity required to trigger an event which

will be processed by the instruments software. Adjustment of the threshold allows reduction of electronic noise and unwanted, non-target particles; and is generally set on the same parameter used to identify the cells of interest (the trigger) (Gasol & del Giorgio 2000). The voltage pulse produced by a particle is passed through either a linear or log amplifier (dependent on sample type) and converted from analog to discrete digital binary information, producing a listmode file which can ultimately be plotted graphically using specialist software. An array of plots can be produced, but the most common include dot plots, contour plots, density plots and histograms (Figure 2.4). Gating can then be performed on plotted data to isolate subsets of a population of cells, and examine their specific parameters in greater detail.

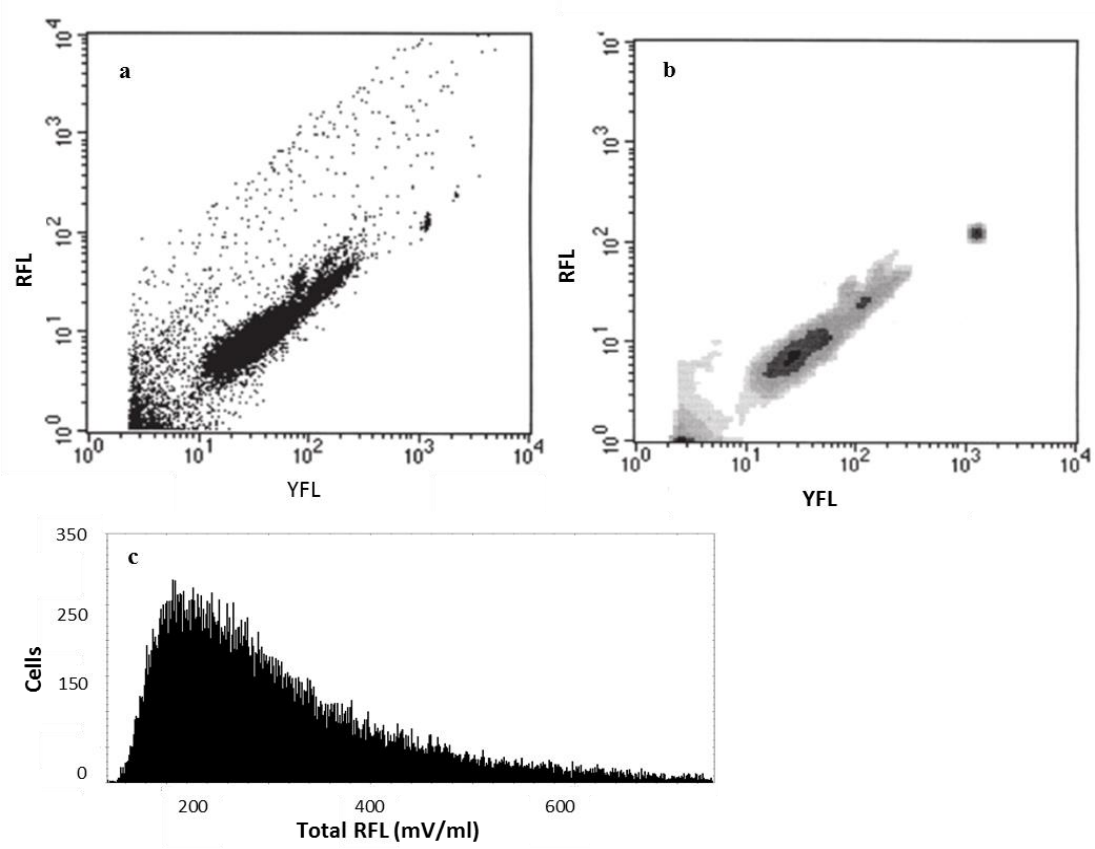

Figure 2.4. Phytoplankton data acquitted by flow cytometry displayed on a) a dot plot; b) a density plot and c) a histogram. Each plot shows either red fluorescence (RFL) or yellow fluorescence (YFL) data.

Phytoplankton data are often acquired using a red fluorescence trigger, which instructs the machine to count only particles with this property which exceed the stated threshold. A freshly inoculated axenic culture of picophytoplanktonic cells will have little background noise, and a low threshold/high sensitivity setting may be used. In contrast, a seawater sample may contain large quantities of debris and dead cells. This will require an increased threshold in order to remove this "noise" and retain focus on the particles of interest.

2.4.3. CytoSense flow cytometer

The CytoSense (CytoBuoy, the Netherlands) flow cytometer is a fixed beam scanning flow cytometer, fitted with a 488 nm blue argon laser. This is a robust and portable machine (cylindrical, approx. 30 cm diameter x 500 cm high) for use in the laboratory or field. The CytoSense differs from other commercial flow cytometers in several key aspects, which made it ideal for use in this research project. Firstly, the CytoSense can analyse particles across the entire size range of phytoplankton allowing particles from 2 to approx. 200 µm to be accurately counted and measured. Many other flow cytometers are restricted in their measurement range: the Accuri C6 for example, is another portable flow cytometer designed for field or laboratory use, but is limited to measurement of particles smaller than 40 µm. Secondly, the CytoSense operates using an internal recirculating sheath fluid system, and unlike many other instruments (e.g. the Becton Dickinson FACScalibur) does not require continuous replenishment and emptying of input and waste tanks. The transport of large quantities of sheath fluid is not necessary and this design also allows the machine to operate without supervision for lengthy periods of analysis. Finally, the CytoSense is also unique in aspects of data output. The multiple data points acquired for each particle are presented as a "pulse shape" alongside the more typical graphical outputs from other machines. The distinct optical signals triggered by each particle and recorded by each PMT and detector are used to produce a profile, much like a fingerprint, which allow the characteristics of each cell to be interpreted at a glance (Figure 2.5). The diatom *Ditylum brightwelli* for example, can be

easily recognised by the distinctive signal produced by its spines and large dual chloroplasts. The optical profiles of cells within different PFT were used throughout this research to increase the ease and speed of PFT delineation and approximate classification. However, pulse-shape analysis was not used to identify cells to species or genus level for two key reasons. Firstly, the accuracy of this technique is dependent upon a library of different pulse-shapes, collected by analysing cultures of known phytoplankton species. Signals from environmental samples are then crosschecked against this pulse-shape archive, allowing species identifications to be made. However, the fluorescence and scatter properties of cultured phytoplankton cells are known to vary with both time and culture conditions. The profile of a cultured species may not necessarily be compable to the profile of its wild counterpart. This issue is further complicated by the often unique specifications of different CytoSense instruments, preventing sharing of accumulated profile libraries between research laboratories. Secondly, the pulse-shape comparison process has not yet been successfully automated. It is extremely time-consuming to compare signals manually, limiting the use of this technique in the analysis of large numbers of cells.

The Cefas CytoSense used throughout this research is fitted with a single 488 nm blue laser, two detectors (for FWS and SWS) and three PMT collecting red (RFL), orange (OFL) and yellow (YFL) fluorescence. The sensitivity of each detector and PMT is adjustable from 0 – 270 mV. The sample intake speed is adjustable from 0.47-9.7 µl/s, allowing effective analysis of a range of cell sizes and concentrations.

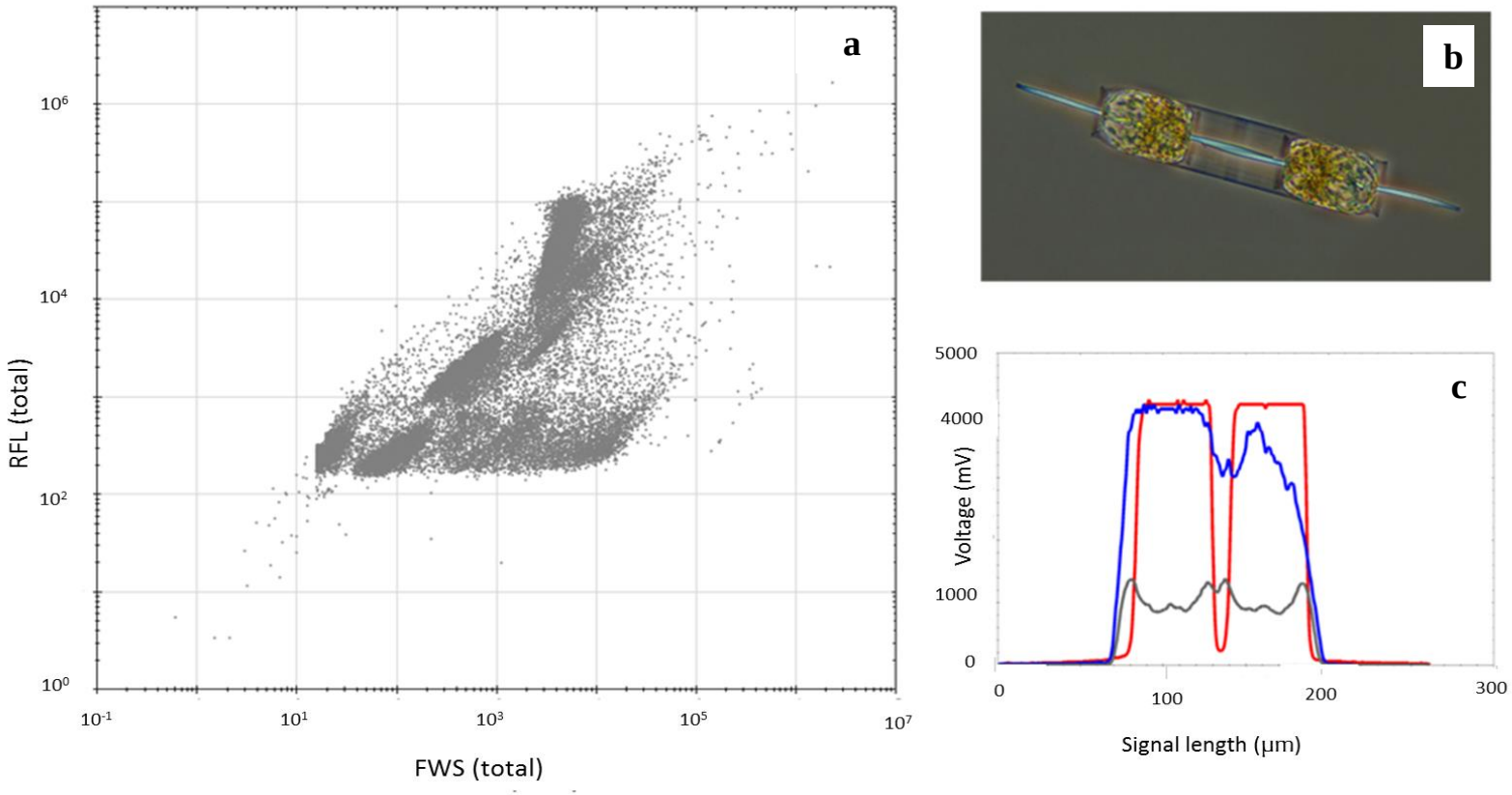

Figure 2.5. Cytoplot of environmental phytoplankton data acquired by the CytoSense (a). Each point on the plot represents a particle. The diatom Ditylum brightwelli (b). The unique pulse shape profile for D. brightwelli (c). Forward scatter (FWS) is represented by the grey line, side scatter (SWS) by the blue, and red fluorescence (RFL) by the red line.

2.4.4. Environmental phytoplankton analysis

Prior to sample analysis, the flow cytometer should be clean and primed with a suitable sheath fluid. It is critical that the sheath fluid used to surround the sample stream is particle free, and of a similar refractive index to the sample stream. For example, during analysis of marine environmental samples, 0.2 µm sterile filtered seawater, or NaCl (35 ppt) should be used. Alternatively, if cells are suspended in a pH neutral buffer, double distilled water is more appropriate. Unless stated, the sheath fluid used throughout this research is 0.2 µm filtered seawater. The CytoSense was powered up and allowed to run at full speed (9.7 µl/s) with the laser off, for at least one hour prior to analysis, to ensure removal of any air bubbles within the system. Data acquisition was performed using CytoUSB v4 (CytoBuoy, the Netherlands).

The seawater sample was homogenised through gentle inversion of the collection bottle, and a 10 ml aliquot was removed to a 40 ml plastic sample pot. This aliquot was briefly examined by eye to check for the presence of high sediment levels, or a bloom, judged by the colour and clarity of the water. If necessary, the sample was diluted with 0.2 µm sterile filtered seawater to prevent clogging of the flow cytometer. Fluorescent or size calibration microspheres were added if required (section 2.4.6.2). A small magnetic flea and stirrer plate were used (minimal rpm), to prevent sedimentation of heavier cells from influencing cell counts. CytoSense acquisition settings were set using a red fluorescence trigger (10 or 25 mV), a flow speed of 4 or 6 µl/s, and an acquisition time of 300 or 600 seconds. The sample inlet tube was placed into the sample, and then flushed through the machine at high speed until the event rate began to rise. The flow rate was then reduced to the acquisition rate, and flushing allowed to continue until the event rate stabilised. Data were then acquired, and on completion, the machine was rinsed using 0.2 µm sterile filtered seawater until the event rate fell below 10 cells per second, indicating the machine was clean.

Within flow cytometry, it is necessary to make compromises between trigger and pump speed as both influence the quality of the data acquired. There are no universal

acquisition settings applicable to every environmental sample due to inherent variation in the cells they contain. For the majority of samples, a red fluorescence trigger set at 25 mV, and a flow rate of 2 µl/s is adequate. However, this is a generalised setting, and requires adjustment depending on the structure of the phytoplankton community present. A high trigger and a fast flow rate will capture more rare events such as very large single cells, but is at the expense of smaller cells below the trigger level which contribute the bulk of the population. Increasing flow rate also impacts upon the stability of the sample stream core, increasing the risk of two particles passing across the laser at the same time (coincidence). Conversely, at lower speeds and trigger levels smaller cells are included, but so are increased levels of noise and debris within the data. Where possible, multiple analyses were performed on the same sample, when sufficient time was available. Data on picophytoplankton were acquired over a short acquisition time (300 seconds) at a red fluorescence trigger of 13 mV and a flow rate of 4 µl/s, whilst microplankton data were preferentially collected at 100 mV at 9.7 µl/s for 1800 seconds.

2.4.5. Treatment of data

The raw datafiles produced by the CytoSense frequently contained large amounts of information irrelevant to the phytoplankton population, such as events caused by debris or microspheres (Figure 2.6). Data files therefore required cleaning and calibration prior to analysis and interpretation. This was achieved using CytoClus v3 data processing software (CytoBuoy, the Netherlands). Each file was opened, and data points displayed in cytoplots. The axes selected depended on the types of cells present, but on most occasions FWS (length) vs. YFL (total) were sufficient to identify microsphere populations. These were gated and removed (cleaned) from the files. Electronic noise and debris were identified using axes of FWS (total) vs. RFL (total), FWS (total) vs. SWS (total), and RFL (total) vs. OFL (total). Unwanted particles were identified using the particle profiler to study pulse shape.

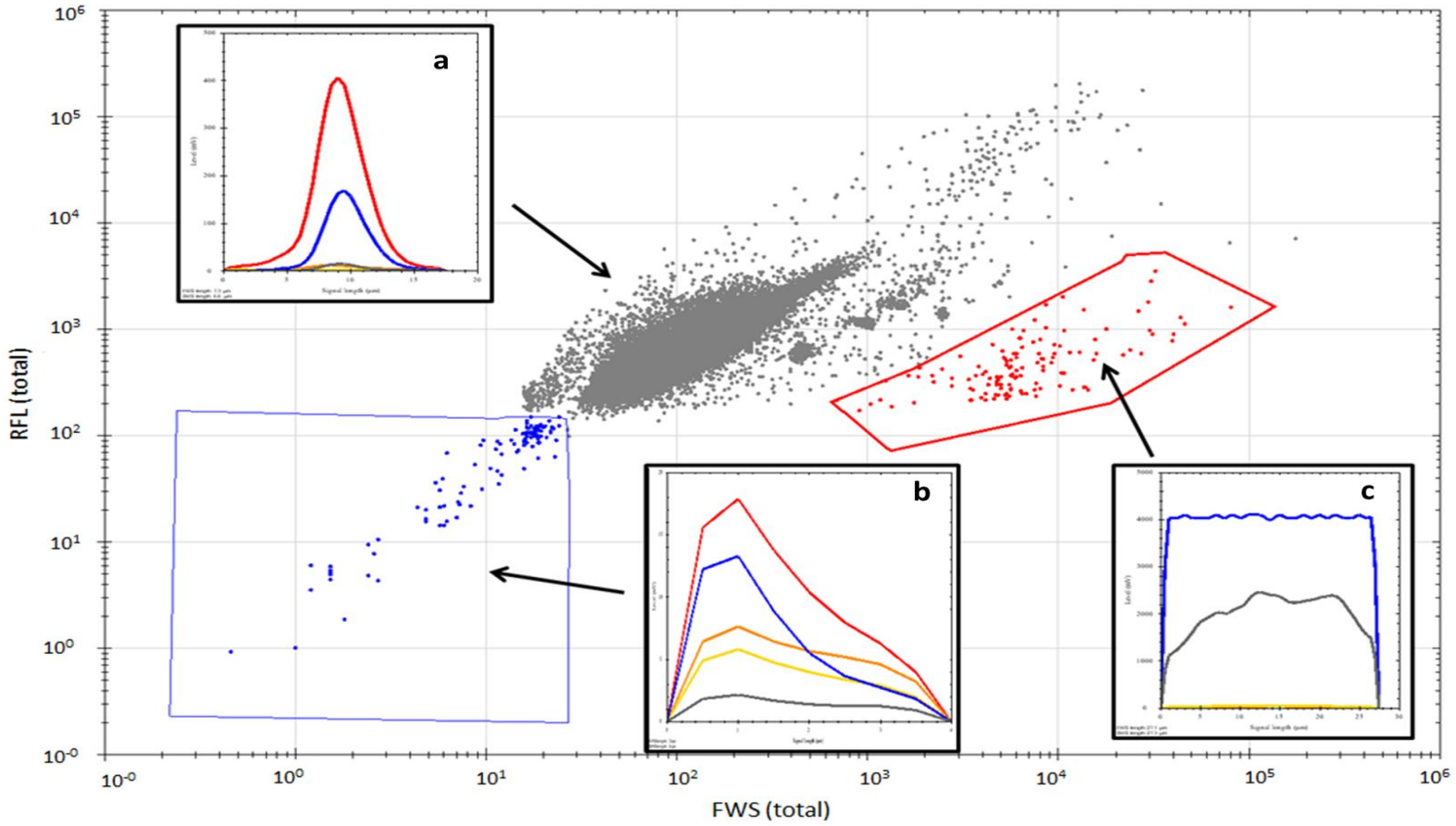

Figure 2.6. Cytoplot of environmental phytoplankton data acquired by the CytoSense. Each point on the plot represents a particle. The pigment and scatter profiles show a phytoplankton cell (a), electronic instrument noise (b) and debris or sediment particle (c). Forward scatter (FWS) is represented by the grey line, side scatter (SWS) by the blue, and red fluorescence (RFL) by the red line.

Electronic noise produces distinct angular fluorescence signals in high contrast to the more rounded pulse shapes produced by phytoplankton cells. Debris was identified by the absence of red fluorescence and high scatter profile.

Clean files were then analysed for phytoplankton content. A gate was drawn around the entire population to produce data on bulk red fluorescence. Groups of PFT within the bulk population were identified based on the fluorescence and scatter properties of each particle. The number of groups identified was highly dependent on sample type, ranging from 4 pico- and nanoplankton groups within open water samples, up to 12 groups spread across the pico-, nano- and microplankton from more diverse coastal samples. These clusters were not identifiable to species level, although in some instances the unique pigment profile of a cell allowed inference of some taxonomic detail. Orange fluorescence (550 to 590 nm) can be used to detect species with phycoerythrin secondary photopigments. This compound is only found in certain cells such as *Synechococcus* spp. and some cryptophytes (Jeffrey & Vesk 2005). This information, combined with an approximation of cell size, allows identification of these groups e.g. *Synechococcus*-like. Calcifying algae such as *E. huxleyi* may also be distinguished on the basis of the high SWS signature produced by the platelets surrounding each cell. Batch processing was then performed to produce numerical data output on the measured parameters for cells within each cluster. Rapid division of fluorescence contributions by cell size were performed using Easyclus v1.17 (Thomas Rutten Projects).

2.4.6. Machine monitoring and maintenance

The accuracy of measurements made by flow cytometry is reliant upon regular calibration and maintenance of the machine. Whilst generally extremely stable, the CytoSense can experience both laser deterioration and pump failure. Monthly checks and approximately biannual servicing were performed to maintain efficient operation and ensure confidence in data produced.

2.4.6.1. Volume calibration

The CytoSense uses a peristaltic pump to control sample flow and supplies measurements of the volume of sample analysed alongside particle event data. Accurate measurements of cell concentration are therefore highly dependent on the operating consistency of this pump. The performance of the pump was closely monitored throughout this research project. Measurements of volume can also be influenced by alterations to tubing or filter arrangements. The total volume of the instrument was checked and re-calibrated after any adjustments or maintenance. Volume and sample pump efficiency were tested by filling a 40 ml sample pot with distilled water, and recording the starting weight. The sample inlet tube to the CytoSense was placed in the pot, and the machine was set to analyse for 600 seconds at a flow rate of 2 µl/s. On completion the pot was re-weighed, and the new weight was recorded. This protocol was repeated a further two times to produce three replicates in total. The sample speed was increased twice more, to 4.2 and 9.7 µl/s, with the entire process repeated for each. This data was then used to calculate the average percentage recovery of water at each speed, permitting correction of volume data produced by the instruments software (Table 2.6). Variations in recovered volume were recorded during this research. All occurred after tubing was replaced, with no instances of unexpected pump decline or failure.

Table 2.6. Example volume calibration data, with calculation of expected and actual percentage recovery of water.

Date	Pump speed (µ/s)	Initial weight (g)	Final weight (g)	Analysis time (s)	Expected volume (speed*time)	Actual volume (initial-final weight)*1000	% recovery (actual/expected)*1000	Average % recovery	SD
24/06/11	2	33.84	32.77	600	1200	1070	89.17	89.17	0.00
	2	32.77	31.7	600	1200	1070	89.17		
	2	31.7	30.63	600	1200	1070	89.17		
	4.2	30.63	28.41	600	2520	2220	88.10	87.96	0.23
	4.2	28.41	26.19	600	2520	2220	88.10		
	4.2	26.19	23.98	600	2520	2220	88.10		
	9.7	23.95	18.92	600	5820	5030	86.43	86.48	0.10
	9.7	18.92	13.89	600	5820	5030	86.43		
	9.7	29.89	24.85	600	5820	5030	86.60		

2.4.6.2. Scatter calibration

As previously described in section 2.3, a flow cytometer does not provide exact measurements of cell size, though FWS and SWS data can be used to give a rough approximation of cell diameter. The CytoSense can reliably distinguish between 5 and 20 µm particles, but struggles to accurately differentiate between smaller size differences. To improve accuracy as far as possible, size estimates produced by the instrument were calibrated using plastic microspheres ranging from 1-15 µm (Molecular Probe, U.S.A.). Prior to use, each solution was vortexed and sonicated to reduce the risk of aggregates. Each size of microsphere was suspended in 0.2 µm filtered natural seawater, both separately and in combination. A magnetic flea was added to each sample pot prior to analysis and the pot was placed on a stirring plate at low rpm, sufficient to prevent settling of the microspheres. Each solution was analysed for 120 seconds, at a flow rate of 4.2 µl/s, using a FWS trigger (25 mV). Analyses were performed in triplicate for each microsphere solution and data are shown in Figure 2.7.

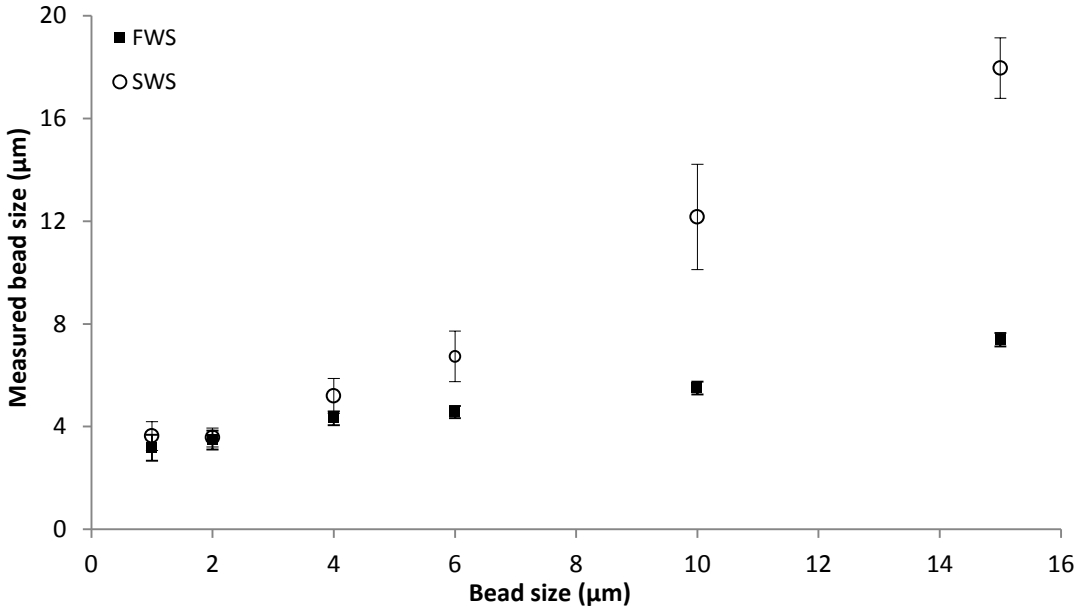

Figure 2.7. Comparison of measured microsphere size derived from measurements of forward (FWS) and side scatter (SWS) and actual size.

Both FWS and SWS overestimated the size of 1 and 2 µm microspheres by 2-3 µm. Since the machine has a lower size limit of 2 µm, these beads are at the very limit of the detection range. The smallest phytoplankton cells encountered during this project were *Synechococcus* sp., at approximately 1 µm. As expected from this calibration work, these were measured as closer to 3 µm in diameter during analysis of environmental samples. Both FWS and SWS produced relatively accurate measurements of 4 and 6 µm microspheres. For the two largest microspheres (10 and 15 µm), FWS greatly underestimated size, whilst SWS provided slightly overestimated measurements. Whilst SWS was closer to actual microsphere size, there was much higher variation between replicates, indicating that this parameter may be less reliable that FWS. This variability in SWS is likely to increase in the analysis of living cells, as SWS is influenced by cellular protuberances and cytoplasmic granularity. These parameters are therefore most informative when used in combination to give a rough estimate of size. As the relationship across the microsphere size range is proportional, they were used to make approximate divisions of particles into pico-, nano- and microplankton categories during later analyses.

2.4.6.3. Laser and PMT calibration

The CytoSense is designed for use in the field and as a consequence the risk of laser or PMT misalignment during transport is low. However, due to the emphasis on fieldwork in this research and the collection of time series data, it was considered important to monitor the consistency of fluorescence measurements over time. Continuity of laser function was checked through the use of fluorescent calibration microspheres as an internal standard. Lasers have a limited life span and their power can decrease without warning. Addition of microspheres to samples permits detection of any sudden drop or shift in laser strength of PMT sensitivity, allowing phytoplankton fluorescence to be calibrated accordingly and preventing loss of data. Microspheres emitting a strong yellow fluorescence signal in addition to red (F8852,

Life Technologies, USA) can be easily differentiated from natural chlorophyll emissions, and were selected for calibration use throughout this research.

The mother stock of microspheres was vortexed and sonicated to break up any aggregations and a working solution was made up with distilled water to a concentration of 1:10,000. Both solutions were stored in the dark at 4 °C. Fluorescent microspheres became unstable and lost fluorescence over time and repeated exposure to light. Fresh working solutions were therefore made up each month. A 25 µl aliquot of the microsphere working solution was added per 10 ml of sample. The sample was then analysed for 600 seconds at either 10 or 25 mV (RFL trigger). On completion of data acquisition, the data file was opened in CytoClus v3, and a plot of length (FWS) vs. YFL (total) was produced. This permitted easy separation of yellow microspheres from photosynthetic cells and debris and detection of single microspheres from doublets. The microsphere cluster was gated and processed to produce average values of fluorescence and scatter. These were checked against previously acquired values through addition to a calibration database, allowing the performance of the CytoSense to be closely tracked throughout this work and ensuring the data collected were available for comparison against data from other instruments.

During the three year sampling period, the CytoSense underwent routine maintenance and repair appropriate to sensitive equipment in continuous use. The instrument was fitted with a new laser, the FWS and SWS detectors were re-aligned and both sample and sheath pumps were replaced. Each separate incident impacted upon flow cytometric data output as shifts in measurements of fluorescence, scatter and volume. However, as internal reference standards were used rigorously throughout the entire sampling period, all data collected were calibrated and ultimately comparable.

2.4. Statistical analyses

Statistical analyses were performed using a variety of specialised software packages for Windows 7. Simple graphical plots, F-tests, t-tests and regression analyses were performed in Microsoft Office Excel version 2010. Univariate and multivariate analyses (ANOVA, MANOVA, MANCOVA) were performed in SPSS version 18.0. Multidimensional scaling analyses of environmental abiotic and abundance data were performed using PRIMER (Plymouth Routines in Multivariate Ecological Research) version 6. Further details on the application of the specific tests performed are supplied within the methodology of the following data chapters.

Chapter 3 Analysis of North Sea phytoplankton biomass by size based PFT during late summer (2010)

Abstract

Phytoplankton are divided into functional types based on cell size: picophytoplankton (≤ 3 μm), nanoplankton (3-20 μm) and microplankton (20-200 μm). Size is an important parameter in terms of carbon turnover, nutrient uptake and trophic transfer efficiency within marine food webs. The North Sea is a temperate shelf sea located between the UK and continental Europe. The spatiotemporal distributions and biomass contributions of nano- and microplankton within this region are well described. North Sea phytoplankton have historically been investigated using light microscopy. Larger phytoplankton cells are readily observed using this technique and as a consequence ecological theories of seasonal relevance and succession have evolved around them. Picophytoplankton are too small to be included within microscopic analyses and their significance to marine systems has only been uncovered over the last 30 years. Flow cytometry is a high speed method for the analysis of microscopic particles. This technique was first applied to oceanography in the 1980s and was influential in increasing knowledge of the picophytoplankton. These cells are now known to dominate phytoplankton cell concentrations and biomass in oligotrophic open water systems, however little information is available on their relevance within shallower and more eutrophic shelf seas. The Cefas International Beam Trawl Survey (IBTS) covered 74 sampling stations located across the northern, central and southern North Sea during late summer 2010. On board flow cytometric analyses of live phytoplankton cells from all three PFT were conducted. Picophytoplankton were shown to dominate cell concentrations whilst nanoplankton dominated biomass. Microplankton contributions to biomass were outweighed by inputs from picophytoplankton. This work highlights the ease with which picophytoplankton cells can be included within regular monitoring programs, with initial results suggesting that assessment of their contribution to North Sea biomass and productivity should not be neglected.

3.1 Introduction

North Sea phytoplankton communities are well documented, with a wealth of literature available on the taxonomy, distribution and abundance of phytoplankton functional types (PFT) within this region, describing their variation in both space and time (Longhurst et al. 1995, Tillmann & Rick 2003, Baretta-Bekker et al. 2009). Primary productivity in coastal or well-mixed waters during spring is dominated by microplankton (20-200 µm) such as large diatom species which utilise replenished surface water nutrients and increased irradiance to form large blooms (Brandt & Wirtz 2010). Summer biomass is composed predominantly of smaller nanoplankton (3-20 µm), typically mixotrophic flagellate or dinoflagellate species better adapted to low nutrient conditions (Tillmann & Rick 2003, Hu et al. 2011). Deeper water becomes stratified during summer months and coccolithophore blooms of *Emiliania huxleyi* may occur in these regions, clearly identifiable on satellite imagery by the 'milky' appearance of surface waters due to the calcium carbonate liths of these cells (Rees et al. 2002). These patterns of PFT distribution were established largely by microscopic observations of preserved phytoplankton (Pannard et al. 2008, Devlin et al. 2009). These studies, and therefore the paradigms they underpin, focus principally on nano-and microplankton, as their larger cell size allows them to be more readily analysed by this technique. However light microscopy cannot account for the smallest phytoplankton cells, the picophytoplankton (≤ 3µm) (Peperzak 2010), resulting in their historical exclusion from models of marine primary productivity.

The relevance of the picophytoplankton to pelagic systems was only fully realised in the early 1980s (Azam et al. 1983) leading to a paradigm shift and the addition of the microbial loop to the conventional model of energy transfers within marine food webs (Pomeroy et al. 2007). At around the same time, transfer of flow cytometric technology from biomedical applications to oceanographic research allowed the first large-scale investigations of picophytoplankton biomass distributions to be conducted (Olson et al. 1983, 1988, Li & Wood 1988, Simon et al. 1994). Flow cytometry is a powerful analytical tool providing rapid access to data on cell abundance, density and size. It is particularly applicable to analysis of phytoplankton

cells as the natural autofluorescence of chlorophyll *a* (chl *a*) and other photosynthetic pigments enables additional assessments of community biomass and diversity. The high throughput nature of flow cytometry in particular allows phytoplankton populations to be studied in greater detail than previously possible. This combination of new theory and technology rapidly led to the discovery of several novel species of picophytoplankton (Waterbury et al. 1979, Chisholm et al. 1988, Courties et al. 1994). Data are now widely available on the prevalence of picophytoplankton within the stratified, low nutrient open ocean where they were found to dominate productivity (Li 1989, Gasol & del Giorgio 2000, Zubkov et al. 2000, Button & Robertson 2001, Pan et al. 2005, Buitenhuis et al. 2012). More recent investigations of picophytoplankton distributions outside of this typical open water habitat have examined the extent of these cells in shallower and more mixed water. Preliminary datasets show that the influence of these cells may extend into regions with more variable environmental conditions and nutrient status (Agawin et al. 2000, Biegala et al. 2003, Mary et al. 2006, Medlin et al. 2006, Maranon et al. 2007). Research conducted within the Bay of Biscay has indicated that picophytoplankton may be more relevant to productivity within shallower or more coastal regions than previously thought (Calvo-Díaz et al. 2004, 2006, 2008). Picophytoplankton contributions to total algal biomass have been estimated at an average of 59% during spring within these temperate coastal waters (Calvo-Díaz et al. 2004). However, there is currently insufficient data available to allow definitive statements on the contributions of picophytoplankton within temperate continental seas to be made.

The North Sea is a marginal sea of the Atlantic Ocean, with a surface area of approximately 575, 000 km^2 situated between the eastern coast of the UK and mainland Europe. It is small and shallow, with an average depth of approximately 74 m (Otto et al. 1990). Notable exceptions are the Norwegian Trench to the north east, a deep intrusion running parallel to the coast of Norway where maximum depth exceeds 700 m (Otto et al. 1990), and the Dogger Bank to the south, where glacial deposits cause water depths of less than 20 m (Veenstra 1965). The North Sea exhibits complex hydrography, influenced by incursions of saline water from the

Atlantic Ocean entering through the English Channel in the south and below the Shetland Islands to the north (Ducrotoy et al. 2000). Baltic seawater enters through the Skagerrak causing areas of lower salinity to the northeast and along the Norwegian coastline (Otto et al. 1990). Towards the south, and particularly along the Dutch and German coastlines, water column mixing and transport processes are more dynamic and are strongly influenced by tidal conditions and riverine input (Otto et al. 1990, Tillmann & Rick 2003, Baretta-Bekker et al. 2009). Seasonal warming does not reach the deepest northern areas, which retain strong vertical temperature gradients in summer, whilst in contrast, complete mixing of the water column is expected in the south (Gieskes & Kraay 1977). Water conditions within the central North Sea are mixed, with a hydrographical front occurring between coastal and oceanic water masses.

Despite the increasing application of flow cytometry to marine research, studies of entire phytoplankton populations within shelf seas remain rare. Within the North Sea, flow cytometric research has focused on specific regions (Rutten et al. 2005), PFT (Zubkov et al. 2001) or a limited size range of chemically preserved cells (Ackleson & Robins 1990, Brandsma et al. 2013). The CytoSense flow cytometer (CytoBuoy, the Netherlands) is unique within the field of flow cytometry. This instrument was designed specifically for field analysis of phytoplankton and is both robust and portable. Furthermore, the CytoSense is able to measure particles ranging from 1-800 µm. These features are in contrast to other instruments which were initially adapted from those used for biomedical analytical purposes and which retain many of the design aspects and properties required by that field. This frequently results in large, complex instruments which are not practical for field deployment and the demands of environmental survey work. The aim of this research was to conduct a flow cytometric survey of North Sea phytoplankton during late summer, encompassing populations across the full range of environmental and physical diversity encountered within the region at this time of year. We aimed to collect distribution and biomass data on live cells from all three size-based PFT through on board analyses with a CytoSense flow cytometer, in order to investigate both

traditional and microbial food webs. As far as we are aware, this was the first survey of its kind within the North Sea.

3.2. Materials and methods

3.2.1. Data collection and processing

Data were collected as part of the International Beam Trawl Survey (IBTS), conducted annually by the Centre for Environment, Fisheries and Aquaculture Science (Cefas), on board the R.V. Cefas Endeavour over 34 days in late summer 2010 (August-September). Surface seawater was collected at 74 locations representative of the northern, central and southern North Sea (Figure 3.1).

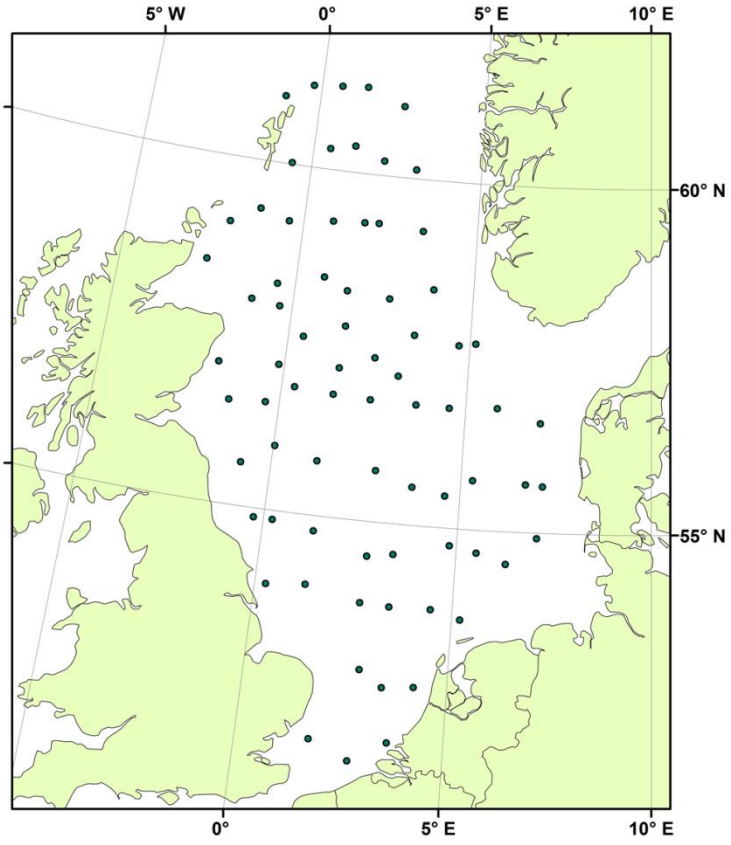

Figure 3.1. Location of the 74 sampling stations within the southern, central and northern North Sea

Discrete samples were collected by 10 L sampling bottles mounted on a Rosette sampler. sampled during the Cefas International Beam Trawl Survey (IBTS) during late summer 2010.

Measurements of salinity, phosphate (PO_4), silicate (Si) and nitrate and nitrite (TOxN) were obtained from surface water samples as described in Chapter 2 (sections 2.3.3 and 2.3.4). Samples for chlorophyll determination by fluorimetry were also collected at each station (Chapter 2, section 2.3.1). Samples for chl *a* determination by high performance liquid chromatography (HPLC) were also collected (as described in Chapter 2, section 2.3.2) at 50 stations located at regular intervals across the sampling grid. Additional information on chlorophyll distributions was obtained from sea colour data acquired remotely from the Medium Resolution Imaging Spectrometer (MERIS). Data were extracted from an online database (https://earth.esa.int accessed 25/11/2013) and used to calculate average values for August across the North Sea. Surface water temperature data were obtained via a Ferrybox system (Petersen et al. 2011) with the exception of stations 1-3 where Ferrybox initialisation issues prevented data collection. Samples for on board phytoplankton analysis by flow cytometry were pre-filtered through a 200 µm nylon mesh to prevent cells or detritus exceeding this size from causing blockages within the instrument. Analyses were conducted on live cells and generally completed within 30 minutes of sample collection. During periods of intensive sampling due to station proximity it was necessary to store samples in dark conditions at 4 ℃ for a maximum of four hours before flow cytometric analyses could be conducted. Samples were analysed using a CytoSense flow cytometer, fitted with a 488 nm blue argon laser. Data were collected using a red fluorescence trigger (RFL) at a threshold of 26 mV and a flow rate of 2 µl/s, using CytoUSB (v4.2) acquisition software (CytoBuoy, the Netherlands). Fluorescent microspheres with a diameter of 1 µm (F8852, Life Technologies, USA) were added to each sample as an internal reference standard. Flow cytometry data were processed using Cytoclus (v3.6) software (CytoBuoy, the Netherlands). Phytoplankton cells were discriminated and enumerated according to their scatter signals and fluorescence properties. Cell

length was approximated from forward scatter (FWS) calibrated against external reference microspheres ranging in size from 1-15 µm (F13838, Life Technologies, USA). Data were divided into contributions by the three size-based PFT. The picophytoplankton were further separated into prokaryotic and eukaryotic cells. Picoprokaryotes were assumed to be *Synechococcus*-like cyanobacterial cells on the basis of their small size and orange autofluorescence (560 - 620 nm) produced by the accessory pigment phycoerythrin. Picoeukaryotes were identified through the presence of red autofluorescence alone (> 670 nm). Further biomass partitioning was conducted using Easyclus v1.17 (Thomas Rutten Projects, the Netherlands) auto clustering software designed specifically for use on large flow cytometry datasets.

3.2.2. Statistical analyses

Environmental and biological data were mapped using ArcGIS v10.1. Kriging was used to infer data estimates in locations that were not sampled allowing generalised North Sea distribution patterns to be plotted. Linear regression analyses between datasets were conducted in Excel (2007) for Windows. Relationships were considered to be significant when $p < 0.05$. Geographic variation in environmental and biological datasets was assessed using PRIMER 6 (Plymouth Routines In Multivariate Ecological Research) statistical software with PERMANOVA+. Environmental data were log transformed and normalised before further analysis, with resemblance matrices constructed based on Euclidean distances. Biological data underwent square root transformations with resemblance matrices assembled using a Bray-Curtis similarity coefficient. Relationships between data points were visualised by principal coordinates analysis (PCO) with data significance assessed by PERMANOVA (999 permutations). Environmental vectors were overlaid onto PCO plots of biological data. Vector direction indicated correlating data, whilst vector length indicated the degree of data correlation. Significant differences between clusters were assessed by PERMANOVA (999 permutations). Distance-based linear modelling (distLM) was used to describe patterns in biological data using environmental variables.

3.3. Results

3.3.1. Characterisation of environmental conditions

North Sea environmental conditions during late summer were variable. A strong north-south divide was observed in both temperature and salinity (Figure 3.2a and b). Water temperature ranged from approximately 12 °C in the northwest, to almost 19 °C along the Dutch, German and Danish coastlines. Salinity was lowest (32.2 PSS) in the south and along the coastline of continental Europe with high salinity levels (35.3 PSS) occurring to the northwest, close to the Shetland Isles. Fluorimetry data recorded increased chlorophyll concentrations in the northwest (Figure 3.2c), peaking at 7.22 µg/l, with a further peak observed along the Dutch coastline (6.18 µg/l). Low concentrations of chlorophyll were detected within open water in the central region of the North Sea. Nutrient levels followed a similar pattern to chlorophyll, with peak concentrations occurring to the extreme northwest and south and lower concentrations within more central areas (Figure 3.2d-f). PO_4 reached a maximum of 0.39 µM in the northwest and a peak of 0.16 µM along the Dutch coastline. As with PO_4, Si levels were high in the northwest, peaking at 5.98 µM. A further region of comparable high Si was also recorded off the Dutch coastline (5.52 µM). Levels of TOxN reached a maximum of 1.70 µM in the northwest but remained low within southern regions.

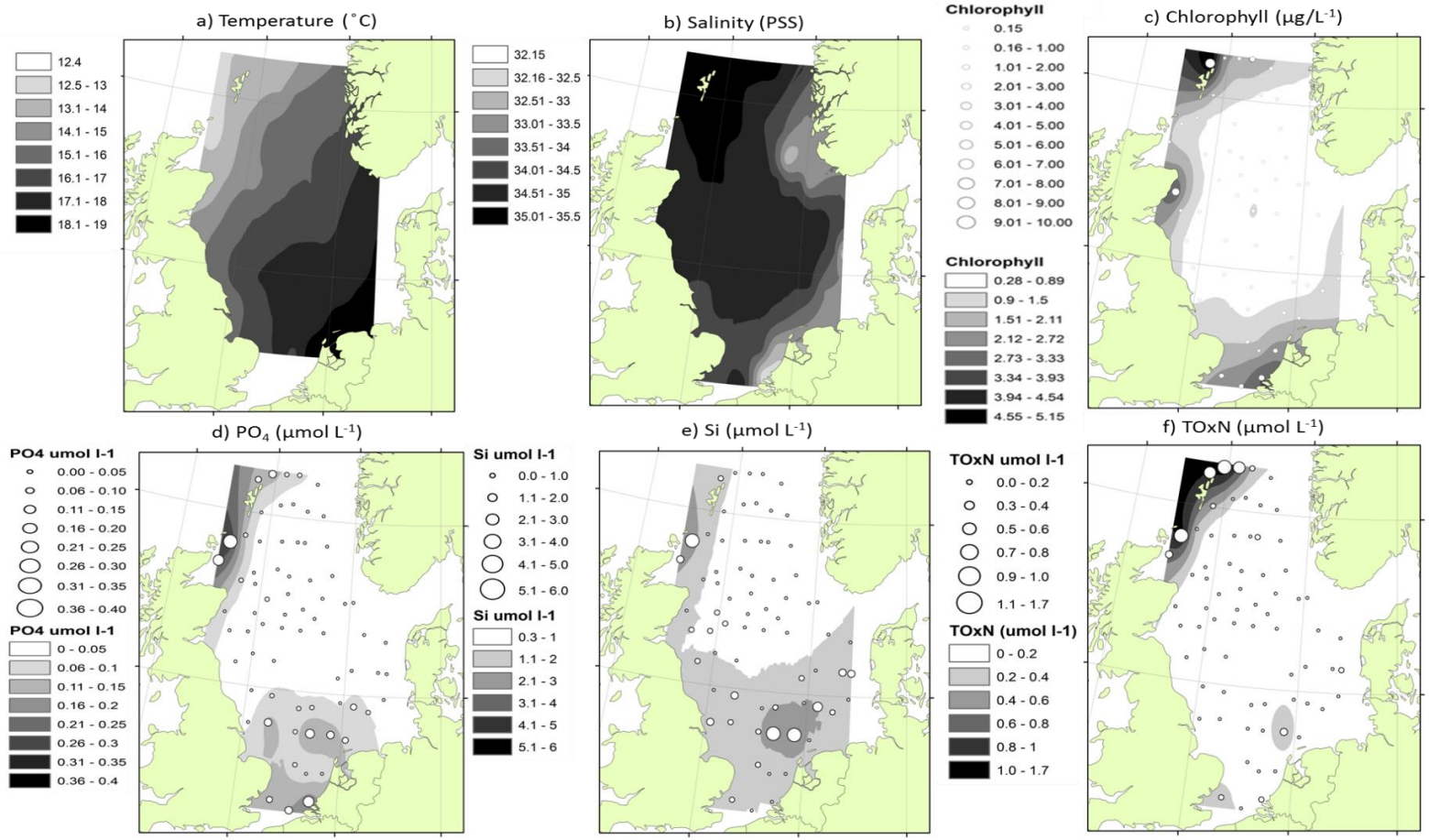

Figure 3.2. Environmental conditions in North Sea surface waters during late summer 2010: temperature (a), salinity (b), concentrations of chlorophyll supplied by fluorimetry (c) ,PO_4 (d), Si (e) and TOxN (nitrate + nitrite) (f). Open circles represent actual recorded data values overlaid onto kriged data.

A cluster analysis of temperature, salinity and nutrient data was conducted by PCO in order to identify areas with similar characteristics. Spatial cluster distributions indicated four approximate hydrographical regions of the North Sea (Figure 3.3) indicated as significantly different by PERMANOVA (p = 0.006).

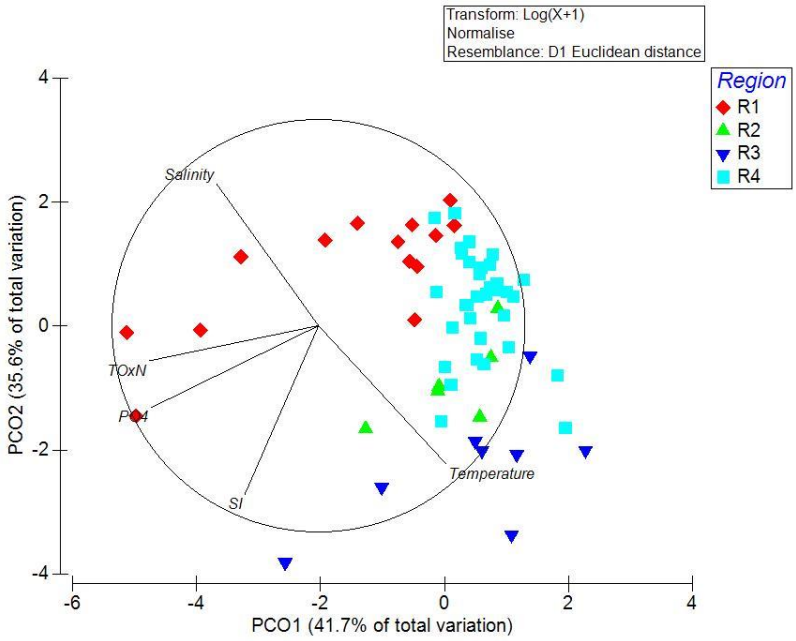

Figure 3.3. Principal coordinates plot (PCO) showing relationships between stations with similar environmental characteristics. Four main regions are identified. Region 1 (R1) represents data from the northwestern North Sea; region 2 (R2) represents the southern North Sea along the eastern UK coastline; region 3 (R3) represents data from the southern North Sea along the coastline of continental Europe and region 4 (R4) represents data from open water in the central North Sea.

Region 1 (R1) contained stations located in deep water in north western corner of the North Sea, close to the Shetland and Orkney Isles (Figure 3. 4). This water mass was influenced by incursions from the North Atlantic, with high salinity and nutrient levels but low temperature. Region 2 (R2) was composed of shallow water stations in the south western North Sea along the UK coastline (Figure 3.4). This region was again liable to influences by the incursion of Atlantic water via the English Channel, but also from estuarine input. Levels of salinity were moderate, with some PO_4 and

Si availability. Region 3 (R3) contained shallow water stations located to the south eastern edge of the North Sea along the coastline of continental Europe and extending towards the Skagerrak (Figure 3.4). Similarly to R2, this area may have received Atlantic water via the channel, but was likely also influenced by drainage from multiple large rivers. R3 had the lowest salinity levels of the survey, with some PO_4 and Si availability. Region 4 (R4) was composed primarily of deeper, open water stations across a range of temperature gradients but with relatively stable salinity. Nutrient availability within this region was extremely limited.

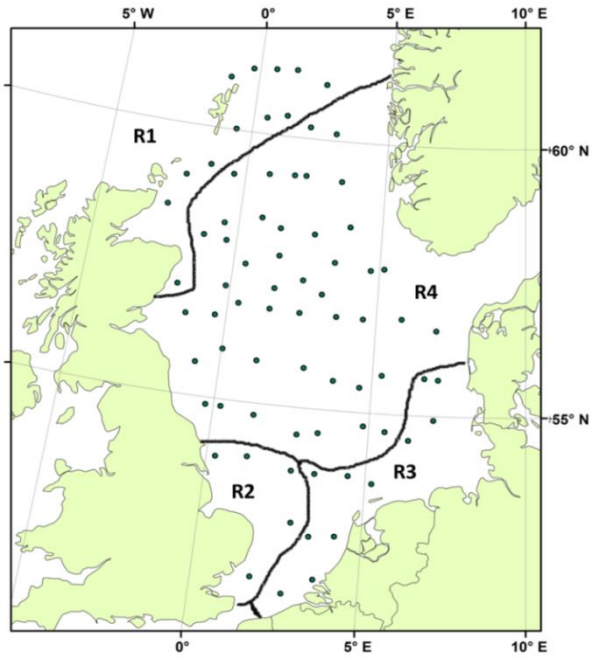

Figure 3.4. Division of North Sea sampling stations into four regions (R) identified by principal coordinates analysis (PCO) and PERMANOVA (p = 0.006).

3.3.2. Comparisons of chlorophyll, chl *a* and RFL measurements

Indications of phytoplankton biomass distribution were acquired using multiple techniques. Greatest comparability was observed in chlorophyll measured by fluorimetry and chl *a* measured by HPLC (R^2 = 0.89, p = 0.03) as shown in Figure 3.5. Whilst weak correlations were observed between total RFL and fluorimetry (R^2

= 0.50) and total RFL and HPLC (R^2 = 0.47) datasets, these were not significant (p = 0.38 and p = 0.94 respectively).

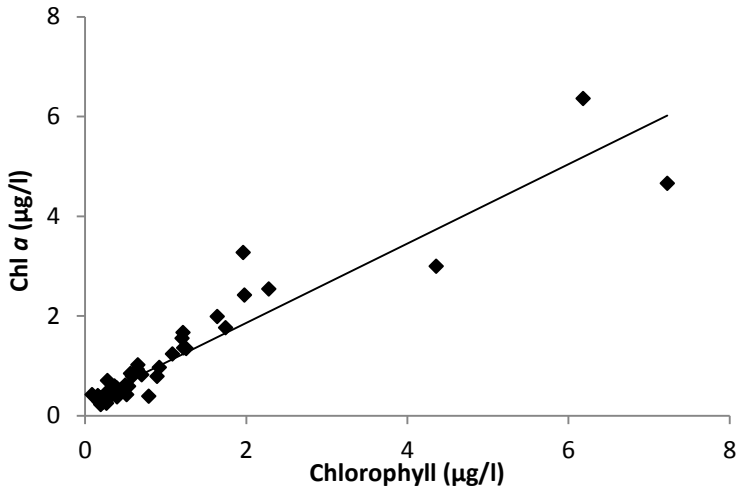

Figure 3.5. Relationship between chlorophyll measured by fluorimetry and chl *a* measured by HPLC (R^2 = 0.89, p = 0.03).

MERIS data represented averages of sea colour at each sampling station for the duration of August, which could not be directly compared against total RFL data. A general indication of the comparability of these methods was achieved by kriging MERIS data points to map areas of high chlorophyll and superimposing total RFL station values onto the same map (Figure 3.6). Both methods clearly indicate low phytoplankton biomass within the open water of R3 whilst identifying high biomass in R1, R2 and R3.

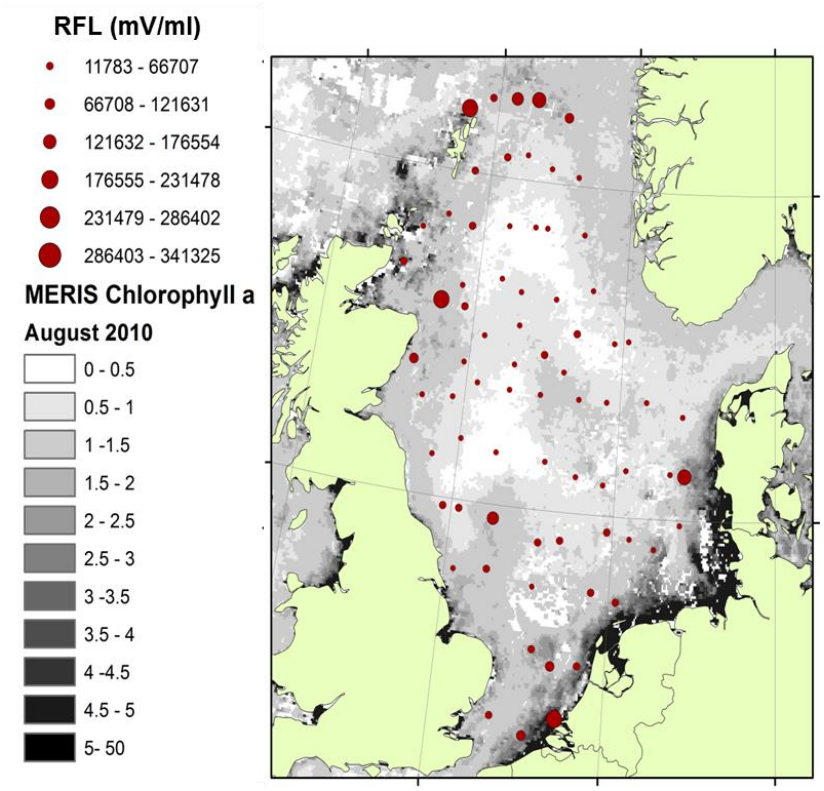

Figure 3.6. Red fluorescence (RFL) data acquired by flow cytometry (circles) overlaid against kriged MERIS data on average surface colour collected during August 2010. General agreement between the two methods on areas of high phytoplankton biomass can be observed around the Shetland Isles, off the north east coast of Scotland, off the eastern coast of England and along the Dutch coastline.

3.3.3. PFT spatial distribution and biomass partitioning

Flow cytometry data revealed picophytoplankton to be ubiquitous and numerically dominant throughout the North Sea (Figure 3.7a). This PFT contributed on average 76% to total phytoplankton cell numbers, with a maximum concentration of 1464 cells/ml in R1 and 69443 cells/ml in R2. Nanoplankton represented on average 23% of phytoplankton numbers and ranged from 230 to a maximum of 17043 cells/ml within R1. Microplankton were absent from many stations and present only in extremely low numbers at others, reaching a maximum concentration of 128 cells/ml in R1.

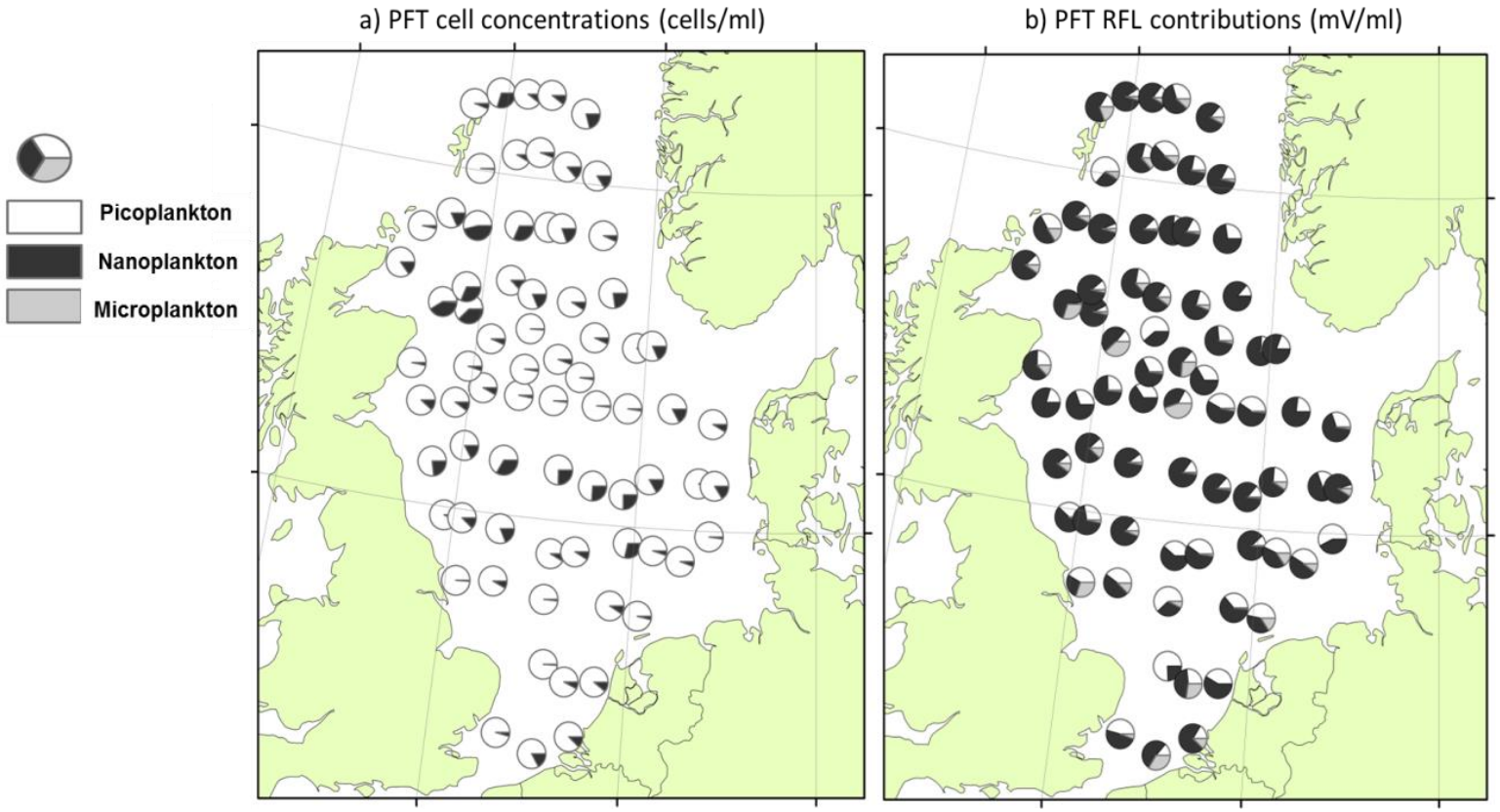

Figure 3.7. Phytoplankton functional type (PFT) contributions to total cell numbers (a) and contribution to total red fluorescence (RFL) (b).

Division of RFL by PFT revealed a different pattern (Figure 3.7b). The clear peaks in maximum total RFL shown in Figure 3.6 were attributable to nanoplankton cells, despite numerical domination by the picophytoplankton. Nanoplankton dominated photosynthetic biomass across the majority of stations, contributing on average 75% to total RFL, with absolute values ranging from 7100 mV/ml in R1 to a maximum of 9500 mV/ml in region 3 (Figure 3.8b).

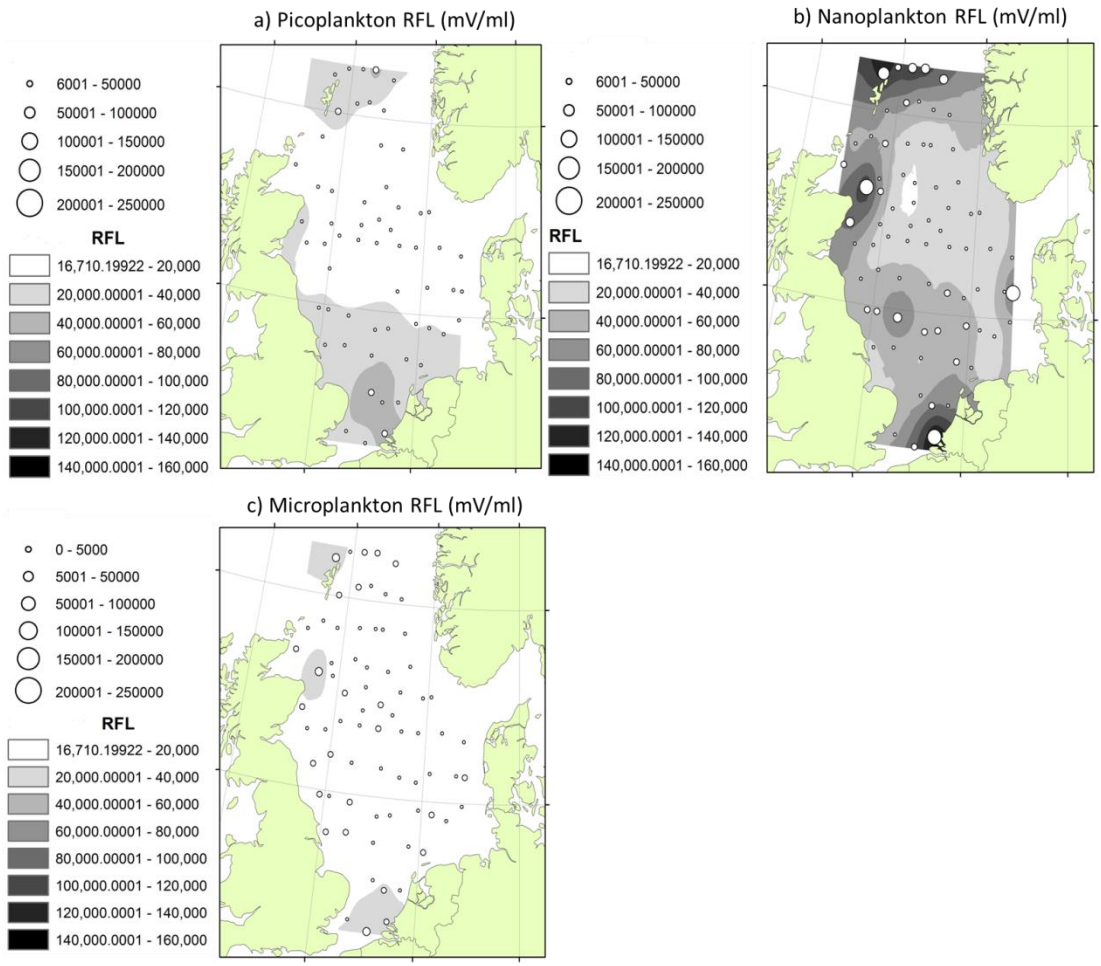

Figure 3.8. Phytoplankton total red fluorescence (RFL) contributions divided by size-based phytoplankton functional types (PFT). Open circles represent recorded data points overlaid on kriged data values. Note that microplankton data shown on plot c is on a different scale to pico- and nanoplankton data due to lower total RFL values.

Picophytoplankton were responsible for on average 17% of RFL with concentrations ranging from 6000 mV/ml in region 1 to 31487 mV/ml in region 2. Picophytoplankton biomass contributions were greatest in the southern North Sea in R2 and R3, but these cells also contributed to areas of high chlorophyll to the northwest in R1 (Figure 3.8a). Microplankton supplied the lowest inputs to RFL, with an average of just 8%. The lowest microplankton contribution was 415 mV/ml (region 4) whilst the highest recorded value was 96223 mV/ml (region 1). Microplankton made small biomass contributions in R1, R2 and R3, but like but like the picophytoplankton these cells were largely absent from open water biomass in R4 (Figure 3.8c). Picophytoplankton biomass was separated into contributions by *Synechococcus*-like prokaryotes and picoeukaryotes (Figure 3.9).

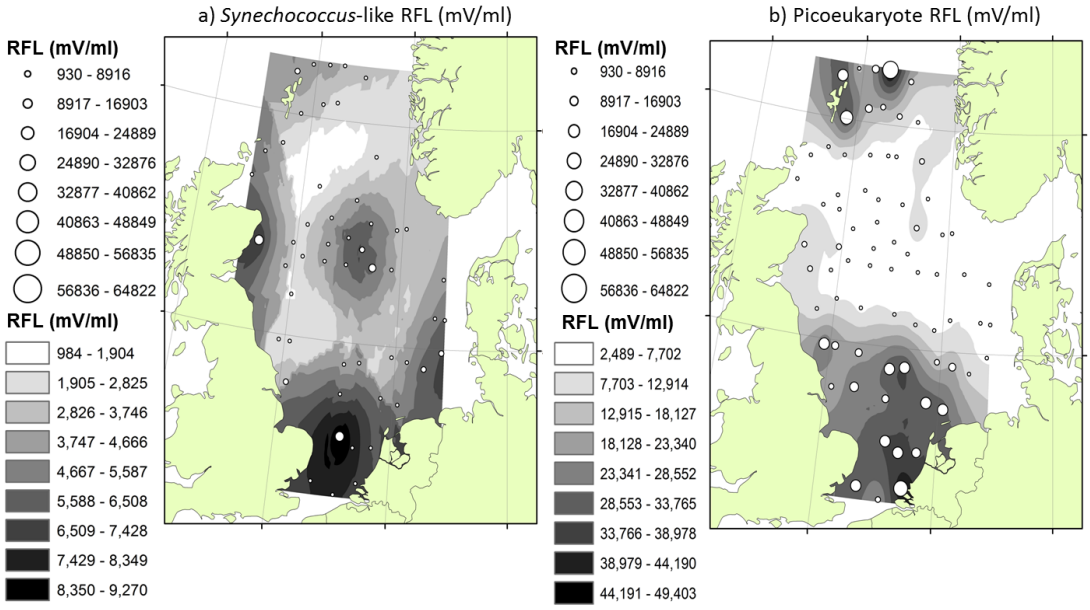

Figure 3.9. Picophytoplankton total red fluorescence (RFL) contributions divided by a) prokaryotic and b) eukaryotic cell groups. Picoprokaryotes were assumed to be *Synechococcus*-like cells on the basis of their orange autofluorescence. Open circles represent recorded data points overlaid onto kriged data values.

The *Synechococcus*-like group contributed on average 37% to picophytoplankton RFL and were present throughout the North Sea. In comparison, picoeukaryotes dominated picophytoplankton RFL, contributing on average 63%, but were less ubiquitous in their distribution. Areas of increased picophytoplankton RFL in R1 and

R2 (Figure 3.8a) appeared attributable to both *Synechococcus*-like prokaryotes and picoeukaryotes, whilst in R1, elevated picophytoplankton RFL levels were linked principally to picoeukaryotes.

Phytoplankton biomass partitioning was further investigated using the Easyclus automated clustering software. Nanoplankton were responsible for the bulk of RFL during this cruise, therefore cells of this PFT were selected for closer examination. The nanoplankton were divided into three sub-groups, consisting of cells from 3-5 µm, 5-10 µm and 10-20 µm. Within each of the four regions, largest RFL contributions were made by cells between 5-10 µm, ranging from 45 to 59%. Biomass partitioning across the three sub-groups was similar within the southern coastal areas of the North Sea covered by R2 and R3, whilst in regions R1 and R4 contributions from the 3-5 and 10-20 µm size ranges were variable (Figure 3.10). Sub-group contributions to nanoplankton chl *a* were not always consistent within regions (Figure 3.11). RFL contributions from each group remained relatively constant across R2 and R4, but were much more variable in R1 and R3.

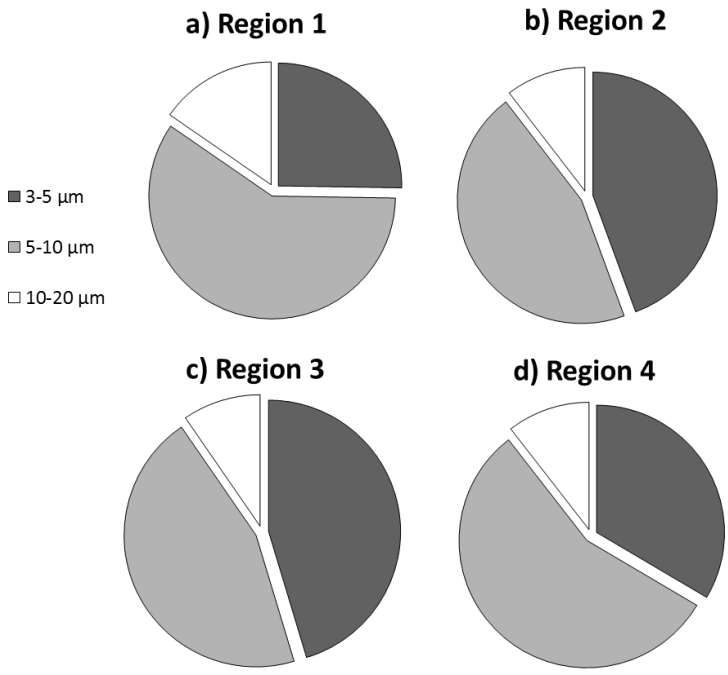

Figure 3.10. Average (%) red fluorescence (RFL) contributions of nanoplankton sub groups within four North Sea regions.

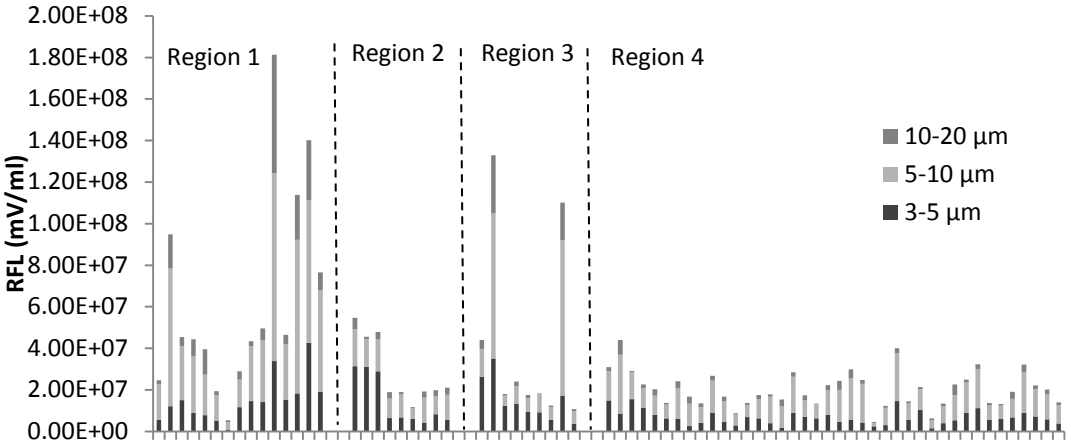

Figure 3.11. Nanoplankton sub-group red fluorescence (RFL) concentrations across four North Sea regions.

3.3.4. Relating environmental parameters to PFT distribution

RFL data from the pico-, nano- and microplankton were visually assessed by PCO (Figure 3.12). Environmental vector data were overlaid and nutrient concentrations were shown to control approximately 64% of the described variation, whilst temperature and salinity were less relevant. Analysis of RFL patterns by distLM using these environmental variables showed TOxN ($p = 0.002$), PO_4 ($p = 0.001$) and temperature ($p = 0.014$) to significantly influence RFL data.

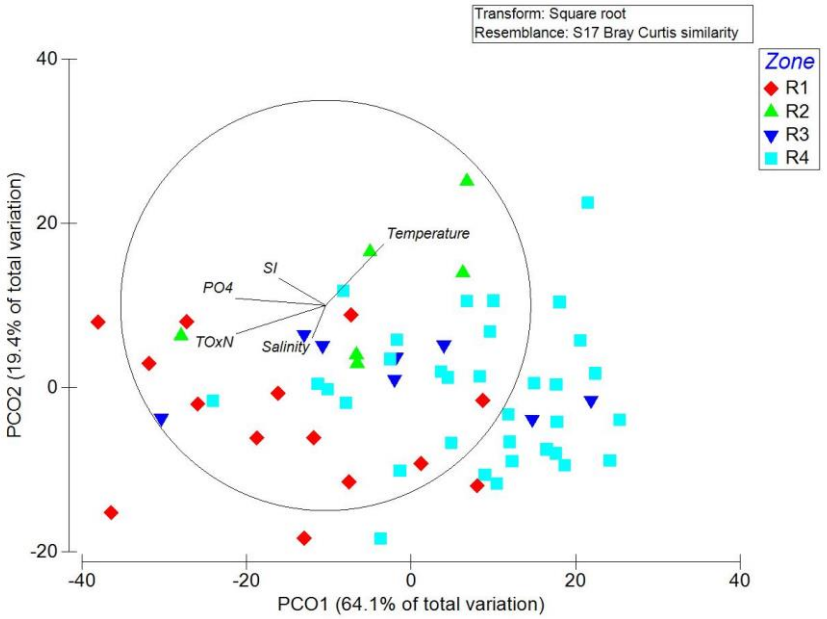

Figure 3.12. Principal coordinates plot (PCO) illustrating the relationships between red fluorescence distributions across four North Sea regions and prevailing environmental conditions.

3.4. Discussion

Environmental data collected confirm conditions within the North Sea during late summer 2010 were typical for the time of year (Gieskes & Kraay 1977, Otto et al. 1990, Tillmann & Rick 2003, Baretta-Bekker et al. 2009, Brandsma et al. 2013). Saline Atlantic Ocean water entered into the northwest corner of the North Sea close to the Shetland Isles, with a secondary, smaller incursion entering via the English Channel in the south. Lower salinity was observed along the Dutch and German coastlines, most likely attributable to riverine input (Otto et al. 1990, Ducrotoy et al. 2000). Whilst inflow of low salinity Baltic seawater via the Skagerrak was not directly detected, due to a lack of stations in the extreme east, its presence was indicated by areas of low salinity water along the Norwegian coastline. A temperature gradient from north to south was also observed, linked to decreased water depth, increased water column mixing and input of warmer water via the English Channel (Ducrotoy et al. 2000, Baretta-Bekker et al. 2009). Nutrient conditions within the North Sea during late summer were in agreement with other data recorded for this time of year (Brandsma et al. 2013) and were low in

comparison to values recorded during spring. Between March to May, Si can reach concentrations of 20 µM, PO_4 levels can increase to 1.4 µM and TOxN can be as high as 25.2 µM (Suratman et al. 2010). This is in contrast to maximum values recorded during late summer 2010 of 5.98, 0.39 and 1.70 µM respectively. Areas of comparatively high PO_4, Si and TOxN may have been caused by nutrient replenishment via North Atlantic input, nutrient recirculation by turbulent conditions, or by riverine discharge in southern regions. The central North Sea is generally too deep for water column mixing to occur and is isolated from both North Atlantic and riverine input. These conditions result in extremely nutrient limited conditions. Chlorophyll distributions displayed a similar pattern to nutrient data, reaching highest concentrations (7.22 µg/l) where all three nutrients were present. This peak was low in comparison to spring chlorophyll values that are known to reach ~ 25 µg/l during North Sea bloom periods (Suratman et al. 2010). Whilst chlorophyll concentrations increased within the southern North Sea with elevated PO_4 and Si, levels were much lower than those observed in the northwest. This suggests that phytoplankton populations within this area may have been TOxN limited. This was confirmed in cluster analyses of phytoplankton RFL data, where TOxN along with PO_4 was indicated to have a strong significant influence on phytoplankton distribution. Si was not a controlling factor of phytoplankton biomass, suggesting diatoms were not dominant within phytoplankton populations at this time. Flow cytometric analyses confirmed the absence of significant numbers of microplankton, generally considered to be composed principally of diatom species (Brandt & Wirtz 2010).

Phytoplankton biomass structure was examined by flow cytometry, using red autofluorescence as a proxy for chl *a*. RFL data showed similarities to MERIS remote sensing data, but was not significantly related to chlorophyll data acquired by fluorimetry or chl *a* data obtained by HPLC, although low levels of correlation were observed. These discrepancies were most likely caused by differences in method sensitivity. Fluorimetry provides a measure of total chlorophyll as contributions of chl *a* from other pigments such as chlorophyll *b* cannot be separated by this technique (Maxwell & Johnson 2000). HPLC offers a more detailed approach and allows quantification of individual pigment concentrations (Aminot & Rey 2000, Jeffrey & Mantoura 2005). However both of these methods are reliant on sample

collection via the concentration of cells upon a membrane, which must then be frozen and stored for later analysis. In contrast, flow cytometry data collected during this cruise were obtained almost immediately from live phytoplankton cells with minimal processing. The production of similar trends in phytoplankton biomass but non-identical datasets is therefore expected given such diverse methodologies.

Within shelf seas and coastal areas, phytoplankton biomass is known to be dominated by nano- and microplankton (Iriarte & Purdie 1994, Tarran et al. 2006). This work found this statement to be partially true within the North Sea during late summer. Nanoplankton dominated phytoplankton RFL across all North Sea regions, in agreement with previous studies (Brandsma et al. 2013), whilst the larger cells of the microplankton made little impact. Autotrophic phytoplankton are dependent on cell surface area for nutrient uptake and cell cross-section for absorption of sunlight (Cermeño et al. 2006). Smaller cell size allows more efficient uptake and assimilation of resources (Raven 1998; Beardall et al. 2009) whilst larger cells have a thicker diffusion boundary layer, causing lower solute exchange volumes and reducing nutrient uptake efficiency (Raven 1998; Agawin et al. 2000). The nutrient limited conditions recorded throughout the cruise were most likely responsible for absence of a significant microplankton contribution to cell numbers or RFL. The application of flow cytometry to data collection allowed the abundance and biomass contributions of live picophytoplankton cells to be included within this broad geographical survey of phytoplankton distribution. These cells were found to be ubiquitous across all areas and overwhelmingly dominant in terms of absolute cell numbers. This numerical dominance was not reflected in biomass due to the very small size of these cells (Li et al. 2006). However, despite their smaller dimensions, picophytoplankton were consistently more relevant to overall phytoplankton RFL than microplankton. Nutrient levels frequently control the distribution of microplankton (Thingstad & Sakshuag 1990) and the environmental data collected during this cruise suggests microplankton were likely nutrient limited during this study, explaining the greater relevance of picophytoplankton within community structure and biomass.

The *Synechococcus*-like picophytoplankton group was ubiquitous across the North Sea, occurring in areas of both high and low nutrients. In contrast to previous

shelf sea studies (e.g. Calvo-Díaz et al. 2004, 2008), this group made largest biomass contributions in nutrient rich conditions rather than low nutrient conditions. Data collected on picoeukaryote distribution and biomass were in agreement with existing data (Calvo-Díaz et al. 2008, Kirkham et al. 2013), with higher contributions to total RFL occurring in areas of increased nutrient availability. This indicates a difference in niche requirements between these two North Sea picophytoplankton groups. *Synechococcus* is known to prevail in the oligotrophic open ocean (Partensky et al. 1999, Zubkov et al. 2000, Button & Robertson 2001, Agustí 2004, Pan et al. 2005). Conditions within R4 during this study most remembled the low nutrient conditions within open water, explaining the prevalence of *Synechococcus*-like cells in this area. Whilst pro- and eukaryotic picophytophytoplankton cells are of similar size and exhibit similar high levels of cell numbers, they in fact represent two very different forms of cellular organisation. This underpins fundamental differences in their ecological traits and functional versatility (Massana & Logares 2013) and therefore accounts for the differences in their dispersal patterns across the North Sea. Cyanobacterial cells such as those likely contained within the *Synechococcus*-like group are able to capitalise on extremely low levels of resources which are considered unsustainable for picoeukaryotic cells and even mixotrophic flagellate cells. This is indicated by the prevalence of *Synechococcus*-like cells within the low nutrient R4 area and the absence of any picoeukaryotic cells in great numbers. Picoeukaryotes are generally considered less resilient to environmental change, as they possess less flexibility to enter into a reversible state of low metabolic activity, particularly in comparison to picoprokaryotes (Massana & Logares 2013).

Division of the nanoplankton into three sub-groups revealed cells between a size range of 5-10 µm contributed on average to over 50% of total RFL. Data of this resolution would be extremely difficult and time consuming to obtain by light microscopy and could not feasibly be acquired in sufficient quantities for use on a macroecological scale. Furthermore, the chemical preservation of cells required for microscopic analysis is known to unpredictably alter cellular dimensions (Menden-Deuer et al. 2001, Zarauz & Irigoien 2008), decreasing the accuracy and relevance of this type of data. Cell size is a key factor in models of marine carbon cycling. This parameter tightly controls the fate of organic carbon through influencing trophic interactions and sinking rates (Le Quere et al. 2005). Detailed knowledge of cell size

distributions, such as that presented here, permits the production of more comprehensive models and aids the development of more robust predictions of ecosystem response to change. Information of this type is also vital for sea-truthing a new generation of remote sensing techniques, which aim to derive phytoplankton size-class information from satellite data (Brewin et al. 2010, Uitz et al. 2010, Li et al. 2013, Brotas et al. 2013, Mustapha et al. 2014).

3.5. Conclusions

The distribution of live picophytoplankton cells in relation to other PFT was mapped for the first time in the North Sea. These data add to the small amount of existing knowledge on proportional picophytoplankton biomass contributions in temperate shelf seas and allowed maps of North Sea phytoplankton distributions to be updated. These results highlight the relevance of picophytoplankton cells in an area outside of the oceanic conditions studied to date and emphasise that the picophytoplankton should not be treated as a homogenous assemblage of cells. These data indicate a clear need for the incorporation of updated analysis techniques to ensure inclusion of the picophytoplankton within future survey work. Flow cytometry offers a high speed method of data acquisition on a larger and more detailed scale than is attainable using current monitoring procedures. Continued advancement of this technology and the logical progression into production of smaller, simpler and cheaper flow cytometers should ultimately increase accessibility to these instruments. Simultaneous development of purpose-designed auto-clustering data analysis software removes the current bottleneck created by the need to process large datasets manually. This combination of instrument and computer technology has the potential to allow flow cytometers to be incorporated into remotely operated, online sampling systems, installed on research vessels or ships of opportunity. This would permit detailed investigations of spatial and temporal variations in phytoplankton standing stock for minimal sampling effort.

Data on isolated PFT are of limited use when constructing and testing ecosystem models. A more holistic view of entire phytoplankton communities is required to obtain accurate representations of the phytoplankton interactions and contributions

necessary for establishing ecological baselines and validating model and satellite data.

Chapter 4 A three-year time series monitoring estuarine pico-, nano- and microplankton phytoplankton communities by flow cytometry

Abstract

Coastal phytoplankton populations are highly variable over seasonal time scales. Biomass and diversity are strongly influenced by shifts in biological, chemical and hydrological forcing parameters and alterations to photosynthetic biomass can impact across multiple higher trophic levels. Phytoplankton are particularly important to sessile filter-feeding bivalves, which occur in natural and farmed populations within the Wash estuary (UK). Conversely, shellfish aquaculture can also influence phytoplankton populations via intensive and selective grazing. Effective management strategies maximising fishery production whilst maintaining ecosystem health require localised data on the spatial and temporal distribution of phytoplankton. Monitoring regimes within the Wash and other similar eutrophic systems frequently use bulk chlorophyll data to track phytoplankton biomass, however this provides no indication of the contribution by phytoplankton functional type (PFT) or community diversity. Data resolution is increased by supplementary microscopic analysis of preserved cells; however this technique excludes small, fragile or rare phytoplankton species. Information on biomass structure in the Wash and other coastal regions is therefore biased towards larger and more robust cells which are easily observed and identified using microscopy. Flow cytometry enables large scale collection of multi parametric data inclusive of all PFT. This technique was applied to phytoplankton community surveys in the Wash estuary over three years. Overall biomass was found to be dominated by nanoplankton cells (3-20 µm), including a *Phaeocystis* bloom recorded in May 2010. Substantial annual variations in the magnitude and composition of phytoplankton blooms were recorded. Resident bivalve populations did not have a significant influence on phytoplankton biomass or diversity. Our data contributes to understanding the role of small phytoplankton cells in coastal eutrophic systems and emphasises the need for updated monitoring procedures utilising new technology.

4.1. Introduction

Coastal environments hold a central role within global cycles of carbon and macronutrients on Earth. Despite their comparatively small volume these diverse transitional systems contribute roughly 25% to oceanic primary productivity (Wollast 1998) and account for approximately 20% of global net inorganic carbon uptake (Thomas et al. 2004). Primary production within coastal regions oscillates with inputs of terrestrial nutrients and their subsequent availability within the water column (Philippart et al. 2000), and with the influence of abiotic forcing mechanisms such as temperature, irradiance and turbidity (Prins et al. 1998, Arndt et al. 2011). Historical anthropogenic exploitation of marine resources promoted the development of human settlements focused around coastal ecosystems. The increased population densities of modern towns combined with the intensive agriculture systems increasingly present along shorelines supply additional or modified inputs to coastal environments, via sewage discharge and chemical and fertiliser run-off (Lotze et al. 2006). As a result, coastal primary production cycles can be more irregular than those in open water and the timing and amplitude of peaks in littoral productivity can be variable in both space and time (Prins et al. 1998, Cloern & Jassby 2008).

Estuarine waters support ecosystems of economic and ecological importance. High primary productivity creates a vital resource for fish, marine mammals and migratory and breeding wading bird colonies, whilst also sustaining farmed populations of aquaculture species. Shifts in the timing, density or composition of phytoplankton communities therefore have the capacity to influence many higher trophic levels. The response of phytoplankton communities to environmental conditions is variable and highly dependent on specific life history characteristics, such as growth curves and storage capacity. Phytoplankton are extremely diverse and display great variation in both physiology and morphology (Leliaert et al. 2011). For ease of analysis, cells are frequently divided into phytoplankton functional types (PFT) independent of species and on the basis of shared properties. Cell size is a commonly used parameter for establishing PFT as it holds a central role in controlling distribution patterns, influences ecological and physiological behaviour and impacts metabolic rates (Margalef 1978, Huete-Ortega et al. 2012). Size can also be determined quickly and simply without requiring species identification or complex sample processing. Phytoplankton are commonly divided into three main

size groups for research purposes, consisting of the picophytoplankton (≤3 µm), nanoplankton (3-20 µm) and microplankton (20-200 µm).

Within the temperate North Sea, coastal phytoplankton populations vary with time, reflecting seasonal fluctuations in the parameters controlling their activities (Not et al. 2007; Schlüter et al. 2012). Blooms are characterised by increased concentrations of chlorophyll *a* (chl *a*) triggered by a combination of environmental conditions and ecosystem variables (Reynolds 2006). Over the course of 12 months two distinct bloom periods are generally observed, a phenomenon which has been particularly well described along the Dutch and German coastlines (Gieskes & Kraay 1977, Townsend et al. 1994, Peperzak et al. 1998, Wiltshire et al. 2008, Brandt & Wirtz 2010, Arndt et al. 2011). Water temperature begins to rise in spring and the water column starts to stabilise. These factors combine with increased day length, leading to greater light intensity within surface waters to produce optimal conditions for phytoplankton growth (Li et al. 2006). Cells are now able to effectively utilise nutrients returned to the euphotic zone by winter turbulence (Simpson & Sharples 2012b). Autotrophic biomass increases quickly, dominated by micro- and nanoplankton species, typically diatoms accompanied by small flagellates. As essential nutrients are exhausted and grazing rates rise, cell numbers drop rapidly and blooms can collapse as suddenly as they appeared (Hasle et al. 1997; Ducklow et al. 2001; Rousseau et al. 2002). Phytoplankton populations remain low over summer, consisting principally of nanoplankton and often dominated by dinoflagellates (Tillmann & Rick 2003). Turbulence in late summer can lead to replenishment of surface water nutrients. If sufficient light intensity remains, a smaller, secondary bloom may occur (Litchman et al. 2007; Hoppenrath et al. 2009).

Blooms are generally beneficial to coastal ecosystems and provide a vital seasonal food source for many organisms. Bloom structure is of high significance to pelagic ecosystems, with species composition determined by the survival of inoculum cells over the winter months (Colijn & Cadée 2003, Schlüter et al. 2012). Diatom dominated blooms contribute heavily to biogeochemical cycling, producing ~ 25% of the total carbon fixed on Earth (Field et al. 1998). These cells have high export to production ratios caused by increased sedimentation rates through aggregate formation and inclusion into rapidly-sinking zooplankton faecal pellets (Smetacek

1999, Leblanc et al. 2012). Some diatom species produce toxins which bioaccumulate within shellfish and pose threats to consumer health (Smayda 1997). Toxic blooms within UK waters are most commonly composed of species of *Pseudo-nitzschia* (Hinder et al. 2011). Dinoflagellate blooms can also be toxic, such as those of *Alexandrium* spp., whilst others are composed of relatively ungrazed species, e.g. *Ceratium* spp. which may cause hypoxia through sedimentation of cells in vast numbers (Carstensen et al. 2007). Blooms of colonial species such as *Phaeocystis globosa* can also impact ecosystems indirectly, through their high biomass and the oxygen depletion caused by colony degradation (Smith et al. 2013).

4.1.1. Phytoplankton analysis techniques

The model of coastal succession outlined above emerged from early observations of phytoplankton distributions and persists today as an established paradigm of North Sea productivity. It accounts principally for the nano- and microplankton as data on their distribution and productivity within coastal regions is widely available. Far less information exists on the role of picophytoplankton in these environments. Distribution data on this PFT are historically limited as the majority of coastal monitoring programmes focus on bulk chl *a* measurements or rely on analysis techniques which cannot account for picophytoplankton cells. Current knowledge of size-based PFT distribution within North Sea coastal waters is built largely on microscopic observations of chemically preserved phytoplankton (e.g. Pannard et al. 2008, Devlin et al. 2009). Microscopic analysis is a slow, laborious and subjective process, and is highly dependent on the skill of the analyst, resulting in relatively small datasets that may not be reproducible (Peperzak 2010, Dromph et al. 2012). Whilst this technique is adequate for quantification of larger cells, picophytoplankton cannot be accurately accounted for by light microscopy (Peperzak et al. 2000). Furthermore, the consequences of preservation vary widely across species: cells contort, contract, expand or are lost entirely depending on their phylogenetic origin (Montagnes et al. 1994, Menden-Deuer et al. 2001). Coastal populations are extremely heterogeneous (Peperzak et al. 2000), making it difficult to account or correct for lost or altered cells. True PFT assessments cannot therefore be obtained in

this manner and the utility of these data to produce robust, inclusive patterns of phytoplankton distribution is limited.

Recent data collected using new technology suggest that the picophytoplankton may make larger contributions to coastal primary productivity than previously realised (Not et al. 2007, Morán 2007, Calvo-Díaz et al. 2008). Flow cytometry is a high-speed technique which gives large volumes of reproducible data across all PFT. Specific combinations of light scatter and fluorescence emissions produced by photosynthetic cells allow separation of physically different individuals into sub-populations (clusters), identifiable to PFT level. Whilst microscopy can provide greater species resolution for phytoplankton samples, data are commonly combined into key taxonomic groups (e.g. diatoms, flagellates etc.) before further processing (Peperzak et al. 2000). Analysis by flow cytometry therefore does not necessarily represent a loss of detail or resolution. Flow cytometry can be performed on fresh or preserved samples, but cells are commonly fixed due to logistical constraints, especially where flow cytometers are not portable or cannot be spared from daily laboratory duties for deployment in the field. In such cases water samples must be returned to shore for laboratory processing at a later date and therefore require fixation before storage and transport. The effects of preservation on phytoplankton cells for analysis by flow cytometry have been widely discussed, though consensus on an optimal procedure is yet to be established. Fixation of cells with 1% glutaraldehyde (final concentration) and storage at -80 º C (Vaulot et al. 1989) is a frequently cited method. However, routine use of this methodology has revealed undesirable impacts on the cellular properties of phytoplankton, with both abundance and red fluorescence (RFL) derived from chl *a* known to decline with sample storage time (Hall 1991, Sato et al. 2006, Katano et al. 2009). These effects may be linked to physical issues, such as cell damage occurring during freezing (Lepesteur et al. 1993). Preservation in this manner can also cause shifts in cell size, with reports of diatom and dinoflagellate cells expanding and contracting unpredictably after treatment with glutaraldehyde (Menden-Deuer et al. 2001). These inconsistencies are likely linked to differences in cell composition across species, however within species variation may be due to cell status at the time of fixation (Menden-Deuer et al. 2001). Reliance on preserved samples can therefore introduce considerable artefacts to phytoplankton measurements and data acquired by either microscopy or

flow cytometry may vary significantly from the original population structure of the fresh sample.

4.1.2. Links between benthic filter feeders and primary production

Cockles (*Cerastoderma edule*) and mussels (*Mytilus edulis*) are both commercially harvested in the Wash estuary (Atkinson et al. 2003). Populations of these bottom-dwelling filter feeders contribute greatly to benthic community biomass, with considerable data showing the wide-ranging impacts of shellfish farming on coastal systems (Crawford et al. 2003, Miron et al. 2005, Cugier et al. 2010). Bivalves directly benefit from primary production in the overlying water column and represent a key link in trophic energy transfers from pelagic to benthic environments (Prins et al. 1998, Grall & Chauvaud 2002). Annual variation in bivalve biomass is largely determined by recruitment densities (van der Meer et al. 2001). Populations spawn in spring, triggered by increases in water temperature (Philippart et al. 2003), producing eggs which develop into pelagic larvae before entering the bottom-dwelling recruitment phase (van der Meer et al. 2001; Philippart et al. 2003). The mortality rates of these juvenile life stages are closely coupled to food availability, as well-fed adults produce larger eggs and because larvae require exogenous food to survive the planktonic stage (Philippart et al. 2003). Food limitation reduces growth rates, increasing exposure to predation and risk of redistribution of larvae to the open sea before metamorphosis (Philippart et al. 2003). As the onset of spring phytoplankton blooms are not solely controlled by temperature, there is potential for mismatch between spawning and optimal food availability (Cushing 1990, Prins et al. 1998, Grall & Chauvaud 2002). Inter-annual variability in the timing and amplitude of phytoplankton blooms may therefore greatly influence bivalve reproduction and biomass (Beukema et al. 2002).

Conversely, bivalve populations also influence phytoplankton populations. Chl *a* depletion has been recorded in areas of intensive aquaculture (Cadée & Hegeman 1974) indicating that top-down control of phytoplankton biomass via active bivalve grazing can outweigh bottom-up control of phytoplankton growth by parameters such as nutrients (Cadée & Hegeman 1974, Cloern 1982, Prins et al. 1998, Chauvaud

et al. 2000). Phytoplankton community composition may be further influenced by grazing selectivity within bivalve populations (Furnas 1990). Certain species provide a more optimal food source, whilst others are inedible (Prins et al. 1998). Preferential grazing may therefore promote dominance of faster growing, less susceptible species (Furnas 1990). Equally, high densities of suspension feeders may also promote phytoplankton biomass. Bivalves are responsible for the recycling and re-suspension of large quantities of particulate matter within the water column, and for the regeneration and reduced storage time of nutrients within photosynthetic biomass (Prins et al. 1998, Grall & Chauvaud 2002). This positive feedback assists in reducing nutrient limitation within ecosystems, thereby encouraging algal growth.

4.1.3. Study area

The Wash estuary system is the largest in the UK spanning an area of 660 km^2, around half of which is permanently covered by water (Murby 1997, Young et al. 1998). The remaining regions are composed of a mixture of mudflat, sandflats and salt marsh (Murby 1997). The Wash embayment receives drainage from approximately 12500 km^2 of eastern England through four main tributary river systems before opening out into the North Sea (Hartwell 2011). The majority of freshwater input is from the turbid and well-mixed Great Ouse (Rendell et al. 1997), with smaller contributions from the rivers Nene, Welland and Witham. The River Steeping also drains into the Wash, but is located at the extreme northerly edge of the embayment (south of Skegness) and is considered of little influence due to its proximity to the open sea. Water depth within the Wash rarely exceeds 10 m (Murby 1997) and water flow is dominated by strong semi-diurnal tides, producing a system which is generally well-mixed both vertically and horizontally (Young et al. 1998, Hartwell 2011). River flow is usually low during late spring and early summer and fluvial influence is considered small compared to tidal processes (Ke et al. 1996). The Wash is surrounded by low-lying fenland, which is heavily used for arable farming purposes (Murby 1997). Large urban conurbations are present at Skegness, Boston, Kings Lynn and Hunstanton (Figure 4.1). The estuary supports important wading and seabird populations, a seal colony and bivalve fisheries and has been

declared a National Nature Reserve (NNR) and Special Protection Area (SPA) by the UK government (Hartwell 2011).

Figure 4.1. The location of the Wash estuary on the UK East Coast (inset), and the location of population centres in the surrounding area (main image). Areas of mud and sandflats exposed at low tide are shown in yellow

Within recent history, bivalve biomass in the Wash estuary has experienced both catastrophic mortalities and an overall general decline (Murby 1997, Atkinson et al. 2003, 2010). These events impacted heavily on both the economic and ecological health of the region. Shellfish beds are vital to the local aquaculture industry and declines have resulted in premature closure of the fishing season and may ultimately lead to loss of the fishery. In addition, the beds are also a critical food resource for large local and migratory bird populations. Previous decreases in shellfish biomass caused mass emigration, starvation and mortality in these dependent populations (Camphuysen et al. 2002, Atkinson et al. 2010).

As outlined in section 4.1.2, phytoplankton community structure and diversity can be tightly coupled to bivalve biomass and ecosystem health. We conducted flow

cytometric observations of phytoplankton biomass variability within the Wash estuary over a three year period from 2010 to 2012. The aims of this work are listed below:

1. Look for evidence of cyclical trends across PFT and relate these to existing paradigms of seasonal succession

2. Record data on annual fluctuations in the timing, strength and composition of spring blooms

3. Determine whether aquaculture of either cockles or mussels influences phytoplankton abundance or diversity.

4.2. Materials and methods

Sample sites were selected to represent the physical and biological diversity present within the Wash. Locations included areas in close proximity to riverine input (Stylemans, Toft, Wreck) and sites situated above large cockle beds (Thief, Wreck, Wrangle) and mussel beds (Gat, Stylemans, Toft). A central location (Buoy) remote from both river flow and aquaculture was chosen to act as a control for comparison with the other sites. Site locations are provided in Figure 4.2. Surface water was collected on our behalf by the Eastern Inshore Fisheries and Conservation Authority (EIFCA, Kings Lynn) on board the RV Three Counties. Water was transported in a cool box to the Cefas Laboratory (Lowestoft) for flow cytometric analysis, filtration for pigment determination and nutrient analyses within 15 hours of collection. Samples were collected on an approximately monthly basis during 2010-2012, unless prevented by adverse weather or mechanical failure. Across the three year period, each of the seven sites was sampled for flow cytometric, pigment and nutrient analyses on 19 separate occasions.

Data on *in-situ* water temperature, salinity and turbidity were intermittently collected at each site through deployment of a handheld probe (YSI 6920 v2, USA). Additional data on the same parameters were collected by a second probe (YSI 6600,

USA) moored at the Buoy sampling site between December 2010 to March 2011, and March 2012 to December 2012. Unfortunately, neither probe was able to collect continuous *in-situ* data due to instrument failure and lengthy repair times. Supplementary information on water temperature and wave height was collected by the Cefas North Well Waverider instrument buoy, moored at the outer edge of the Wash (Figure 4.2). Surface levels of photosynthetically active radiation (PAR) were recorded with a LI-COR (LI-192) Underwater Quantum Sensor (Nebraska, USA) at the North Sea Dowsing instrumental mooring (not shown, located 25 miles off the north Norfolk coast at 53.531N, 1.053E).

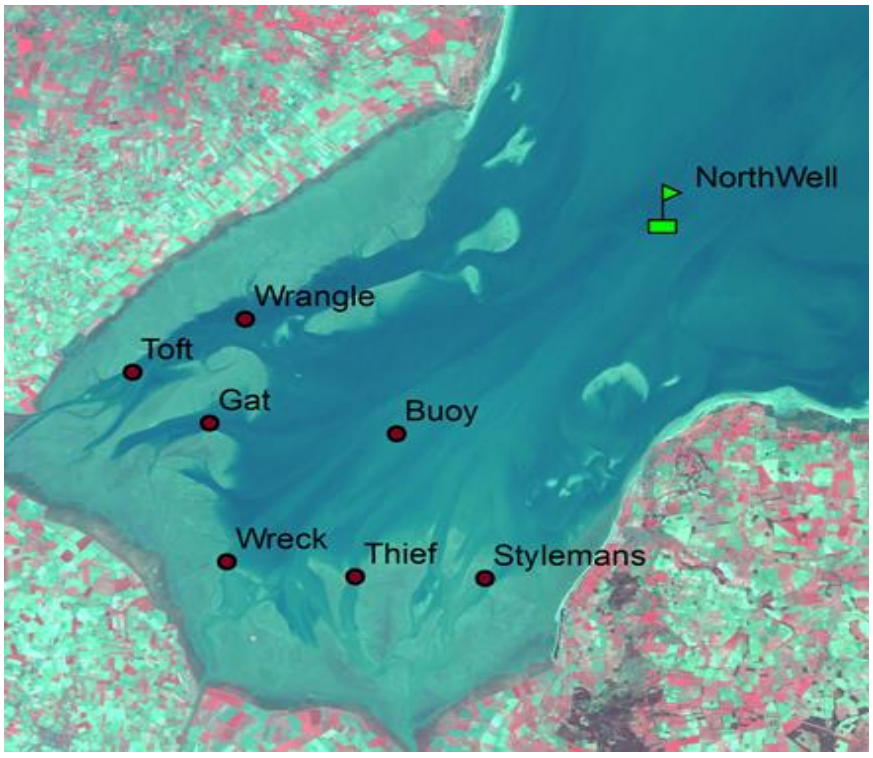

Figure 4.2. Location of the seven sampling sites within the Wash estuary and the position of the North Well Waverider.

No flow data for the river Great Ouse were available for the sampling period. An indication of freshwater input to the Wash was obtained from rainfall data within the Great Ouse catchment area. These were obtained from the UK government meteorological office database (http://www.metoffice.gov.uk/climate/uk/stationdata/cambridgedata.txt, accessed

May 2013). Measurements of salinity, chlorophyll and dissolved nutrients including phosphate (PO_4), silicate (Si), ammonium (NH_4), nitrate (NO_3) and nitrite (NO_2) were acquired from a discrete surface water sample at each site during monthly sampling. Seawater was processed and analysed as described in Chapter 2 sections 2.3.1, 2.3.3 and 2.3.4). Unfortunately, the salinity dataset is incomplete due to damage of sample bottles during transit. At the Buoy, Stylemans, Toft and Wreck sites an aliquot of seawater was removed for pigment analysis by HPLC as described in Chapter 2 (section 2.3.3). On board flow cytometry was not possible during this research programme due to sampling frequency and restrictions on instrument availability. Hence, seawater aliquots were removed at each site, filtered through a 200 µm nylon mesh and returned to the Cefas laboratory as described in Chapter 2 (section 2.3)

Flow cytometric analysis of phytoplankton samples should be conducted within a short period of time after collection. When this is not possible, chemical fixation of water samples is a technique frequently used to allow delayed analysis of phytoplankton cells. However, this method can cause multiple issues in data accuracy, as described in section 4.1.2. Transportation of fresh, unpreserved samples to the laboratory for analysis within 24 hours offers an alternative solution, however the impacts of this technique upon phytoplankton cells are unknown. Samples underwent filtration (200 µm) immediately after collection in order to remove large grazing organisms, but smaller grazers may have remained, potentially altering phytoplankton diversity and density during transport. Transportation time or conditions may have caused cells to become stressed, leading to shifts in the strength of fluorescence signals. It was therefore necessary to compare both protocol options, in order to select the most appropriate technique. Trials were conducted on multiple occasions throughout 2010 and 2011 ensuring each protocol was tested against the full range of phytoplankton diversity present in the Wash.

Aliquots were removed from samples at each site and fixed in 1% glutaraldehyde as described by Vaulot et al. (1989). However, neither liquid nitrogen nor -80 º C storage facilities were available on this research vessel. Glutaraldehyde-fixed samples were therefore kept at -20 º C for no more than 15 hours until returned to the laboratory, where they were transferred to storage at -80 º C and analysed within 30

days (Troussellier et al. 1999, Button & Robertson 2001). On board flow cytometry was conducted on two separate occasions during May 2011 and July 2012 where aliquots were removed from each sample for immediate analysis. This allowed comparison of "fresh" phytoplankton data against data acquired from the same sample during laboratory analyses up to 15 hours later. The impact of 200 µm filtration on phytoplankton populations was tested via fluorimetric analysis of chlorophyll as described in Chapter 2 (section 2.3.3). During March, April, May and October (2012) data were collected from filtered and non-filtered aliquots of the same seawater sample, to allow comparison of the bulk quantities of chlorophyll present in each.

Flow cytometric analyses were done with a CytoSense flow cytometer (Cytobuoy B.V., the Netherlands) using CytoUSB 5 data acquisition software and analysed using Cytoclus v3.6 (both Cytobuoy, the Netherlands). Data were acquired using a red fluorescence (RFL) trigger (26 mV) at a flow rate of 2 µl/s for a period of ten minutes for both fresh and glutaraldehyde-fixed samples. Multiple settings and analyses designed specifically for data collection from each PFT within a sample were not possible due to the high number of sampling sites and associated time constraints. The settings described were selected to collect data as representative as possible of all three PFT during a single analysis run. Cell size derived from forward scatter (FWS) data and red fluorescence (RFL) were calibrated monthly against averaged values attained from 1 µm microspheres with yellow fluorescence (F8852, Life Technologies, USA) added to each sample. The use of an internal reference standard ensured data comparability across the three year project. Further detailed descriptions of data acquisition, cluster details and analysis are given in Chapter 2 sections 2.3.4 and 2.3.5.

4.2.1. Statistical analyses

Cell concentrations and fluorescence after transportation and fixation were assessed for variance using F-tests (Excel 2007). Data were examined for significant differences using t-tests of equal or unequal variance (Excel 2007). Linear regression analyses were used to compare chl *a* datasets acquired by different methodologies

and for performing correlation analyses on environmental and biological data. Significant results were reported when $p < 0.05$. Monthly diversity in phytoplankton community composition was analysed using the Shannon Index (Shannon & Weaver 1949) calculated using the following formula:

$$H' = -\sum pi\ln(pi)$$

Where:

H' = the Shannon Index

pi = the relative abundance of each group of organisms

This method provides a quantitative approach to measuring the abundance and evenness of species present within a community. High index values are representative of a diverse and equally distributed community, whilst low values indicate communities with few species. Biological abundance data and environmental data were not normally distributed. Standard deviation of the data was generally proportional to the mean, therefore data were normalised by log transformation in order to stabilise variance before further analysis. MANOVAs (SPSS v18) were performed on these data to simultaneously assess the effects of multiple independent variables (site, month and year). MANOVAs consisted of four separate multivariate analyses: Pillai's Test, Wilks' Lambda, Hotelling's Trace and Roy's Largest Root with significant differences reported when $p < 0.05$. Step-down ANOVAs were performed to clarify specific significant variations within the data. MANCOVAs were used to study the co-variance of year by month on flow cytometry and pigment data. Compositional similarities across data were further investigated using PRIMER 6 (Plymouth Routines In Multivariate Ecological Research) statistical software. Environmental data were log transformed and normalized before further analysis whilst biological data underwent square root transformations. Similarity matrices were constructed using Euclidean distance for environmental data and a Bray-Curtis similarity coefficient for biological data. Multidimensional scaling (MDS) and the production of 2-D ordination plots were used to visualise groups of similar data. Data points were plotted in multiple dimensions, with the distance between each point illustrating their relative similarity

or dissimilarity. Plots were compressed into two or three dimensions and a stress factor was supplied indicating how well each plot represented full MDS. Plots were only considered to be representative when stress factors were below a threshold of 0.2. Exploratory factor analyses were performed to allow identification and summation of any highly correlated variables into a single group before principal coordinates analyses (PCO) were conducted. Environmental vectors were overlaid onto PCO plots, with vector direction indicating correlating data, whilst vector length indicated the degree of data correlation. Significant differences between clusters were assessed by PERMANOVA (999 permutations).

4.3. Results

Flow cytometric analyses of water samples revealed 12 phytoplankton clusters identifiable throughout the duration of this survey. An example of community structure showing the typical fluorescence properties of some of these clusters is shown in Figure 4.3. A brief description of the properties of each cluster and their PFT assignation is provided in Table 4.1.

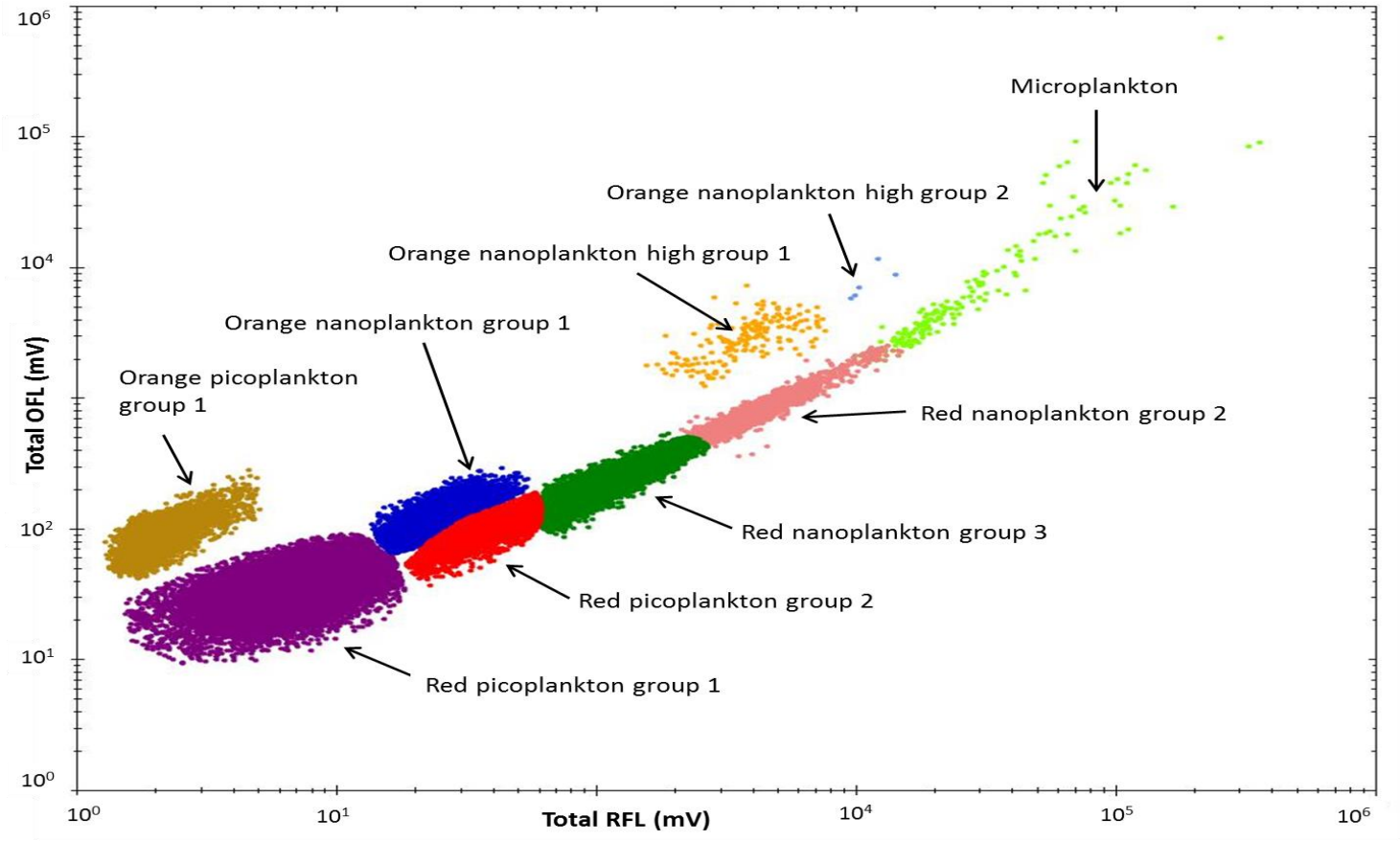

Figure 4.3. Typical clusters produced by flow cytometry for some of the phytoplankton groups identified within the Wash estuary. Each separate cluster is represented by different coloured markers. Axes show the total red fluorescence (RFL) of a cell versus the total orange fluorescence (OFL). Data shown were collected from the Wrangle site during spring 2012.

Table 4.1. Description of phytoplankton functional types (PFT) identified by flow cytometric analysis of water samples from the Wash estuary during 2010-2012, on the basis of their scatter and fluorescence properties. RFL and OFL represent red and orange fluorescence respectively. Picophytoplankton are defined as cells ≤ 3 µm, nanoplankton are cells between 3 – 20 µm, microplankton are cells from 20 – 200 µm.

ID	PFT	Features	Description
Orange picophytoplankton (group 1)	Picophytoplankton	Unicellular, RFL and OFL	Cyanophyceae
Orange picophytoplankton (group 2)	Picophytoplankton	As above, with slightly increased RFL	Cyanophyceae
Red picophytoplankton (group 1)	Picophytoplankton	Unicellular flagellates, RFL	Prymesiophyceae, Chlorophyceae, Prasinophyceae
Red picophytoplankton (group 2)	Picophytoplankton	Unicellular flagellates, RFL	As above
Orange nanoplankton (group 1)	Nanoplankton	Unicellular flagellates, RFL and OFL	Cryptophyta, Rhodophyta,
Red nanoplankton (group 1)	Nanoplankton	Unicellular flagellates or diatoms, RFL	Bacillariophyceae, Dinophyceae, Prymesiophyceae. Includes *Phaeocystis* spp.
Red nanoplankton (group 2)	Nanoplankton	Unicellular flagellates or diatoms, RFL	As above
Red nanoplankton (group 3)	Nanoplankton	Unicellular flagellates, RFL	As above, rarest of the three red nanoplankton groups
Orange nanoplankton high (group 1)	Nanoplankton	Unicellular flagellates or dinoflagellates, RFL and strong OFL	Cryptophyceae, Rhodophyceae
Orange nanoplankton high (group 2)	Nanoplankton	Unicellular flagellates or dinoflagellates, RFL and strong OFL	As above
Orange nanoplankton high (group 3)	Nanoplankton	Unicellular flagellates or dinoflagellates, RFL and strong OFL	As above
Microplankton	Microplankton	Unicellular or chain-forming diatom or dinoflagellate cells, high RFL	Bacillariophyceae, Dinophyceae,

4.3.1. Impacts of glutaraldehyde fixation on phytoplankton cells

Data on total cell concentration, total RFL and average cell size at each of the seven sites were grouped to produce a single mean value for each month. This was performed for both glutaraldehyde-fixed and live samples in order to compare between the two methods (Figure 4.4).

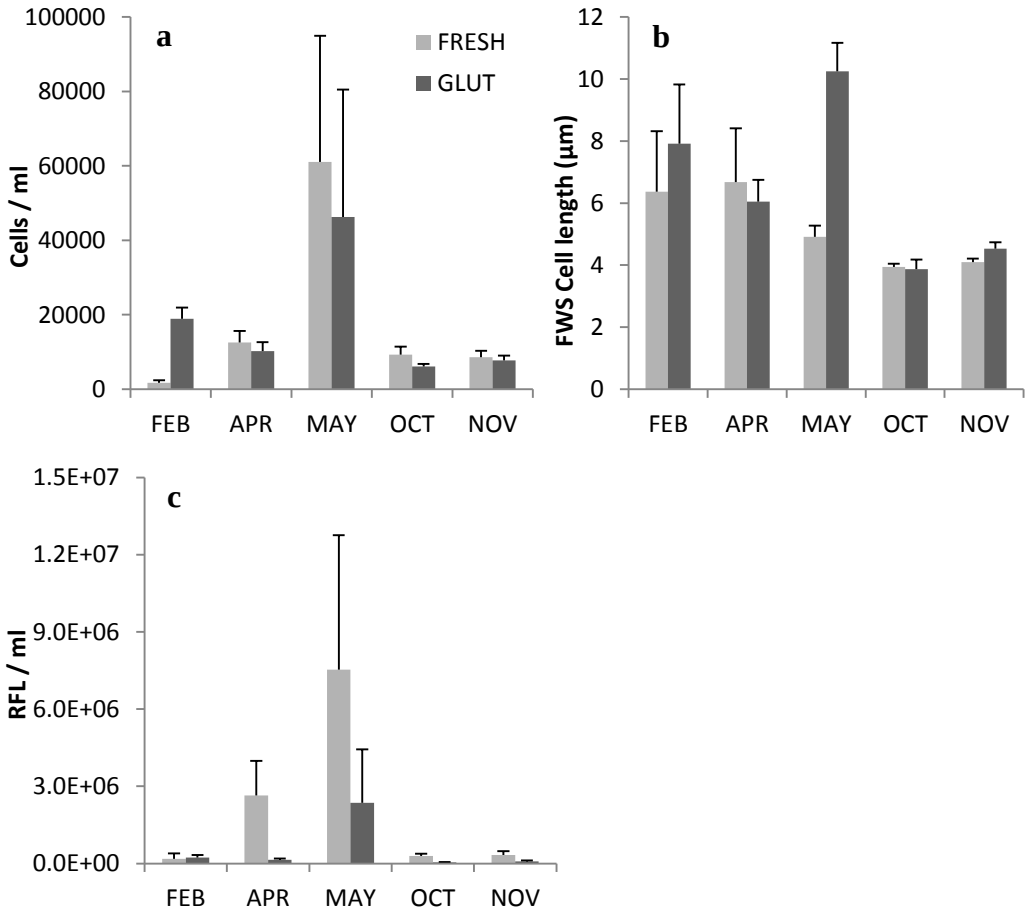

Figure 4.4. The averages and standard deviations (n = 7) of total cell concentration (a), cell length derived from forward scatter (FWS); (b), and total red fluorescence (RFL); (c) for live (FRESH) and glutaraldehyde fixed (GLUT) phytoplankton samples across five months in 2010.

Cell concentration increased significantly from 1.77E+03 to 1.89E+04 after fixation in February ($p = 0.000$) but significantly decreased from 9.28E+03 to 6.09E+03 in October ($p = 0.004$). Average cell size also varied significantly after preservation, increasing from 4.92 µm to 10.25 µm in May ($p = 0.000$). Significantly reduced

levels of total RFL per ml were recorded in fixed samples across all months apart from February, with greatest decreases observed in April (from 2.65E+06 to 1.42E+05; p = 0.001) and May (from 7.53E+06 to 2.35E+06; p = 0.02). Data on total cell concentration, total RFL and average cell size for each PFT across the seven sites were averaged in order to produce mean monthly values for each PFT. This was again performed for both glutaraldehyde-fixed and live samples in order to allow comparisons between the two methods (Table 4.2).

Table 4.2. P values produced by t-test analyses showing significant differences in averages of cell concentration, cell size and total red fluorescence (RFL) of PFT between live and glutaraldehyde fixed phytoplankton samples.

Group	Cell abundance (per ml)	FWS Cell size (µm)	RFL (mV/ml)
Orange picoplankton 1	0.427	0.266	0.000*
Orange picoplankton 2	0.458	0.478	0.186
Red picoplankton 1	0.004*	0.297	0.026*
Red picoplankton 2	0.357	0.155	0.008*
Orange nanoplankton 1	0.454	0.000*	0.005*
Red nanoplankton 1	0.024*	0.001*	0.030*
Red nanoplankton 2	0.076	0.429	0.008*
Red nanoplankton 3	0.281	0.272	0.070
Orange nanoplankton high 1	0.001*	0.000*	0.084
Orange nanoplankton high 2	0.008*	0.000*	0.071
Orange nanoplankton high 3	0.000*	0.001*	0.027*
Microplankton	0.462	0.377	0.029*

* indicates significant p value (< 0.05)

Significant increases in average cell concentrations were recorded in red picophytoplankton group 1 (p = 0.004), where cell numbers rose by 288% in February. In orange nanoplankton high groups 1-3, cell concentrations significantly decreased with average losses of approximately 46% (group 1 p = 0.001; group 2 p = 0.008; group 3 p = 0.000). These three groups also showed significant increases in average cell size (group 1 p = 0.000; group 2 p = 0.000; group 3 p = 0.001), as did orange nanoplankton group 1 (p = 0.000) and red nanoplankton group 1 (p = 0.001). Significant losses in total RFL were observed across all cells after glutaraldehyde

preservation, with the exception of orange picophytoplankton group 2, red nanoplankton group 3 and orange nanoplankton high groups 1 and 2 (Table 4.2). Highest RFL losses were observed in April and May, where total RFL decreased on average by 50% after preservation.

4.3.2. Impacts of delayed analysis on live phytoplankton cells

Data on total cell concentration, total RFL and average cell size at each of the seven sites were grouped to produce average values for May 2010 and July 2011. This was performed for samples analysed immediately on board and also for samples which underwent delayed laboratory analysis in order to make comparisons between the two methods. No significant differences in any of these three parameters were observed after delayed analysis of samples in either month (Figure 4.5).

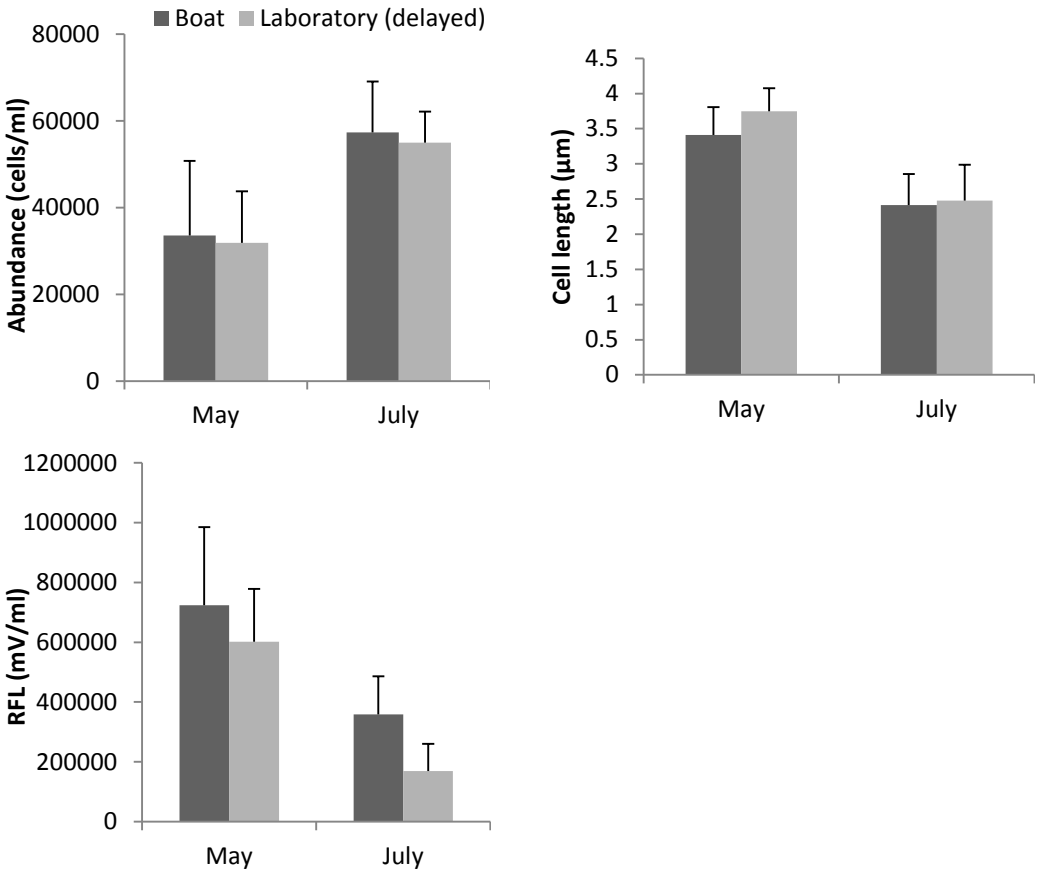

Figure 4.5. The averages and standard deviations (n = 7) of total cell concentration (a), cell length derived from forward scatter (FWS); (b), and total red fluorescence (RFL); (c) between live samples analysed immediately by on board flow cytometry (Boat) and live samples analysed in the laboratory after a delay due to transport (Laboratory).

PFT data for each site were combined to produce monthly average values in order to examine data for group-specific effects (Table 4.3). No significant differences were observed in any PFT with the exception of orange nanoplankton group high 2, where cell size significantly increased by approximately 2 µm after delayed analysis in comparison to cell size measured during immediate analysis.

Table 4.3. P values produced by t-test analyses showing significant differences in averages of cell concentration, cell size and total red fluorescence (RFL) across PFT in live cells analysed immediately and after a 15 hour (maximum) delay.

Group	Cell abundance (per ml)	FWS Cell size (µm)	RFL (mV/ml)
Orange picoplankton 1	0.427	0.266	0.000*
Orange picoplankton 2	0.458	0.478	0.186
Red picoplankton 1	0.004*	0.297	0.026*
Red picoplankton 2	0.357	0.155	0.008*
Orange nanoplankton 1	0.454	0.000*	0.005*
Red nanoplankton 1	0.024*	0.001*	0.030*
Red nanoplankton 2	0.076	0.429	0.008*
Red nanoplankton 3	0.281	0.272	0.070
Orange nanoplankton high 1	0.001*	0.000*	0.084
Orange nanoplankton high 2	0.008*	0.000*	0.071
Orange nanoplankton high 3	0.000*	0.001*	0.027*
Microplankton	0.462	0.377	0.029*

* indicates significant p value (< 0.05)

4.3.3. Impact of 200 µm filtration on chlorophyll content

Fluorimetric measurements of chlorophyll before and after filtration (Figure 4.6) produced similar data ($r^2 = 0.64$, $p = 0.04$). Chlorophyll data from each of the seven sites were combined to produce a mean value for each month, for each protocol. No significant differences in chlorophyll were observed between the two protocols, with the exception of October. In this month, chlorophyll increased slightly after filtration (Figure 4.7). Therefore hereafter only chlorophyll data derived from 200 µm filtered water samples are presented and discussed.

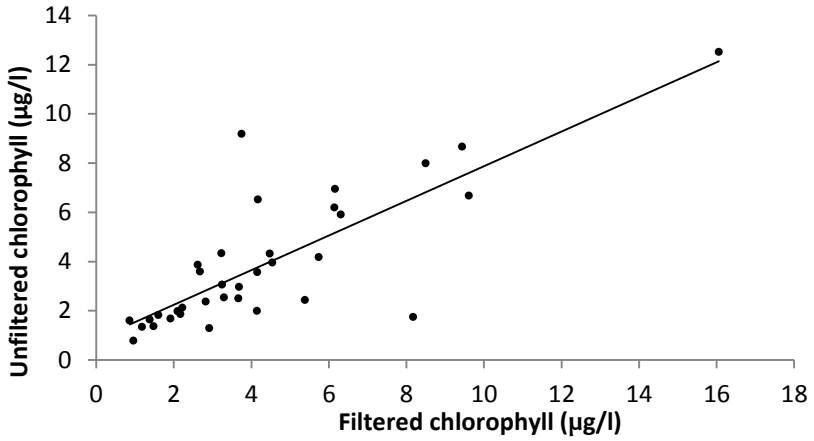

Figure 4.6. Relationship between chlorophyll (µg/l) measured by fluorimetry before and after 200 µm filtration (r2 = 0.64, p = 0.04).

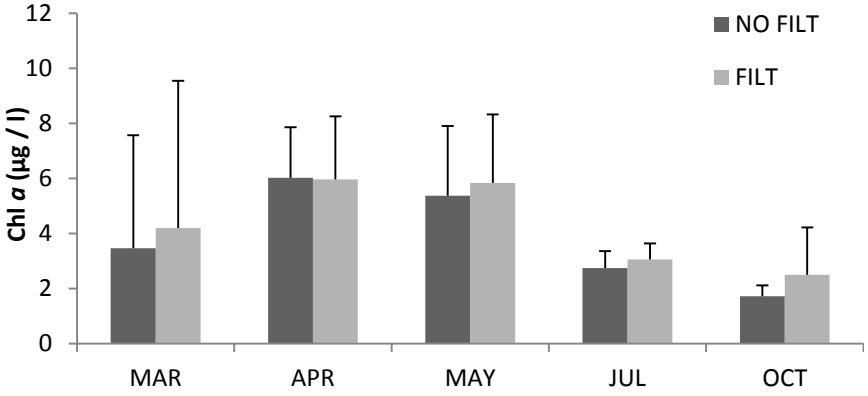

Figure 4.7. The averages and standard deviations (n = 7) of chlorophyll (µg/l) measured by fluorimetry before (NO FILT) and after 200 µm filtration (FILT) across five months during 2010.

4.3.4. Analysis of environmental data

Data on water temperature collected by the *in-situ* probe at Buoy and by handheld probe across the seven sampling sites were compared with data obtained from the Waverider instrumental buoy (see Appendix I). Temperature data were combined and averaged to produce generalised monthly values for the Wash, however no data were available from any source for January 2010. Averaged data from January 2011 and 2012 were therefore used to give an estimated value (Figure 4.8). Surface irradiance data collected by the Dowsing Smartbuoy from 2010-2012 and

chlorophyll data determined by fluorimetry are also provided in Figure 4.8. An index calculated from irradiance and turbidity data was used to provide an indication of light availability within surface waters. Both temperature and irradiance showed consistent cyclical trends which peaked in June of each year and remained low over winter. Water temperature reached the highest value in July 2010 at 18 °C, with the lowest value of 3 °C occurring in February of the same year. Surface irradiance ranged from 3 mol photon/m^2 d^{-1} in January 2010 up to 40 mol photon/m^2 d^{-1} in July 2011. Light availability showed a similar pattern in 2010 and 2011, increasing in spring with a secondary peak occurring in late summer. Maximum irradiance occurred in April 2011. Levels were less predictable in 2012 when highest light availability occurred in June, followed by a peak of similar magnitude in August. Chlorophyll peaks occurred at a similar time to increases in each of these parameters, although their magnitude was not proportional to chlorophyll intensity.

Salinity data were acquired from laboratory analysis of water samples with additional information from both probes. As previously stated in section 4.2.2, probe data were intermittent across the three year sampling period and unfortunately many of the samples collected for laboratory analysis were lost due to broken bottles. These issues resulted in a sporadic data set, with missing or minimal data for some months (Appendix II). In order to produce a coherent dataset from the available information, data from each site and technique were combined to produce a monthly average. No salinity data were available for July 2011. In this instance, data from July 2010 and July 2012 were averaged to produce an estimated value of salinity (indicated by a star marker in Figure 4.9). Turbidity data were also available from multiple sources (Appendix III) and data were again combined to produce an average value for each month (Figure 4.9). Monthly wave height indicated by the Waverider instrument buoy and rainfall during the sampling period are also shown in Figure 4.9.

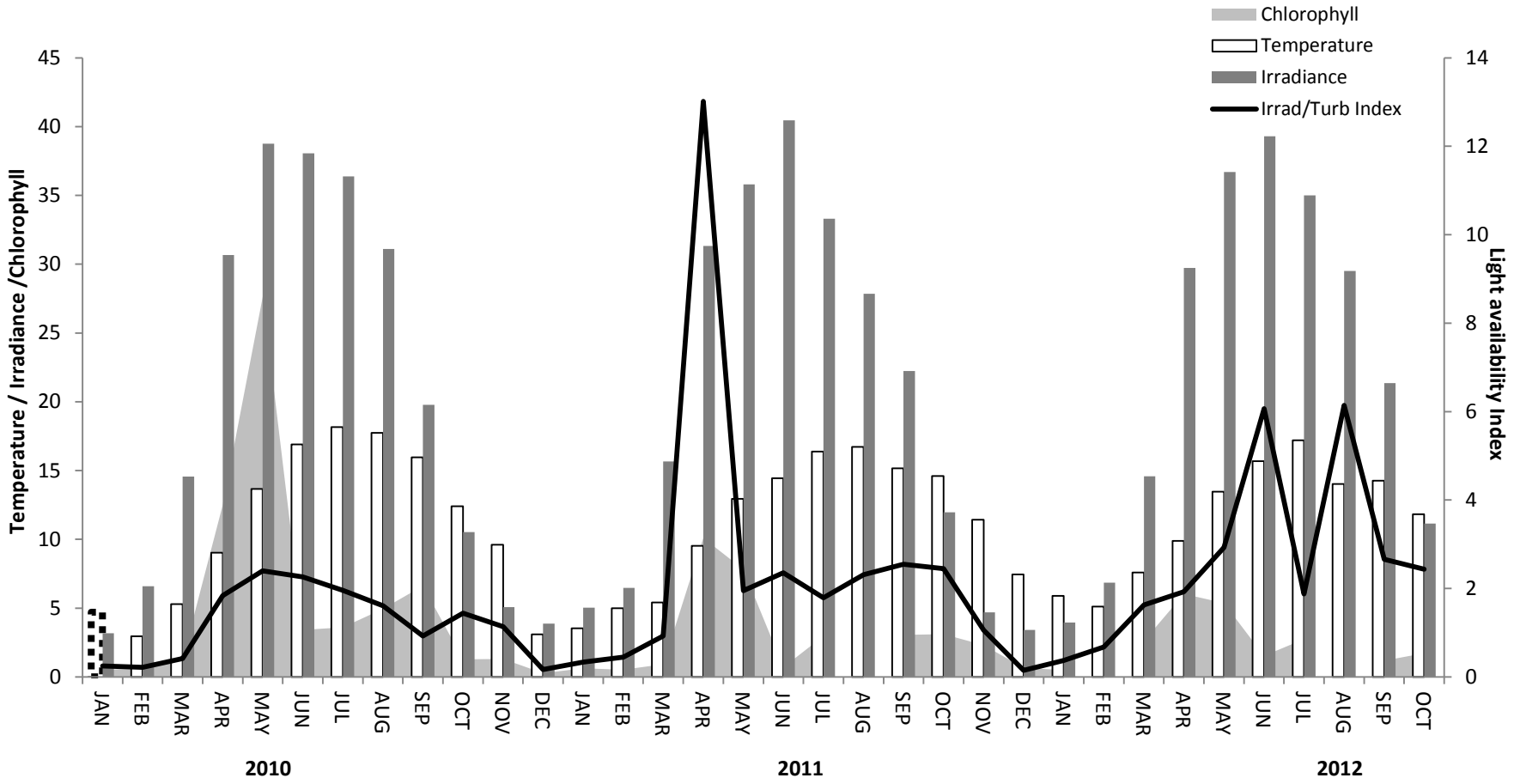

Figure 4.8. Averaged water temperature (º C), surface irradiance (mol photon/m), chlorophyll (µg/l) obtained by fluorimetry and a light availability index between January 2010 and October 2012 in the Wash Estuary.

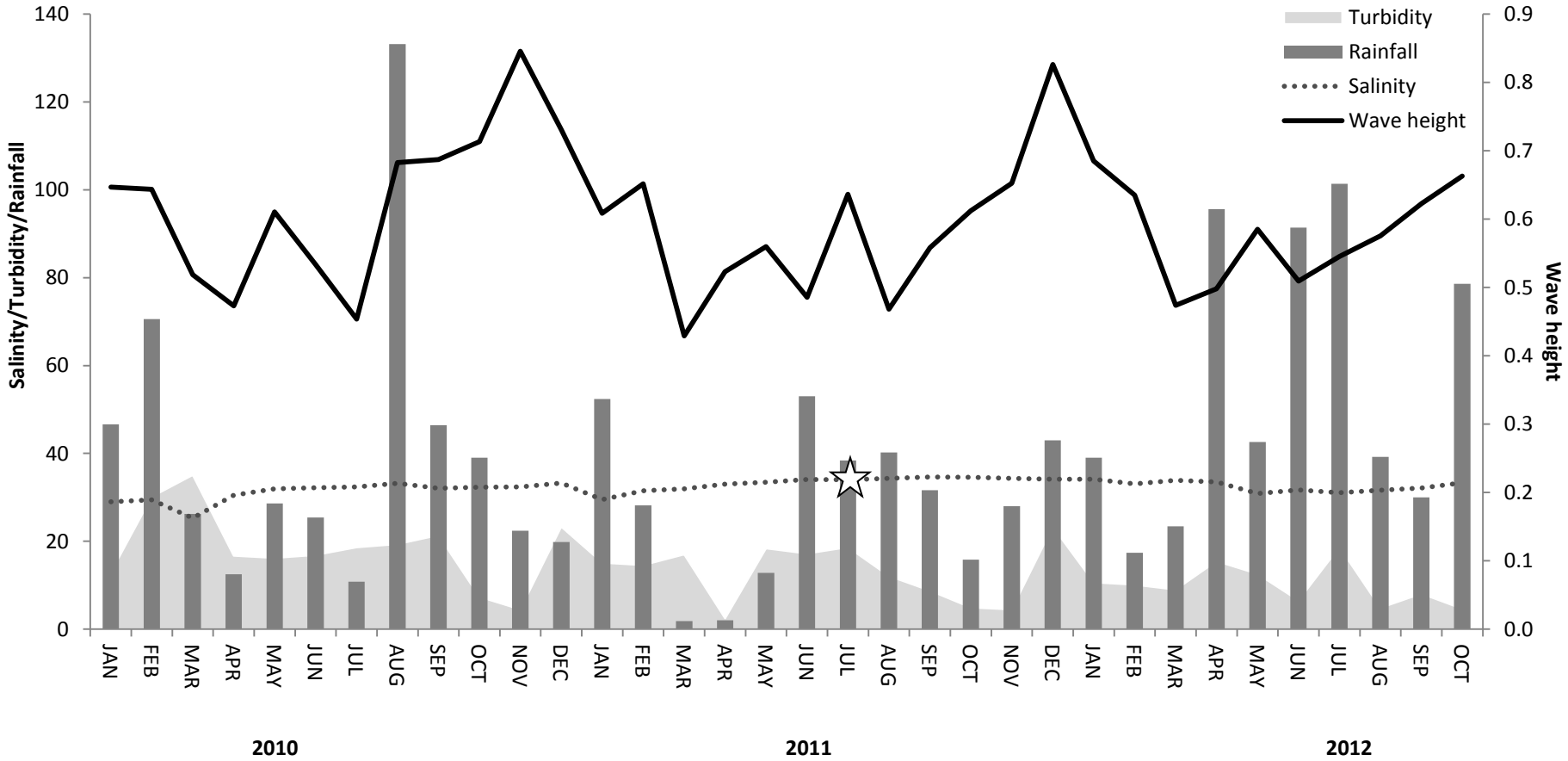

Figure 4.9. Averaged data of salinity (PSS), turbidity (NTU), rainfall (mm) and wave height (m) between January 2010 and October 2012 in the Wash Estuary. A missing data point for salinity in July 2011 was extrapolated from averaged data from corresponding months in 2010 and 2012. This data point is indicated by a star marker.

Salinity levels ranged from 25.3 PSS in March 2010 to a peak of 34.3 PSS in September 2011. Low salinity in March co-occurred with maximum turbidity levels of 35 nephelometric turbidity units (NTU), however a similar association was not observed in January 2011 when salinity fell again (29.5 PSS, 15 NTU). Turbidity patterns varied throughout the study period, with an overall peak (35 NTU) recorded in early 2010 as previously described. Turbidity was lowest in April 2011, falling to 2.4 NTU. General patterns of high turbidity during winter and early spring were recorded across all three years, although this was most noticeable in 2010. Wave height also increased during winter months, particularly in 2010 and 2011. Maximum wave height (0.85 m) was recorded in November 2010, with the lowest reading collected in March 2011 (0.43 m). Increased wave height also co-occurred with elevated rainfall, particularly in early and late summer in 2010. Rainfall within the catchment area of the Great Ouse peaked at 133 mm in August 2010 and again during April (96 mm) and July (101 mm) of 2012 (Figure 4.9). These peaks did not co-occur with high turbidity within the Wash, with one exception. In early 2010 (February-March), peak turbidity occurred after high levels of rainfall. The timing of chlorophyll peaks (Figure 4.8) did not coincide with elevated or decreased levels of salinity, wave height or rainfall, but appeared to increase after periods of high turbidity in April and May of each year.

Correlation analyses were performed on these environmental parameters in order to statistically assess any relationships between them. The variability of each parameter with chlorophyll was also tested. A weak relationship was observed between temperature and irradiance data, although this was not significant (R^2 = 0.54, p = 0.6). Chlorophyll was not found to directly correlate with any environmental parameter. Temporal and spatial variations in environmental data were tested for significance by MANOVA. Rainfall was excluded as these data only provided an approximation of potential freshwater flow into the Wash. Sampling location was not found to significantly influence environmental data. Sampling month was found to have a strong influence on environmental conditions as all four multivariate tests returned significant results (p = 0.000). Individual ANOVAs showed temperature, irradiance and wave height to vary significantly between months (p = 0.000 for each). A MANCOVA was performed to test for the influence of year on these data. Each of the four multivariate tests returned significant results

($p = 0.000$) indicating that the effect of month on temperature, irradiance and wave height remained significant after controlling for annual variation.

4.3.5. Analysis of nutrient data

NO_3, NO_2 and NH_4 concentrations were combined to produce an average concentration of total dissolved inorganic nitrogen (DIN) at each site. Nutrient data repeated similar trends at each location over the three year sampling period (Figure 4.10). Variations in the peak intensity of each nutrient across the sites are shown in Table 4.4. Nutrients were highest between January and April of each of the three years and remained low over the summer months, with the exception of PO_4 which continued to fluctuate. Silicate levels ranged from 0.34 µM in April 2010 up to a high of 91.98 µM in March 2010. Concentrations of DIN varied greatly, from 0.2 µM in July 2011 to 393.2 µM in March 2010. PO_4 levels showed the lowest range, from 0.07 µM in May 2012 to a maximum of 3.11 µM in January 2012.

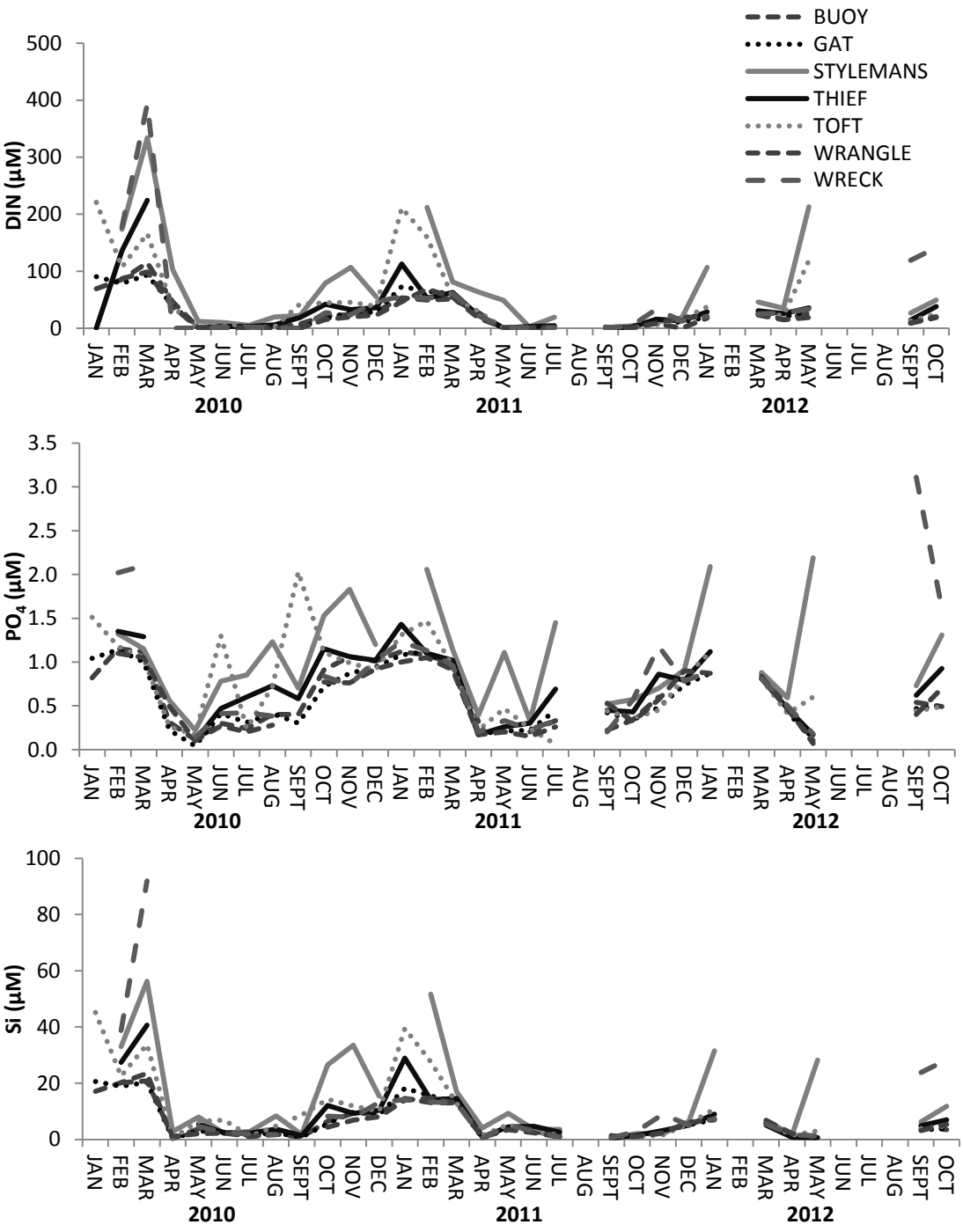

Figure 4.10. Variations in dissolved organic nitrogen (DIN), consisting of NO_3, NO_2 and NH_4, phosphate (PO_4) and silicate at each site between 2010 and 2012.

Table 4.4. Minimum (Min) and maximum (Max) values (µM) for DIN, PO_4 and Si across each of the seven sampling sites for 2010, 2011 and 2012.

		DIN		PO_4		Si	
Year	Month	Min	Max	Min	Max	Min	Max
2010	January	90.32	220.97	0.82	1.51	17.09	20.63
	February	78.36	177.14	1.1	2.02	18.93	38.71
	March	93.52	393.19	1	2.1	20.3	91.98
	April	36.98	102.94	0.22	0.56	0.34	2.81
	May	0.3	11.6	0.04	0.22	2.12	7.95
	June	1.39	9.73	0.27	1.3	2.12	6.92
	July	0.65	5.03	0.2	0.85	1.05	2.84
	August	0.52	19.94	0.28	1.23	1.65	8.42
	September	1.06	42.4	0.3	2.03	0.83	8.71
	October	15.17	79.13	0.72	1.53	4.4	26.53
	November	19.87	106.58	0.74	1.83	7.91	33.56
	December	23.03	54.88	0.94	1.2	8.1	15.39
2011	January	46.22	211.17	1.00	1.43	13.98	39.48
	February	49.25	212.13	1.05	2.06	13.09	51.70
	March	51.19	80.90	0.91	1.14	12.76	16.91
	April	18.09	63.88	0.17	0.39	0.45	2.05
	May	0.51	48.91	0.20	1.11	3.99	9.28
	June	0.79	2.98	0.15	0.33	2.37	4.67
	July	0.20	19.06	0.06	1.45	0.87	2.56
	September	0.50	2.46	0.20	0.52	0.54	1.28
	October	0.56	3.72	0.32	0.57	0.99	2.97
	November	5.77	32.88	0.45	1.18	1.60	9.00
	December	11.49	18.91	0.74	0.91	5.07	6.38
2012	January	17.88	106.72	0.86	2.09	6.73	31.52
	March	23.20	45.76	0.81	0.88	5.12	6.79
	April	14.98	35.02	0.41	0.59	0.81	2.14
	May	18.83	213.04	0.07	2.19	0.47	28.27
	July	8.53	37.83	0.18	0.71	4.64	9.88
	September	8.72	119.16	0.40	3.11	3.21	23.80
	October	18.58	141.13	0.49	1.61	3.46	11.77

Relationships between nutrients were tested and a significant correlation was recorded between DIN and Si ($R^2 = 0.88$. $p = 0.000$), shown in Figure 4.11.

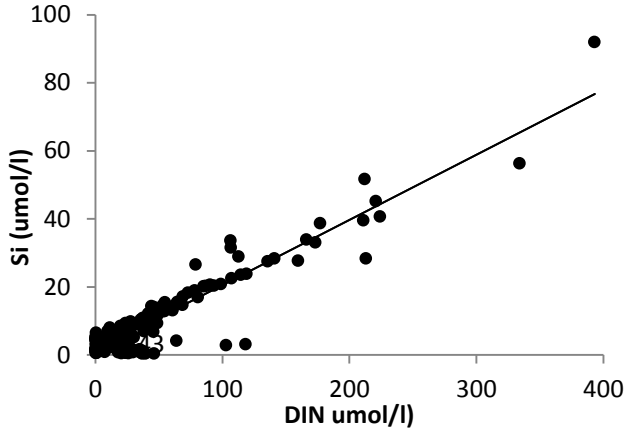

Figure 4.11. Relationship between dissolved inorganic nitrogen (DIN) and silicate (Si) in the Wash estuary between 2010 and 2012 (R^2 = 0.88. p = 0.000).

Temporal and spatial variations in environmental data were tested for significance by MANOVA. Sampling location was not found to significantly influence variations in nutrient concentrations. Averaged monthly nutrient data for the Wash were therefore produced by combining data from each of the seven sampling sites. Peaks in both DIN and Si were closely followed by peaks in chlorophyll derived from fluorimetric analysis, particularly in early 2010 and 2011 (Figure 4.12).

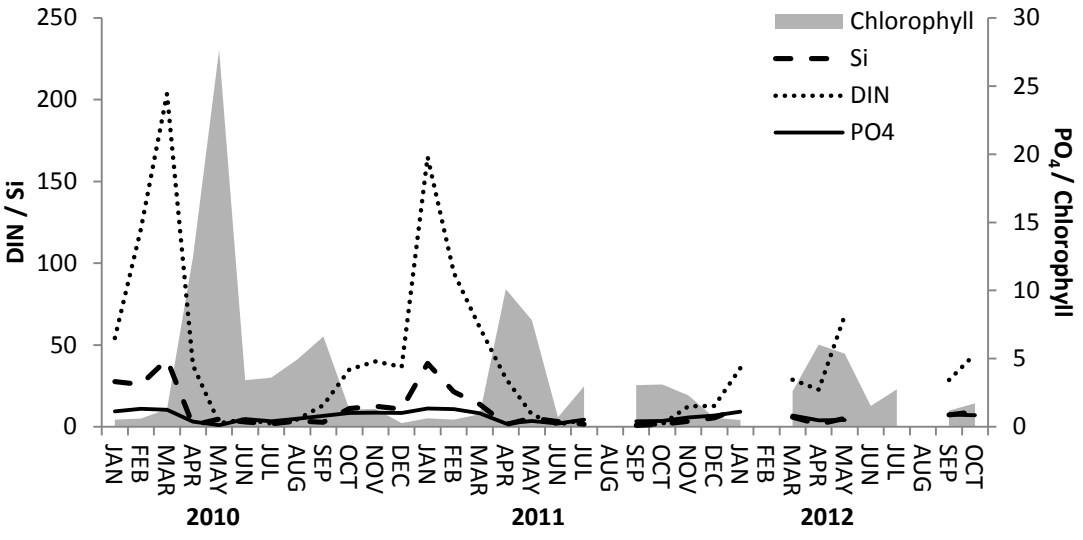

Figure 4.12. Averaged values for dissolved inorganic nitrogen (DIN), phosphate (PO_4) and silicate (Si) (µM) for all seven sampling sites shows negative correlation with chlorophyll derived by fluorimetry (µg/l).

A second MANOVA was performed in order to test the influence of sampling time on nutrient levels. All four multivariate tests were highly significant ($p = 0.000$), indicating that month exerted strong control over nutrient levels. Step-down ANOVAs showed that each nutrient varied significantly by month ($p = 0.000$). A MANCOVA was performed to test for the influence of annual variation on monthly nutrient levels. Data remained significant (for all four tests $p = 0.000$), indicating that month was the controlling factor on nutrient levels within the Wash.

4.3.6. Comparison of environmental and nutrient data

Relationships between environmental and nutrient data were assessed by PCO. Correlation analyses indicated a clear association between DIN and Si, therefore these variables were combined into a single group in order to reduce components in the following analyses. Similarly, turbidity and irradiance measurements were replaced by the light availability index previously described, further reducing the experimental components. A strong relationship was observed between water temperature and light availability, with some association noted between DIN and PO_4 (Figure 4.13). Temperature and salinity appeared to control the majority of variation across the three year sampling period, with all five parameters accounting for 76% of total variation. These data were then assessed by PERMANOVA. Data were grouped by season prior to analysis in order to balance the model and ensure the robustness of this statistical procedure. Significant variation in environmental and nutrient data was observed by both season and year (both $p = 0.001$), whilst sampling location was not found to influence variance.

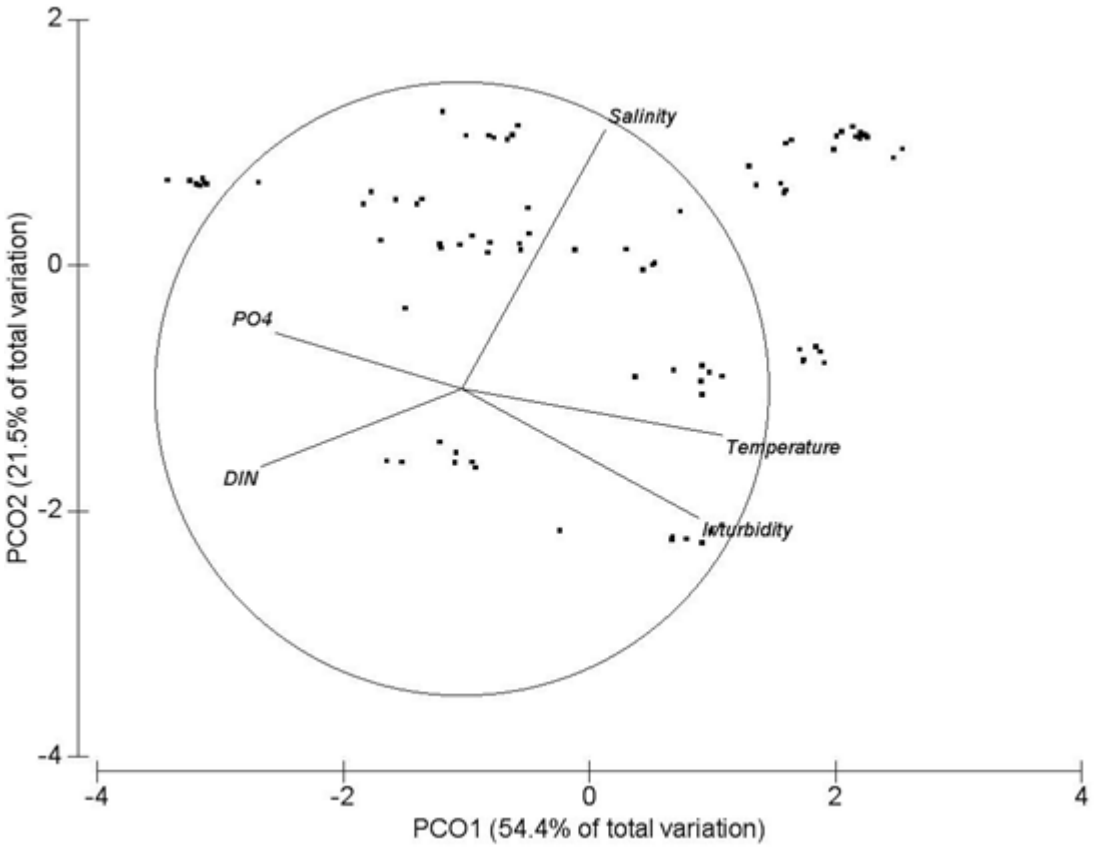

Figure 4.13. Principal coordinates analysis (PCO) plot with environmental parameters overlaid as vectors, indicating the associations between temperature and light availability (Irr/turbidity) and DIN and PO_4 within data.

4.3.7. Comparison of RFL and chlorophyll measurements

Measurements of RFL by flow cytometry, chlorophyll data derived from fluorimetry and chl *a* measured by HPLC were averaged by month and compared. Each of the three separate techniques recognised clear data peaks which occurred annually in May and which were particularly notable during 2010 and 2011 (Figure 4.14). A smaller secondary peak was also recorded in late summer (August-September).

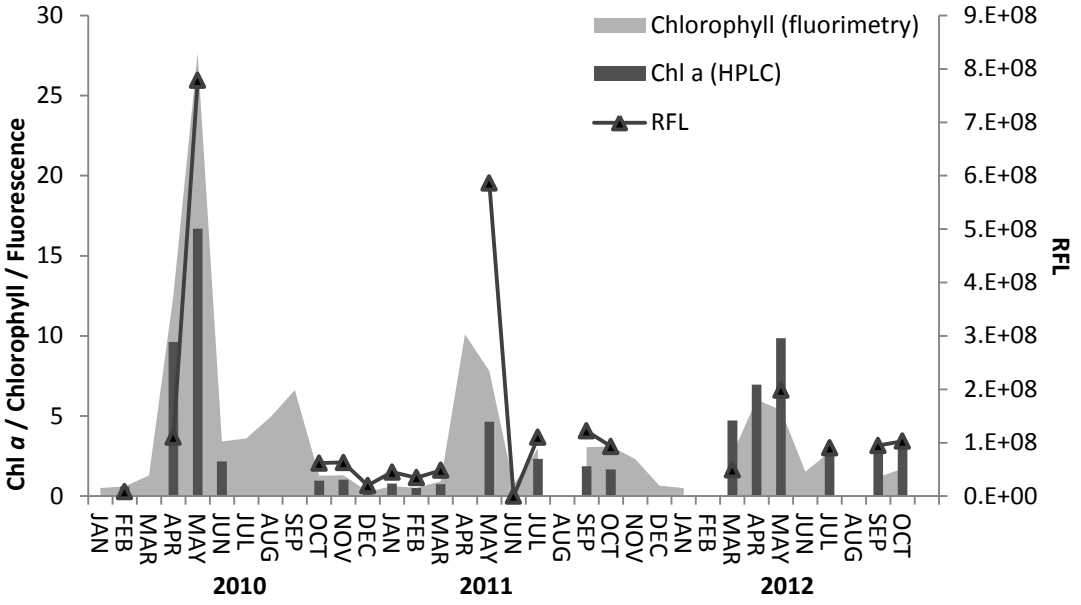

Figure 4.14. Monthly averages of red fluorescence measured by *in-situ* sonde measurements, chlorophyll *a* (chl *a*) measured by HPLC analysis (µg/l), chlorophyll content determined by fluorimetry (RFU) and red fluorescence (RFL) determined by flow cytometry (mV/ml) from 2010 to 2012.

Chl *a* concentrations measured by HPLC were approximately half of chlorophyll values observed by fluorimetry (Figure 4.14). This was expected, and was due to differences in technique sensitivity. HPLC analysis allows differentiation between chlorophyll *b* (chl *b*) and chl *a*. This is not possible with fluorimetry, resulting in higher values of total chlorophyll. Further examination of RFL and HPLC chl *a* data by site and month indicated clear separation of data collected in May 2010 and 2011 from other months across the three year sampling period (Figure 4.15). Data from the Stylemans site in May 2010 are notably isolated from the other sites at that time.

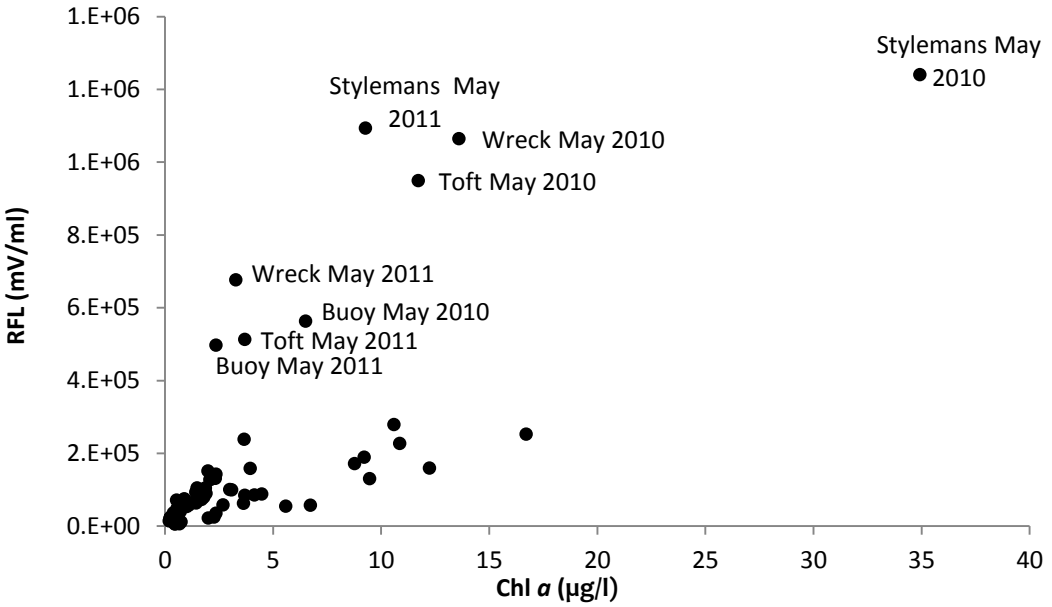

Figure 4.15. Relationship between total red fluorescence (RFL) measured by flow cytometry and chl *a* measured by high performance liquid chromatography (HPLC).

4.3.8. Flow cytometric analysis of phytoplankton distribution and diversity

Flow cytometric cluster data were combined into five PFT based on cell size and fluorescence emissions. These were: orange picophytoplankton, red picophytoplankton, red nanoplankton, orange nanoplankton, and microplankton. These categories were selected as the remaining PFT were considered sub-categories of these divisions, e.g. red picophytoplankton group 1 and red picophytoplankton group 2 were reduced to a single red picophytoplankton group. This decrease in taxonomic resolution was necessary to establish general overall patterns of biomass distribution within the Wash. Relative contributions of RFL (%) by each PFT were used as an indicator of their biomass. Data from each of the seven different sampling locations were not found to be significantly different and were therefore treated as replicates (n = 7) for each month. Monthly RFL variations in PFT were assessed by MANOVA and were found to be significant ($p = 0.000$ for all four multivariate analyses). Step-down ANOVAs were used to further examine the influence of month on each PFT, with high significance found for all five ($p = 0.000$ for all). A MANCOVA was used to examine whether monthly variation remained significant after consideration of annual variation. All four multivariate tests again returned

highly significant results ($p = 0.000$ for all), indicating that month strongly impacted temporal PFT contribution and was not influenced by annual variation. These analyses were repeated using year as the independent variable. All multivariate tests again returned significant results ($p = 0.000$). Separate ANOVAs revealed year had a significant effect on all PFT (orange picophytoplankton $p = 0.035$, all other PFT $p = 0.000$). A MANCOVA controlling for the effect of month showed significant results in each multivariate test ($p = 0.000$ for all). It can therefore be concluded that PFT contributions to RFL and therefore biomass in the Wash estuary were significantly different on both monthly and annual timescales. This variation was further investigated by MDS and PERMANOVA. Monthly RFL data were grouped by season (spring and autumn) in order to create a balanced model. A 2-D ordination plot (stress = 0.07) revealed the presence of distinct data clusters, representing differing PFT composition. Data collected during autumn months across all three years show similar PFT structure (Figure 4.16a), whilst data collected in spring shows much greater variability ($p = 0.001$). Examination by year revealed data from 2010 to show the widest variation in PFT (Figure 4.16b). RFL data from 2011 showed slightly more comparability, whilst data from 2012 showed the most homogeneity in PFT throughout the sampling year ($p = 0.036$).

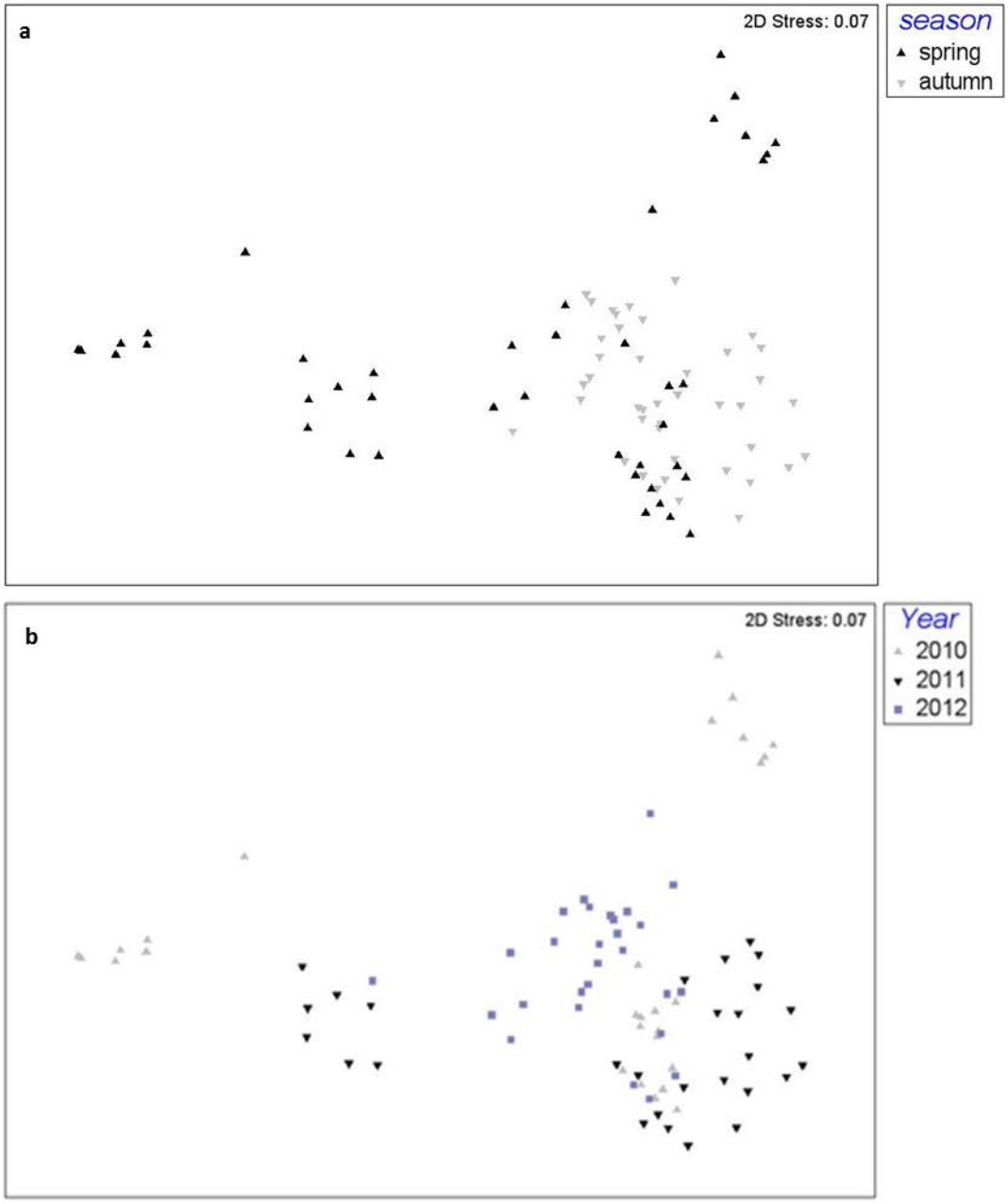

Figure 4.16. Multidimensional scaling (MDS) of the relative abundance of PFT represented visually in a two dimensional ordination plot. Distribution similarities across the Wash estuary are show by season (a) and by year (b).

The diversity of these 5 PFT was investigated using absolute data (RFL mV/ml) in order to permit greater resolution of distributions specific to different months and years. Assessment by PCO showed PFT present in May 2010 and 2011 to be very distinct from those recorded throughout the rest of the three year sampling period, accounting for close to 20% of total variation (Figure 4.17).

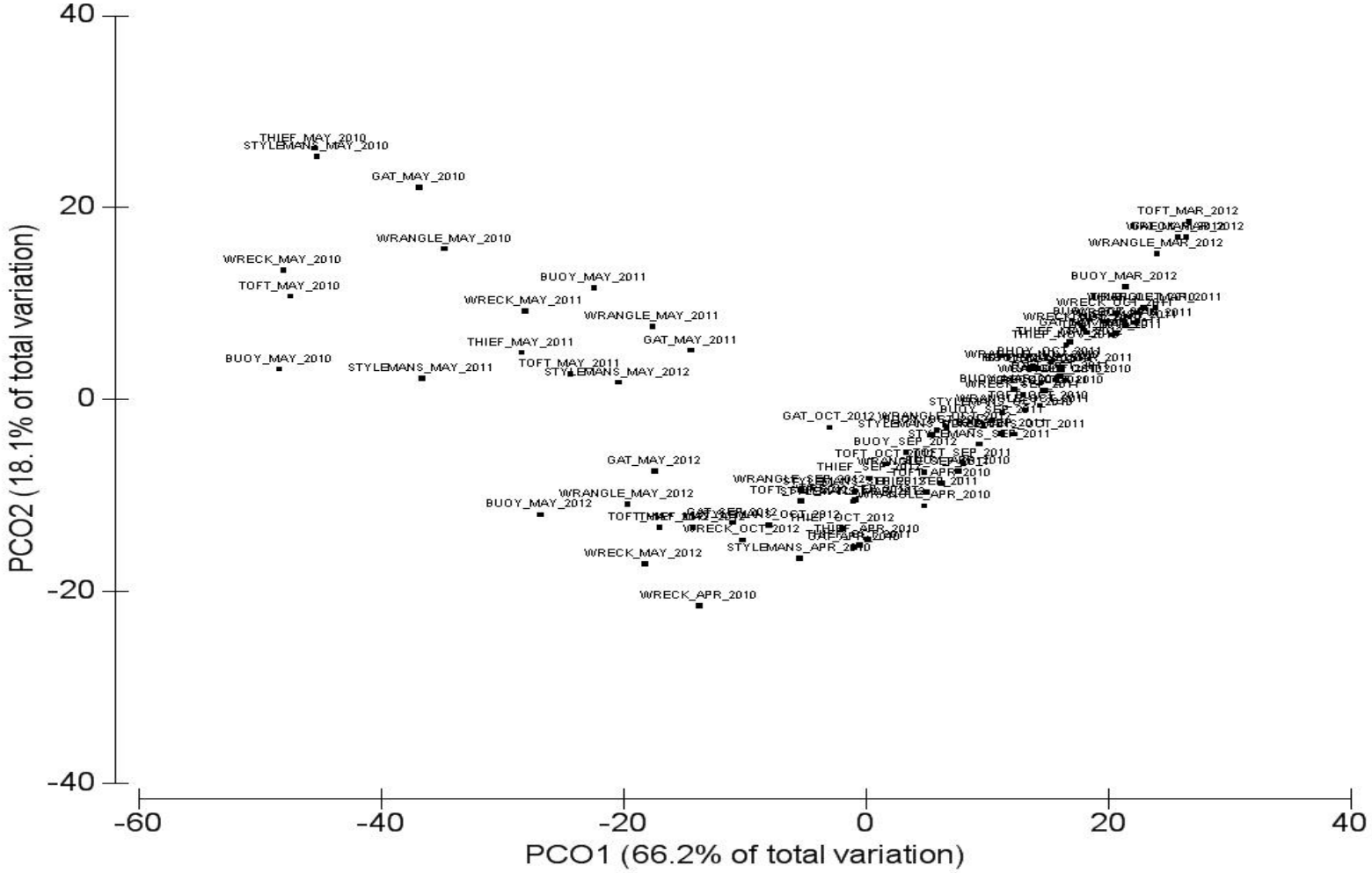

Figure 4.17. Principal coordinates analysis (PCO) plot of absolute values of total red fluorescence (RFL) representing diversity of the five main phytoplankton

Further assessments of phytoplankton diversity were performed on proportional data (% RFL) from all 12 PFT. A measure of monthly phytoplankton diversity was derived from the Shannon index (*H'*) and compared against total chl *a* acquired by HPLC (Figure 4.18). A pattern of low diversity during March to May, followed by increased diversity over summer and winter months was seen in both 2010 and 2011. During 2012, community diversity was more constant, falling only slightly during May. Diversity correlated negatively with chl *a*, particularly in May 2010 when chl *a* reached the highest levels observed across the three year sampling period.

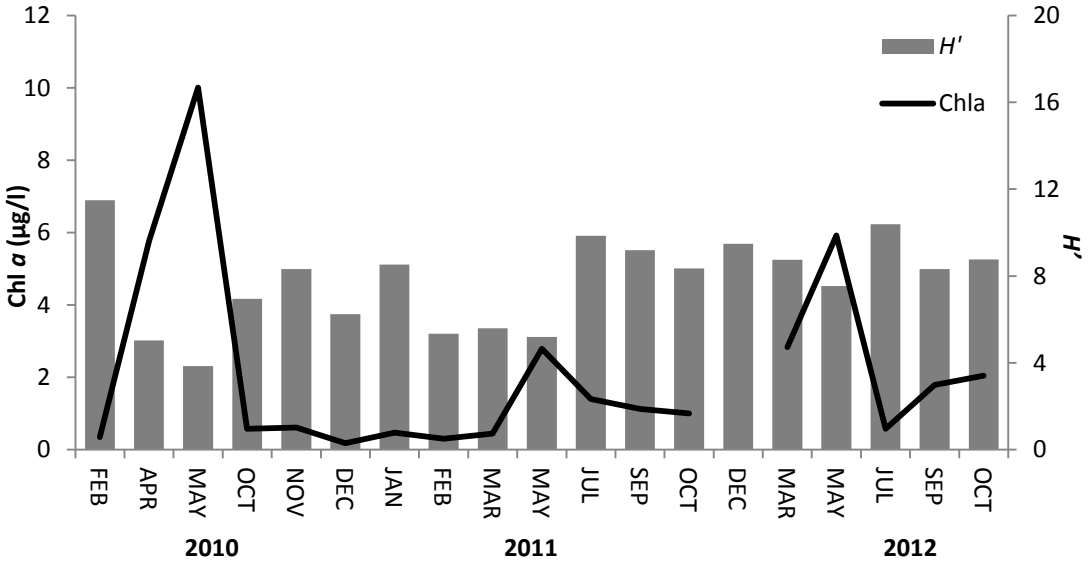

Figure 4.18. Comparison between phytoplankton diversity derived using the Shannon Index (*H'*) calculated from the total red fluorescence of each of the 12 phytoplankton functional types (PFT), and chlorophyll *a* concentration (chl *a*) derived from HPLC analyses during February 2010 and October 2012.

Peak chlorophyll and therefore phytoplankton blooms occurred in May of each year. The structure of phytoplankton bloom communities was different each year. Analysis of the 12 different PFT showed lowest diversity in May 2010, increasing through 2011 with the highest diversity observed in May 2012 (Figure 4.19). In 2010, the bloom population was dominated by red nanoplankton groups 1 and 2, which jointly contributed 96% to total RFL. Microplankton were present, but contributed on average only 4% of total RFL.

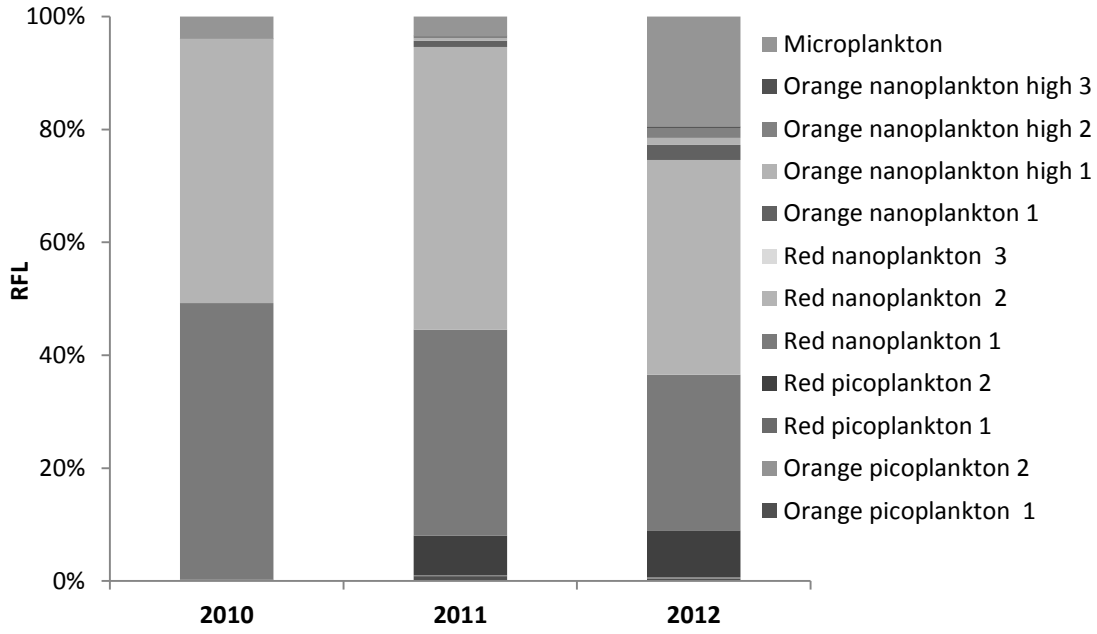

Figure 4.19. The relative contributions of the twelve phytoplankton functional types (PFT) to total red fluorescence (RFL) during May 2010, 2011 and 2012.

During analysis of samples from May 2010, water samples were observed to contain a colonial species consisting of cells contained within a sticky matrix, causing aggregation of debris and other cells observable with the naked eye.
This was noted during on board 200 µm filtration of water samples, and also in the laboratory due to repeated blockages within the flow cytometer during analysis. Further examination of these water samples by light microscopy identified these cells as a colonial form of *Phaeocystis*, most likely *P. globosa* (Hasle et al. 1997). In May 2011, red nanoplankton groups continued to dominate total RFL (87%) but to a slightly lesser extent than in 2010. Bloom diversity slightly increased, with total RFL contributions from both red picophytoplankton group 2 (7%) and microplankton (3%). RFL contributions were clearly most diverse in May 2012, when input from the largest number of different phytoplankton clusters was recorded. Whilst red nanoplankton groups 1 and 2 still supplied over half of total RFL (66%), microplankton were more dominant than in previous years (19%). Red picophytoplankton group 1 again made fluorescence contributions (8%), and there

were more notable contributions from orange nanoplankton groups (6%) than in 2010 and 2011.

4.3.9. Phytoplankton community pigment analysis by HPLC

Data on chl *a* and phaeopigments (chlorophyllide, pheophorbide and pheophytin) were removed from the HPLC dataset to allow investigation of accessory pigment diversity. The pigments croccoxanthin and antheraxanthin were present very infrequently and only in trace quantities (< 0.0001 µg/l) and were also removed from further analysis. A brief description of the diagnostic properties of the remaining accessory pigments analysed is supplied in Table 4.5. Similarly to previous datasets, sampling location did not significantly influence pigment abundances. A MANOVA was used to assess shifts in monthly pigment composition. Each of the four multivariate tests returned significant results (Pillai's Test $p = 0.009$, all other tests $p = 0.000$), indicating that pigment distributions were strongly influenced by month. The effect of month on each pigment was tested individually by ANOVA (Table 4.6) and was found to be significant in all pigments apart from dinoxanthin.

Table 4.5. A summary of microalgal pigments common to coastal waters identifiable by high performance liquid chromatography (Jeffrey et al. 2011).

Class	Division	Chlorophylls (chl)	Carotenoids
Cyanophyceae	Cyanophyta	chl *a*	Zeaxanthin, β,β-carotene myxoxanthophyll
Rhodophyceae	Rhodophyta	chl *a*	Zeaxanthin β,β-carotene
Bacillariophyceae	Heterokontophyta	chl *a*, chl c_1, chl c_2, chl c_3	Fucoxanthin, diadinoxanthin, diatoxanthin, β,β-carotene, occasionally 19'-butanoyloxyfucoxanthin
Chrysophyceae	Heterokontophyta	chl *a*, chl c_1, chl c_2	Fucoxanthin, violaxanthin, zeaxanthin, β,β-carotene
Dictyochophyceae	Heterokontophyta	chl *a*, chl c_1, chl c_2, chl c_3	Fucoxanthin, β,β-carotene, diadinoxanthin, diatoxanthin, 19'-butanoyloxyfucoxanthin, violaxanthin, zeaxanthin
Eustigmatophyceae	Heterokontophyta	chl *a*	Violaxanthin, zeaxanthin, β,β-carotene
Pelagophyceae	Heterokontophyta	chl *a*, chl c_2, chl c_1, chl c_3 variable	Diadinoxanthin, diatoxanthin, fucoxanthin 19'-butanoyloxyfucoxanthin, gyroxanthin-diester
Raphidophyceae	Heterokontophyta	chl *a*, chl c_1, chl c_2	Fucoxanthin, violaxanthin, zeaxanthin, β,β-carotene
Pavlovophyceae	Haptophyta	chl *a*, chl c_1, chl c_2	Fucoxanthin, diadinoxanthin, diatoxanthin β,β-carotene
Prymnesiophyceae	Haptophyta	chl *a*, chl c_3, chl c_2, chl c_1	Fucoxanthin, diadinoxanthin, diatoxanthin, β,β-carotene, 19'-butanoyloxyfucoxanthin, gyroxanthin-diester, 19'-hexanoyloxyfucoxanthin
Crytptophyceae	Cryptophyta	chl *a*, chl c_2	Alloxathin, crocoxanthin
Dinophyceae	Dinophyta	chl *a*, chl c_2	Peridinin in many species, other pigments depend on endosymbionts (e.g. haptophytes, diatoms, cryptophytes, prasinophytes)
Euglenophyceae	Euglenophyta	chl *a*, chl *b*	Diadinoxanthin, diatoxanthin, β,β-carotene
Chlorarachniophyceae	Chlorarachniophyta	chl *a*, chl *b*	Neoxanthin, violoxanthin, lutein, β,β-carotene, zeaxanthin
Chlorophyceae	Chlorophyta	chl *a*, chl *b*	Lutein, violoxanthin, neoxanthin, β,β-carotene, zeaxanthin
Prasinophyceae	Prasinophyta	chl *a*, chl *b*	Lutein, violoxanthin, neoxanthin, β,β-carotene, zeaxanthin, prasinoxanthin

Table 4.6. ANOVA results showing the significant influences of month and year on HPLC accessory pigments.

	Month		Year	
Pigment	**df**	**Sig.**	**df**	**Sig.**
Chlorophyll c_3	10	.000*	2	.031
Chlorophyll c_2	10	.000*	2	.197
Chlorophyll c_1	10	.000*	2	.000*
Peridinin	10	.006*	2	.031
19–but-fucoxanthin	10	.000*	2	.265
Fucoxanthin	10	.000*	2	.056
Neoxanthin	10	.000*	2	.055
Prasinoxanthin	10	.000*	2	.004*
Violaxanthin	10	.000*	2	.529
19-hex-fucoxanthin	10	.000*	2	.000*
Astaxanthin	10	.000*	2	.000*
Diadinoxanthin	10	.001*	2	.309
Myxoxanthophyll-like	10	.031*	2	.005*
Dinoxanthin	10	.059	2	.000*
Alloxanthin	10	.000*	2	.210
Diatoxanthin	10	.000*	2	.576
Zeaxanthin	10	.000*	2	.865
Lutein	10	.000*	2	.982
Gyroxanthin-diester	10	.003*	2	.276
Chlorophyll *b*	10	.005*	2	.037*
$\alpha + \beta$ carotene	10	.013*	2	.159

*** Indicates significant results**

The effect of month on pigment data was further tested by MANCOVA, controlling for annual variation by using year as a covariate factor. All four multivariate tests again returned significant results ($p = 0.000$). A second MANOVA was conducted to assess whether pigment composition also varied on an annual basis. All multivariate tests were significant ($p = 0.000$) indicating pigments differed between years. The influence of year on individual pigments was further examined by ANOVA. A significant effect was found on seven of the twenty one pigments tested (Table 4.5). These temporal variations in pigment abundance were further investigated by MDS and PERMANOVA. Monthly

HPLC data were grouped by season (spring and autumn) to prevent data imbalance within the model. A 2-D ordination plot (stress = 0.08) revealed high variation throughout spring in comparison to the relatively similar pigment composition observed in autumn (Figure 4.20a, p = 0.001).

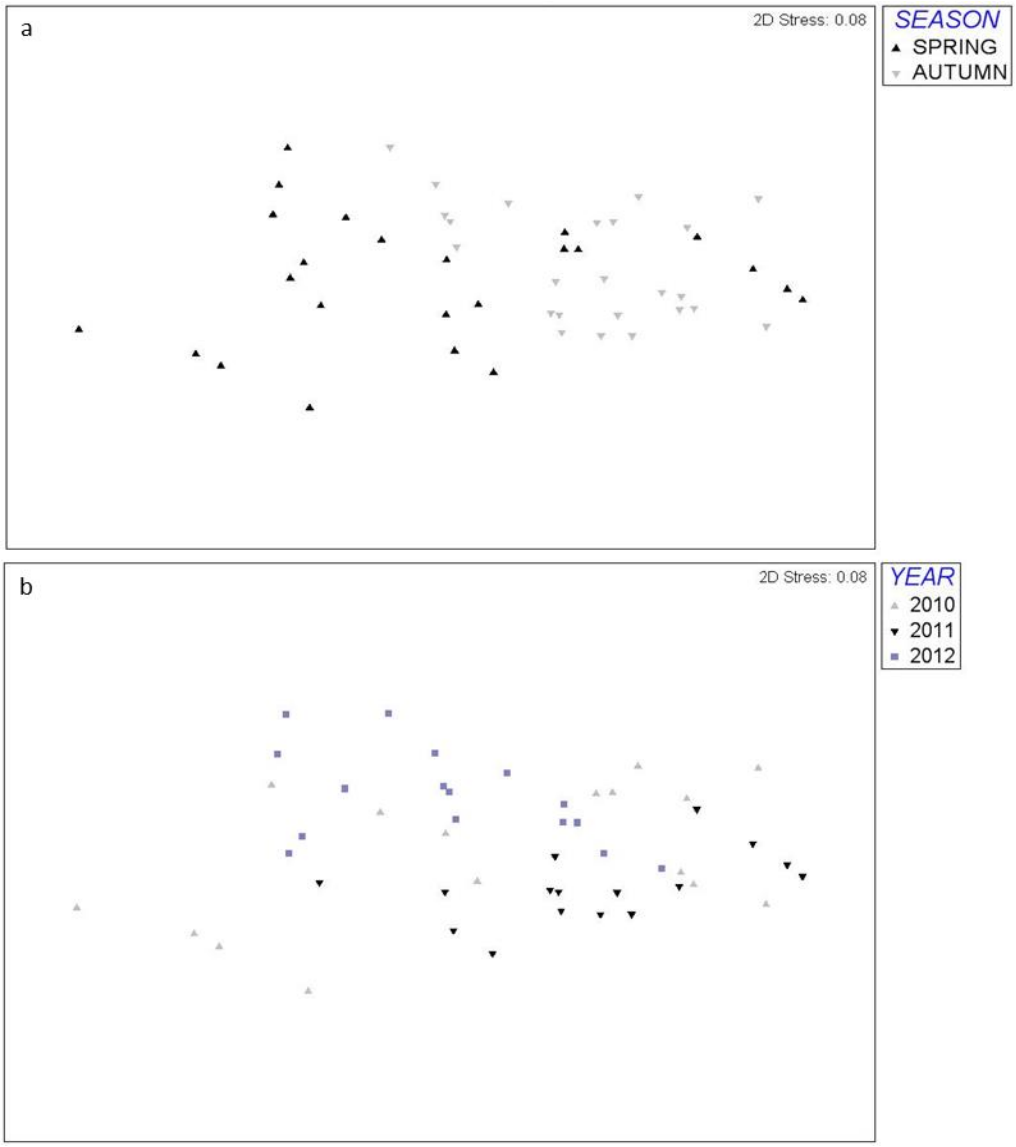

Figure 4.20. Multidimensional scaling (MDS) of phytoplankton accessory pigment composition represented visually in a two dimensional ordination plot. Distribution similarities across the Wash estuary are show by season (a) and by year (b).

Data from 2010 again exhibited the greatest variation and highest dissimilarity from the other two years, with greatest similarities across pigment data recorded in 2012 (Figure 4.20b, p = 0.001). Pigment data were also analysed by PCO, which like the flow cytometry data again revealed data from May 2010 to be distinct not only from the rest of the dataset (Figure 4.21), but also from the other years, accounting for 12% of total described variation (75%).

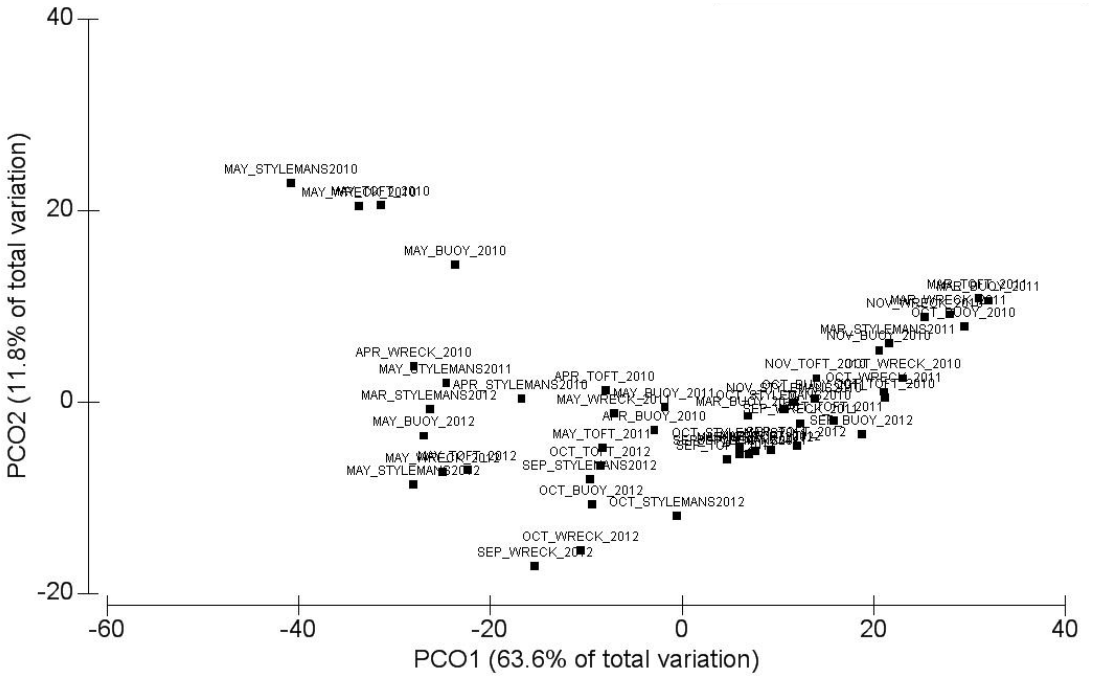

Figure 4.21. Principal coordinates analysis (PCO) plot of phytoplankton accessory pigment diversity within the Wash Estuary. Data from May 2010 and 2011 account for ~12% of total variation within the dataset.

The relative contributions (%) of each pigment were used to assess their abundance in May of each year (Figure 4.22). During May 2010 and 2011 there was little variation in pigment concentrations across sites. In May 2010, pigments were dominated by fucoxanthin (52%) and chlorophylls c_2 (16%) and c_3 (19%). There were small contributions from 19-hex-fucoxanthin (2%) and diadinoxanthin (5%). Pigments in May 2011 showed a similar pattern. Fucoxanthin again dominated (55%) with chlorophylls c_2

(12%) and c_3 (8%). Minor pigment contributions were more varied than in 2010, with input from prasinoxathin (3%), diadinoxanthin (6%), chlorophyll *b* (5%) and α + β carotene (4%). May 2012 exhibited highest pigment diversity, and also the most variation between sites during May of the three years. The principal pigment groups of fucoxanthin (54%) and chlorophyll c_2 (12%) remain, however chlorophyll c_3 is reduced (3%). Further contribution were made by diadinoxanthin (7%), α + β carotene (6%), chlorophyll *b* (5%) and alloxanthin (4%).

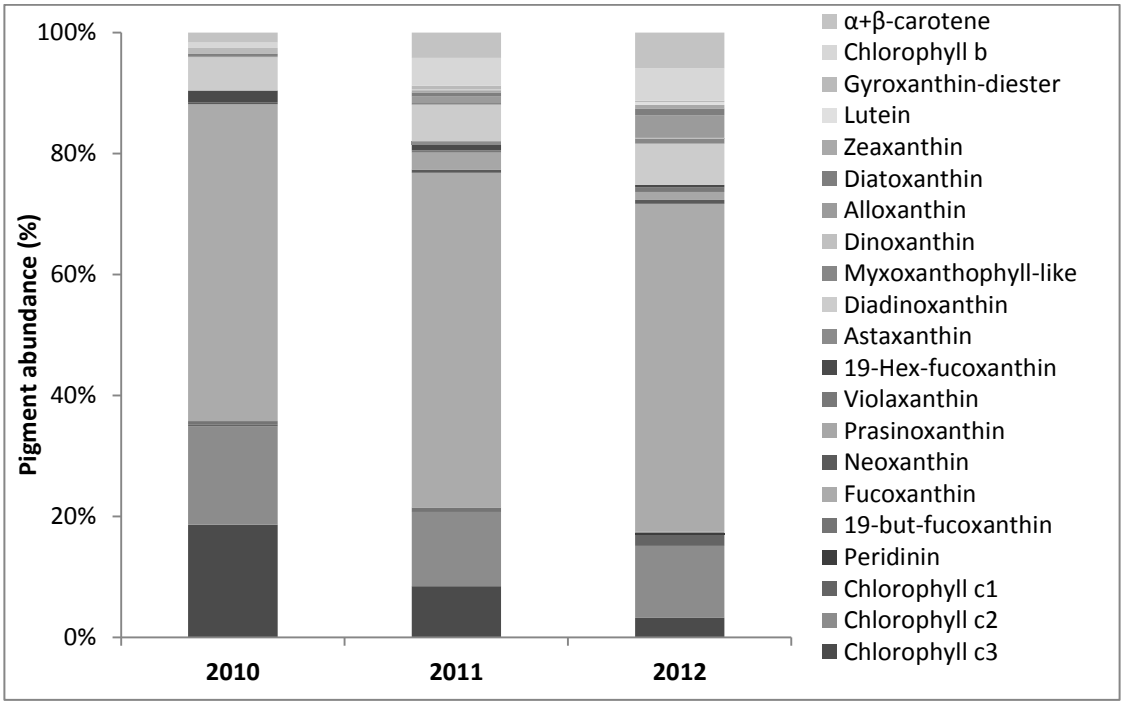

Figure 4.22. The relative contributions of accessory pigments in the Wash estuary during May 2010, 2011 and 2012.

4.3.10. Comparison of flow cytometric and HPLC data

Both flow cytometry and HPLC are techniques which analyse pigments contained within phytoplankton cells. Whilst flow cytometry can also supply data on cell size, HPLC offers taxonomic resolution to phytoplankton communities through the use of

diagnostic pigment analyses. Correlations between PFT and accessory pigment data would therefore be mutually beneficial to each technique and increase their utility and investigative strength. Relationships between accessory pigment data measured by HPLC and PFT total RFL data were tested by linear regression. No significant relationships were observed between orange picophytoplankton or microplankton and any accessory pigments. Red picophytoplankton correlated with chl *b* ($R^2 = 0.40$, $p = 0.025$), orange picophytoplankton correlated with alloxanthin ($R^2 = 0.40$, $p = 0.000$) and red nanoplankton correlated with six different accessory pigments (Table 4.7).

Table 4.7. Significant correlations between accessory pigments and three phytoplankton functional types (PFT).

Group	Cell abundance (per ml)	FWS Cell size (µm)	RFL (mV/ml)
Orange picoplankton 1	0.427	0.266	0.000*
Orange picoplankton 2	0.458	0.478	0.186
Red picoplankton 1	0.004*	0.297	0.026*
Red picoplankton 2	0.357	0.155	0.008*
Orange nanoplankton 1	0.454	0.000*	0.005*
Red nanoplankton 1	0.024*	0.001*	0.030*
Red nanoplankton 2	0.076	0.429	0.008*
Red nanoplankton 3	0.281	0.272	0.070
Orange nanoplankton high 1	0.001*	0.000*	0.084
Orange nanoplankton high 2	0.008*	0.000*	0.071
Orange nanoplankton high 3	0.000*	0.001*	0.027*
Microplankton	0.462	0.377	0.029*

4.3.11. Relating environmental parameters to phytoplankton distributions

MDS analyses were performed in order to determine which environmental or nutrient factors most influenced phytoplankton communities. These variables were overlaid onto ordination plots as vectors in order to visualise their influence. PERMANOVA were

conducted in order to assess the significance of these relationships. Significant seasonal variations in RFL ($p = 0.002$) were driven by a variety of factors during spring with temperature and light availability causing the majority of this variation, whilst DIN and salinity were also influential (Figure 4.23a).

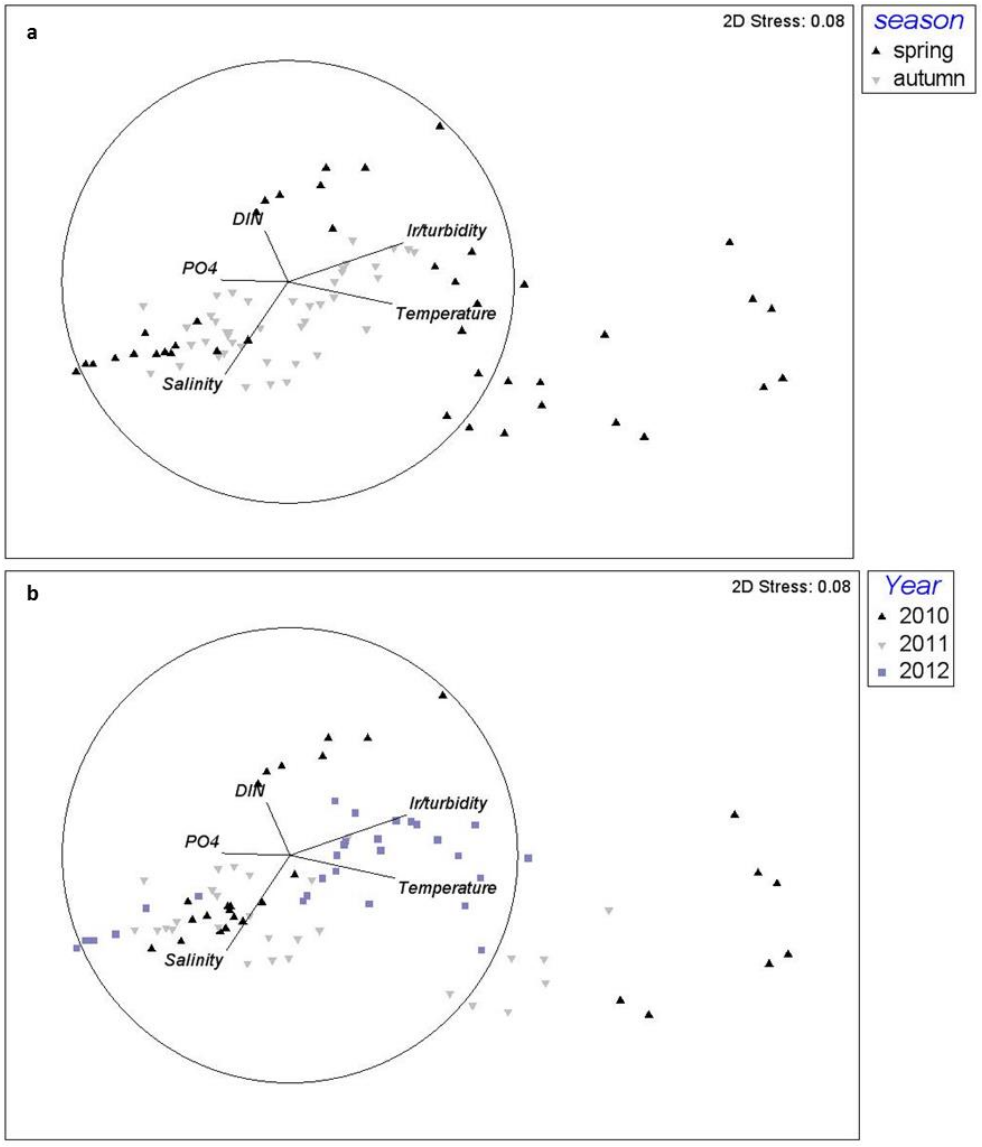

Figure 4.23. Multidimensional scaling (MDS) of the parameters influencing variation in seasonal (a) and annual (b) phytoplankton biomass in the Wash estuary from 2010 to 2012.

Spring phytoplankton biomass was not linked to PO_4 availability. Phytoplankton biomass during autumn was less variable, and appeared to be driven principally by salinity, with some influence from temperature, light availability and PO_4. In comparison, DIN availability appeared to have little impact. Variations in annual biomass ($p = 0.024$) were controlled principally by salinity and DIN in 2010, although much variation remained unexplained by these parameters (Figure 4.23b). Similarly large intra annual variation was observed in 2011 and this was again controlled by salinity, with additional input from PO_4 and to a lesser extent, temperature. Biomass data from 2012 showed the least variation and were also the most well explained, as both light availability and temperature were clearly influential in this year.

4.4. Discussion

Glutaraldehyde preservation of phytoplankton cells as described by Vaulot et al. (1989) significantly influenced the accuracy of the analysis. Alterations to cell concentrations, total RFL and size were observed in preserved samples. Further analysis revealed the impacts of preservation to be variable across PFT, with significant reductions in total RFL observed in orange picophytoplankton group 1, red picophytoplankton groups 1 and 2, red nanoplankton groups 1 and 2, orange nanoplankton group 1, orange nanoplankton high group 3 and microplankton. This is in contrast to observations of increased RFL in cultured species after fixation reported by Vaulot et al. (1989), but in agreement with the results on preserved environmental samples studied by Sato et al. (2006). Cell concentrations were affected in red picophytoplankton group 1, red nanoplankton group 1 and orange nanoplankton high groups 1-3; and cell size alterations were observed in orange nanoplankton group 1, red nanoplankton group 1 and orange nanoplankton high groups 1-3. Nanoplankton groups were most affected by glutaraldehyde preservation, showing losses and increased FWS as noted by Sato et al. (2006). These effects were most likely attributable to the preservation and freezing process causing cell membranes to become compromised and leading to expansion or destruction of cells (Menden-Deuer et al. 2001, Sato et al. 2006). Interestingly, preservation caused cell numbers to increase in red picophytoplankton

group 1. A similar effect was also observed by Sato et al. (2006) and may have been caused by increased FWS signals allowing picophytoplanktonic cells previously below flow cytometry cell size detection thresholds to enter into the analysis range, thereby increasing cell concentrations in this group. The variation observed across monthly datasets for preserved cells was therefore linked to the PFT present at the time of sampling and consequently their varying response to preservation. These results supplement existing data confirming glutaraldehyde preservation of phytoplankton to cause data bias (Hall 1991, Lepesteur et al. 1993, Menden-Deuer et al. 2001, Sato et al. 2006) and reinforce the need for careful interpretation of data acquired in this manner. This is of particular importance in areas dominated by nanoplankton cells, shown to be most affected by this technique. Alternative chemicals and protocols for phytoplankton preservation are available, including fixation with paraformaldehyde (Marie et al. 2000) and techniques targeting specific species (Eschbach et al. 2001), however all forms of aldehyde preservation may cause artificial changes to cell structure. A recently developed technique for phytoplankton analysis by electron microscopy may offer an alternative approach. The rapid freezing and freeze substitution (RFS) method has been shown to preserve the structural integrity of a diverse range of environmental PFT (Kimura et al. 2012), but has yet to be tested for flow cytometry purposes.

In contrast, a delay of less than 15 hours between sample collection and analysis had minimal impact on phytoplankton, with significant effects observed only in one PFT. Both cell size and total RFL were shown to increase in orange nanoplankton high group 2 after flow cytometric analysis was delayed. The selection of this method as preferential to sample preservation was therefore confirmed, particularly as the orange nanoplankton high groups were comparatively scarce throughout the duration of the study. This method should therefore be considered as a viable alternative to sample preservation for near shore coastal phytoplankton monitoring.

Environmental data from the Wash during 2010-2012 followed trends previously observed within temperate estuarine systems (Iriarte & Purdie 1994, Tillmann & Rick 2003, Wiltshire et al. 2008). Temperature and irradiance increased in early spring whilst

wave height and turbidity levels decreased, creating optimal conditions for phytoplankton growth (Brussaard et al. 1996). Wave height is associated with wind speed, and may be linked to increased turbidity levels within surface waters due to stormy conditions. However, this was not the case in March 2010, suggesting high turbidity at this time was linked to alternative factors. The Wash estuary is surrounded by large areas of arable farmland. Extended rainfall onto exposed soils is known to cause elevated levels of sediment particles to be washed into rivers and to augment river flow (Howarth 2008). The Wash receives input from four major rivers, suggesting that these two parameters may have led to the increased turbidity noted in March 2010. Nutrient levels were also consistent with expectations and peaked in early spring each year. DIN and Si showed a strong correlation indicating they may originate from the same source. Si within coastal systems is generally derived from terrestrial sources and is often supplied in river water from dissolution of rocks and soil minerals (Lancelot et al. 1987). Both environmental and nutrient data were relatively homogenous across the seven sampling locations, most likely due to the highly tidal and well-mixed nature of the estuary. No discernible differences in either set of parameters were noted at sites above cockle or mussel beds, or those close to riverine discharge.

Peaks in chl *a* closely tracked nutrient peaks and appeared annually each May. Interestingly, whilst peaks of DIN and Si were immediately followed by spikes in chl *a*, these nutrients showed large interannual variation in their concentration which was not reflected in chl *a* intensity. Measurements of both chl *a* during May 2010 were more than double those observed in 2011, however nutrient levels preceding the 2011 bloom were equivalent to or double those in 2010. This reinforces the importance of multiple biological, chemical and environmental factors in bloom formation as described in other studies of temperate coastal systems (Brussaard et al. 1996, Schlüter et al. 2012). Chl *a* levels remained low over summer, with a smaller secondary peak occurring only in late summer 2010. Within Southampton Water, an estuary on the south coast of England, chl *a* was also shown to peak in May, reaching a maximum of 9.7 µg/l (Iriarte & Purdie 1994) in comparison to an average yearly maximum of 10.13 µg/l recorded within the Wash. Phytoplankton biomass within the Wash therefore followed the cyclical trends of

timing and interannual variability in peak chl *a* commonly observed at other temperate coastal regions, but which should not assumed (Cloern & Jassby 2008). Flow cytometric analysis of PFT showed phytoplankton diversity to follow the seasonal patterns predicted for eutrophic temperate ecosystems (Tillmann & Rick 2003, Not et al. 2007, Schlüter et al. 2012). Diversity was low during blooms, but increased over summer and winter months when chl *a* levels decreased. This inverse relationship is commonly observed within coastal systems (Forster et al. 2006).

Flow cytometric analyses allowed phytoplankton bloom structure to be closely studied and allowed detailed population comparisons to be made between each year. Within North Sea coastal regions, bloom biomass and productivity are typically dominated by diatoms (Medlin et al. 2006, Pannard et al. 2008, Schlüter et al. 2012), particularly large microplanktonic genera such as *Odontella* or *Ditylum* (Rousseau et al. 2002, Weston et al. 2008). Diatoms are frequently the main consumers of NO_3 in nutrient replete systems, but require Si for cell wall construction (Kudela & Dugdale 2000). The rapid declines observed in both DIN and Si prior to spikes in chl *a* are therefore symptomatic of the presence of diatom cells. However, whilst microplankton diatom species were present, flow cytometry indicated that spring bloom biomass was dominated by nanoplankton cells, a phenomenon also observed in the Southern Bight (Druzhkov & Druzhkova 2000). This was particularly true in May 2010, where microplankton contributed less than 4% to total RFL. Furthermore, picophytoplankton cells which are traditionally excluded from classical theories of coastal primary productivity were shown to make more relevant contributions to total RFL than microplankton in two of the three surveyed years (2010 and 2011). This is in agreement with recent data from the Bay of Biscay which also indicated strong relevance of picophytoplankton within eutrophic systems (Calvo-Díaz et al. 2004, 2006, 2008).

Comparison of HPLC accessory pigment data to the total RFL data of PFT clusters supplied taxonomic resolution to flow cytometry data. Significant correlations occurred primarily within the red nanoplankton, as these cells were abundant throughout the three year sampling period, allowing more statistically robust comparisons to be made.

Pigment data indicated this group contained a broad diversity of species, including diatom cells, pelagophytes, euglenophytes, chrysophytes and prymnesiophytes (Jeffrey & Vesk 2005). The orange nanoplankton PFT was linked to concentrations of the accessory pigment alloxanthin, suggesting the presence of cryptophytes within this group. Red picophytoplankton were shown to possess chl *b*, indicating that this group may have contained euglenophytes, chlorarachniophytes, chlorophytes and prasinophytes (Jeffrey & Vesk 2005).

It is unlikely that the Wash estuary forms an exception to established ecological theories of phytoplankton succession, particularly due to the conformity exhibited in all other aspects of this study. The absence of significant microplankton diatom contributions within the data collected is interesting, as their presence within the phytoplankton community was clearly indicated by annual exhaustion of Si each spring. This may point to the presence of small diatom cells within the nanoplankton whose optical signals could not be separated from flagellate cells of similar size. However this effect is more likely to have been attributable to the presence of benthic diatom communities excluded from surface water sampling techniques. Benthic diatoms are common within shallow estuarine systems (Kromkamp et al. 1995) and could have caused the observed depletion of Si whilst their position in the water column would have excluded them from biomass estimates. A further explanation for this effect may be insufficient sampling frequency as diatom blooms occur rapidly and disappear suddenly when Si becomes depleted, due to high sedimentation rates and rapidly increasing grazing levels (Rousseau et al. 2002). In May 2010 the surface bloom biomass was dominated by *Phaeocystis*, identified by field and laboratory observations of the distinctive colonial cells of this genus. This was confirmed by the strong presence of the accessory pigment chlorophyll c_3 and traces of 19-hex-fucoxanthin, both frequently used as an indicator pigments of *Phaeocystis* species (Breton et al. 2000). Within North Sea coastal regions, diatom blooms in early spring are regularly followed by blooms of *Phaeocystis* (Mills et al. 1994, Brussaard et al. 1996, Brunet et al. 1996, Peperzak et al. 1998, Rousseau et al. 2002). Whilst Si concentrations are high, *Phaeocystis* cells cannot compete with diatoms for DIN and PO_4 (Egge & Aksnes 1992). However, since

Phaeocystis does not require Si, once this nutrient is exhausted colony formation occurs rapidly allowing *Phaeocystis* cells to reach bloom numbers (Reid et al. 1990, Brussaard et al. 1995). The bloom fails only when levels of DIN become limiting (Riegman et al. 1992). It is therefore possible that our data only partially captured the full extent of the spring bloom community within the Wash and this may be especially true for May 2010. Interestingly, no notable quantities of 19-hex-fucoxanthin were recorded in 2011 or 2012. For many years, North Sea *Phaeocystis* blooms were thought to be dominated by *P. pouchetti* (Lancelot et al. 1987), however *P. globosa* is now known to be the prevalent species (Baumann et al. 1994). The 19-hex-fucoxanthin content of *P. globosa* is much lower or even absent compared to that of *P. pouchetti*, now generally considered to be a cold water species (Vaulot et al. 1994). The Phaeocystis bloom of 2010 may therefore be linked to an incursion of cooler Atlantic water transporting cells of *P. pouchetti* into the region.

Whilst supplying a useful indicator of preceding diatom biomass, monitoring of irregular *Phaeocystis* blooms such as that observed in May 2010 has further ecological significance. *Phaeocystis* is recognised by the Water Framework Directive (WFD) as an indicator species for eutrophication (Lancelot et al. 2008), and is classified as a harmful algal bloom (HAB) species due to significant indirect effects of blooms upon local ecosystems (Smith et al. 2013). Reductions in the clearance rates of mussels and stunted growth in other bivalves have previously been linked to blooms of this algae (Pieters et al. 1980; Beukema & Cadée 1991). Species within the *Phaeocystis* genus have a complex life cycle consisting of both solitary and colonial cell phases (Rousseau et al. 2007). The success of *Phaeocystis* blooms is partly due to the enclosure of colonial cells within gelatinous organic mucilage reducing herbivore grazing (Daro et al. 2008) and the presence of an intra-colonial space which may act as a nutrient reservoir affording higher growth rates to colonial cells (Veldhuis et al. 2005, Smith et al. 2013). Mucous production constitutes a major part of primary production within *Phaeocystis* species; however high acrylate accumulation and low nitrogen content means bacterial degradation of mucous occurs more slowly than in other organic material (Rousseau et al. 2007). As a consequence, when blooms begin to fail, dissolved mucus accumulates in

high concentrations and produces a dense foam when agitated by wind or wave action, which is ultimately deposited on shorelines. In this manner, a large portion of bloom primary production escapes cycling within the pelagic food web (Lancelot et al. 1987). Furthermore, the extent of *Phaeocystis* blooms is also relevant on a climatological scale. *Phaeocystis* species release significant amounts of the aerosol dimethylsulphide (DMS) (Stefels & van Boekel 1993) which plays an important role in the global sulphur cycle and in climate cooling through aerosol and cloud formation (Malin et al. 1992).

Bivalve populations have previously been shown to influence nutrient status via rapid recycling and resuspension of particulate matter within the water column, thereby reducing nutrient storage time within photosynthetic biomass (Prins et al. 1998, Philippart et al. 2000, Grall & Chauvaud 2002). No consistent alterations to chlorophyll, chl *a* or total RFL were observed above cockle or mussel beds, in comparison to data from the Buoy control site where shellfish beds were absent. In similar estuarine environments with dense levels of bivalve aquaculture, e.g. in Mont Saint Michel Bay (France), bivalve biomass is known to exert strong control over primary productivity (Cugier et al. 2010). PFT biomass and accessory pigment data also showed little variation across sampling sites, indicating that the presence of aquaculture did not influence phytoplankton community structure or diversity. This contrasts with data from the Oosterchelde estuary (the Netherlands), where cockle and mussel filtration has been linked to both decreased primary production and shifts in size structure of phytoplankton communities (Smaal et al. 2013). It therefore appears that current levels of cockle and mussel aquaculture in the Wash estuary are sustainable and within the carrying capacity of the ecosystem.

4.5. Conclusions

Whilst the population dynamics of terrestrial plants are well-studied, there is still much to learn about species succession within the phytoplankton. Flow cytometry provides a simple method for the investigation of phytoplankton community properties to PFT level. Our data provide information on the key role of nanoplankton cells within

seasonal cycles of succession which may otherwise have been underestimated by more routine observation methods. This highlights the importance of careful interpretation of phytoplankton data obtained from preserved samples. The absence of picophytoplankton from existing descriptions of bloom populations has been due principally to historical difficulties in accurately quantifying cells of this size. Our data shows the ease with which flow cytometric analyses can include data on this PFT within monitoring regimes, and supplements existing research indicating the relevance of these cells outside of open ocean systems. Whilst we did not uncover links between phytoplankton community structure and bivalve biomass, we provided evidence of interannual variation in the magnitude and composition of spring blooms within the Wash estuary. Our data also identified the presence of a HAB species, a potentially damaging occurrence which may lead to future food limitation within bivalve populations.

Flow cytometry gives detailed data on a scale that is unattainable with existing monitoring techniques. Our data underline the need to incorporate new technology into routine surveys of marine communities. Development of low-cost, reliable flow cytometers would increase the feasibility of on board or *in-situ* instruments to the wider scientific community and reduce reliance on preserved samples. Increased instrument accessibility would promote increased sampling frequency required to obtain data on rapid shifts in phytoplankton community structure and will help build towards the ultimate aim of online, high-frequency automated sampling within coastal systems. Estuarine management strategies operate against a complex background of changing nutrient inputs and forcing parameters. Accurate assessment of primary productivity and the diversity of the phytoplankton is essential in order to form reliable overviews of ecosystem health and status. The underlying causes of biomass shift at higher trophic levels cannot be confidently determined without a comparative baseline documenting typical cycles of flux, intensity and composition within phytoplankton communities.

4.6. Appendices

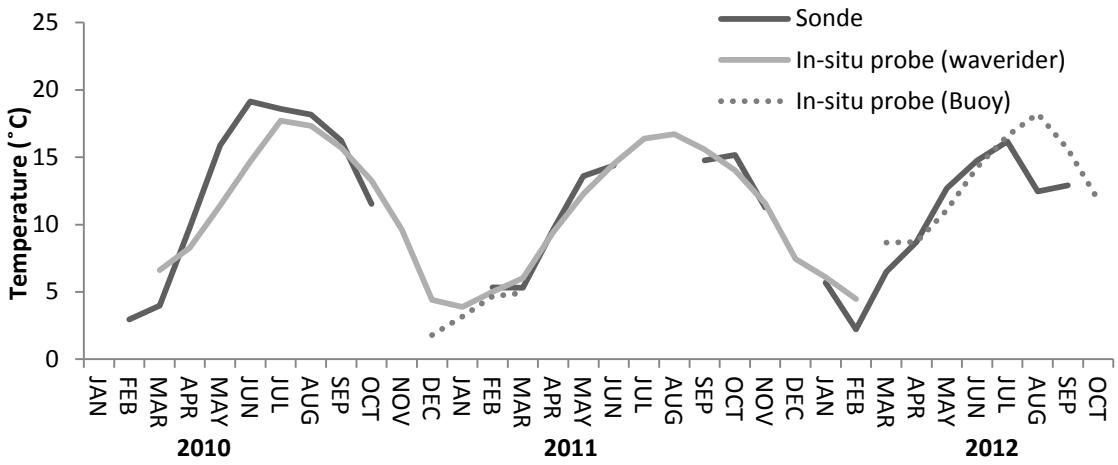

Appendix I. Comparison of temperature data collected by three independent instruments. Data were collected by a handheld sonde probe and by two in-situ probes, moored at the Buoy sampling site and attached to a Waverider instrumental buoy.

Appendix II. Comparison of turbidity data collected by two independent instruments. Data were collected by a handheld sonde probe and by an *in-situ* probe moored at the Buoy sampling site.

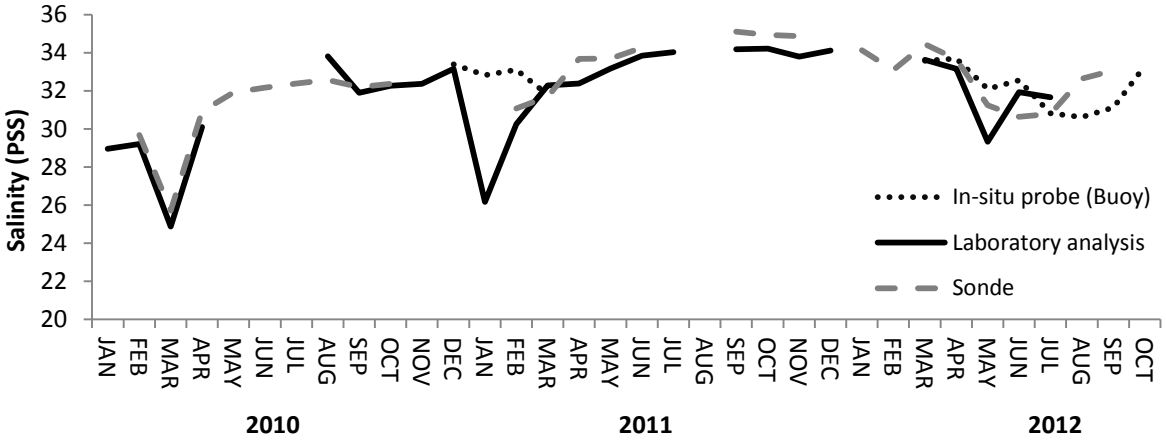

Appendix III. Comparison of salinity data collected by three independent instruments. Data were measured by a handheld sonde probe , an *in-situ* probe moored at the Buoy sampling site and laboratory salinity analysis.

Chapter 5 Estimation of carbon content in phytoplankton cells by flow cytometry in cultured and environmental populations.

Abstract

Accurate partitioning of biomass between phytoplankton functional types (PFT) is essential for robust ecosystem models of carbon cycling. Chlorophyll *a* (chl *a*) is widely used as a biomarker for estimation of bulk photosynthetic biomass, but it is influenced by environmental parameters such as temperature, light history and nutrient status, and provides no information on community structure. Quantifying the DNA content of phytoplankton cells provides an alternative means of measuring biomass. Intracellular DNA exhibits a stable relationship with cell size and carbon content. We propose a simple staining protocol combined with flow cytometric analysis to provide an efficient means of assessing cellular DNA content to measure phytoplankton carbon. Methanol-fixed cells were further permeabilised through addition of DMSO prior to staining with the DNA fluorochrome PicoGreen. The fluorescence intensity of the DNA-dye complex produced was related to fluorescence emitted by stained chicken erythrocyte nuclei (CEN) to quantify phytoplankton DNA. We tested the method on cultured species encompassing the diversity representative of natural communities. Satisfactory staining was achieved within and across different cell types, with minimal cell damage and losses. Further testing established the method was transferable to the DNA quantification of environmental samples. This method permits better estimates of DNA partitioning across phytoplankton communities; provides supplementary carbon biomass data and could help to increase the relevance and robustness of ecosystem models through supplying an alternative biomarker to chl *a*.

5.1. Introduction

Marine biogeochemical processes are closely linked to phytoplankton community assemblage. Cell abundance and biomass are a measure of the successful conversion of inorganic to organic carbon and net primary production. Carbon estimates are therefore often used to analyse metabolism and energy transfers within marine environments, with carbon frequently used as a currency within ecosystem models (Gosselain et al. 2000). Phytoplankton play a critical role in the "biological pump", a mechanism describing photosynthetic fixation of CO_2 by phytoplankton cells in surface waters. This carbon is stored either temporarily or permanently as these phytoplankton cells sink and transport organic matter downwards through the water column (Anderson 2005). The size-based phytoplankton functional types (PFT) present within a community are critical to these processes. Cells are generally divided into picophytoplankton (≤3 µm), nanoplankton (3-20 µm) and microplankton (20-200 µm) groups (Sieburth et al. 1978, Vaulot et al. 2008). Differences in cell size govern variations in cellular carbon content (Uysal 2000, Litchman et al. 2007) and influence cell fate (Berelson 2001, Le Quere et al. 2005). Reduced diameters equate to lower sedimentation rates promoting participation within the microbial loop and recycling of carbon within surface waters (Azam et al. 1983, Fenchel 2008). In contrast, larger diameters can increase settling rates, resulting in the loss of carbon from surface waters (Raven 1998, Scharek et al. 1999). Subsequent re-circulation to the euphotic zone is then highly dependent on the depth and mixing of the water mass (Berelson 2001, Le Quere et al. 2005).

Ecosystem models describing marine biogeochemical cycling can be simplistic, lacking articulation of the distinct roles of size-based PFT. Cells are aggregated into a catch-all "phytoplankton" group, regardless of size or ecosystem role (Six & Maier-Reimer 1996, Palmer & Totterdell 2001, Aumont et al. 2002). This is a generalisation frequently referred to as a "black box" within models and does not utilise information available on phytoplankton physiology to create more dynamic representations of marine systems (Le Quere et al. 2005, Anderson 2005, Jardillier et al. 2010). Whilst simpler models successfully capture net ecosystem properties, such as seasonal blooms and general areas of oceanic fertility (Jeffrey & Mantoura 2005; Anderson 2005),

accurate simulation of the processes involved in biogeochemical cycling ideally require data on carbon partitioning across phytoplankton populations.

High-quality abundance data permitting division of phytoplankton biomass by PFT are therefore fundamental in the development of robust biogeochemical ocean models. Ascertaining the carbon content of a cell is a critical step in establishing its ecological relevance. However, no direct method for measurement of phytoplankton carbon biomass is currently available. Instead, data are obtained using a proxy parameter common to all phytoplankton. Chlorophyll *a* (chl *a*) is a photosynthetic pigment universal to all algal phyla and widely recognized as a useful indicator of phytoplanktonic biomass (Jeffrey & Mantoura 2005). Data on chl *a* can be collected with relative ease through measurements of *in-situ* chl *a* fluorescence (Proctor & Roesler 2010) or through extraction and analysis via spectrophotometry, fluorimetry or high performance liquid chromatography (Aminot & Rey 2000, Jeffrey 2005, Ediger et al. 2006). Biomass is calculated by transformation of this data into values of carbon, using published single or averaged conversion factors (Riemann et al. 1989; Cloern et al. 1995; Zubkov et al. 1998; Veldhuis & Kraay 2000; Morán 2007). However, despite ubiquitous use of chl *a* derived carbon biomass, there are limitations on the data it provides. Information on community structure and the relative biomass contribution by different PFT is poorly resolved, as most data acquired in this manner are in bulk form (Havskum et al. 2004, Cornet-Barthaux et al. 2007). This information contributes to synoptic surveys of phytoplankton and supplements remote sensing satellite data permitting mapping of inter-annual variability and productivity hotspots (Le Quere et al. 2005; Ribalet et al. 2010); but has little or no provision for allocation of carbon to PFT (Toepel et al. 2004). This approach assumes a constant relationship between chl *a* and carbon (Riemann et al. 1989). The link between phytoplankton carbon biomass and chl *a* concentration is in fact non-linear, due to the complex combined influences of fluctuating environmental parameters such as irradiance, temperature and nutrient availability (Cloern et al. 1995; Fukuda et al. 1998; Veldhuis & Kraay 2000; Calvo-Diaz & Moran 2006). Ratios of chl *a* to carbon can shift by an order of magnitude within a single species, with potential for greater variation over different temporal and spatial

scales (Sosik et al. 1989; Veldhuis et al. 1997; Veldhuis & Kraay 2000; Calvo-Diaz 2004). Attempts to increase the accuracy of conversion factors via laboratory manipulations of cultured phytoplankton populations are not always helpful. Species tested are usually those easiest to maintain in culture and may not necessarily be indicative of the response of a species or functional type as a whole (Le Quere et al. 2005).

Phytoplankton biomass can be more accurately measured by transformation of individual cell volume into units of carbon. Volume is derived from optical measurements of cell size, typically obtained from chemically preserved samples by light microscopy (Bratbak 1985; Hillebrand et al. 1999; Konoplya & Soares 2011). Species specific geometric shape formulae are available for volume calculation of most cell shapes and structures (Hillebrand et al. 1999), with a variety of carbon to volume conversion values reported for different phytoplankton groups (Mullin et al. 1966; Strathmann 1967; Lee & Fuhrman 1987; Verity et al. 1992; Montagnes et al. 1994; Menden-Deuer & Lessard 2000; Leblanc et al. 2012). Despite the utility of this correlation, this approach is rarely used, due principally to difficulties in acquiring sufficient quantities of data to produce accurate representations of microbial communities. Microscopy is time-consuming and labour intensive and the preservation of cells required may contort their dimensions making accurate measurements difficult (Menden-Deuer & Lessard 2000). Flow cytometry offers some resolution to this issue. The light scatter signals recorded by this technique are not exact proxies for cellular properties, however calibrated data can supply an approximate indication of size (Gasol & Del Giorgio 2000; Felip & Catalan 2000). This is sufficient to assign analysed particles to a size-based PFT. Information on chl *a* via quantification of natural pigment autofluorescence can also be acquired via flow cytometry. Nonetheless this data still suffers from the same carbon conversion issues as more traditional techniques.

Analysis of phytoplankton DNA content by flow cytometry offers an alternative means of measuring carbon. The overall DNA content of phytoplankton is low, composing at most 3% of total cell carbon (Veldhuis et al. 1997). However genome size

is a conservative parameter within phytoplankton; a phenomenon termed the DNA C-value paradox (Thomas 1971; Cavalier-Smith 1978; Veldhuis et al. 1997; Gregory & Hebert 1999). It is independent of both cellular complexity and external environmental conditions (Holm-Hansen 1969; Cavalier-Smith 1978; Olson and Chisholm 1986; Boucher et al. 1991; Gregory 2001). Critically, phytoplankton DNA content is influenced by cell size: a scaleable correlation which extends across all phyla (Boucher et al. 1991; Veldhuis et al. 1997; Veldhuis & Kraay 2000). This co-variation allows total DNA content to be used as an estimate of carbon without requiring measurement of cell size or chl *a*.

Exploitation of this relationship using the high throughput capacity of flow cytometry could provide a feasible means of PFT biomass assessment. The use of nucleic acid specific fluorochromes in combination with flow cytometry is widespread in laboratory and field research for quantitative detection of phytoplankton DNA (Veldhuis et al. 1997; Gasol et al. 1999; Boelen et al. 2001; Button & Robertson 2001; Zubkov et al. 2006), but has yet to be specifically applied to estimating environmental carbon biomass of entire phytoplankton communities across a range of nutrient regimes. This is partially related to the particle size restrictions of some flow cytometers which limit the measurement range, but principally to a lack of preparation and staining protocols applicable to the physiological variation in phytoplankton encountered across oceanic and coastal communities. Marine ecosystems are characterised by large species diversity so a methodology which permeabilises the silica frustules of diatoms to allow a stain to enter may destroy the structural integrity of more fragile flagellate cells (Tsuji & Yanagita 1981). Here, we introduce a simple protocol for effective DNA staining across PFT exhibiting different cell size, strucutre and composition. The protocol was applied initially to laboratory cultures to determine DNA content and estimate cellular carbon. Results were compared to data obtained via volume: carbon calculations and also by elemental carbon analysis, permitting comparative evaluation of each technique. Finally, the staining protocol was used to estimate carbon biomass in different environmental phytoplankton communities, confirming utility of the methodology in the field.

5.2. Materials and Methods

5.2.1. Phytoplankton cultures

Thirteen phytoplankton strains (non-axenic) representative of the physiology and phylogeny present within North Sea communities were selected (Table 5.1).

Table 5.1. A summary of the phytoplankton species investigated. Names, origins and culture conditions are described. Strains were obtained from the Culture Collection of Marine Phytoplankton (CCMP) now re-named the National Centre for Marine Alga and Microbiota (NCMA), the Culture Collection of Algae and Protozoa (CCAP) and the Centre for Fisheries and Aquaculture Science (Cefas).

Domain	Class	Species	Strain	Growth medium	Origin
Prokarya	Cyanophyceae	*Synechococcus*	CCMP 2370	SN	Sargasso Sea
Eukarya	Prymnesiophyceae	*Isochrysis galbana*	CCAP 927/1	f/2	Isle of Man, UK
	Prymnesiophyceae	*Emiliania huxylei**	CCAP 920/8	K	Bergen, Norway
	Eustigmatophyceae	*Nannochloropsis salina*	CCAP 849/6	f/2	Long Island, USA
	Prasinophyceae	*Micromonas pusilla*	CCAP 1965/4	f/2	Plymouth, UK
	Chlorophyceae	*Tetraselmis suecica*	CCAP 66/22A	f/2	Suffolk, UK
	Dinophyceae	*Amphidinium carterae*	CCAP 1102/5	L1	Scarborough, UK
	Dinophyceae	*Prorocentrum minimum*	CCAP 1136/16	L1	Loch Etive, UK
	Dinophyceae	*Pyrocystis lunula*	CCAP 1131/1	L1	Unknown
	Bacillariophyceae	*Amphora coffeaeformis*	CCAP 1001/2	f/2 + Si	California, USA
	Bacillariophyceae	*Thalassiosira punctigera*	CCAP 1085/19	f/2 + Si	Oban, UK
	Bacillariophyceae	*Thalassiosira weissflogii*	CCAP 1085/18	f/2 + Si	Hawaii, USA
	Bacillariophyceae	*Stephanopyxis turris*	Cefas W001	f/2 + Si	The Wash, UK

*****Calcifying strain

Phytoplankton were grown in media recommended by the culture collection and as described in Chapter 2 (section 2.1.1). SN media was prepared according to Waterbury et al. (1986), f/2 and f/2 + Si as described by Guillard & Ryther (1962), K as described by Keller et al. (1978) and L1 as directed by Guillard & Hargraves (1993). Cultures

were maintained in an incubator (MLR-351 Plant Growth Chamber, Sanyo, Loughborough, UK) at 17 °C with fluorescent light supplied on a 12 h light: 12 h dark cycle, at 40-50 µmol $m^{-2}s^{-1}$ light intensity. Each strain was grown in batch culture, in 250 ml Erlenmeyer flasks. Cultures were maintained by transfer to fresh medium approximately every 14 days. Cells were harvested for experimentation in late exponential phase to maximise numbers and reduce bacterial contamination.

5.2.2. Elemental analysis of phytoplankton carbon content

Aliquots were removed from each culture with the exceptions of *Synechoccocus*, *S. turris* and *P. lunula*. These cultures were deemed to be of poor quality at the time of analysis and were therefore excluded from this method. Aliquots were analysed by flow cytometry to provide cell concentration measurements for each species. Cells were harvested by gentle vacuum filtration (< 10 kPa) through a 13 mm diameter GF/F filter (Whatman, UK), previously combusted at 450 ºC for 4 hours in a muffle furnace. The quantity of culture filtered varied between 10 to 20 ml depending on cell density which ranged from 7.57E+04 for *A. carterae* to 6.82E+08 for *M. pusilla*. Each filter was folded in half and placed in a sterile microcentrifuge tube. Filters were dried at 60 ºC for 48 hours then placed into nickel capsules for carbon-hydrogen-nitrogen (CHN) analysis. Analyses were performed using an elemental analyser (CE440, Exeter Analytical, Coventry, UK) by technicians at the School of Environmental Sciences (University of East Anglia). Values of carbon per cell were calculated using the concentration of each culture (cells/ml) determined from flow cytometry data.

5.2.3. Cell fixation, permeabilisation and DNA staining

PicoGreen shows limited and highly variable staining when applied to live cells (Veldhuis et al. 1997). Fixation of phytoplankton was therefore necessary to permeabilise cells prior to further analysis. Cells were removed from suspension via centrifugation (10 minutes, 600 G at 17 °C). The non-ionic surfactant Pluronic (10%,

Sigma-Aldrich) was added (10 µl/ml) prior to all centrifugation in order to ensure cell suspension and increase efficiency of cell recovery (Biegala et al. 2003). The resulting supernatant was removed and cell pellets were re-suspended in methanol (Sigma-Aldrich 99.9% laboratory grade) for overnight fixation at 4°C. Aldehyde preservation is commonly used in phytoplankton fixation, particularly in preparation for flow cytometric analysis. However, the most popular choice, glutaraldehyde, is known to produce yellow-green background fluorescence (Veldhuis et al. 1997, Vives-Rego et al. 2000) and was therefore avoided to prevent interference with the emission signals of cells stained with PicoGreen. Additionally, fixation by methanol causes denaturisation and precipitation of intracellular proteins, leading to permeabilisation of cell membranes (Bozzola & Russell 1999). Alcohol preservation also leads to extraction of photosynthetic pigments (Olson et al. 1983), which may further aid accessibility to DNA. Centrifugation was repeated to allow removal of methanol and the re-suspension of cells in a solution of one of two chemicals: Triton X-100 or dimethylsulfoxide (DMSO) at 1% (v/v). Triton X-100 (Sigma-Aldrich) is a non-ionic detergent known to cause increased dispersal and reduced aggregation of cells. Concentrations of 0.5-1% can lyse chloroplasts and increase stain access (Boucher et al. 1991, Marie et al. 1996, Veldhuis et al. 1997, Dolezel & Bartos 2005). DMSO (Sigma-Aldrich) is a highly polar organic solvent known to assist permeabilisation of eukaryotic cell membranes; however effects are variable between species, dependent on concentration and occasionally detrimental (Veldhuis & Kraay 2000; Vives-Rego et al. 2000).

PicoGreen (Invitrogen, USA) is a proprietary fluorochrome with high affinity for double stranded DNA (dsDNA), generating a high fluorescence yield when bound to DNA molecules (Marie et al. 1996, Veldhuis et al. 1997). PicoGreen is intercalating and shows no base pair specificity (Veldhuis et al. 1997) in contrast to stains such as DAPI which favour AT over GC pairs (Lin et al. 1977, Smarda et al. 2012). Strong yellow-green emissions (approx. 520 nm) are produced upon excitation of this dye-DNA complex by a blue laser (488 nm). PicoGreen stock solution was divided into aliquots upon receipt and kept frozen at -20 °C. Working solutions were made by 10 fold dilution of PicoGreen with 0.2 µm sterile filtered deionised water, stored at -20 °C for a

maximum of four weeks (Veldhuis et al. 1997). A freshly defrosted working solution was used for each day of analysis. The specificity of dsDNA-stain complexes was ensured through the addition of 20 µl RNase (R-4875, Sigma-Aldrich) per ml of sample (0.2 mg ml^{-1} final volume) according to Veldhuis et al. (1997). The concentration and incubation times for PicoGreen were tested to ensure acceptable staining efficiency (see sections 5.3.5 and 5.3.6). All subsequent staining was conducted with a 1% final concentration of PicoGreen. Samples were thoroughly mixed and incubated in the dark at room temperature for 45 minutes, then analysed immediately.

5.2.4. DNA calibration

An ideal DNA reference standard should have a genome size close to the target species, be stable with constant genome size, easy to use and available in sufficient quantities (Dolezel & Bartos 2005). However, these requirements are hard to satisfy and result in the use of many different DNA standards including trout, calf and chicken cells and human leukocytes (Dolezel & Bartos 2005). In this study, DNA-dye fluorescence was calibrated using chicken erythrocyte nuclei (CEN) as an internal calibration standard (Kapraun 2005). Isolated CEN (ab4527, Abcam, UK) were re-suspended in aliquots of buffer as per the manufacturer's instructions. The nuclei are 5 µm in diameter, with a published DNA content of 3 picograms (Rasch 1985, Tiersch et al. 1989, Johnston et al. 1999, Riechmann et al. 2000). CEN are commonly used as DNA calibration standards (Johnston et al. 1999), but have been reported to show inconsistent mean values of fluorescence across different preparations, despite apparently constant DNA content (Johnston et al. 1999). As these are isolated nuclei lacking cell walls and cytoplasm, they are less stable than stained phytoplankton cells and prone to damage. However, use of isolated nuclei permits accurate estimation of genome size unachievable when whole cells (e.g. chicken red blood cells) are used, and allows phytoplankton DNA measurements to be expressed as quantitative values rather than the relative or arbitrary units of DNA produced in other studies (e.g.Veldhuis et al. 1997, Veldhuis & Kraay 2004).

CEN were tested extensively prior to use as a DNA standard, to ensure stability and adequate staining by PicoGreen. They were centrifuged and permeabilised following the methodology above, with the addition of re-suspension in Tris-HCl buffer (T5941, Sigma-Aldrich). It was concluded that unlike whole cell calibration standards, CEN could not be treated in the same manner as phytoplankton cells. Exposure to this protocol resulted in varied and unpredictable fluorescence emissions after staining or complete destruction of nuclei (see section 5.3.5). CEN were therefore added to samples concurrently with PicoGreen, minimising damage and stabilising fluorescence emissions. Fresh suspensions of CEN were made as required from stocks frozen at -80 °C. Phytoplankton DNA content was calculated relative to the CEN signal, producing absolute values of DNA and quantitative measurement of genome size.

5.2.5. Environmental samples

Phytoplankton samples were collected from two North Sea locations during May and July 2012 (Figure 5.1). Coastal phytoplankton communities were represented within water collected from the Wash estuary (52.942N, 0.318E), whilst open water populations were sampled at the Dowsing instrumental mooring (53.531N, 1.053E). Samples were pre-filtered through a 200 µm nylon mesh to remove zooplankton and concentrated via tangential flow (Millipore) to ensure sufficient cell numbers for robust testing of the staining protocol. Staining was carried out in accordance with the protocol described in section 5.2.4 and data were converted to units of carbon after calibration with CEN. Volume and therefore carbon data were divided into the following groups on the basis of FWS-derived cell size: ≤ 3, 3-5, 5-8, 8-12, 12-15, 15-20 and ≥ 20 µm. Data from particles below a 1 µm size threshold were removed in order to exclude bacterial cells from analyses.

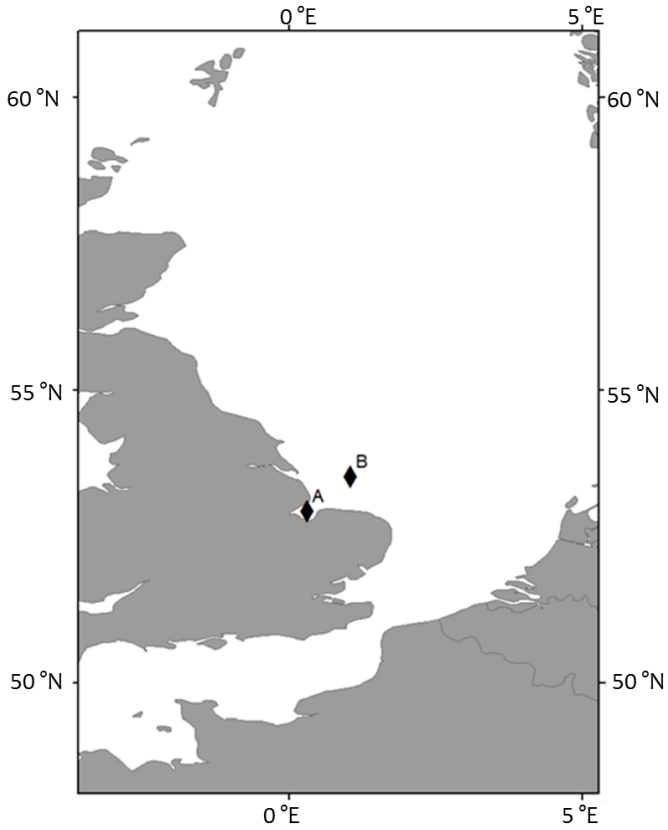

Figure 5.1. Environmental samples were collected from the Wash estuary (52.942N, 0.318E) at location A and the Dowsing Smartbuoy instrumental mooring (53.531N, 1.053E) at location B.

5.2.6. Flow cytometry analysis

Phytoplankton samples were analysed on a CytoSense flow cytometer fitted with a 488 nm blue argon laser, using CytoUSB 5 data acquisition software for Windows. The re-circulating internal fluidic system was modified for analysis of stained samples, bypassing transport of waste fluid through the inline sheath filters. This is similar to the operational protocol of other flow cytometers and was performed to prevent accumulation of stained particles within the instrument. Unstained cells from fresh samples were analysed using a red fluorescence (RFL) trigger parameter whilst stained samples were analysed using a yellow-green fluorescence trigger parameter (YFL). The trigger levels (mv) and flow rates (µl/s) were adapted according to the cell size and density of each sample. A minimum of 5000 events were recorded for each sample. A

0.2 µm filtered seawater sheath fluid was used to analyse live cells in fresh samples, whilst 0.2 µm filtered distilled water was used for stained samples. Sheath fluids were changed in order to avoid measurement variations caused by differences in the refractive index between sheath and sample fluid streams. All experimental data were normalised to fluorescence (F8852, Life Technologies, USA) and size (F13838, Life Technologies, USA) calibration microspheres before further analysis. Flow cytometry data were processed using Cytoclus 3 software for Windows to identify and gate target cell populations on the basis of their scatter and fluorescence emission profiles.

5.2.7. Statistical analyses

Cell fluorescence and FWS were found to be normally distributed in all phytoplankton culture data. Significant differences were reported when $p < 0.05$. A repeated measures ANOVA (SPSS 18 for Windows 7) was used to test for significant differences in the means of cell scatter and concentrations between untreated cells and cells during different stages of the staining process. The sphericity of the data was determined using Mauchly's Test (SPSS 18 for Windows 7). When sphericity was violated ($p < 0.05$), Greenhouse-Geisser corrected values were used. Differences in cellular fluorescence variations produced by Triton X-100 and DMSO were tested for significance by t-test (Microsoft Office Excel 2007). Cell volume and carbon data were normalised by log transformation before further analysis. Carbon to volume relationships were determined by model I regression as described by Menden-Deuer & Lessard (2000). Regression analyses were performed using Microsoft Office Excel (2007) and the statistical significance of regressions was tested by ANOVA (SPSS 18 for Windows 7).

5.3. Results

5.3.1. Cell length and volume

Cell length was measured by flow cytometry and microscopy (Table 5.2). FWS and SWS data produced similar measurements of length ($R^2 = 0.93$, $p = 0.01$) which correlated well with microscopy data ($R^2 = 0.82$, $p = 0.04$ for FWS and $R^2 = 0.71$, $p = 0.03$ for SWS). Three different methods were used to estimate cell volume (Table 5.2). Greatest similarities were observed between FWS and microscopy datasets which both estimated volume assuming spherical shape ($R^2 = 0.89$, $p = 0.01$). These FWS data showed comparability to data based on microscopic measurements of true (geometric) cellular dimensions ($R^2 = 0.72$, $p = 0.03$); although assumption of spherical shape caused cell volume to be overestimated in cells with more variable structure. A similar correlation was observed between spherical and geometric volume estimates produced by microscopy ($R^2 = 0.70$, $p = 0.02$). Assumption of spherical form again resulted in comparatively larger estimates of volume in cells with more irregular shape. Data from the two largest species analysed, *S. turris* (75 µm) and *P. lunula* (80 µm), were not included within these statistical comparisons as their distance from the next largest species (*T. suecica*, 12 µm) negatively influenced relationship significance despite the production of similar R^2 values.

Table 5.2. Data on average cell volume derived from FWS measurements assuming cells are spherical in shape (FWS volume). Within each sample approximately 5000 cells were analysed (n=3). Cell dimensions determined by microscopy were used in geometric equations relating to true cell shape to produce median cell volume estimates (Volume – Shape). Approximately 100 cells were analysed from each sample (n=3). Microscopy measurements were also used to produce volume data assuming spherical shape (Volume – Sphere). All volume data were calculated using equations in Hillebrand et al. (1999).

					Flow cytometry (FWS)	Microscopy	
Species	Cell shape*	FWS cell length (µm)	SWS cell length (µm)	Microscopy cell length (µm)	Volume - Sphere (μm^3)	Volume - Sphere (μm^3)	Volume - Shape (μm^3)
Synechococcus	S	1.50**	1.50**	1.50**	1.77	1.77	1.77
M. pusilla	PS	2.64	3.36	2.86	9.60	12.19	7.95
I. galbana	PS	3.07	3.82	3.53	15.20	22.94	19.94
N. salina	S	3.57	3.95	3.83	23.80	29.31	29.31
E. huxylei	S	4.62	4.94	4.86	51.63	60.11	60.11
A. coffeaeformis	Cym	6.05	5.90	5.4	116.09	82.63	19.49
T. weissflogii	Cyl	8.87	8.32	8.92	365.12	371.04	346.41
A. carterae	E	10.21	9.51	16.8	556.94	2483.03	588.18
P. minimum	E	10.45	11.93	13.05	598.37	1163.82	318.18
T. punctigera	Cyl	11.55	10.64	10.33	807.65	577.00	200.30
T. suecica	PS	12.42	7.31	14.35	1002.72	1547.43	950.46
S. turris	Cyl	75.23	84.17	63.02	222960.60	130941.28	2947.98
P. lunula	E	80.39	85.48	69.50	272076.65	175796.14	25582.75

*****S = sphere, PS = prolate spheroid, Cyl = cylinder, E = ellipsoid, Cym = Cymbelloid****** Cell length of *Synechococcus* was estimated from cell size data provided by NCMA

5.3.2. Pre-treatment and permeabilisation

The pre-treatment and permeabilisation stages of the staining protocol were assessed for potential negative impacts upon a selection of phytoplankton strains. Cell concentrations appeared stable throughout centrifugation, fixation, permeabilisation with chemicals and staining (Table 5.3). Data sphericity assumptions were violated for both Triton X-100 x^2 (5) = 31.5, p = 0.00 and DMSO x^2 (5) = 37.6, p = 0.000. Degrees of freedom were therefore corrected using Greenhouse-Geisser estimates (ε =0.42 and 0.36 respectively). No significant changes to cell concentrations were seen at any stage after centrifugation, fixation and suspension in Triton X-100 (F= 1.27, 8.90 = 0.58, p = 0.5) or DMSO (F= 1.07, 7.51 = 0.85, p = 0.395). Cell size also appeared unaffected throughout pre-treatment and permeabilisation stages (Table 5.4). Data sphericity was similarly violated during analysis of FWS variation during treatment stages: for Triton X-100 x^2 (5) = 16.08, p = 0.08 and for DMSO x^2 (5) = 11.601, p = 0.45. Degrees of freedom were again corrected (ε = 0.45 and 0.61 respectively). No significant shifts in cell scatter were noted at any stage for either Triton X-100 (F= 1.36, 8.13 = 0.85, p = 0.714), or DMSO (F= 2.97, 53.27 = 0.334, p = 0.704).

Table 5.3 Cell concentrations across sequential stages of the pre-treatment and staining protocol (n = 3). Untreated cells removed from culture were initially analysed. Analysis was repeated after primary centrifugation (1) and again after methanol fixation and secondary centrifugation of cells (2). Triton X-100 and DMSO refer to cells suspended in these chemicals after fixation and prior to staining.

					Flow cytometry (FWS)	Microscopy	
Species	Cell shape*	FWS cell length (µm)	SWS cell length (µm)	Microscopy cell length (µm)	Volume - Sphere (μm^3)	Volume - Sphere (μm^3)	Volume - Shape (μm^3)
Synechococcus	S	1.50**	1.50**	1.50**	1.77	1.77	1.77
M. pusilla	PS	2.64	3.36	2.86	9.60	12.19	7.95
I. galbana	PS	3.07	3.82	3.53	15.20	22.94	19.94
N. salina	S	3.57	3.95	3.83	23.80	29.31	29.31
E. huxylei	S	4.62	4.94	4.86	51.63	60.11	60.11
A. coffeaeformis	Cym	6.05	5.90	5.4	116.09	82.63	19.49
T. weissflogii	Cyl	8.87	8.32	8.92	365.12	371.04	346.41
A. carterae	E	10.21	9.51	16.8	556.94	2483.03	588.18
P. minimum	E	10.45	11.93	13.05	598.37	1163.82	318.18
T. punctigera	Cyl	11.55	10.64	10.33	807.65	577.00	200.30
T. suecica	PS	12.42	7.31	14.35	1002.72	1547.43	950.46
S. turris	Cyl	75.23	84.17	63.02	222960.60	130941.28	2947.98
P. lunula	E	80.39	85.48	69.50	272076.65	175796.14	25582.75

Table 5.4. Cell length derived from forward scatter (FWS) across sequential stages of the pre-treatment and staining protocol (n = 3). Untreated cells removed from culture were initially analysed. Analysis was repeated after primary centrifugation (1) and again after methanol fixation and secondary centrifugation of cells (2). Triton X-100 and DMSO refer to cells suspended in these chemicals after fixation and prior to staining.

Species	Untreated cells		(1) After centrifugation		(2) Methanol preservation and centrifugation		Cells suspended in Triton X-100		Cells suspended in DMSO	
	Length (µm)	SD	Length (µm)	SD	Length (um)	SD	Length (µm)	SD	Length (µm)	SD
M. pusilla	2.99	0.44	3.13	0.47	3.43	0.59	4.62	0.42	4.70	0.41
E. huxleyi	4.66	0.45	3.94	0.32	6.09	0.49	3.15	0.31	3.15	0.31
A. carterae	10.09	2.43	10.15	2.25	11.99	2.11	8.84	2.70	8.31	1.29
P. minimum	10.12	1.67	9.06	1.37	13.02	2.77	8.86	1.95	11.42	1.75
T. punctigera	12.40	1.25	11.50	1.41	7.94	1.66	20.45	2.99	8.41	1.42
T. suecica	12.03	2.11	11.77	2.10	8.18	1.27	9.65	1.28	9.32	0.96
S. turris	74.91	33.12	70.52	32.01	74.06	32.43	72.31	38.67	72.34	39.39

5.3.3. DNA-dye fluorescence

Further analyses were performed to determine whether Triton X-100 or DMSO promoted higher staining across phytoplankton cells (Table 5.5). DMSO was found to significantly increase fluorescence emissions across all species ($p < 0.05$) apart from in *Synechococcus* and *S. turris*, where no difference was observed and in *T. punctigera* where Triton X-100 produced greater values of yellow fluorescence per cell ($p = 0.03$).

Table 5.5. Mean yellow fluorescence emissions (mV) per cell after permeabilisation with Triton X-100 or DMSO (n = 3).

Species	Triton X-100		DMSO	
	YFL	SD	YFL	SD
Synechococcus	181.45	26.39	178.27	24.56
M. pusilla	489.11	44.44	520.63	55.05
I. galbana	598.62	132.59	944.79	185.98
N. salina	1024.32	371.40	1375.57	349.83
E. huxleyi	6827.15	1175.04	12805.05	1023.54
T. weissflogii	47109.79	17409.89	73426.58	22427.40
A. carterae	36412.09	5875.40	56102.24	7060.01
P. minimum	106248.52	8527.78	152392.42	11155.03
T. punctigera	59394.10	14888.00	46120.00	10856.34
T. suecica	29306.74	6998.76	33101.37	10373.87
S. turris	651477.42	204816.07	590702.28	224996.09

Staining quality was assessed visually on the quantity of background fluorescence, variation within clusters and cluster resolution displayed on cytoplots of stained cells. In some species, two separate cell clusters were clearly observed (Figure 5.2). These most likely represented cells in the G1 and G2 cell cycle phases. Cell division within phytoplankton is accompanied by bimodal distribution of DNA, with cells containing exactly one or two copies of the genome (Veldhuis & Kraay 2000). However, as the smaller, secondary G2-like cluster was not present or well resolved in all cases, the data analyses described throughout were performed only on the numerically dominant primary (G1) population. Inclusion of both clusters would have introduced data variation unrelated to the staining protocol and made true

comparisons of efficiency difficult. Further visual assessments of staining were performed using epifluorescence microscopy (DM12, Leica, Ernst-Leitz-Strasse, Germany). This allowed comparison of stain specificity across treatments. Cells stained after treatment with DMSO were observed to emit brighter staining, judged to be more specific to the nucleus.

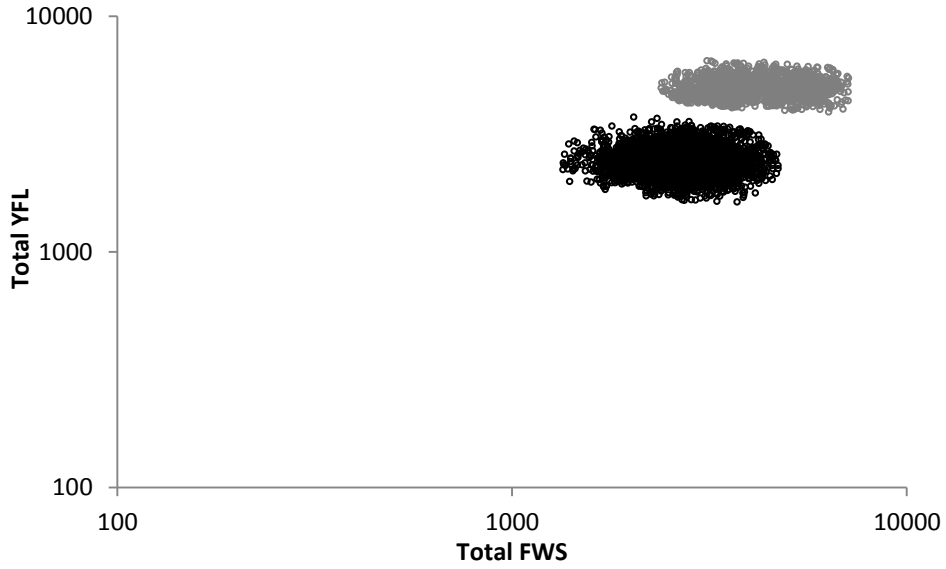

Figure 5.2. Cytoplot showing total yellow fluorescence (YFL) and total forward scatter (FWS) of *I. galbana* after treatment with DMSO. The G1 cell cluster is indicated by the black markers with G2-like cells in grey.

5.3.4. Optimisation of phytoplankton and chicken erythrocyte nuclei (CEN) fluorescence

T-tests were performed to quantify the impact of PicoGreen concentration on fluorescence emissions from *I. galbana* and *P. minimum* (Table 5.6). Increasing stain concentration from 1 to 5% (v/v) produced significantly more fluorescence in *I. galbana* cells permeabilised with both Triton X-100 ($p = 0.014$) and DMSO ($p = 0.001$).

Table 5.6. Average yellow fluorescence emissions (mV) in phytoplankton species *I. galbana* and *P. minimum*, and in isolated chicken erythocyte nuclei (CEN) after addition of 1 or 5% PicoGreen (n = 3). Average yellow fluorescence emissions in CEN after addition of 1% PicoGreen and incubation over three different time periods are also shown.

	1% PicoGreen				5% PicoGreen			
	DMSO		Triton X-100		DMSO		Triton X-100	
Species	YFL	SD	YFL	SD	YFL	SD	YFL	SD
I. galbana	1582	354	1666	301	3063	404	2198	312
P. minimum	111647	10762	105879	10854	157216	24271	124301	16365
CEN	38615	3763	27247	4462	46451	4261	40805	3910
CEN 20	48232	5285	38272	4398				
CEN 40	47717	5250	42064	3816				
CEN 60	46138	6014	38316	4454				

In cells of *P. minimum*, fluorescence increased only in DMSO permeabilised cells ($p = 0.012$). This reinforced earlier data (Table 5.5) and indicated DMSO was preferable to Triton X-100 on the basis of stain accessibility and fluorescence stability. Whilst addition of 5% PicoGreen produced highest levels of fluorescence, observation of cells with epifluorescence microscopy established that this was frequently attributable to non-specific staining, with yellow-green fluorescence present throughout the cytoplasm. The stability of CEN was analysed prior to use as a calibration standard. Fluorescence emissions after repeated centrifugation, exposure to methanol and re-suspension in in Triton X-100, DMSO and the neutral buffer Tris-HCl were found to be extremely variable (Figure 5.3). DNA-dye fluorescence ranged from ~ 5500 to 38500 mV across treatments, with similar high variation within between treatment replications on independent batches of CEN.

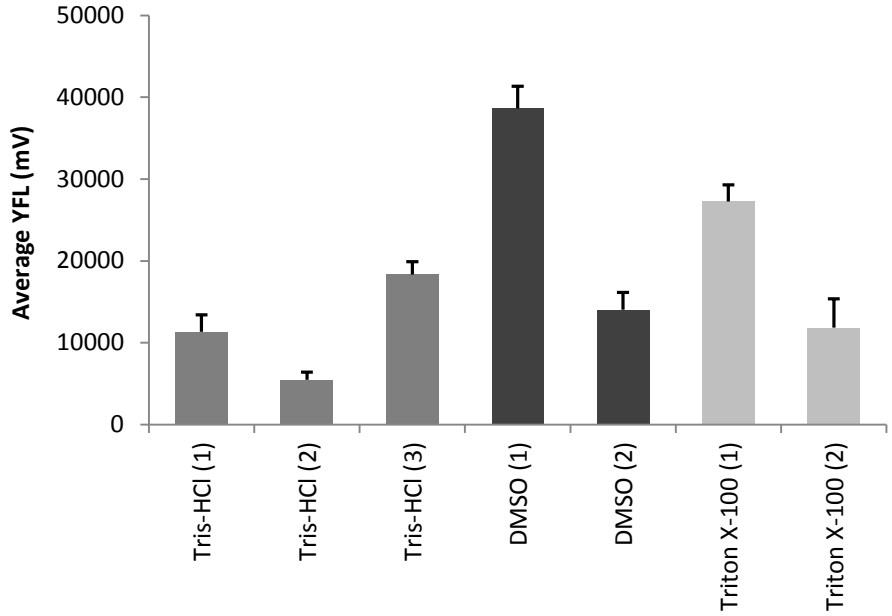

Figure 5.3. Average yellow fluorescence (YFL) emissions of isolated chicken erythrocyte nuclei (CEN) after exposure to methanol and centrifugation. The number in brackets denotes to independent batches of CEN undergoing identical treatment (n = 3).

Addition of freshly defrosted nuclei directly to Triton X-100 or DMSO without exposure to centrifugation or methanol fixation stabilised fluorescence emissions (Table 5.6). Increasing the concentration of PicoGreen from 1 to 5% significantly increased fluorescence in CEN exposed to Triton X-100 ($p = 0.001$), but had no effect on CEN suspended in DMSO. CEN fluorescence was higher overall after exposure to DMSO at both 1 and 5% PicoGreen ($p = 0.001$, $p = 0.045$). No significant differences in staining efficiency were seen after 20, 40 or 60 minutes of incubation with PicoGreen in either Triton X-100 or DMSO (Table 5.6). Given that optimal phytoplankton staining was also observed using DMSO as a permeabilisation agent, this chemical was selected for use within this protocol. Whilst addition of 5% PicoGreen again produced highest staining levels, similarly to phytoplankton data this fluorescence was attributable to undesirable, non-specific staining within CEN. Hence, 1% PicoGreen was used in further protocol development.

5.3.5. Phytoplankton DNA and carbon content

Phytoplankton genome data correlated with existing data on DNA content (where available) for the species tested (Table 5.7). DNA represents 3% of total cellular carbon within phytoplankton (Veldhuis et al. 1997). Values of DNA were therefore multiplied to produce cellular carbon content (Table 5.7). Carbon content by DNA staining showed a positive relationship with cell volume estimated by FWS (R^2 = 0.63, p = 0.02) as shown in Figure 5.4. These DNA derived carbon data were compared against carbon values based on microscopy measurements of true (geometric) cell volume and against carbon derived by CHN analysis (Table 5.7).

Table 5.7. Estimations of phytoplankton carbon content based on DNA content, microscopic estimations of geometric volume and carbon-hydrogen-nitrogen (CHN) elemental analysis. Estimations of DNA content are compared to those listed by Boucher et al. (1991). Phytoplankton species are listed in ascending size order.

Species	DNA (pg cell^{-1})	DNA (C pg cell^{-1})	Volume (C pg cell^{-1})	CHN (C pg cell^{-1})	Literature DNA values (pg cell^{-1})
Synechococcus	0.01	0.43	0.40	-	0.02^{+}
M. pusilla	0.03	1.09	1.79	0.77	-
I. galbana	0.07	2.23	5.04	9.28	0.42^{+}
N. salina	0.10	3.40	6.01	9.41	-
E. huxylei	0.77	25.67	13.50	18.61	-
A. coffeaeformis	21.87	729.16	6.59	4.54	-
T. weissflogii	2.95	98.24	117.06	84.09	4.7^{+}
A. carterae	10.03	334.36	137.26	282.63	6.5^{+}
P. minimum	11.14	371.47	121.95	393.66	-
T. punctigera	16.12	537.33	67.69	106.28	-
T. suecica	2.03	67.51	221.80	49.93	-
S. turris	26.40	880.02	996.18	-	-
P. lunula	33.43	1114.17	2621.66	-	-

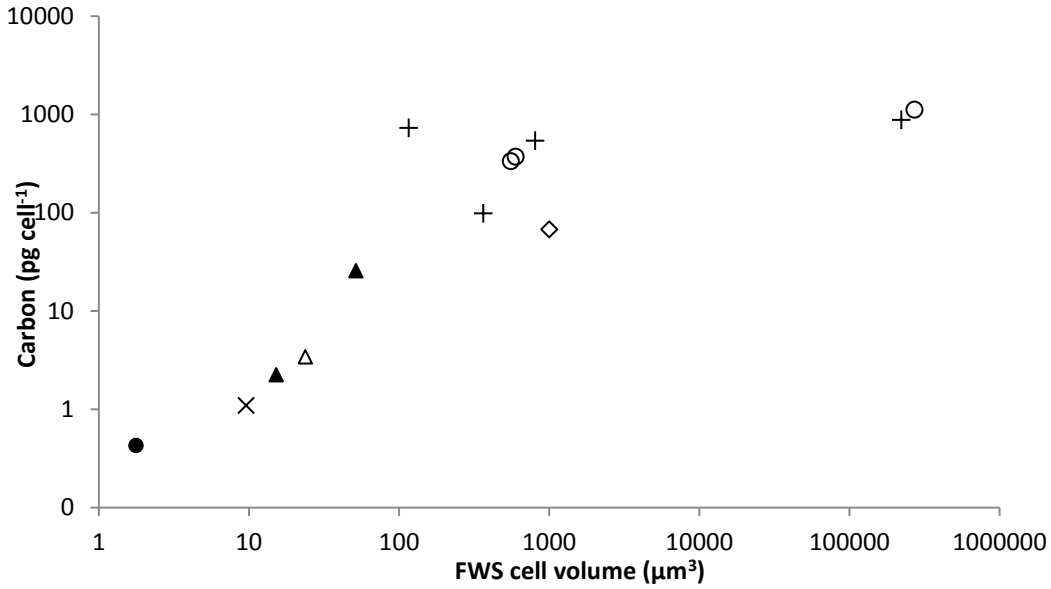

Figure 5.4. The cellular carbon content (pg cell^{-1}) of 13 phytoplankton species estimated via DNA staining and flow cytometry. Cell volume (log) derived from forward scatter (FWS) is plotted against DNA-derived carbon data (log), with the exception of *Synechococcus* (cyanobacteria) where cell volume was calculated from estimated cell size. Phytoplankton data are grouped as follows: the diatoms (+) , the dinoflagellates (○), chlorophytes (◊), prasinophytes (x), eustigmatophytes (Δ), prymnesiophytes (▲) and cyanobacteria (●).

For most species, variations in carbon content between the methods were within 1-2 orders of magnitude (Table 5.7). For the dinoflagellates *A. carterae* and *P. minimum*, DNA and CHN carbon data were comparable whilst carbon calculated from volume produced much lower values. This trend was reversed within the largest dinoflagellate species *P. lunula*, where carbon calculated from volume was higher than DNA derived data. The diatom species *A. coffeaeformis* and *T. punctigera* produced higher DNA carbon values in comparison to data produced from both volume and CHN analysis.

5.3.6. Environmental testing of staining protocol

At each sampling station DNA content increased with cell size regardless of location (Figure 5.5) with positive correlations between these parameters at both the Dowsing instrumental mooring ($R^2 = 0.79$, $p = 0.03$) and the Wash estuary ($R^2 =$

0.94, p = 0.03). Carbon content data derived from the DNA of environmental phytoplankton species showed the same trend with cell volume observed in cultured species (Figure 5.5). Data from *A. coffeaeformis* and *T. punctigera* were removed from this comparison due to their unusually high DNA-derived carbon values. Average carbon values ranged from 1.65 (Dowsing) to 3.49 C pg cell^{-1} (Wash estuary) for picophytoplankton cells and from 143.28 (Dowsing) to 342.87 C pg cell^{-1} (Wash estuary) for microplankton cells.

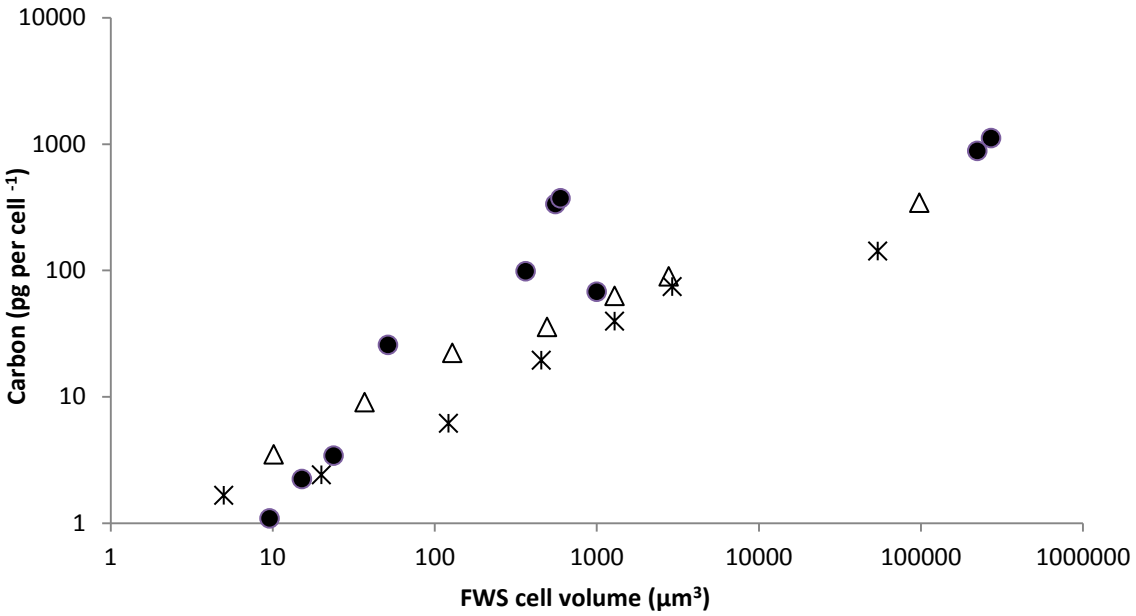

Figure 5.5. Averaged carbon content (pg per cell) derived from DNA for each size-based environmental phytoplankton group. Groups were defined as follows: 0-3, 3-5, 5-8, 8-12, 12-15, 15-20 and ≥ 20 µm. Data from the Dowsing instrumental mooring are represented by star markers (R^2 = 0.79, p = 0.31) and data from the Wash estuary are repesented by triangular markers (R^2 = 0.94, p = 0.08). Carbon data from cultured phytoplankton species, with the exception of *Synechococcus*, are supplied for comparison, indicated by filled circle markers.

5.4. Discussion

In agreement with existing data (e.g. Felip et al. 2007), both FWS and SWS measurements gave reasonable estimates of cell size across all phytoplankton cultures proportional to measured cell volume, with the exception of *Synechococcus*. Within the literature, FWS is frequently interpreted as cell size (Peperzak et al. 2000,

Tzur et al. 2011) however this relationship should not be assumed. Light scatter signals are influenced by factors other than cell size: intracellular composition; the refractive indices of suspension and sheath fluids; and differences in flow cytometer construction specifications such as light source wavelength and angles of scatter collection are all known to influence data (Cucci & Sieracki 2001; Shapiro 2003; Tzur et al. 2011). Differences in scatter may therefore not always be indicative of differences in size particularly in small variations within taxa (Veldhuis & Kraay 2000; Shapiro 2003). Careful instrument calibration with both microsphere and microscopy data is therefore vital before division of cells into size-based PFT, particularly in populations where cyanobacterial cells are abundant.

Assumed spherical volume calculated from FWS measurements was comparable with spherical volume derived by microscopy. There were also correlations between both flow cytometry and microscopy spherical volume methods and geometric volume data produced by microscopy. Microscopic measurement of cell size and conversion to volume assuming a spherical shape is a popular method within the literature (Verity et al. 1992; Zarauz & Irigoien 2008; Taylor et al. 2011; Chekalyuk et al. 2012). This data showed that spherical volume datasets acquired by flow cytometry are comparable to those produced by microscopy. Assumption of cell shape can produce overestimations of cell volume in comparison to values based on actual cell structure; dependent on phytoplankton community composition. However, the rapid analysis rate and the automated nature of flow cytometry greatly increase the sample size achievable, thereby increasing the robustness of carbon data acquired in this manner.

The protocol described here provides for the first time an efficient method of DNA staining, applicable to phytoplankton cells across a wide range of size, morphology and species in both laboratory and field environments. The DNA content of each species scaled with cell size as expected (Boucher et al. 1991, Veldhuis et al. 1997). Within the dinoflagellates *A. carterae* and *P. minimum*, carbon values from DNA and CHN analyses were similar, whilst volume derived carbon data were much lower. Dinoflagellates possess genetic characteristics which separate them from other eukaryotes, notably a large amount of cellular DNA, ranging from 3-250 pg/cell, compared to an average of 0.54 pg DNA/cell for eukaryotic algae

(Spector 1984, Rizzo 1991). These disproportionately large genomes are partly attributable to numerous seemingly identical chromosomes which remain condensed throughout the cell cycle (Rizzo 2003). This unique feature may explain the deviation of these two species from the general pattern within the data, also noted in other studies (Boucher et al. 1991, Veldhuis et al. 1997). Additionally, many species of dinoflagellates exhibit green autofluorescence (GAF) within the cytoplasm during certain life stages (Shapiro et al. 1989; Elbrächter 1994), known to interfere with green fluorescence staining within this group (Tang & Dobbs 2007). However, flow cytometric analysis of dinoflagellate cells prior to staining did not reveal the presence of GAF in our species. The similarity of DNA derived carbon content to values produced by CHN analysis further indicates that these elevated DNA contents are not linked to increased fluorescence as a consequence of GAF. The potential influence of GAF is rarely discussed within the literature but should be carefully considered in future staining work. Interestingly, the third dinoflagellate, *P. lunula*, did not exhibit this pattern. In this species, carbon estimated from volume produced higher values than those derived from DNA content. The cell structure of *P. lunula* forms a crescent shape which is difficult to measure by microscopy, leading to inaccuracies in cell volume estimates in this species. Furthermore, organelles are concentrated within the central region of these cells, with the majority of the interior space filled only by transparent cytoplasmic extensions (Seo & Fritz 2006). This may therefore produce inaccuracies in volume to carbon conversions which assume dinoflagellate cells to be densely packed, such as in *A. carterae* or *P. minimum*. It seems likely that a combination of both factors caused an overestimation of the volume-derived carbon content of this species. It should therefore be noted that assessments of dinoflagellate biomass reliant on volume methodology alone could significantly miscalculate carbon contributions from this group.

Similar conversion issues may also occur in larger diatom species. Transformation of cell volume to units of carbon are based on measurements of external frustule dimensions which do not necessarily correlate with those of the cytoplasm (Leblanc et al. 2012) leading to disruption of assumed relationships between volume and carbon content. Diatoms possess large vacuoles and may therefore contain less carbon per unit of volume than anticipated from their external size (Cornet-Barthaux et al. 2007). It is difficult to correct for these inert cell

structures, as vacuole proportions vary both phylogenetically and physiologically (Sicko-Goad et al. 1984, Hillebrand et al. 1999), ranging in volume from 22-70% relative to total diatom cell volume (Sicko-Goad et al. 1984). This issue, combined with difficulties in obtaining accurate measurements of complex diatom cell structures, produces cumulative complications in determing carbon content and probable overestimations of carbon biomass contributions by these cells. Whilst this issue is widely recognised, a satisfactory solution has yet to be found. Estimation of carbon calculated from DNA content circumnavigates both of these issues and may offer a more straight forward means of diatom biomass assessment.

The DNA derived carbon contents of the pennate diatom *A. coffeaeformis* and the chain-forming diatom *T. punctigera* appeared particularly large in comparison to the other two methods of carbon estimation and also in comparison to the known DNA content of other diatoms (Créach et al. 2006). Benthic species such as *A. coffeaeformis* exude polysaccharides that promote attachment of cells to flat surfaces (Hodson et al. 2012), frequently leading to the formation of clumps or aggregates when cultured. As such, it is difficult to fully separate cells prior to analysis and multiple stained individuals may have crossed the path of the laser simultaneously. The chain forming nature of *T. punctigera* may have produced a similar effect. However, cell scatter signals for both species were closely observed during analysis and coincidence events were rare. Furthermore, these events are easily eliminated from analyses due to their observably larger FWS and SWS signals. Elevated DNA contents may therefore be attributable to cell status at the time of analysis. Separate G1 and G2 phase subpopulations were not identifiable in these two species, most likely due to the masking effect of aggregations or chains of cells present within these cultures. It therefore seems likely that increased DNA/carbon levels were caused by unintentional inclusion of G2 subpopulations in the final stages of division within analyses.

Field testing of the protocol with environmental samples was successful. Cells across a wide size range from both coastal and open water environments were successfully stained and data showed DNA and therefore carbon content to increase with cell size. Whilst picophytoplankton cells stained well, there were issues in the accurate estimation of their size. The CytoSense flow cytometer is able to detect and

enumerate cells ranging from 2 - 200 µm, however the diameter of cells outside this range cannot be accurately measured. This restricts the utility of flow cytometry carbon data obtained from estimates of cell volume alone, although carbon values acquired from DNA are unaffected by this problem. This further underlines the inaccuracies inherent in carbon datasets based on a singular cellular property. DNA derived carbon data also revealed clear differences in carbon partitioning across the phytoplankton communities present at each location, with PFT values from the open water Dowsing site lower than those recorded at the Wash estuary. High resolution data of this type are essential for determining the ecological relevance of PFT in environments of different nutrient status and for tracking the ecosystem impact of any future shifts in biotic and abiotic parameters. Bacterial cells were also well stained by this protocol, although these were not targeted in further analyses. Bacterial populations are equally relevant in the flux of marine carbon via their participation within the microbial loop, however these cells are excluded from biomass estimates derived from light microscopy studies or based on measurements of chl *a*. This DNA staining protocol therefore offers an inclusive assessment of carbon partitioning across both large and small marine microbial forms, previously unattainable by a single analysis technique and essential for advancing comprehension of the processes underpinning marine biogeochemical cycling.

DNA analysis by fluorochrome staining and flow cytometry is a relative measurement and the quality of the data produced is constrained by the DNA reference standard used. There is little information and even less uniformity across the literature on the acquisition, preparation and use of DNA standards. We have found CEN to be a popular choice in algal DNA calibration, but they are sourced, fixed and utilised in a variety of ways (Tiersch et al. 1989, Johnston et al. 1999, Dolezel & Bartos 2005, Kapraun 2005). Mean CEN fluorescence has varied within different preparations of nuclei even though the DNA content is apparently the same (Johnston et al. 1999). This disparity can cause significant problems with estimations of DNA content, particularly in the discrimination of small differences in genome size. Whilst isolated nuclei allowing the expression of absolute DNA values are preferable, they are fragile and easily damaged, and reliability must be ascertained before use. An estimated DNA content of approx. 3 pg per nuclei is generally used for calibration purposes, however this is assumed and may be influenced by

inconsistencies in DNA content between chicken lines (Bennett & Leitch 1995). Furthermore, the genome size of CEN can be 10-20 times larger than those of many phytoplankton cells (Vaulot et al. 1994), introducing a risk of nonlinearity and offset errors (Dolezel & Bartos 2005). Despite their widespread acceptance, animal nuclei may therefore not be the best choice for estimations of genome size in plants. Plant standards, such as those used in terrestrial plant research (Johnston et al. 1999) may prove to be more relevant for phytoplankton analysis. Vaulot et al. (1994) used a strain of *Phaeocystis* as an internal DNA standard, however this approach is rare within phytoplankton genome research. Further research into the development of widely available phytoplankton standards for use in DNA calibration is clearly required and would be extremely relevant to this protocol.

5.5. Conclusions

Currently, calculation of volume using geometric shape equations is only possible via microscopy. Whilst preferable, this technique cannot supply data on the scale required for comprehensive ecosystem modelling. We have demonstrated that estimates of spherical biovolume produced from calibrated flow cytometric cell size measurements can provide an efficient alternative data source, on a scale relevant for macroecological studies. Flow cytometric analysis has the potential to play a key role in experimental verification of ecosystem models and can contribute much more than measurements of red fluorescence and approximations of community composition. As the popularity of flow cytometry for marine monitoring increases, it is essential to continue development of new applications at the cutting edge of this technology. We have demonstrated that basic flow cytometric analyses can be modified to target alternative cellular properties producing much greater resolution of phytoplankton community structure and function for little extra effort. This study successfully achieved a phytoplankton DNA staining protocol appropriate to both cultured and environmental cells and applicable to diverse environmental locations. DNA derived carbon measurements offer a third dimension of information to assessments of photosynthetic standing stock and can provide the size-based PFT data required by ecosystem models. The link between DNA and carbon may prove extremely useful in the analysis of phytoplankton communities across light or nutrient gradients; e.g. vertical profiling. This protocol also offers potential for applications beyond use as a

platform for biomass estimations. The staining of what appear to be G1 and G2 phase subpopulations of cells within many species indicates utility for cell cycle studies in field samples. Clarification of the relationship between cell cycle and cell growth in natural communities may assist in predictions of population growth rates. Whilst this study focused on applying DNA staining to explore the ecological relevance of cells within marine systems, there remains much to discover about the evolutionary significance of DNA content and the C-value enigma, especially within the dinoflagellates. This methodology offers high-speed analysis of genome size, which may be of particular use in laboratory investigation of inter- and intraspecies genetic diversity.

It is apparent that further examination and increased methodological clarity into the use of DNA standards within staining flow cytometry is required. This is vital to ensure ultimate data comparability between different machines and protocols. Reference standards require careful selection and rigorous compatibility testing prior to, and during, experimentation in order to ensure optimal data quality. As the use of flow cytometric analysis within marine research grows, the matter of data comparability is an increasingly pertinent issue. Development and consensus on the use of appropriate, widely available DNA reference standards is vital to ensure a benchmark of comparability in future work.

Chapter 6 Synthesis: progress and perspectives

This research aimed to assess and document the natural variability of phytoplankton populations within North Sea waters, focusing specifically on the distribution and contribution of the micro-, nano- and picophytoplankton functional types. Flow cytometry supplied a powerful investigative tool for the examination of phytoplankton cells across all three size-based functional types, allowing comparative examinations of the relevance of each group to cell concentrations and biomass. In this section, I describe the issues investigated throughout this thesis. The main results are summarised and discussed in relation to the progress achieved and from the perspective of further research development.

6.1. Flow cytometric analysis of North Sea phytoplankton biomass during late summer (Chapter 3)

Objective 1: *Spatial investigation of phytoplankton distribution and biomass partitioning through participation in the Cefas International Beam Trawl Survey Research Cruise, August 2010.*

The extent of picophytoplankton (≤ 3 µm) contributions to food webs and therefore carbon cycling were only fully realised in the early 1980s. The first applications of flow cytometry to oceanographic research at around the same time allowed picophytoplankton communities to be comprehensively studied on a wide scale. As a consequence, these cells are now known to proliferate in the oligotrophic open ocean and populations within these systems are well described (Li et al. 1981, Platt et al. 1983, Howard & Joint 1989, Zubkov et al. 1998). More recently, the relevance of the picophytoplankton to temperate coastal systems has begun to be examined (Calvo-Díaz et al. 2004, 2006, 2008, Morán 2007). This thesis aimed to address gaps in the knowledge of picophytoplankton contributions to phytoplankton community structure and biomass outside of typical oceanic environments. Within the North Sea, information on phytoplankton distribution and biomass partitioning is

frequently derived from limited datasets. These are restricted in the cell size range included within the analysis (Brandsma et al. 2013), focus on a single PFT to the exclusion of others (Howard & Joint 1989, Riegman & Noordeloos 1998, Baudoux et al. 2008), or are constrained in size and reproducibility due to the analysis technique used (Baretta-Bekker et al. 2009). Picophytoplankton cell size discounts them from accurate quantification by light microscopy, whilst many flow cytometers have upper or lower particle size limits which prevent complete measurements of phytoplankton biomass. Consequently, picophytoplankton contributions relative to North Sea nano- (3-20 µm) and microplankton (20-200 µm) biomass have yet to be widely examined. Developments in flow cytometric design have produced a new generation of instruments specifically designed for analysis of environmental samples in the field. The CytoSense (Cytobuoy, the Netherlands) is robust, portable and able to process cells from 1 to 800 µm. This instrument was used to conduct on board analyses of live cells from all three size-based phytoplankton functional types (PFT) during late summer 2010. This was the first flow cytometric survey of this kind to cover the North Sea.

Picophytoplankton cells were shown to be ubiquitous across the North Sea, numerically dominating phytoplankton communities. Total red fluorescence (RFL) contributions were dominated by nanoplankton and were focused around areas of higher nutrients. Further analysis of the group revealed cells between 5-10 µm contributed on average to over 50% of total nanoplankton RFL. Minimal contributions from microplankton cells were observed in terms of both cell concentrations and RFL. A *Synechococcus*-like picoprokaryote group contributed to phytoplankton biomass in areas of both high and low nutrient status, in contrast to data from previous studies of picophytoplankton in shelf seas (e.g. Calvo-Díaz et al. 2004, 2008). Overall values of total RFL representing complete phytoplankton community contributions were compared to MERIS ocean colour satellite data and were shown to produce similar maps of biomass distribution and magnitude.

The combination of on board high speed flow cytometry and automated data processing software was successfully used to provide novel insights into North Sea phytoplankton community structure. These data emphasise the huge potential of flow

cytometry for the collection of detailed datasets which require a greatly reduced sampling effort in comparison to more standardised techniques. Furthermore, use of specialised flow cytometry data processing software such as Easyclus (Thomas Rutten Projects) allowed automated division of RFL data into contribution by multiple, customisable cell size classes, with minimal operator input. As flow cytometers become more accessible and more widely used within marine research, the need for standardisation of analysis techniques and methodological clarity become increasingly important. Flow cytometry datasets such as this form an extremely valuable resource, useful for scientific purposes ranging from biogeochemical model and satellite data validation to assessments of fish stocks. However, unless flow cytometric data on cell size and fluorescence are carefully calibrated, datasets cannot be compared and therefore cannot be effectively used within wider research.

Whilst this survey only provided a synoptic overview of phytoplankton distributions at this time, the need for future inclusion of picophytoplankton within phytoplankton research in temperate zones was clear. Although the relevance of picophytoplankton to shelf sea biomass may ultimately prove trivial when compared to other PFT, they hold potential as indicator species of future environmental change (Morán 2007, Li et al. 2009). Alterations in the distribution patterns of the picophytoplankton may supply a valuable biomarker for subtle shifts in ecosystem state and a population baseline, similar to those in place for larger cells, should be established.

6.2. A three-year time series monitoring estuarine pico-, nano-and microplankton phytoplankton communities by flow cytometry (Chapter 4).

Objective 2: *Temporal investigation of PFT distributions and diversity in the Wash estuary (UK) from 2010-2012*

Coastal environments hold a central role within global cycles of carbon and macronutrients on Earth, contributing roughly 25% to oceanic primary productivity

despite their comparatively small volume (Wollast 1998). These highly productive regions form a vital resource for fish, mammals and birds, and support aquaculture industries. Coastal phytoplankton populations vary with time, reflecting seasonal fluctuations in the parameters controlling their activities (Not et al. 2007; Schlüter et al. 2012). Two distinct bloom periods of high photosynthetic biomass are observed along North Sea coastlines during spring and late summer, a phenomenon which coincides with optimal physicochemical conditions (Gieskes & Kraay 1977, Townsend et al. 1994, Peperzak et al. 1998, Wiltshire et al. 2008, Brandt & Wirtz 2010, Arndt et al. 2011). Within these regions, bloom biomass and productivity are typically dominated by large microplanktonic diatom genera, accompanied by smaller nanoflagellate cells (Rousseau et al. 2002, Pannard et al. 2008, Weston et al. 2008, Schlüter et al. 2012). This seasonal distribution model was built primarily on data supplied by microscopic observations of chemically preserved cells (Pannard et al. 2008, Devlin et al. 2009). The ecological state of UK marine waters is currently assessed by the European Water Framework Directive (WFD). Phytoplankton community data are compared against an 'ideal' of species composition, abundance, average biomass and bloom occurrence (Devlin et al. 2009). Re-evaluation of the WFD and the use of light microscopy methods is ongoing, as light microscopy is labour intensive, subjective and produces relatively small datasets which exclude the picophytoplankton (Peperzak et al. 2000, Peperzak 2010, Dromph et al. 2012). Cell preservation is known to unpredictably alter cellular properties, creating data bias and complicating PFT assessments (Montagnes et al. 1994, Menden-Deuer et al. 2001, Sato et al. 2006, Katano et al. 2009). Flow cytometry provides a faster means of acquiring larger and more reproducible datasets, but is also routinely applied to preserved cells due to logistical rather than technical constraints. A CytoSense flow cytometer was used to track phytoplankton cells within the Wash estuary over a three year period. The measurement range of this instrument allowed pico-, nano- and microplankton cells to be analysed simultaneously. Data were collected from seven sampling sites within the estuary, including four locations in close proximity to farmed bivalve populations. On board flow cytometry was not possible and an alternative method of sample transportation was developed, avoiding the need for chemical preservation. Preservation was shown to significantly alter cell fluorescence ($p = 0.001$), abundance ($p = 0.0000$) and size ($p = 0.000$), particularly within the nanoplankton. This work supplemented existing studies signalling the

need for careful interpretation of data acquired in this manner and provides a viable alternative to fixation protocols.

Bivalve aquaculture did not influence phytoplankton biomass or composition. The timing of RFL peaks were consistent with existing models and closely tracked optimal nutrient conditions. Significant interannual variations were recorded in the magnitude of bloom biomass, particularly in spring 2010 where RFL values were larger than in subsequent years ($7.8x10^8$ mV/ml compared to $5.9x10^8$ in 2011 and $2x10^8$ in 2012). Whilst microplankton and diatoms were present within bloom communities, as indicated by flow cytometry data and silicate depletion, bloom biomass was dominated by nanoplankton across all three years, contributing 96% (2010), 87% (2011) and 66% (2012) to RFL. Furthermore, in 2011 picophytoplankton represented 7% of bloom RFL, in comparison to contributions of 3% from the microplankton. In 2010 spring bloom biomass was composed of the harmful algal bloom (HAB) species *Phaeocystis*, a unique event not repeated in the subsequent two years.

This dataset showed some discrepancies with established ecological theories of phytoplankton distribution patterns. Nanoplankton cells dominated surface water blooms, whilst the contribution of microplankton was outweighed by that of picophytoplankton in 2011. Reduced silicate levels were most likely attributable to the presence of benthic diatom species undetected by surface water sampling procedures. These data raise several important points for discussion. Nanoplankton cells were more affected by preservation techniques than any other group. This suggests great potential for miscalculation of their contribution to photosynthetic biomass based only on data acquired from preserved cells. Picophytoplankton are not included within models of coastal succession, yet our data show these cells can periodically contribute more surface biomass than microplankton. This is in agreement with recent data from the Bay of Biscay which outlined the significant contribution of picophytoplankton within eutrophic systems (Calvo-Díaz et al. 2004, 2006, 2008). Efforts should therefore be made to include this PFT within monitoring programmes of coastal phytoplankton communities, particularly the WFD. Furthermore, it appears that large and ecologically relevant benthic diatom

communities have been overlooked by standardised surface water sampling techniques. Accurate representations of annual variations in phytoplankton biomass within the Wash estuary may therefore require the collection of multiple samples throughout the water column. This work also showed the variable nature of phytoplankton community composition. *Phaeocystis* is an indicator of eutrophication, a HAB species known to lower bivalve productivity (Lancelot et al. 2008, Smith et al. 2013) and can indirectly negatively influence carbon recirculation within ecosystems. In regions of high ecological and economic importance such as the Wash, it is critical to establish detailed monitoring procedures capable of reliably tracking the strength and frequency of *Phaeocystis* bloom events. The inclusion of flow cytometry in future survey work within the Wash would permit efficient collection of the data required for continued monitoring of these issues.

6.3. Estimation of carbon content in phytoplankton cells by flow cytometry in cultured and environmental populations (Chapter 5)

Objective 3: *Advancement of flow cytometric techniques for phytoplankton analysis through the development of protocols using cell volume and DNA content for carbon estimation.*

Accurate partitioning of phytoplankton biomass by PFT is essential for robust ecosystem models of carbon cycling. Chl *a* is common to all phytoplankton species and is a frequently used proxy for estimates of photosynthetic carbon (Gosselain et al. 2000, Jeffrey & Mantoura 2005). However, the relationship between chl *a* and carbon is non-linear, as chl *a* varies with temperature, light history and nutrient status (Cloern et al. 1995, Fukuda et al. 1998, Veldhuis & Kraay 2000). Chl *a* data are also generally in the form of bulk community measurements (Cornet-Barthaux et al. 2007). Cell carbon may be more accurately derived from microscopic measurements of cell volume (Hillebrand et al. 1999), however the complex nature of this technique limits dataset size. Phytoplankton DNA content exhibits a stable relationship with cell volume, as genome size is a conservative parameter unaltered by environmental forcing (Holm-Hansen 1969, Cavalier-Smith 1978, Gregory 2001b). This parameter therefore offers a stable basis for carbon conversions but is not widely used due to

the lack of a DNA measurement protocol applicable to multiple PFT (Gall et al. 1993, Marie et al. 1996, Veldhuis et al. 1997). This thesis developed a simple phytoplankton DNA staining procedure compatible with flow cytometric analysis and suitable for use across a range of species. The accuracy of cell volume data acquired by flow cytometry was also tested against microscopically acquired values. Phytoplankton DNA content was calibrated against isolated chicken erythrocyte nuclei (CEN), supplying the first absolute values of DNA from all three size-based PFT. In agreement with existing data, DNA content scaled with cell size (Boucher et al. 1991, Veldhuis et al. 1997) at both coastal ($R^2 = 0.94$, $p = 0.03$) and open water sampling locations ($R^2 = 0.79$ $p = 0.03$). Conversion of DNA to carbon showed the average carbon contents of PFT to vary geographically. Coastal values ranged from 4 pg C cell^{-1} in the picophytoplankton to 343 pg C cell^{-1} in the microplankton, whilst values in open water were much lower, ranging from 2 pg C cell^{-1} (picophytoplankton) to 143 pg C cell^{-1} (microplankton). Cell volume measurements derived from carefully calibrated flow cytometry data were similar to those produced by microscopy ($R^2 = 0.89$, $p = 0.01$). Whilst microscopic measurements of cell size are popular (Verity et al. 1992; Zarauz & Irigoien 2008; Taylor et al. 2011; Chekalyuk et al. 2012), this study showed that calibrated flow cytometry data produces datasets of equal accuracy on a scale more relevant to macroecological studies. Phytoplankton carbon data acquired by DNA staining were comparable to values obtained from cell volume conversions and CHN elemental analysis. Exceptions to this trend were seen in dinoflagellates, where volumetric estimates both under and overestimated carbon content due to variations in the DNA density of their cells, and therefore carbon content, between species. Consequently, these data indicate that biomass estimations based solely on volumetric calculations may contain significant errors when dinoflagellate species are present. Interestingly, DNA content was larger than expected in two diatom species, most likely due to accidental inclusion of G2 subpopulations within data analyses. The successful staining of both G1 and G2 cell cycle phases suggests this protocol may be useful for future research into population growth of environmental phytoplankton communities.

This study proposed two alternative methods of measuring phytoplankton carbon content by flow cytometry in addition to more characteristic analyses of RFL. These

protocols supplement chl *a* as biomarkers for estimates of carbon biomass, supplying supplementary datasets for investigations of phytoplankton community structure. This work reinforces the flexibility of flow cytometry as an analytical technique and underlines its suitability for detailed surveys of marine microbial communities. However, whilst the large datasets produced by flow cytometry increase statistical and therefore model validity, data quality is highly dependent on the use of careful calibration and standardisation procedures. There is little information and even less uniformity across the literature on the acquisition, preparation and use of flow cytometry standards, for both fluorescence and size parameters. Flow cytometry has the potential to play a key role in experimental verification of ecosystem models and can contribute much more than measurements of fluorescence. As the popularity of flow cytometry for use in marine research increases, it is essential to develop new applications at the cutting edge of this technology, whilst continuing to promote methodological clarity and use of appropriate reference standards.

6.4 Conclusions

Phytoplankton drive global biogeochemical cycles and underpin intricate trophic systems. The structure and composition of phytoplankton communities are central to ecosystem functioning and knowledge of biomass partitioning across cell size categories is critical for increasing understanding of these complex processes and interactions. North Sea phytoplankton have been studied for more than 200 years, during which time the initial perceptions of Viktor Hensen have evolved to produce the ecological paradigms of phytoplankton temporal and spatial distributions in place today. Phytoplankton analysis techniques have advanced at a slower rate. Light microscopy played a key role in early analyses of marine biota and it remains integral to modern monitoring procedures. The advent of flow cytometry in the 1930s and the application of this technique to oceanography in the 1980s marked a new era in phytoplankton research. It is now possible to collect data across the entire cell size range of phytoplankton species in larger and more accurate datasets than ever before. This project utilised flow cytometric technology to its full extent in order to examine the distribution and biomass partitioning of North Sea phytoplankton communities. Research focused on inclusion of the picophytoplankton

alongside nano- and microplankton within both spatial and temporal investigations of phytoplankton communities. The data collected were then used to re-examine existing ecological theories on phytoplankton distribution within temperate shelf seas. Established views on the relevance of picophytoplankton to phytoplankton community structure and seasonal succession were challenged in both coastal and open water North Sea environments. The previously undocumented contributions of picophytoplankton cells to spring bloom dynamics within the Wash estuary and the differing distributions of pro- and eukaryotic picophytoplankton cells across the North Sea clearly indicate that much remains to be discovered about this PFT. Picophytoplankton can no longer be considered of little importance outside of oligotrophic systems and should not be treated as a homogenous group. The need for inclusion of all three PFT within both targeted research of specific communities and routine monitoring regimes was clearly demonstrated throughout this thesis.

Flow cytometry was shown to be an ideal technique for collection of inclusive phytoplankton data throughout the North Sea. These instruments are increasingly used within oceanographic research but are equally applicable to marine monitoring. The development of cheaper, portable and more multi-functional flow cytometers increases their accessibility to a wider scientific community, creating more opportunities for data collection across all PFT. Throughout this project the CytoSense has proven equally suited to both offshore fieldwork and experimental laboratory analyses. Incorporation of instruments such as this into routine phytoplankton monitoring programmes would reduce the need for, and costs associated with, sample preservation, transportation and laboratory analyses. These savings would help to offset the initial costs of acquiring a flow cytometer. Whilst other instruments are also suitable for data collection in the laboratory or field (Picot et al. 2012), the CytoSense offers a unique range of modifications which greatly enhance its multipurpose capabilities and increase its versatility in data collection (http://www.cytobuoy.com, accessed 21/04/2014). A standard bench top CytoSense can be made submersible and capable of deployment to a maximum depth of 200 m. The CytoSense can also be adapted for placement on fixed moorings, collecting high frequency data for months at a time (Thyssen et al. 2011) without the need for regular deployment of research vessels. An additional second laser can be fitted for identification of optimum species (Rutten et al. 2005), whilst an in-flow camera

system can be purchased allowing photographs to be taken of the particles analysed (Picot et al. 2012). Data acquired from CytoSense instruments with imaging capabilities are of particular use in the continued efforts to construct reliable libraries of phytoplankton pulse-shapes and identify species contained within clusters (Malkassian et al. 2011, Pereira & Ebecken 2011). They are also relevant to monitoring programmes within environments such as the Wash estuary, where the presence of commercial shellfish beds necessitates regular screening of water samples for the presence of toxic phytoplankton (HAB) species. This is currently performed by light microscopy, however automated flow cytometry imaging systems in the Gulf of Mexico were recently used to detect the first toxic *Dinophysis* bloom recorded in the US (Campbell et al. 2010). This combination of technologies therefore has great potential to enhance the detection of toxic species in UK waters and provide a similar automated early warning system.

Continued development of automated flow cytometry is now culminating in the placement of completely automated flow cytometers on board research vessels (Swalwell et al. 2011). Recent trials have demonstrated the successful installation and remote operation of a CytoSense flow cytometer on board the RV Cefas Endeavour during Spring 2014 (Véronique Créach, Cefas, personal communication). Seawater samples are collected, analysed, processed by autoclustering software and transmitted automatically, allowing real time data to be viewed online. The CytoSense was also linked to an automated Ferrybox system, allowing flow cytometry data to be combined with information on temperature, salinity, fluorescence, turbidity and position (Créach, personal communication). Installation of combined automated systems on ships of opportunity, such as passenger ferries and freight vessels, would exponentially increase the quantity of information collected for comparatively little cost and sampling effort. This would supply phytoplankton datasets on a previously unattainable scale, ideal for calibrating remote sensing data and validating ecosystem models (Brotas et al. 2013). The practicality of this type of data collection is tightly coupled to the continued development and improvement of automated clustering software, such as EasyClus which was trialled in this thesis. It is essential that both flow cytometric technology and analytical power advance in parallel, to ensure that data collected are not constrained by a processing bottleneck. The release of new software on open source

platforms such as R (Poisson-Caillault et al. 2009, Wacquet 2011) will facilitate this process by increasing accessibility and promoting collaboration.

Detailed information on phytoplankton populations is essential for accurate representations of the relationships between primary productivity, carbon cycling and phytoplankton community structure and for relevant modelling predictions on the effects of future environmental change. Alterations to global climate are expected to modify oceanic environments over the next 100 years (Meehl et al. 2007), with consequences for both phytoplankton primary production and standing stock (Irwin & Finkel 2008). Increases in atmospheric CO_2 and temperature are linked to shifts in ocean chemistry and circulation patterns, likely to cause changes in both light and nutrient regimes (Finkel et al. 2009, Maranon et al. 2012). Clear evidence documenting increasing temperature and decreasing pH in some regions of the upper ocean has already been published (Meehl et al. 2007, Boyd et al. 2013). Ongoing warming may lead to declines in total phytoplankton biomass (Behrenfeld et al. 2006) via a gradual shift towards smaller primary producers (Morán et al. 2010), a trend already observed in Mediterranean waters (Cabrini et al. 2012, Giani et al. 2012, Mozetič et al. 2012). Temperature is known to be positively linked to the relative contribution of smaller cells to total primary production, but not to total chlorophyll. Chl *a* may therefore not provide an ideal biomass biomarker for cells of this size range (Agawin et al. 2000). The development of supplementary methods of biomass estimation, such as the DNA content protocol developed in this thesis, may therefore become of increasing relevance.

More than 70% of the surface of the Earth is covered by seas and oceans (Suttle 2007) and the phytoplankton contained within them are responsible for approximately half of global primary production (Field et al. 1998). However, whilst the population dynamics of terrestrial plants are well-studied, there remains much to learn about the distribution and activity of phytoplankton. Marine ecosystems are characterised by wide species diversity yet the succession and distribution of the main taxa are not fully understood. The potential impact of climate change on phytoplankton communities remains uncertain. Large scale shifts in community size structure could lead to alterations in oceanic ecosystem function and biogeochemical cycling (Morán et al. 2010). A movement towards smaller cell size could decrease

primary production available to food webs and increase availability to the microbial loop (Hansson et al. 2012), with potentially negative consequences for reliant higher trophic organisms. The range of phytoplankton species may shift in order to adapt to environmental change, leading to the appearance of warm water HAB species in formerly temperate areas. Additional stress factors such as ocean acidification, eutrophication, pollution and overfishing will combine to place additional pressure on marine ecosystems. Dominance of smaller cells may decrease the efficiency of the biological pump, reducing the amount of carbon transported from the surface to the oceans interior and the drawdown of CO_2. This could impact greatly upon carbon cycling, potentially promoting climate change and strengthening global warming via a positive feedback loop (Mousing et al. 2014).

A more in-depth understanding of the structure and function of phytoplankton is crucial to creating accurate ecosystem models and allowing regional paradigms of distribution and primary productivity to be overhauled and redefined. These data in turn are critical to elucidating the roles of shifting environmental parameters in their assemblages, knowledge which is vital in order to predict and mitigate the effects of global climate change on pelagic ecosystems.

References

Ackleson SG, Robins DB (1990) Flow cytometric determinations of North Sea phytoplankton optical properties. Netherlands J Sea Res 25:11–18

Adachi M, Ito A, Ishida A, Kadir W, Ladpala P, Yamagata Y (2011) Carbon budget of tropical forests in Southeast Asia and the effects of deforestation: an approach using a process-based model and field measurements. Biogeosciences 8:2635–2647

Agawin NSR, Duarte CM, Agustı S (2000) Nutrient and temperature control of the contribution of picoplankton to phytoplankton biomass and production. Limnol Oceanogr 45:591–600

Agustí S (2004) Viability and niche segregation of *Prochlorococcus* and *Synechococcus* cells across the Central Atlantic Ocean. Aquat Microb Ecol 36:53–59

Alldredge A, Passow U, Logan B (1993) The abundance and significance of a class of large, transparent organic particles in the ocean. Deep Sea Res Part I Oceanogr Res Pap 40:1131–1140

Amann R, Fuchs BM (2008) Single-cell identification in microbial communities by improved fluorescence *in situ* hybridization techniques. Nat Rev Microbiol 6:339–48

Amann RI, Ludwig W, Schleifer K-H (1995) Phylogenetic identification and *in situ* detection of individual Microbial Cells without Cultivation. Microbiol Rev 59:143–169

Aminot A, Rey F (2000) Standard procedure for the determination of chlorophyll *a* by spectroscopic methods. ICES Tech Mar Environ Sci:1–25

Andersen R (2004) Biology and systematics of heterokont and haptophyte algae. Am J Bot 91:1508–22

Anderson TR (2005) Plankton functional type modelling: running before we can walk? J Plankton Res 27:1073–1081

Arndt S, Lacroix G, Gypens N, Regnier P, Lancelot C (2011) Nutrient dynamics and phytoplankton development along an estuary–coastal zone continuum: A model study. J Mar Syst 84:49–66

Atkinson P, Clark N, Bell M, Dare P, Clark J, Ireland P (2003) Changes in commercially fished shellfish stocks and shorebird populations in the Wash, England. Biol Conserv 114:127–141

Atkinson P, Maclean I, Clark N (2010) Impacts of shellfisheries and nutrient inputs on waterbird communities in the Wash, England. J Appl Ecol 47:191–199

Aumont O, Belviso S, Monfray P (2002) Dimethylsulfoniopropionate (DMSP) and dimethylsulfide (DMS) sea surface distributions simulated from a global three-dimensional ocean carbon cycle model. J Geophys Res 107:1–19

Azam F, Fenchel T, Field J, Gray J, Meyer-Reil L, Thingstad F (1983) The ecological role of water-column microbes in the sea. Mar Ecol Prog Ser 10:257–263

Baretta JW, Ebenhöh W, Ruardij P (1995) The European regional seas ecosystem model, a complex marine ecosystem model. Netherlands J Sea Res 33:233–246

Baretta-Bekker J, Baretta J, Latuhihin M, Desmit X, Prins T (2009) Description of the long-term (1991-2005) temporal and spatial distribution of phytoplankton carbon biomass in the Dutch North Sea. J Sea Res 61:50–59

Bar-Zeev E, Berman-Frank I, Stambler N, Vázquez Domínguez E, Zohary T, Capuzzo E, Meeder E, Suggett D, Iluz D, Dishon G, Berman T (2009) Transparent exopolymer particles (TEP) link phytoplankton and bacterial production in the Gulf of Aqaba. Aquat Microb Ecol 56:217–225

Baudoux A, Veldhuis M, Noordeloos A, Noort G van, Brussaard C (2008) Estimates of virus-vs. grazing induced mortality of picophytoplankton in the North Sea during summer. Aquat Microb Ecol 52:69–82

Baumann MEM, Lancelot C, Brandini FP, Sakshaug E, John DM (1994) The taxonomic identity of the cosmopolitan prymnesiophyte *Phaeocystis*: a morphological and ecophysiological approach. J Mar Syst 5:5–22

Behrenfeld M, O'Malley R, Siegel D (2006) Climate-driven trends in contemporary ocean productivity. Nature 444:752–755

Bennett M, Leitch I (1995) Nuclear DNA amounts in Angiosperms. Ann Bot 76:113–176

Berelson W (2001) Particle settling rates increase with depth in the ocean. Deep Sea Res Part II 49:237–251

Beukema J, Cadée G (1991) Growth rates of the bivalve *Macoma balthica* in the Wadden Sea during a period of eutrophication: relationships with concentrations of pelagic diatoms and flagellates. Mar Ecol Prog Ser 68:249–256

Beukema J, Cadée G, Dekker R (2002) Zoobenthic biomass limited by phytoplankton abundance: evidence from parallel changes in two long-term data series in the Wadden Sea. J Sea Res 49:111–125

Bidigare RR, Heukelem L Van, Trees CC (2005) Analysis of Algal Pigments by High-Performance Liquid Chromatography. In: Andersen R. (ed) Algal Culturing Techniques. Elesevier Academic Press

Biegala I, Not F, Vaulot D, Simon N (2003) Quantitative assessment of picoeukaryotes in the natural environment by using taxon-specific oligonucleotide probes in association with Tyramide Signal Amplification-Fluorescence *In Situ* Hybridization and flow cytometry. Appl Environ Microbiol 69:5518–5529

Boelen P, Veldhuis M, Buma A (2001) Accumulation and removal of UVBR-induced DNA damage in marine tropical plankton subjected to mixed and simulated non-mixed conditions. Aquat Microb Ecol 24:265–274

Boran J, Camphuysen K, Evans P, Leo[old M, Northridge S, Reid J, Tasker M, Weir C (2003) Atlas of cetacean distribution in north-west European waters (JB Reid, PGH Evans, and SP Northridge, Eds.). Joint Nature Conservation Committee, Peterborough

Boucher N, Vaulot D, Partensky F (1991) Flow cytometric determination of phytoplankton DNA in cultures and oceanic populations. Mar Ecol Prog Ser 71:75–84

Bouman HA, Lepère C, Scanlan DJ, Osvaldo U (2012) Phytoplankton community structure in a high-nutrient, low-chlorophyll region of the eastern Pacific Subantarctic region during winter-mixed and summer-stratified conditions. Deep Sea Res Part I Oceanogr Res Pap 69:1–11

Bourne W (1983) Birds, fish and offal in the North Sea. Mar Pollut Bull 14:294–296

Boyd PW, Rynearson TA, Armstrong EA, Fu F, Hayashi K, Hu Z, Hutchins DA, Kudela RM, Litchman E, Mulholland MR, Passow U, Strzepek RF, Whittaker KA, Yu E, Thomas MK (2013) Marine phytoplankton temperature versus growth responses from polar to tropical waters - outcome of a scientific community-wide study. PLoS One 8:e63091

Bozzola JJ, Russell LD (1999) Specimen preparation for transmission electron microscopy.In: Electron microscopy: principles and techniques for biologists, 2nd edn. Jones and Bartlett Publishers, p 16–47

Brandsma J, Martínez J, Slagter HA, Evans C, Brussaard CPD (2013) Microbial biogeography of the North Sea during summer. Biogeochemistry 113:119–136

Brandt G, Wirtz KW (2010) Interannual variability of alongshore spring bloom dynamics in a coastal sea caused by the differential influence of hydrodynamics and light climate. Biogeosciences 7:371–386

Bratbak G (1985) Bacterial biovolume and biomass estimations. Appl Environ Microbiol 49:1488–1493

Bratbak G, Jacquet S, Larsen A, Pettersson L, Sazhin A, Thyrhaug R (2011) The plankton community in Norwegian coastal waters -abundance, composition, spatial distribution and diel variation. Cont Shelf Res 31:1500–1514

Breton E, Brunet C, Sautour B, Brylinski J (2000) Annual variations of phytoplankton biomass in the Eastern English Channel: comparison by pigment signatures and microscopic counts. J Plankton Res 22:1423–1440

Brewin RJW, Hardman-Mountford NJ, Lavender SJ, Raitsos DE, Hirata T, Uitz J, Devred E, Bricaud A, Ciotti A, Gentili B (2011) An intercomparison of bio-optical techniques for detecting dominant phytoplankton size class from satellite remote sensing. Remote Sens Environ 115:325–339

Brewin RJW, Lavender SJ, Hardman-Mountford NJ (2010) Mapping size-specific phytoplankton primary production on a global scale. J Maps 448:462

Brotas V, Brewin RJW, Sá C, Brito AC, Silva A, Mendes CR, Diniz T, Kaufmann M, Tarran G, Groom SB, Platt T, Sathyendranath S (2013) Deriving phytoplankton size classes from satellite data: validation along a trophic gradient in the eastern Atlantic Ocean. Remote Sens Environ 134:66–77

Brownlee C, Taylor AR (2002) Algal calcification and silification. Encycl Life Sci:1–6

Brunet C, Brylinski JM, Bodineau L, Thoumelin G, Bentley D, Hilde D (1996) Phytoplankton dynamics during the spring bloom in the south-eastern English Channel. Estuar Coast Shelf Sci 43:469–483

Brussaard C, Gast G, Duyl F van, Riegman R (1996) Impact of phytoplankton bloom magnitude on a pelagic microbial food web. Mar Ecol Prog Ser 144:211–221

Brussaard CPD, Riegman R, Noordeloos AAM, Cadee GC, Witte H, Kop AJ, Nieuwland G, Duyl FC Van, Bak RPM (1995) Effects of grazing, sedimentation and phytoplankton cell lysis on the structure of a coastal pelagic food web. Mar Chem 123:259–271

Buck KRK, Chavez FFP, Campbell L (1996) Basin-wide distributions of living carbon components and the inverted trophic pyramid of the central gyre of the North Atlantic Ocean, summer 1993. Aquat Microb Ecol 10:283–298

Buitenhuis ET, Li WKW, Vaulot D, Lomas MW, Landry MR, Partensky F, Karl DM, Ulloa O, Campbell L, Jacquet S, Lantoine F, Chavez F, Macias D, Gosselin M, McManus GB (2012) Picophytoplankton biomass distribution in the global ocean. Earth Syst Sci Data 4:37–46

Button D, Robertson B (2001) Determination of DNA content of aquatic bacteria by flow cytometry. Appl Environ Microbiol 67:1636–1645

Cabrini M, Fornasaro D, Cossarini G, Lipizer M, Virgilio D (2012) Phytoplankton temporal changes in a coastal northern Adriatic site during the last 25 years. Estuar Coast Shelf Sci 115:113–124

Cadée G, Hegeman J (1974) Primary production of phytoplankton the Wadden Sea. Netherlands J Sea Res 8:240–259

Calvo-Díaz A, Moran X, Nogueira E, Bode A, Varela M (2004) Picoplankton community structure along the northern Iberian continental margin in late winter-early spring. J Plankton Res 26:1069–1081

Calvo-Díaz A, Morán X, Calvo-D A, Moran X (2006) Seasonal dynamics of picoplankton in shelf waters of the southern Bay of Biscay. Aquat Microb Ecol 42:159–174

Calvo-Díaz A, Moran X, Suarez L (2008) Seasonality of picophytoplankton chlorophyll *a* and biomass in the central Cantabrian Sea, southern Bay of Biscay. J Mar Syst 72:271–281

Campbell L, Olson RJ, Sosik HM, Abraham A, Henrichs DW, Hyatt CJ, Buskey EJ (2010) First harmful *Dinophysis* (Dinophyceae, Dinophysiales) bloom in the U.S. is revealed by automated imaging flow cytometry. J Phycol 46:66–75

Camphuysen C, Berrevoets C, Cremers H, Dekinga A, Dekker R, Ens B, Have T van der, Kats R, Kuiken T, Leopold M, Meer J van der, Piersma T (2002) Mass mortality of common eiders (*Somateria mollissima*) in the Dutch Wadden Sea, winter 1999/2000: starvation in a commercially exploited wetland of international importance. Biol Conserv 106:303–317

Carrick H, Schelske C (1997) Have we overlooked the importance of small phytoplankton in productive waters? Limnol Oceanogr 42:1613–1621

Carstensen J, Henriksen P, Heiskanen A-S (2007) Summer algal blooms in shallow estuaries: definition, mechanisms, and link to eutrophication. Limnol Oceanogr 52:370–384

Cavalier-Smith T (1978) Nuclear volume control by nucleoskeletal DNA, selection for cell volume and cell growth rate, and the solution of the DNA C-Value paradox. J Cell Sci 34:247–278

Cembella A (2003) Chemical ecology of eukaryotic microalgae in marine ecosystems. Phycologia 42:420–447

Cermeño P, Marañón E, Harbour D, Harris RP (2006) Invariant scaling of phytoplankton abundance and cell size in contrasting marine environments. Ecol Lett 9:1210–1215

Chauvaud L, Jean F, Ragueneau O (2000) Long-term variation of the Bay of Brest ecosystem: benthic-pelagic coupling revisited. J Exp Mar Bio Ecol 227:83–111

Chekalyuk A, Landry M, Goericke R, Taylor A, Hafez M (2012) Laser fluorescence analysis of phytoplankton across a frontal zone in the California Current ecosystem. J Plankton Res 34:761–777

Chisholm SW, Olson RJ, Zettler ER, Goericke R, Waterbury J, Welschmeyer N (1988) A novel free-living prochlorophyte abundant in the oceanic euphotic zone. Lett to Nat 334:340–343

Cloern J (1982) Does the benthos control phytoplankton biomass in south San Francisco Bay? Mar Ecol Prog Ser 9:191–202

Cloern JE, Grenz C, Vidergar-Lucas L (1995) An empirical model of the phytoplankton chlorophyll: carbon ratio - the conversion factor between productivity and growth rate. Limnol Oceanogr 40:1313–1321

Cloern J, Jassby A (2008) Complex seasonal patterns of primary producers at the land-sea interface. Ecol Lett 11:1294–303

Cloern J, Jassby A (2009) Patterns and scales of phytoplankton variability in estuarine–coastal ecosystems. Estuaries and Coasts 33:230–241

Colijn F, Cadée G (2003) Is phytoplankton growth in the Wadden Sea light or nitrogen limited? J Sea Res 49:83–93

Collier J (2000) Flow cytometry and the single cell in phycology. J Phycol 36:628–644

Cornet-Barthaux V, Armand L, Quéguiner B (2007) Biovolume and biomass estimates of key diatoms in the Southern Ocean. Aquat Microb Ecol 48:295–308

Courties C, Vaquer A, Troussellier M, Lautier J (1994) Smallest eukaryotic organism. Nature 370:255

Crawford C, McLeod C, Mitchell I (2003) Effects of shellfish farming on the benthic environment. Aquaculture 224:127–168

Créach V, Ernst A, Sabbe K, Vanelslander B, Vyverman W, Stal L (2006) Using quantitative PCR to determine the distribution of a semicryptic benthic diatom, *Navicula phyllepta* (Bacillariophyceae). J Phycol 42:1142–1154

Crosland-Taylor P (1953) A device for counting small particles suspended in a fluid through a tube. N 171:37–38

Cucci T, Sieracki M (2001) Effects of mismatched refractive indices in aquatic flow cytometry. Cytometry 44:173–8

Cugier P, Struski C, Blanchard M, Mazurié J, Pouvreau S, Olivier F, Trigui JR, Thiébaut E (2010) Assessing the role of benthic filter feeders on phytoplankton production in a shellfish farming site: Mont Saint Michel Bay, France. J Mar Syst 82:21–34

Cushing D (1990) Plankton production and year class strength in fish populations: an update of the match/mismatch hypothesis. Adv Mar Biol 26:249–293

de la Rocha CL (2003) The Biological Pump. Treatise on Geochemistry 6:1–29

Devlin M, Barry J, Painting S, Best M (2009) Extending the phytoplankton tool kit for the UK Water Framework Directive: indicators of phytoplankton community structure. Hydrobiologia 633:151–168

Dolah F Van (2000) Marine Algal Toxins: origins, health effects and their increased occurrence. Environ Heal Perspect 108:133–242

Dolezel J, Bartos J (2005) Plant DNA flow cytometry and estimation of nuclear genome size. Ann Bot 95:99–110

Dromph K, Agusti S, Basset A, Franco J, Henriksen P, Icely J, Lehtinen S, Moncheva S, Revilla M, Roselli L, Sorensen K (2012) Sources of uncertainty in assessment of marine phytoplankton communities. Hydrobiologia 704:253–264

Druzhkov N V, Druzhkova EI (2000) The dynamics of the nanophytoplankton community in the coastal ecosystem of the Southern Bight (North Sea) during the winter–spring period. J Sea 43:105–111

Dubelaar GBJ, Gerritzen PL (2000) CytoBuoy: a step forward towards using flow cytometry in operational oceanography. Sci Mar 64:255–265

Ducklow H, Steinberg D, Buesseler K (2001) Upper Ocean Carbon Export and the Biological Pump. Oceanography 14:50–58

Ducrotoy J-P, Elliott M, Jonge VN de (2000) The North Sea. Mar Pollut Bull 41:5–23

Ediger D, Soydemir N, Kideys AE (2006) Estimation of phytoplankton biomass using HPLC pigment analysis in the southwestern Black Sea. Deep Sea Res Part II Top Stud Oceanogr 53:1911–1922

Egge J, Aksnes D (1992) Silicate as regulating nutrient in phytoplankton competition. Mar Ecol Prog Ser 83:281–289

Elbrächter M (1994) Green autofluorescence: a new taxonomic feature for living dinoflagellate cysts and vegetative cells. Rev Palaeobot Palynol 84:101–105

Engel A (2002) Direct relationship between CO_2 uptake and transparent exopolymer particles production in natural phytoplankton. J Plankton Res 24:49–53

Eschbach E, Reckermann M, John U, Medlin L (2001) A simple and highly efficient fixation method for *Chrysochromulina polylepis* (Prymnesiophytes) for analytical flow cytometry. Cytometry 44:126–32

Falkowski P, Katz M, Knoll A, Quigg A, Raven J, Schofield O, Taylor F (2004) The evolution of modern eukaryotic phytoplankton. Science 305:354–60

Felip M, Andreatta S, Sommaruga R, Straskrábová V, Catalan J, Straskra V (2007) Suitability of flow cytometry for estimating bacterial biovolume in natural plankton samples: comparison with microscopy data. Appl Environ Microbiol 73:4508–4514

Felip M, Catalan J (2000) The relationship between phytoplankton biovolume and chlorophyll in a deep oligotrophic lake: decoupling in their spatial and temporal maxima. J Plankton Res 22:91–105

Fenchel T (2001) How Dinoflagellates Swim. Protist 152:329–338

Fenchel T (2008) The microbial loop – 25 years later. J Exp Mar Bio Ecol 366:99–103

Field C, Behrenfeld M, Randerson J, Falkowski P (1998) Primary production of the biosphere: integrating terrestrial and oceanic components. Science 281:237–240

Finkel Z V., Beardall J, Flynn KJ, Quigg A, Rees TA V., Raven JA (2009) Phytoplankton in a changing world: cell size and elemental stoichiometry. J Plankton Res 32:119–137

Forster R, Créach V, Sabbe K, Vyverman W, Stal L (2006) Biodiversity-ecosystem function relationship in microphytobenthic diatoms of the Westerschelde estuary. Mar Ecol Prog Ser 311:191–201

Frada M, Not F, Probert I, Vargas C de (2006) $CaCO_3$ optical detection with Fluorescent *In Situ* Hybridization: a new method to identify and quantify calcifying microorganisms from the oceans. J Phycol 42:1162–1169

Franklin D, Airs R, Fernandes M, Bell T, Bongaerts R, Berges J, Malin G (2012) Identification of senescence and death in *Emiliania huxleyi* and *Thalassiosira pseudonana*: Cell staining, chlorophyll alterations, and dimethylsulphoniopropionate (DMSP) metabolism. Limnol Oceanogr 57:305–317

Franklin DJ, Steinke M, Young J, Probert I, Malin G (2010) Dimethylsulphoniopropionate (DMSP), DMSP- lyase activity (DLA) and dimethylsulphide (DMS) in 10 species of coccolithophore. Mar Ecol Prog Ser 410:13–23

Froneman PW, Pakhomov EA, Balarin MG (2004) Size-fractionated phytoplankton biomass, production and biogenic carbon flux in the eastern Atlantic sector of the Southern Ocean in late austral summer 1997 – 1998. Deep Sea Res Part II 51:2715–2729

Fukuda R, Ogawa H, Nagata T, Koike I (1998) Direct determination of carbon and nitrogen contents of natural bacterial assemblages in marine environments. Appl # Environ Microbiol 64:3352–3358

Fuller NJ, Campbell C, Allen DJ, Pitt FD, Zwirglmaier K, Gall F Le, Vaulot D, Scanlan DJ (2006) Analysis of photosynthetic picoeukaryote diversity at open ocean sites in the Arabian Sea using a PCR biased towards marine algal plastids. Aquat Microb Ecol 43:79–93

Furnas MJ (1982) Growth rates of summer nanoplankton (<10 µm) populations in lower Narragansett Bay, Rhode Island, USA. Mar Biol 70:105–115

Furnas M (1990) In situ growth rates of marine phytoplankton: approaches to measurement, community and species growth rates. J Plankton Res 12:1117–1151

Gaerdes A, Iversen M, Grossart H-P, Passow U, Ulrich M (2010) Diatom associated bacteria are required for aggregation of *Thalassiosira weissflogii*. ISME:1–10

Gall Y Le, Brown S, Marie D, Mejjad M, Kloareg B (1993) Quantification of nuclear DNA and G-C content in marine macroalgae by flow cytometry of isolated nuclei. Protoplasma 173:123–132

Garel E, Ferreira Ó (2011) Monitoring estuaries using non-permanent stations: practical aspects and data examples. Ocean Dyn 61:891–902

Gasol J, Giorgio P del (2000) Using flow cytometry for counting natural planktonic bacteria and understanding the structure of planktonic bacterial communities. Sci Mar 64:197–224

Gasol J, Zweifel U, Peters F, Fuhrman J, Hagström A (1999) Significance of size and nucleic acid content heterogeneity as measured by flow cytometry in natural planktonic bacteria. Appl Environ Microbiol 65:4475–4483

Gee K (2010) Offshore wind power development as affected by seascape values on the German North Sea coast. Land Use Policy 27:185–194

Gerdts G, Luedke G (2006) FISH and chips: marine bacterial communities analyzed by flow cytometry based on microfluidics. J Microbiol Methods 64:232–40

Ghosal S, Rogers M, Wray A (2000) The turbulent life of phytoplankton. Cent Turbul Res Proceeding:31–45

Giani M, Djakovac T, Degobbis D, Cozzi S, Solidoro C, Umani SF (2012) Recent changes in the marine ecosystems of the northern Adriatic Sea. Estuar Coast Shelf Sci 115:1–13

Gieskes W, Kraay G (1977) Continuous plankton records: Changes in the plankton of the North Sea and its eutrophic Southern Bight from 1948 to 1975. Netherlands J Sea Res 11:334–364

Giovannoni SJ, Britschgi TB, Moyer CL, Field KG (1990) Genetic diversity in Sargasso Sea bacterioplankton. Nature 345:60-63

Gomez F (2012) A quantitative review of the lifestyle, habitat and trophic diversity of the dinoflagellates (Dinoflagellata, Alveolata). Syst Biodivers 10:267–275

Gonzalez JM, Zimmermann J, Saiz-Jimenez C (2005) Evaluating putative chimeric sequences from PCR-amplified products. Bioinformatics 21:333–7

Gosselain V, Hamilton P, Descy J-P (2000) Estimating phytoplankton carbon from microscopic counts: an application for riverine systems. Hydrobiologia 438:75–90

Graham L, Wilcox L (2000) Introduction to the algae - occurrence, relationships, nutrition, definition, general features. In: Graham L, Wilcox L (eds) Algae. Prentice-Hall, New Jersey, p 1–21

Grall J, Chauvaud L (2002) Marine eutrophication and benthos: the need for new approaches and concepts. Glob Chang Biol 8:813–830

Gregory TR (2001a) The bigger the C-value , the larger the cell : genome size and red blood cell size in vertebrates. Blood Cells Mol Dis 27:830–843

Gregory TR (2001b) Coincidence, coevolution, or causation? DNA content, cell size, and the C-value enigma. Biol Rev Camb Philos Soc 76:65–101

Gregory TR, Hebert PDN (1999) The modulation of DNA content: proximate causes and ultimate consequences. Genome Res 9:317–324

Guillard R (1975) Culture of phytoplankton for feeding marine invertebrates. In: Smith W, Chanley M (eds) Culture of Marine Invertebrate Animals. Plenum Press, New York, USA, p 26–60

Guillard R, Hargraves P (1993) *Stichochrysis immobilis* is a diatom, not a chrysophyte.Phycologia 32:234–236

Guillard R, Ryther J (1962) Studies on marine planktonic diatoms: 1. *Cyclotella nana* (Hustedt) and *Detonula confervacae* (Cleve). J Microbiol 8:229–239

Guillou L, Pedro C, Massana R, Balague V, Balagué V, Pedrós-Alió C (2004) Picoeukaryotic diversity in an oligotrophic coastal site studied by molecular and culturing approaches.FEMS Microbiol Ecol 50:231–43

Hackett J, Anderson D, Erdner D, Bhattacharya D (2004) Dinoflagellates: A Remarkable Evolutionary Experiment. Am J Bot 91:1523–1534

Hall JA (1991) Long-term preservation of picophytoplankton for counting by fluorescence microscopy. Br Phycol J 26:169–174

Hamm CE, Merkel R, Springer O, Jurkojc P, Maier C, Prechtel K, Smetacek V (2003) Architecture and material properties of diatom shells provide effective mechanical protection. Nature 421:841–3

Hansson L-A, Nicolle A, Granéli W, Hallgren P, Kritzberg E, Persson A, Björk J, Nilsson PA, Brönmark C (2012) Food-chain length alters community responses to global change in aquatic systems. Nat Clim Chang 3:228–233

Hartwell V (2011) The Wash Biodiversity Action Plan. The Wash Estuary Project, Spalding, Lincolnshire

Hasle GR, Syvertsen EE, Throndsen J, Steidinger KA, Jangen K, Heimdal BR (1997) Identifying Marine Phytoplankton (CR Tomas, Ed.). Academic Press

Havskum H, Schlüter L, Schareck R, Berdalet E, Jacquet S (2004) Routine quantification of phytoplankton groups - microscopy or pigment analyses? Mar Ecol Prog Ser 273:31–42

Heukelem L Van, Thomas CS (2001) Computer-assisted high-performance liquid chromatography method development with applications to the isolation and analysis of phytoplankton pigments. J Chromatogr A 910:31–49

Hillebrand H, Durselen C-D, Kirschtel D, Pollingher U, Zohary T (1999) Biovolume calculation for pelagic and benthic microalgae. J Phycol 35:403–424

Hinder SL, Hays GC, Brooks CJ, Davies AP, Edwards M, Walne AW, Gravenor MB (2011) Toxic marine microalgae and shellfish poisoning in the British Isles: history, review of epidemiology, and future implications. Environ Heal 10:1-12

Hodson O, Monty J, Molino P, Wetherbee R (2012) Novel whole cell adhesion assays of three isolates of the fouling diatom *Amphora coffeaeformis* reveal diverse responses to surfaces of different wettability. Biofouling J Bioadhesion Biofilm Res 28:381–393

Holm-Hansen O (1969) Determination of microbial biomass in ocean profiles. Limnol Oceanogr 14:740–747

Hoppenrath M, Elbrachter M, Drebes G (2009) Introduction. In: Mosbrugger V (ed) Marine Phytoplankton. Selected microphytoplankton species from the North Sea around Helgoland and Sylt. E. Schweizerbart'sche Verlagsbuchhandlung, Stuttgart, p 12–20

Houdan A, Probert I, Lenning K Van, Lefebvre S (2005) Comparison of photosynthetic responses in diploid and haploid life-cycle phases of *Emiliania huxleyi* (Prymnesiophyceae). Mar Ecol Prog Ser 292:139–146

Howard KM, Joint IR (1989) Physiological ecology of picoplankton in the North Sea. Mar Biol 281:275–281

Howarth RW (2008) Coastal nitrogen pollution: A review of sources and trends globally and regionally. Harmful Algae 8:14–20

Hu H, Zhang J, Chen W (2011) Competition of bloom-forming marine phytoplankton at low nutrient concentrations. J Environ Sci 23:656–663

Huete-Ortega M, Cermeño P, Calvo-Díaz A, Marañón E (2012) Isometric size-scaling of metabolic rate and the size abundance distribution of phytoplankton. Proc R Soc B 279:1815–23

Huete-Ortega M, Maranon E, Varela M, Bode a. (2009) General patterns in the size scaling of phytoplankton abundance in coastal waters during a 10-year time series. J Plankton Res 32:1–14

Inouye I, Kawachi M (1994) The haptonema. In: Green J, Leadbeater S (eds) The haptophyte algae. Clarendon Press, Oxford, UK, p 73–89

Iriarte A, Purdie D (1994) Size distribution of chlorophyll *a* biomass and primary production in a temperate estuary (Southampton Water): the contribution of photosynthetic picoplankton. Mar Ecol Prog Ser 115:283–297

Irigoien X, Flynn K, Harris R (2005) Phytoplankton blooms : a “loophole” in microzooplankton grazing impact? J Plankton Res 27(4):313-327

Irwin A, Finkel Z (2008) Mining a sea of data: deducing the environmental controls of ocean chlorophyll. PLoS One 3:e3836

Janssen F, Schrum C, Backhaus JO (1999) A climatological data set of temperature and salinity for the Baltic Sea and the North Sea. Ger J Hydrol 51:5–245

Jardillier L, Zubkov M V, Pearman J, Scanlan DJ (2010) Significant CO_2 fixation by small prymnesiophytes in the subtropical and tropical northeast Atlantic Ocean. ISME J Int Soc Microb Ecol 4:1180–92

Jeffrey SW (2005) Application of pigment methods to oceanography. In: Jeffrey SW, Mantoura RFC, Wright SW (eds) Phytoplankton Pigments in Oceanography: Guidlines to Modern Methods, 2nd edn.p 127–166

Jeffrey S, Mantoura R (2005) Development of pigment methods for oceanography: SCOR-supported Working Groups and objectives. In: Jeffrey SW, Mantoura RFC, Wright SW (eds) Phytoplankton Pigments in Oceanography: Guidlines to Modern Methods, 2nd edn. United Nations Educational, Scientific and Cultural Organisation, p 19–36

Jeffrey S, Vesk M (2005) Introduction to marine phytoplankton and their pigment signatures. In: Jeffrey SW, Mantoura RFC, Wright SW (eds) Phytoplankton Pigments in Oceanography: Guidlines to Modern Methods, 2nd edn. UNESCO Publishing, p 37–84

Jeffrey S, Wright S, Zapata M (2011) Microalgal classes and their signature pigments. In: Roy S, Llewellyn C, Egeland E, Johnsen G (eds) Phytoplankton pigments. Characterisation, chemotaxonomy and applications in oceanography. 2nd edn. Cambridge University Press, Cambridge, p 3–77

Jennings S, Mélin F, Blanchard JL, Forster RM, Dulvy NK, Wilson RW (2008) Global-scale predictions of community and ecosystem properties from simple ecological theory. Proc Biol Sci 275:1375–83

Jin X, Gruber N, Frenzel H, Doney SC, Mcwilliams JC (2007) The impact on atmospheric CO_2 of iron fertilization induced changes in the ocean's biological pump. Biogeosciences Discuss 4:3863–3911

Johnson ZI, Zinser ER, Coe A, McNulty NP, Woodward EMS, Chisholm SW (2006) Niche partitioning among *Prochlorococcus* ecotypes along ocean-scale environmental gradients. Science 311:1737–40

Johnston JS, Bennett MD, Rayburn AL, Galbraith DW, Price HJ (1999) Reference standards for determination of DNA content of plant nuclei. Am J Bot 86:609–13

Jonker R, Groben R, Tarran G, Medlin L, Wilkins C, Garcia L, Zabala L, Boddy L (2000) Automated identification and characterisation of microbial populations using flow cytometry: the AIMS project. Sci Mar 64:225–234

Kamentsky LA (1965) Rapid biological cell identification by spectroscopic analysis. Proc 18th Ann Conf Eng Biol Med 7:178

Kapraun DF (2005) Nuclear DNA content estimates in multicellular green, red and brown algae: phylogenetic considerations. Ann Bot 95:7–44

Katano T, Nakano S (2006) Growth rates of *Synechococcus* types with different phycoerythrin composition estimated by dual-laser flow cytometry in relationship to the light environment in the Uwa Sea. J Sea Res 55:182–190

Katano T, Yoshida M, Lee J, Han M-S, Hayami Y (2009) Fixation of *Chattonella antiqua* and *C. marina* (Raphidophyceae) using Hepes-buffered paraformaldehyde and glutaraldehyde for flow cytometry and light microscopy. Phycologia 48:473–479

Ke X, Evans G, Collins M (1996) Hydrodynamics and sediment dynamics of the Wash embayment, eastern England. Sedimentology 43:157–174

Keeling PJ, Burger G, Durnford DG, Lang BF, Lee RW, Pearlman RE, Roger AJ, Gray MW (2005) The tree of eukaryotes. Trends Ecol Evol 20:670–6

Keller M, Selvin R, Claus W, Guillard R (1978) Media for the culture of oceanic ultraphytoplankton. J Phycol 23:633–63

Kerby TK, Cheung WW, Engelhard GH (2012) The United Kingdom's role in North Sea demersal fisheries: a hundred year perspective. Rev Fish Biol Fish 22:621–634

Kim J-M, Lee K, Shin K, Yang E, Engel A, Karl D, H-C K (2011) Shifts in biogenic carbon flow from particulate to dissolved forms under high carbon dioxide and warm ocean conditions. Geophys Res Lett 38:1-5

Kimura K, Tomaru Y, Nagasaki K (2012) Ultrastructural observation of natural field phytoplankton cells by using rapid freezing and freeze substitution. Plankt Benthos Res 7:126–134

Kirkham AR, Lepere C, Jardillier LE, Not F, Bouman H, Mead A, Scanlan D (2013) A global perspective on marine photosynthetic picoeukaryote community structure. ISME 7:922–936

Kirkwood D (1996) Nutrients: practical notes on their determination in seawater. ICES Tech Mar Environ Sci:23 pp

Koester JA, Swalwell JE, Dassow P von, Armbrust EV (2010) Genome size differentiates co-occurring populations of the planktonic diatom *Ditylum brightwellii* (Bacillariophyta). BMC Evol Biol 10:1

Konoplya B, Soares F (2011) New geometric models for calculation of microalgal biovolume. Brazilian Arch Biol Technol 54:527–534

Kostadinov T, Siegel D, Maritorena S (2009) Retrieval of the particle size distribution from satellite ocean color observations. J Geophys Res 114:1–22

Kroger S, Parker E, Metcalfe J, Greenwood N, Forster R, Sivyer D, Pearce D (2009) Sensors for observing ecosystem status. Ocean Sci Discuss 6:765–798

Kromkamp J, Peene J, Rijswijk P van, Sandee A, Goosen N (1995) Nutrients, light and primary production by phytoplankton and microphytobenthos in the eutrophic, turbid Westerschelde estuary (The Netherlands). Hydrobiologia 311:9–19

Kudela R, Dugdale R (2000) Regulation of phytoplankton new production as determined by enclosure experiments with nutrient additions in Monterey Bay, California. Deep Sea Res Part II 47:1023–1053

Lalli C, Parsons T (1993) Biological oceanography: an introduction. Pergamon Press, Oxford, UK

Lancelot C, Billen G, Sournia A, Weisse T, Colijn F, Veldhuis M, Davies A, Wassman P (1987) *Phaeocystis* blooms and nutrient enrichment in the continental coastal zones of the North Sea. Ambio 16:38–46

Lancelot C, Rousseau V, Gypens N (2008) Ecologically based indicators for *Phaeocystis* disturbance in eutrophied Belgian coastal waters (Southern North Sea) based on field observations and ecological modelling. J Sea Res 61:44–49

Lebedev V (2002) Macroecological patterns of phytoplankton in the northwestern North Atlantic Ocean. 419:154–157

Leblanc K, Armand L, Assmy P, Beker B, Bode A, Breton E, Cornet V, Gibson J, Kopczynska E, Marshall H, Peloquin J, Piontkovski S, Poulton AJ, Schiebel R, Shipe R, Stefels J, Leeuwe MA Van, Varela M, Widdicombe C, Yallop M (2012) A global diatom database – abundance, biovolume and biomass in the world ocean. Earth Sytem Sci Data 4:149–165

Le Quere C, Harrison S, Prentice C, Buitenhuis E, Aumont O, Bopp L, Claustre H, Cotrim Da Cunha L, Geider R, Giraud X, Klaas C, Kohfield K, Legendre L, Manizza M, Platt T, Rivkin R, Sathyendranath S, Uitz J, Watson A, Wolf-

Gladrow D (2005) Ecosystem dynamics based on plankton functional types for global ocean biogeochemistry models. Glob Chang Biol 11:2016–2040

Lee S, Fuhrman JA (1987) Relationships between biovolume and biomass of naturally derived marine bacterioplankton. Appl Environ Microbiol 53:1298–303

Leliaert F, Verbruggen H, Zechman FW (2011) Into the deep: new discoveries at the base of the green plant phylogeny. BioEssays news Rev Mol Cell Dev Biol 33:683–92

Lepesteur M, Martin J, Fleury A (1993) A comparative study of different preservation methods for phytoplankton cell analysis by flow cytometry. Mar Ecol Prog Ser 93:55–63

Levine NM, Varaljay VA, Toole DA, Dacey JWH, Doney SC, Moran MA (2012) Environmental, biochemical and genetic drivers of DMSP degradation and DMS production in the Sargasso Sea. Environ Microbiol 14:1210–23

Lewis L, McCourt R (2004) Algae and the origin of land plants. Am J Bot 91:1535–1556

Li WKW, Roa D, Harrison W, Smith J, Cullen J, Irwin B, Platt T (1981) Autotrophic picoplankton in the tropical ocean. Science 219:2–5

Li WKW, Wood A (1988) Vertical distribution of North Atlantic ultraphytoplankton: analysis by flow cytometry and epifluorescence microscopy. Deep Res 35:1615–1638

Li WKW (1989) Shipboard analytical flow cytometry of oceanic ultraphytoplankton. Cytometry 10:564–79

Li WKW, Dickie PM (2001) Monitoring Phytoplankton, Bacterioplankton, and Virioplankton in a Coastal Inlet (Bedford Basin) by Flow Cytometry. Cytometry 44:236 –246

Li WKW, Harrison WG, Head E (2006) Coherent assembly of phytoplankton communities in diverse temperate ocean ecosystems. Proc R Soc B 273:1953–1960

Li WKW (2009) From cytometry to macroecology: a quarter century quest in microbial oceanography. Aquat Microb Ecol 57:239–251

Li WKW, Mclaughlin FA, Lovejoy C, Carmack EC (2009) Smallest algae thrive as the Arctic Ocean freshens. Science 326:539

Li Z, Li L, Song K, Cassar N (2013) Estimation of phytoplankton size fractions based on spectral features of remote sensing ocean color data. J Geophys Res Ocean 118:1445–1458

Lin M, Comings D, Alfi O (1977) Optical studies of the interaction with DNA and metaphase chromosomes. Chromosoma 60:15–25

Lindström E, Weisse T, Stadler (2002) Enumeration of small ciliates in culture by flow cytometry and nucleic acid staining. J Microbiol Methods 49:173–82

Liss P, Hatton A, Malin G, Nightingale P, Turner S (1997) Marine sulphur emissions. Philos Trans R Soc B 352:159–169

Litchman E, Klausmeier C a C, Schofield OMO, Falkowski PPG (2007) The role of functional traits and trade-offs in structuring phytoplankton communities: scaling from cellular to ecosystem level. Ecol Lett 10:1170–81

Longhurst A, Sathyendranath S, Platt T, Caverhill C (1995) An estimate of global primary production in the ocean from satellite radiometer data. J Plankton Res 17:11245–1271

Lotze HK, Lenihan HS, Bourque BJ, Bradbury RH, Cooke RG, Kay MC, Kidwell SM, Kirby MX, Peterson CH, Jackson JBC (2006) Depletion, degradation, and recovery potential of estuaries and coastal seas. Science 312:1806–1809

Mackey M, Higgins H, Mackey D, Wright S (1997) CHEMTAX User's Manual: a program for estimating class abundances from chemical markers - application to HPLC measurements of phytoplankton pigments. CSIRO Marine Laboratories, Tasmania

Malin G, Turner S, Liss P (1992) Sulfur: the plankton/climate connection. J Phycol 28:590–597

Malkassian A, Nerini D, Dijk M a van, Thyssen M, Mante C, Gregori G (2011) Functional analysis and classification of phytoplankton based on data from an automated flow cytometer. Cytometry A 79:263–75

Maranon E, Cermeno P, Latasa M, Tadonleke R (2012) Temperature, resources, and phytoplankton size structure in the ocean. Limnol Oceanogr 57:1266–1278

Maranon E, Cermeno P, Rodrigues J, Zubkov M, Harris R (2007) Scaling of phytoplankton photosynthesis and cell size in the ocean. Limnol Oceanogr 52:2190–2198

Margalef R (1978) Life-forms of phytoplankton as survival alternatives in an unstable environment. Oceanol Acta 1:493–509

Marie D, Partensky F, Jacquet S, Vaulot D (1997) Enumeration and cell cycle analysis of natural populations of marine picoplankton by flow cytometry using the nucleic acid stain SYBR Green I. Appl Environ Microbiol 63:186–93

Marie D, Pierre U, Curie M, Simon N, Vaulot D (2005) Phytoplankton cell counting by flow cytometry. In: Andersen R (ed) Algal Culturing Techniques. Elesevier Academic Press, p 253–268

Marie D, Shi XL, Rigaut-jalabert F, Vaulot D (2010) Use of flow cytometric sorting to better assess the diversity of small photosynthetic eukaryotes in the English Channel. FEMS Microbiol Ecol 72:165–178

Marie D, Simon N, Guillou L, Partensky F, Vaulot D (2000) Current Protocols in Cytometry. Curr Protoc Cytom 11.12.1

Marie D, Vaulot D, Partensky F (1996) Application of the novel nucleic acid dyes YOYO-1, YO-PRO-1, and PicoGreen for flow cytometric analysis of marine prokaryotes. Appl Environ Microbiol 62:1649–1655

Martiny JBH, Bohannan BM, Brown JH, Colwell RK, Fuhrman JA, Green JL, Horner-Devine MC, Kane M, Krumins JA, Kuske CR, Morin PJ, Naeem S, Ovreås L, Reysenbach A-L, Smith VH, Staley JT (2006) Microbial biogeography: putting microorganisms on the map. Nat Rev Microbiol 4:102–12

Mary I, Cummings D, Biegala I, Burkill P, Archer S, Zubkov M (2006) Seasonal dynamics of bacterioplankton community structure at a coastal station in the western English Channel. Aquat Microb Ecol 42:119–126

Massana R, Logares R (2013) Eukaryotic versus prokaryotic marine picoplankton ecology. Environ Microbiol 15:1254–61

Maxwell K, Johnson GN (2000) Chlorophyll fluorescence - a practical guide. J Exp Bot 51:659–68

Medlin LK, Metfies K, Mehl H, Wiltshire K, Valentin K (2006) Picoeukaryotic plankton diversity at the Helgoland time series site as assessed by three molecular methods. Microb Ecol 52:53–71

Meehl G, Stocker T, Collins W (2007) Global climate projections. In: Solomon S, Qin D, Manning M, Chen Z, Marquis M, Averyt K, Tignor M (eds) Climate Change 2007: The Physical Science Basis. Contribution of Working Group I to the Fourth Assessment Report of the Intergovernmental Panel on Climate Change. Cambridge University Press, Cambridge

Meer J van der, Beukema JJ, Dekker R (2001) Long-term variability in secondary production of an intertidal bivalve population is primarily a matter of recruitment variability. J Anim Ecol 70:159–169

Meersche K Van den, Rijswijk P Van, Soetaert K, Middelburg JJ, Meersche K Van Den (2009) Autochthonous and allochthonous contributions to mesozooplankton diet in a tidal river and estuary: Integrating carbon isotope and fatty acid constraints. Limnol Oceanogr 54:62–74

Menden-Deuer S, Lessard E (2000) Carbon to volume relationships for dinoflagellates, diatoms and other protist plankton. Limnol Oceanogr 45:569–579

Menden-Deuer S, Lessard E, Satterberg J (2001) Effect of preservation on dinoflagellate and diatom cell volume, and consequences for carbon biomass predictions. Mar Ecol Prog Ser 222:41–50

Mills D, Tett P, Novarino G (1994) The spring bloom in the south western North Sea in 1989. Netherlands J Sea Res 33:65–80

Miron G, Landry T, Archambault P, Frenette B (2005) Effects of mussel culture husbandry practices on various benthic characteristics. Aquaculture 250:138-154

Modigh M, Saggiomo V, Alcala MR (1996) Conservative features of picoplankton in a Mediterranean eutrophic area, the Bay of Naples. J Plankton Res 18:87–95

Moldovan A (1934) Photo-electric technique for the counting of microscopical cells. Science 80:188–189

Montagnes D, Berges J, Harrison P, Taylor F (1994) Estimating carbon, nitrogen, protein, and chlorophyll *a* from volume in marine phytoplankton. Limnol Oceanogr 39:1044–1060

Moon-van der Staay SY, Wachter R De, Vaulot D (2001) Oceanic 18S rDNA sequences from picoplankton reveal unsuspected eukaryotic diversity. Nature 409:607–10

Morán X (2007) Annual cycle of picophytoplankton photosynthesis and growth rates in a temperate coastal ecosystem: a major contribution to carbon fluxes. Aquat Microb Ecol 49:267–279

Morán XAG, López-Urrutia Á, Calvo-Díaz A, Li WKW (2010) Increasing importance of small phytoplankton in a warmer ocean. Glob Chang Biol 16:1137–1144

Mousing EA, Ellegaard M, Richardson K (2014) Global patterns in phytoplankton community size structure - evidence for a direct temperature effect. Mar Ecol Prog Ser 497:25–38

Mozetič P, Francé J, Kogovšek T, Talaber I, Malej A (2012) Plankton trends and community changes in a coastal sea (northern Adriatic): bottom-up vs. top-down control in relation to environmental drivers. Estuar Coast Shelf Sci 115:138–148

Mullin M, Sloan P, Eppley R (1966) Relationship between carbon content, cell volume and area in phytoplankton. Limnol Oceanogr 11:307–311

Mur L, Skulberg O, Utkilen H (1999) Cyanobacteria in the environment. In: Chorus I, Bartram J (eds) Toxic Cyanobacteria in Water - a guide to their public health consequences, monitoring and management. Spoon Press Taylor and Francis Group

Murby P (1997) The Wash: Natural Area Profile. English Nature, Grantham, Lincolnshire

Mustapha Z Ben, Alvain S, Jamet C, Loisel H, Dessailly D (2014) Automatic classification of water-leaving radiance anomalies from global SeaWiFS imagery: application to the detection of phytoplankton groups in open ocean waters. Remote Sens Environ 146:97–112

Muyzer G, Smalla K (1998) Application of denaturing gradient gel electrophoresis (DGGE) and temperature gradient gel electrophoresis (TGGE) in microbial ecology. Antonie Van Leeuwenhoek 73:127–41

Nishino S, Kikuchi T, Yamamoto-Kawai M, Kawaguchi Y, Hirawake T, Itoh M (2011) Enhancement/reduction of biological pump depends on ocean circulation in the sea-ice reduction regions of the Arctic Ocean. J Oceanogr 67:305–314

Not F, Simon N, Biegala IC, Vaulot D (2002) Application of fluorescent *in situ* hybridization coupled with tyramide signal amplification (FISH-TSA) to assess eukaryotic picoplankton composition. Aquat Microb Ecol 28:157–166

Not F, Zapat M, Pazos Y, Campana E, Doval M, Rodriguez F (2007) Size-fractionated phytoplankton diversity in the NW Iberian coast: a combination of microscopic, pigment and molecular analyses. Aquat Microb Ecol 49:255–265

Not F, Latasa M, Scharek R, Viprey M, Karleskind P, Balague V, Ontoriaoviedo I, Cumino A, Goetze E, Vaulot D (2008) Protistan assemblages across the Indian Ocean, with a specific emphasis on the picoeukaryotes. Deep Sea Res Part I Oceanogr Res Pap 55:1456–1473

Olaizola M, Ziemann DA, Bienfang PK, Walsh WA, Conquest LD (1993) Eddy-induced oscillations of the pycnocline affect the floristic composition and depth distribution of phytoplankton in the subtropical Pacific. Mar Biol 116:533–542

Olson R, Frankel S, Chisholm S (1983) An inexpensive flow cytometer for the analysis of fluorescence signals in phytoplankton: chlorophyll and DNA distributions. J Exp Mar Bio Ecol 68:129–144

Olson R, Vaulot D, Chisholm S (1985) Marine phytoplankton distributions measured using shipboard flow cytometry. Deep Sea Res 32(10):1273-1280

Olson R, Chisholm S (1986) Effects of light and nitrogen limitation on the cell cycle of the dinoflagellate *Amphidinium carteri*. J Plankton Res 8:785–793

Olson R, Chisholm S, Zetter E, Armbrust E (1988) Analysis of *Synechococcus* pigment types in the sea using single and dual beam flow cytometry. Deep Sea Res Part A Oceanogr Res Pap 35:425–440

Olson RJ, Chisholm SW, Zetrler ER, Altabet M (1990) Spatial and temporal distributions of prochlorophyte picoplankton in the North Atlantic Ocean. Deep Res 37(6):1033-1051

Otto L, Zimmerman J, Furnes G, Mork M, Saetre R, Becker G (1990) Review of the physical oceanography of the North Sea. Netherlands J Sea Res 26:161–238

Palmer J, Totterdell I (2001) Production and export in a global ecosystem model. Deep Res I 48:1169–1198

Palsson C, Graneli W (2004) Nutrient limitation of autotrophic and mixotrophic phytoplankton in a temperate and tropical humic lake gradient. J Plankton Res 26:1005–1014

Pan L, Zhang L, Zhang J, Gasol J, Chao M (2005) On-board flow cytometric observation of picoplankton community structure in the East China Sea during the fall of different years. FEMS Microbiol Ecol 52:243–53

Pannard A, Claquin P, Klein C, Roy B Le, Veron B (2008) Short-term variability of the phytoplankton community in coastal ecosystem in response to physical and chemical condition changes. Estuar Coast Shelf Sci 80:212–224

Partensky F, Blanchot J, Vaulot D (1999) Differential distribution and ecology of *Prochlorococcus* and *Synechococcus* in oceanic waters: a review. Bull Oceanogr MONACO-NUMERO Spec:457–476

Partensky F, Hess WR (1999) *Prochlorococcus*, a marine photosynthetic prokaryote of global significance. 63:106–127

Passow U (2012) The abiotic formation of TEP under different ocean acidification scenarios. Mar Chem 128-129:72–80

Paxinos R, Mitchell JG (2000) A rapid Utermöhl method for estimating algal numbers. J Plankton Res 22:2255–2262

Peperzak L (2010) An objective procedure to remove observer-bias from phytoplankton time-series. J Sea Res 63:152–156

Peperzak L, Colijn F, Gieskes W, Peeters J (1998) Development of the diatom-*Phaeocystis* spring bloom in the Dutch coastal zone of the North Sea: the silicon depletion versus the daily irradiance threshold hypothesis. J Plankton Res 20:517–537

Peperzak L, Vrieling E, Sandee B, Rutten T (2000) Immuno flow cytometry in marine phytoplankton research. Sci Mar 64:165–181

Pereira GC, Ebecken NFF (2011) Combining in situ flow cytometry and artificial neural networks for aquatic systems monitoring. Expert Syst Appl 38:9626–9632

Pernthaler A, Pernthaler J, Amann R (2002) Fluorescence in situ hybridization and catalyzed reporter deposition for the identification of marine bacteria. Appl Environ Microbiol 68:3094–3101

Petersen W, Schroeder F, Bockelmann F-D (2011) FerryBox - application of continuous water quality observations along transects in the North Sea. Ocean Dyn 61:1541–1554

Philippart CJ, Gerhard C, Raaphorst W van, Riegman R (2000) Long-term phytoplankton-nutrient interactions in a shallow coastal sea: algal community structure, nutrient budgets, and denitrification potential. Limnol Oceanogr 45:131–144

Philippart CJM, Aken HM van, Beukema JJ, Bos OG, Cade GC, Dekker R (2003) Climate-related changes in recruitment of the bivalve *Macoma balthica*. Limnol Oceanogr 48:2171–2185

Picot J, Guerin CL, Van Kim C Le, Boulanger CM (2012) Flow cytometry: retrospective, fundamentals and recent instrumentation. Cytotechnology 64:109–30

Pieters H, Kluytmans J, Zandee D, Cadée G (1980) Tissue composition and reproduction of *Mytilus edulis* in relation to food availability. Netherlands J Sea Res 14:349–361

Platt T, Subba D, Irwin B (1983) Photosynthesis of picoplankton in the oligotrophic ocean. Nature 301:702–704

Poisson-Caillault É, Hebert P-A, Wacquet G (2009) Dissimilarity-based classification of multidimensional signals by conjoint elastic matching: application to phytoplanktonic species recognition. In: EANN, 11th International Conference of Engineering Applications of Neural Networks.p 152–164

Pomeroy L (1975) The ocean's food web, a changing paradigm. Bioscience 24:499–504

Pomeroy L, Williams PJ leB, Azam F, Hobbie J (2007) The microbial loop. Oceanography 20:28–33

Porra R, Pfundel E, Engel N (2005) Metabolism and function of photosynthetic pigments. In: Phytoplankton Pigments in Oceanography: Guidlines to Modern Methods.p 85–126

Prins TC, Smaal AC, Dame RF (1998) A review of the feedbacks between bivalve grazing and ecosystem processes. Aquat Ecol 31:349–359

Proctor R, Holt J, Allen J, Blackford J (2003) Nutrient fluxes and budgets for the North West European Shelf from a three-dimensional model. Sci Total Environ 314-316:769–785

Proctor C, Roesler C (2010) New insights on obtaining phytoplankton concentration and composition from in situ multispectral chlorophyll fluorescence. Limnol Oceanogr Methods 8:696–708

Qiu D, Huang L, Liu S, Lin S (2011) Nuclear, mitochondrial and plastid gene phylogenies of *Dinophysis miles* (Dinophyceae): evidence of variable types of chloroplasts. PLoS One 6:e29398

Rasch E (1985) DNA “standards” and the range of accurate DNA estimates by Feulgen absorption microspectrophotometry. PubMed 196:137–166

Raven JA (1998) The twelfth Tansley Lecture. Small is beautiful: the picophytoplankton. Funct Ecol 12:503–513

Raven JA, Beardall J, Allen D, Bragg J, Finkel Z V, Flynn KJ, Quigg A, Rees TA V, Richardson A (2009) Allometry and stoichiometry of unicellular, colonial and multicellular phytoplankton. New Phytol 181:295–309

Rees AP, Woodward EM., Robinson C, Cummings DG, Tarran G a, Joint I (2002) Size-fractionated nitrogen uptake and carbon fixation during a developing coccolithophore bloom in the North Sea during June 1999. Deep Sea Res Part II Top Stud Oceanogr 49:2905–2927

Reid P, Edwards M (2001) Long-term changes in the pelagos, benthos and fisheries of the North Sea. Senckenbergiana maritima 31:107–115

Reid P, Lancelot C, Gieskes W, Hafmeier E, Weichart G (1990) Phytoplankton of the North Sea and its dynamics: a review. Netherlands J Sea Res 26:295–331

Rendell A, Horrobin T, Jickells T, Edmunds H, Brown J, Malcolm S (1997) Nutrient cycling in the Great Ouse Estuary and its impact on nutrient fluxes to The Wash, England. Estuar Coast Shelf Sci 45:653–668

Reynolds C (2006) The Ecology of Phytoplankton. Cambridge University Press, Cambridge

Ribalet F, Marchetti A, Hubbard KA, Brown K, Durkin CA, Morales R, Robert M, Swalwell JE, Tortell PD, Armbrust E V (2010) Unveiling a phytoplankton hotspot at a narrow boundary between coastal and offshore waters. Proc Natl Acad Sci U S A 107:16571–6

Riechmann J, Heard J, Martin G, Reuber L, Jiang C-Z, Keddie J, Adam L, Pineda O, Ratcliffe O, Samaha R, Creelman R, Pilgrim M, Broun P, Zhang JZ, Ghandehari D, Sherman B, Yu G-L (2000) Arabidopsis transcription factors: genome-wide comparative analysis among eukaryotes. Science 290:2105–2110

Riegman R, Noordeloos A (1998) Size-fractionated uptake of nitrogenous nutrients and carbon by phytoplankton in the North Sea during summer 1994. Mar Ecol Prog Ser 173:95–106

Riegman R, Noordeloos AAM, Cadee GC (1992) Phaeocystis blooms and eutrophication of the continental coastal zones of the North Sea. Mar Biol 484:479–484

Riemann B, Simonsen P, Stensgaard L (1989) The carbon and chlorophyll content of phytoplankton from various nutrient regimes. J Plankton Res 11:1037–1045

Rizzo PJ (1991) The enigma of the dinoflagellate chromosome. J Eukaryot Microbiol 38:246–252

Rizzo PJ (2003) Those amazing dinoflagellate chromosomes. Cell Res 13:215–7

Röttgers R, Press AIN, Rottgers R (2007) Comparison of different variable chlorophyll *a* fluorescence techniques to determine photosynthetic parameters of natural phytoplankton. Deep Sea Res Part I Oceanogr Res Pap 54:437–451

Round F, Crawford R, Mann D (2007) The Diatoms, biology & morphology of the genera. Cambridge University Press

Rousseau V, Leynaert a, Daoud N, Lancelot C (2002) Diatom succession, silicification and silicic acid availability in Belgian coastal waters (Southern North Sea). Mar Ecol Prog Ser 236:61–73

Rousseau V, Chretiennot-Dinet M-J, Jacobsen A, Verity P, Whipple S (2007) The life cycles of *Phaeocystis*: state of knowledge and presumptive role in ecology. Biogeochemistry 83:29–47

Rutten TPA, Sandee B, Hofman ART (2005) Phytoplankton monitoring by high performance flow cytometry: a successful approach? Cytom Part A 26:16–26

Sato M, Takeda S, Furuya K (2006) Effects of long-term sample preservation on flow cytometric analysis of natural populations of pico- and nanophytoplankton. J Oceanogr 62:903–908

Scanlan D, West N (2002) Molecular ecology of the marine cyanobacterial genera *Prochlorococcus* and *Synechococcus*. FEMS Microbiol Ecol 40:1–12

Scharek R, Tupas LM, Karl DM (1999) Diatom fluxes to the deep sea in the oligotrophic North Pacific gyre at Station ALOHA. Mar Ecol Prog Ser 182:55–67

Schiayno MR, Unrein F, Gasol JM, Farias ME, Estevez C, Balagué V, Izaguirre I, Schiaffino MR (2009) Comparative analysis of bacterioplankton assemblages from maritime Antarctic freshwater lakes with contrasting trophic status. Polar Biol 32:923–936

Schillings C, Wanderer T, Cameron L, Wal JT van der, Jacquemin J, Veum K (2012) A decision support system for assessing offshore wind energy potential in the North Sea. Energy Policy 49:541–551

Schlüter MH, Kraberg A, Wiltshire KH (2012) Long-term changes in the seasonality of selected diatoms related to grazers and environmental conditions. J Sea Res 67:91–97

Seljom P, Rosenberg E (2011) A study of oil and natural gas resources and production. Int J Energy Sect Manag 5:101–124

Seo KS, Fritz L (2006) Karyology of a marine non-motile dinoflagellate, *Pyrocystis lunula*. Hydrobiologia 563:289–296

Shannon C, Weaver W (1949) The mathematical theory of communication. The University of Illinois Press, Urbana, IL

Shapiro HM (2003) Practical Flow Cytometry, 4th edn. Wiley-Liss, New Jersey

Shapiro HM (2004) The Evolution of Cytometers. Cytom Part A 58A:13–20

Shapiro L, Haugen E, Carpenter E (1989) Occurrence and abundance of green-fluorescing dinoflagellates in surface waters of the northwest Atlantic and northeast Pacific Oceans. J Phycol 35:189–191

Shaw GE (1983) Bio-controlled thermostasis involving the sulfur cycle. Clim Change 5:297–303

Shi XL, Marie D, Jardillier L, Scanlan DJ, Vaulot D (2009) Groups without cultured representatives dominate eukaryotic picophytoplankton in the oligotrophic South East Pacific Ocean. PLoS One 4:e7657

Shumway S (1989) Toxic algae, a serious threat to shellfish aquaculture. World Aquac 20:65–74

Sicko-Goad LM, Schelske CL, Stoermer EF (1984) Estimation of intracellular carbon and silica content of diatoms from natural assemblages using morphometric techniques. Limnol Oceanogr 29:1170–1178

Sieburth JM, Smetacek V, Lenz J (1978) Pelagic ecosystem structure: heterotrophic compartments of the plankton and their relationship to plankton size fractions. Limnol Oceanogr 23:1256–1263

Sigman DM, Haug GH (2003) The Biological Pump in the Past. Treatise on Geochemistry 6:491–528

Simon N, Barlow R, Marie D, Partensky F, Vaulot D (1994) Characterisation of oceanic photosynthetic picoeukaryotes by flow cytometry. J Phycol 30:922–935

Simon N, Campbell L, Ornolfsdottir E, Groben R, Guillou L, Lange M, Medlin LLK (1988) Oligonucleotide probes for the identification of three algal groups by dot blot and fluorescent whole-cell hybridization. J Eukaryot Microbiol 47:76–84

Simon N, Cras A, Foulon E, Lemée R (2009) Diversity and evolution of marine phytoplankton. C R Biol 332:159–70

Simpson JH, Sharples J (2012a) Physical forcing of the shelf seas: what drives the motion of the ocean. In: Simpson JH, Sharples J (eds) Introduction to the Physical and Biological Oceanography of Shelf Seas. Cambridge University Press, Cambridge, p 424

Simpson JH, Sharples J (2012b) Seasonal stratification and the spring bloom. In: Simpson JH, Sharples J (eds) Introduction to the Physical and Biological Oceanography of Shelf Seas. Cambridge University Press, Cambridge, p 424

Six K, Maier-Reimer E (1996) Effects of plankton dynamics on seasonal carbon fluxes in an ocean general circulation model. Global Biogeochem Cycles 10:559–583

Smaal A, Schellekens T, Stralen M van, Kromkamp J (2013) Decrease of the carrying capacity of the Oosterschelde estuary (SW Delta, NL) for bivalve filter feeders due to overgrazing. Aquaculture 404-405:28–34

Smarda P, Bureš P, Smerda J, Horová L (2012) Measurements of genomic GC content in plant genomes with flow cytometry: a test for reliability. New Phytol 193:513–21

Smayda TJ (1997) Harmful algal blooms: their ecophysiology and general relevance to phytoplankton blooms in the sea. Limnol Oceanogr 42:1137–1153

Smetacek V (1999) Revolution in the ocean. Nature 401:27570

Smith WO, Liu X, Tang KW, DeLizo LM, Doan NH, Nguyen NL, Wang X (2013) Giantism and its role in the harmful algal bloom species *Phaeocystis globosa*. Deep Sea Res Part II Top Stud Oceanogr 5:1–12

Spector D (1984) Dinoflagellate nuclei. In: Spector D (ed) Dinoflagellates. Academic Press, New York, p 107–147

Stefels J, Boekel W van (1993) Production of DMS from dissolved DMSP in axenic cultures of the marine phytoplankton species *Phaeocystis* sp. Mar Ecol Prog Ser 97:11–18

Strathmann RR (1967) Estimating the organic carbon content of phytoplankton from cell volume or plasma. Limnol Oceanogr 12:411–418

Suratman S, Weston K, Greenwood N, Sivyer DB, Pearce DJ, Jickells T (2010) High frequency measurements of dissolved inorganic and organic nutrients using instrumented moorings in the southern and central North Sea. Estuar Coast Shelf Sci 87:631–639

Suttle C (2005) Viruses in the sea. Nature 437:356–61

Suttle C a (2007) Marine viruses-major players in the global ecosystem. Nat Rev Microbiol 5:801–12

Swalwell JE, Ribalet F, Armbrust EV (2011) SeaFlow: A novel underway flow-cytometer for continuous observations of phytoplankton in the ocean. Limnol Oceanogr Methods 9:466–477

Tang YZ, Dobbs FC (2007) Green autofluorescence in dinoflagellates, diatoms, and other microalgae and its implications for vital staining and morphological studies. Appl Environ Microbiol 73:2306–13

Tarran G a., Heywood JL, Zubkov M V. (2006) Latitudinal changes in the standing stocks of nano- and picoeukaryotic phytoplankton in the Atlantic Ocean. Deep Sea Res Part II Top Stud Oceanogr 53:1516–1529

Taylor F (1980) Phytoplankton ecology before 1900: Supplementary notes to the "Depths of the Ocean." In: Sears M, Merriman D (eds) Oceanography: the Past. Springer-Verlag, New York, p 509–521

Taylor A, Landry M, Selph K, Yang E (2011) Biomass, size structure and depth distributions of the microbial community in the eastern equatorial Pacific. Deep Sea Res Part II Top Stud Oceanogr 58:342–357

Thingstad T, Sakshuag E (1990) Control of phytoplankton growth in nutrient recycling ecosystems.Theory and terminology. Mar Ecol Prog Ser 63:261–272

Thomas C (1971) The genetic organisation of chromosomes. Annu Rev Genet 5:237–256

Thomas H, Bozec Y, Elkalay K, Baar H de (2004) Enhanced open ocean storage of CO_2 from shelf sea pumping. Science 304:1005–1008

Thurman H V (1997) Introductory Oceanography, 8th edn. Prentice-Hall, New Jersey

Thyssen M, Mathieu D, Garcia N, Denis M (2008) Short-term variation of phytoplankton assemblages in Mediterranean coastal waters recorded with an automated submerged flow cytometer. J Plankton Res 30:1027–1040

Thyssen M, Garcia N, Denis M (2009) Sub meso scale phytoplankton distribution in the North East Atlantic surface waters determined with an automated flow cytometer.Biogeosciences 6:569–583

Thyssen M, Beker B, Ediger D, Yilmaz D, Garcia N, Denis M (2011) Phytoplankton distribution during two contrasted summers in a Mediterranean harbour: combining automated submersible flow cytometry with conventional techniques. Environ Monit Assess 173:1–16

Tiersch TR, Chandler RW, Wachtel SS, Elias S (1989) Reference standards for flow cytometry and application in comparative studies of nuclear DNA content. Cytometry 10:706–710

Tillmann U, Rick H-J (2003) North Sea Phytoplankton: a Review. Senckenbergiana maritima 33:1–69

Toepel J, Wilhelm C, Meister A, Becker A, Carmen Martinez-Ballesta M del (2004) Cytometry of freshwater phytoplankton. Methods Cell Biol 75:375–407

Totterdell IJ, Armstrong RA, Drange H (1993) Trophic Resolution. In: Evans G., Fasham MJR (eds) Towards a Model of Ocean Biogeochemical Processes. NATO ASI, Vol. I 10. Springer-Verlag, Berlin, p 71–92

Townsend D, Cammen L, Holligan P, Campbell D, Pettigrew N (1994) Causes and consequences of variability in the timing of spring phytoplankton blooms. Deep Res I 41:747–765

Troussellier M, Courties C, Lebaron P, Servais P (1999) Flow cytometric discrimination of bacterial populations in seawater based on SYTO 13 staining of nucleic acids. FEMS Microbiol Ecol 29:319–330

Tsuji T, Yanagita T (1981) Improved fluorescent microscopy for measuring the standing stock of phytoplankton including fragile components. Mar Biol 64:207–211

Tzur A, Moore JK, Jorgensen P, Shapiro HM, Kirschner MW (2011) Optimizing optical flow cytometry for cell volume-based sorting and analysis. PLoS One 6:e16053

Uitz J, Claustre H, Gentili B, Stramski D (2010) Phytoplankton class-specific primary production in the world's oceans: seasonal and interannual variability from satellite observations. Global Biogeochem Cycles 24:1–19

Uitz J, Claustre H, Morel A, Hooker SB (2006) Vertical distribution of phytoplankton communities in open ocean: An assessment based on surface chlorophyll. J Geophys Res 111

Utermöhl von H (1931) Neue Wege in der quantitativen Erfassung des Planktons. (Mit besondere Beriicksichtigung des Ultraplanktons). Verh Int Verein Theor Angew Limnol 5:567–595

Uysal Z (2000) Pigments, size and distribution of *Synechococcus* spp. in the Black Sea. J Mar Syst 24:313–326

Vaulot D, Courties C, Partensky F, Biologique S (1989) Heterogeneity in fragility and other biophysical properties: a simple method to preserve oceanic phytoplankton for flow cytometric analyses through division by the corresponding parameters. Cytometry 10:629–635

Vaulot D, Birrien J-L, Marie D, Casotti R, Veldhuis M, Kraay G (1994) Morphology, ploidy, pigment composition and genome size of cultured strains of *Phaeocystis* (Prymnesiophyceae). J Phycol 30:1022–1035

Vaulot D, Eikrem W, Viprey M, Moreau H (2008) The diversity of small eukaryotic phytoplankton (< or =3 micron) in marine ecosystems. FEMS Microbiol Rev 32:795–820

Veenstra H (1965) Geology of the Dogger Bank Area, North Sea. Mar Geol 3:245–262

Veldhuis MJW, Cucci TL, Sieracki ME (1997) Cellular DNA content of marine phytoplankton using two new fluorochromes: taxonomic and ecological implications. J Phycol 33:527–541

Veldhuis MJW, Kraay GWK (2000) Application of flow cytometry in marine phytoplankton research: current applications and future perspectives. Sci Mar 64:121–134

Veldhuis MJW, Kraay GWK, Timmermans K (2001) Cell death in phytoplankton : correlation between changes in membrane permeability, photosynthetic activity , pigmentation and growth. Eur J Phycol 36:167–177

Veldhuis MJW, Kraay GWK (2004) Phytoplankton in the subtropical Atlantic Ocean: towards a better assessment of biomass and composition. Deep Sea Res Part I Oceanogr Res Pap 51:507–530

Veldhuis MJW, Timmermans KR, Croot P, Wagt B Van Der (2005) Picophytoplankton ; a comparative study of their biochemical composition and photosynthetic properties. J Sea Res 53:7–24

Verdy A, Follows M, Flierl G (2009) Optimal phytoplankton cell size in an allometric model. Mar Ecol Prog Ser 379:1–12

Verity PG, Robertson CY, Tronzo CR, Andrews MG, Nelson JR, Sieracki ME (1992) Relationships between cell volume and the carbon and nitrogen content of marine photosynthetic nanoplankton. Limnol Oceanogr 37:1434–1446

Viprey M, Guillou L, Ferréol M, Vaulot D (2008) Wide genetic diversity of picoplanktonic green algae (Chloroplastida) in the Mediterranean Sea uncovered by a phylum-biased PCR approach. Environ Microbiol 10:1804–22

Vives-Rego J, Lebaron P, Nebe-von Caron G (2000) Current and future applications of flow cytometry in aquatic microbiology. FEMS Microbiol Rev 24:429–48

Volk T, Hoffert MI (1985) Ocean carbon pumps: analysis of relative strengths and efficiencies in ocean-driven atmospheric CO_2 changes. Geophys Monogr Ser 32:99–110

Volpi E V, Bridger JM (2008) FISH glossary : an overview of the fluorescence *in situ* hybridization technique. Biotechniques 45:385–409

Wacquet G (2011) Classification spectrale semi-supervisée. Application à la surveillance de l'écosystème marin. Université du Littoral Côte d'Opale, Calais

Waterbury J, Watson S, Guillard R, Brand L (1979) Widespread occurrence of a unicellular,marine, planktonic, cyanobacterium. Nature 227:293–294

Waterbury J, Watson S, Valois F, Franks D (1986) Biological and ecological characterization of the marine unicellular cyanobacterium *Synechococcus*. Can Bull Fish Aquat Sci 214:71–120

Weston K, Greenwood N, Fernand L, Pearce DJ, Sivyer DB (2008) Environmental controls on phytoplankton community composition in the Thames plume, U.K. J Sea Res 60:246–254

Wiltshire KH, Malzahn AM, Wirtz K, Greve W, Janisch S, Mangelsdorf P, Manly BFJ, Boersma M (2008) Resilience of North Sea phytoplankton spring bloom dynamics: an analysis of long-term data at Helgoland Roads. Limnol Oceanogr 53:1294–1302

Wollast R (1998) Evaluation and comparison of the global carbon cycle in the coastal zone and in the open ocean. In: Brink K, Robinson A (eds) The Sea. Wiley, New York, p 152–213

Yentsch CS, Yentsch CM (1979) Fluorescent spectral signatures: the characterisation of phytoplankton populations by the use of excitation and emission spectra. J Mar Res 37:471–483

Young E, Bigg G, Grant A, Walker P, Brown J (1998) A modelling study of environmental influences on bivalve settlement in The Wash, England. Mar Ecol Prog Ser 172:197–214

Zarauz L, Irigoien X (2008) Effects of Lugol's fixation on the size structure of natural nano-microplankton samples, analyzed by means of an automatic counting method. J Plankton Res 30:1297–1303

Zehr JP, Bench SR, Carter BJ, Hewson I, Niazi F, Shi T, Tripp HJ, Affourtit JP (2008) Globally distributed uncultivated oceanic N_2-fixing cyanobacteria lack oxygenic photosystem II. Science 322:1110–1112

Zhu F, Massana R, Not F, Marie D, Vaulot D (2005) Mapping of picoeukaryotes in marine ecosystems with quantitative PCR of the 18S rRNA gene. FEMS Microbiol Ecol 52:79–92

Zubkov M, Sleigh M, Tarran G, Burkill P, Leakey R (1998) Picoplanktonic community structure on an Atlantic transect from 50 N to 50 S. Deep Sea Res Part I Oceanogr Res Pap 45:1339–1355

Zubkov M, Sleigh M, Burkhill P (2000) Assaying picoplankton distribution by flow cytometry of underway samples collected along a meridional transect across the Atlantic Ocean. Aquat Microb Ecol 21:13–20

Zubkov M V, Fuchs BM, Stephen D, Kiene RP, Amann R, Burkill H (2001) Linking the composition of bacterioplankton to rapid turnover of dissolved dimethylsulphoniopropionate in an algal bloom in the North Sea. Environ Microbiol 3:304–311

Zubkov M, Tarran G, Fuchs B (2004) Depth related amino acid uptake by *Prochlorococcus* cyanobacteria in the Southern Atlantic tropical gyre. FEMS Microbiol Ecol 50:153–161

Zubkov M, Burkill P, Topping J (2006) Flow cytometric enumeration of DNA-stained oceanic planktonic protists. J Plankton Res 29:79–86

Zwirglmaier K, Jardillier L, Ostrowski M, Mazard S, Garczarek L, Vaulot D, Not F, Massana R, Ulloa O, Scanlan DJ (2008) Global phylogeography of marine *Synechococcus* and *Prochlorococcus* reveals a distinct partitioning of lineages among oceanic biomes. Environ Microbiol 10:147–61